DOKUZ EYLÜL UNIVERSITY
GRADUATE SCHOOL OF NATURAL AND APPLIED SCIENCES

THE GEOLOGY OF YATAĞAN COALFIELD AND INVESTIGATION OF MINERALOGICAL AND PETROGRAPHICAL PROPERTIES OF THE COALS, SW TÜRKİYE

Işık HACIMUSTAFAOĞLU

August, 2025
İZMİR

THE GEOLOGY OF YATAĞAN COALFIELD AND INVESTIGATION OF MINERALOGICAL AND PETROGRAPHICAL PROPERTIES OF THE COALS, SW TÜRKİYE

A Thesis Submitted to the Graduate School of Natural and Applied Sciences of Dokuz Eylül University In Partial Fulfillment of the Requirements for the Degree of Doctor of Philosophy in Geological Engineering, Economic Geology Program

by

Işık HACIMUSTAFAOĞLU

August, 2025

İZMİR

Ph.D. THESIS EXAMINATION RESULT FORM

We have read the thesis entitled "**THE GEOLOGY OF YATAĞAN COALFIELD AND INVESTIGATION OF MINERALOGICAL AND PETROGRAPHICAL PROPERTIES OF THE COALS, SW TÜRKİYE**" completed by **IŞIK HACIMUSTAFAOĞLU** under supervision of **ASSOCIATE PROF. DR. MEHMET AKBULUT** and **PROF. DR. KIMON CHRISTANIS** and we certify that in our opinion it is fully adequate, in scope and in quality, as a thesis for the degree of Doctor of Philosophy.

.....

Assoc.Prof.Dr. Mehmet AKBULUT

Supervisor

.....	.....
Prof. Dr. Tolga OYMAN	Prof. Dr. M. Kemal ÖZFIRAT
Thesis Committee Member	Thesis Committee Member
.....	.....
Prof. Dr. Macid Fikret SUNER	Assoc.Prof. Dr. Ceren KÜÇÜKUYSAL
Examining Committee Member	Examining Committee Member

Prof.Dr. Abdullah SEÇGİN

Director

Graduate School of Natural and Applied Sciences

ACKNOWLEDGEMENTS

I would like to thank my thesis supervisor, Associate Prof. Dr. Mehmet AKBULUT and the co-supervisor, Prof. Em. Dr. Kimon CHRISTANIS from the University of Patras (Greece) for sharing their knowledge and experience with me in the field and the laboratory work, and throughout the compiling of the current thesis. I am particularly grateful to Prof. Dr. Hülya İNANER, who, along with both supervisors, contributed to the planning of the thesis and actively participated in all stages of the study. Her support, as well as Prof. Dr. Tolga OYMAN's support throughout my doctoral education, is highly appreciated. I am also grateful to Prof. Dr. Ali İhsan KARAYİĞİT from Hacettepe University, Ankara, for his valuable contributions for the development of this thesis. Much appreciation goes to the staff of the Yatağan Thermal Energy Mining Directorate Mr. H. Tanzer AYDEMİR, Deputy Head of the Mining Department, Mr. Şahin YILDIRIM, General Manager of Thermal Power Plants, Mr. İbrahim YÖRÜK, former Underground Operation Manager, and Mr. Kaan KARABULUT, former Chief Planning Engineer, for their assistance during the field work and for providing the coal analysis data.

I would like to express my sincere gratitude to: Ms. Maria KALABOKA and Mrs. Golfo KORDOPATI from the Instrumental Analysis Laboratory, University of Patras, for performing the ultimate analyses; Assoc. Prof. Dr. Pasraskevi LAMBROPOPOULOU and Mr. Konstantinos PERLEROS from the Department of Geology, University of Patras, for repeating the XRD analyses of selected coal samples. My gratitude goes to Dr. İsmail İŞİNTEK for his guidance during the evaluation of microscope studies; Dr. Zeynep BÜÇKÜN for her suggestions and support during the evaluation of the results; Ms. Burcu ERECEK, who actively participated in the field and microscope studies.

Finally, I would like to thank my family for supporting me both financially and morally throughout their lives: my husband, Dr. Ramazan Hacımustafaoğlu, for his support and patience at every stage of my work; and my sons, Doğukan and Furkan Hacımustafaoğlu, for their love, interest and support.

Işık HACIMUSTAFAOĞLU

THE GEOLOGY OF YATAĞAN COALFIELD AND INVESTIGATION OF MINERALOGICAL AND PETROGRAPHICAL PROPERTIES OF THE COALS, SW TÜRKİYE

ABSTRACT

This doctoral thesis aims by studying the geological properties, coal quality, petrographic, geochemical and mineralogical compositions, to reconstruct the palaeoenvironmental conditions and to determine the controlling factors, which affected the Yatağan coal seam. The studied samples derived from cores I-18, I-23 and I-25 retrieved from the recently discovered lignite field near the Yatağan Thermal Power Plant in the Yatağan District of Muğla Province. The average total moisture is 35% (on as-received basis; ar); the ash yield 33% (on dry basis; db); the volatile matter yield 58% (on dry, ash-free basis; daf); the fixed carbon content yield 42% (daf); the sulphur content 2.5% (ar); the gross calorific value 12.18 MJ/kg (on moist, ash-free basis; maf). The coal rank is ortholignite. The petrographic composition of the samples shows the predominance of huminite (>78.6 vol.%), whereas liptinite and inertinite are contained in lesser amounts. The mean random huminite reflectance is 0.28%. Based on the maceral contents determined, facies diagrams infer that the lignite derived from herbaceous helophyte remains accumulated in a palaeomire under telmatic/limnotelmatic, rheotrophic, and anoxic conditions. The trace element contents determined by P-XRF comprise, on average, Si 4.58%, Al 2.81%, Fe 1.17%, Ca 4.34%, Mg 0.96%, Ti 0.09%, and P 0.03%, Zr 37 ppm, Ni 34 ppm, As 38 ppm, Cd 23 ppm, and Se 3 ppm. In addition, the mineralogical and elemental composition of the lignite and the inorganic intercalations were examined using XRD and SEM-EDX. The lignite contains clay minerals, quartz, feldspar, pyrite, mica, calcite, and aragonite. The inorganic intercalations contain mainly clay minerals and quartz, which were washed out from the basin margins by surface water and transported into the palaeomire. In light of all this data, the coal field under study shares similar characteristics with other fields in the Muğla Basin.

Keywords: Lignite, coal petrology, geochemistry, mineralogy, Yatağan, Muğla

YATAĞAN KÖMÜR SAHASININ JEOLOJİSİ, KÖMÜRLERİN MİNERALOJİK VE PETROGRAFİK ÖZELLİKLERİNİN İNCELENMESİ, GB TÜRKİYE

ÖZ

Bu doktora tezi, jeolojik özellikleri, kömür kalitesini, petrografik, jeokimyasal ve mineralojik bileşimleri inceleyerek, Yatağan kömür damarını etkileyen paleoçevresel koşulları yeniden oluşturmayı ve kontrol faktörlerini belirlemeyi amaçlamaktadır. İncelenen numuneler, Muğla ilinin Yatağan ilçesindeki Yatağan Termik Santrali yakınlarında yeni keşfedilen linyit sahasından alınan I-18, I-23 ve I-25 karotlarından elde edilmiştir. Ortalama toplam nem oranı %35 (aldığı haliyle; ar); kül verimi %33 (kuru bazda; db); uçucu madde verimi %58 (kuru, külsüz bazda; daf); sabit karbon içeriği verimi %42 (daf); kükürt içeriği %2,5 (ar); brüt kalorifik değer %12,18 MJ/kg'dır (nemli, külsüz bazda; maf). Kömürün sınıfı ortolinyittir. Örneklerin petrografik bileşimi, huminitlerin (>%78,6 hacim) baskın olduğunu gösterirken, liptinit ve inertinit daha az miktarda bulunmaktadır. Ortalama rastgele huminit yansıtma oranı %0,28'dir. Belirlenen maseral içeriklerine dayanarak, fasiyes diyagramları, telmatik/limnotelmatik, reotrofik ve anoksik koşullar altında paleomirede biriken otsu helofit kalıntılarından türetilen linyitin olduğunu göstermektedir. P-XRF ile belirlenen eser element içerikleri ortalama olarak Si %4,58, Al %2,81, Fe %1,17, Ca %4,34, Mg %0,96, Ti %0,09 ve P %0,03, Zr 37 ppm, Ni 34 ppm, As 38 ppm, Cd 23 ppm ve Se 3 ppm'dir. Ayrıca, linyitin mineralojik ve elementel bileşimi ile inorganik interkalasyonlar XRD ve SEM-EDX kullanılarak incelenmiştir. Linyit, kil mineralleri, kuvars, feldispat, pirit, mika, kalsit ve aragonit içermektedir. İnorganik interkalasyonlar ise, yüzey suları tarafından havza kenarlarından yıkanarak paleomire taşınan kil mineralleri ve kuvars içermektedir. Tüm bu veriler ışığında, incelenen kömür sahası Muğla Havzasındaki diğer sahalarla benzer özellikler taşımaktadır.

Anahtar Kelimeler: Linyit, kömür petrolojisi, jeokimya, mineraloji, Yatağan, Muğla

CONTENTS

Page

THESIS EXAMINATION RESULT FORM ii
ACKNOWLEDGEMENTS iii
ABSTRACT iv
ÖZ v
LIST OF FIGURES x
LIST OF TABLES xiii

CHAPTER ONE - INTRODUCTION 1

1.1 Coal Quality and Reserves in Türkiye 1
1.2 Bibliography Review 5
1.3 Study Area 11
1.4 Aim of the Study 13

CHAPTER TWO – GEOLOGICAL SETTING 14

2.1 Tectonic Development of Muğla Basin 14
2.2 The Yatağan Area 18
2.2.1 Pre-Neogene Rocks 18
2.2.2 Neogene Formations 19
2.2.2.1 Turgut Formation 19
2.2.2.2 Sekköy Formation 19
2.2.2.3 Yatağan Formation 19
2.2.2.4 Milet Formation 20
2.2.3 Quaternary Formations 20

CHAPTER THREE–MATERIALS AND METHODS 22

3.1 Field Work 23

CHAPTER FOUR - RESULTS **27**

4.1 Lithological Features 27
4.2 Laboratory Determinations 29
4.2.1 Proximate Analysis 29
4.2.2 Ultimate Analysis 31
4.2.3 Coal Petrography 32
4.2.3.1 Definitions of the Maceral Groups 33
4.2.3.1.a Huminite/Vitrinite Group 34
4.2.3.1.b Inertinite Group 34
4.2.3.1.c Liptinite Group 34
4.2.3.2 Maceral Composition of Yatağan Coal 35
4.2.3.3 Huminite Reflectance 42
4.2.4 Mineralogical Composition 45
4.2.4.1 Inorganic Sediments 47
4.2.5 SEM-EDX Analysis of Coal Samples 49
4 2.6 PXRF Evaluation of Yatağan Coal and Inorganic Rock Sample 54
4.2.6.1 Trace Element Chemistry 55
4.2.6.2 Petrographic Analysis of Inorganic Samples 60

CHAPTER FIVE - DISCUSSION **62**

5.1 Coal Rank 62
5.2 Depositional Environment 64
5.3 Inferences from The Mineral Matter 69
5.3.1 Correlation of Trace Element Contents in The Yatağan Lignite 71
5.3.2 Characterization of inorganic rocks and inferences 76
5.4 Evaluation ofthe Coal Petrography Data in relation with the Available Borehole Spatial Data 80
5.5 Comparison of Reflectance Measurements between Huminite Macerals 84
5.6 Comparison to other coal fields in the Muğla Basin 85

CHAPTER SIX - CONCLUSION **88**

REFERENCES **90**

APPENDICES **103**

APPENDIX I: Drilling and core sampling in the Yatağan lignite field 104
APPENDIX II: Laboratory studies 107
APPENDIX III: Characterization of Macerals in Coal 111
APPENDIX IV: Photomicrographs of the Yatağan lignite 114
APPENDIX V: Histograms of the reflectance measurement 122
APPENDIX VI: XRD Analysis 129
APPENDIX VII: SEM-EDX Analysis 132
APPENDIX VIII: Petrographic analysis of inorganic samples. 144

LIST OF FIGURES

Page

Figure 1.1 Distribution of Coal Consumption by Sectors in Türkiye for 2022 (ETKB, 2024)..... 1
Figure 1.2 Fossil Fuel Deposits of Türkiye (from Nakoman and İnaner, 2004; MTA, 2010)..... 3
Figure 1.3 Lignite Production in Türkiye from 2012 to 2022 (ETKB, 2024)..... 4
Figure 1.4 Major lignite fields in the Muğla Basin (İnaner et al., 2008)..... 12
Figure 2.1 Present tectonic setting of the Aegean extensional province and related graben systems in Western Anatolia (from Yağmurlu, 2000)..... 14
Figure 2.2(a) Geological map of the Miocene Muğla Basin, SW Türkiye (after Querol et al., 1999), and Geological cross-section of the Muğla and Gökova Gulf region. (b) Cross-section of the Muğla Basin (vertical scale is exaggerated), (from Gürer et al., 2013)..... 16
Figure 2.3 Lithostratigraphic column of Muğla Basin (modified from Sun and Karaca, 2000)..... 17
Figure 2.4 Geological map of the Yatağan Basin (Ünal, 1989; Bulut et al., 2001). 18
Figure 2.5 Generalized stratigraphic column of Muğla-Yatağan Basin (from Gürsoy et al., 1993, and İnaner, 1994)..... 21
Figure 3.1 Flowchart of the methodology applied in the study on Yatağan lignite samples. 22
Figure 3.2 Sketch map of the drilling sites within the license area of the Yatağan Thermal Energy Mining Directorate. 24
Figure 4.1 The I-18 borehole profile (the red circles correspond to inorganic, the blue ones to coal samples)..... 27
Figure 4.2 The I-23 borehole profile (the red circles correspond to inorganic, the blue ones to coal samples)..... 28
Figure 4.3 The I-25 borehole profile (the red circles correspond to inorganic, the blue ones to coal samples)..... 28
Figure 4.4 Maceral group composition and reflectance values of the samples from I-18 well. 39

Figure 4.5 Maceral group composition and reflectance values of the samples from I-23 well. 40
Figure 4.6 Maceral group composition and reflectance values of the samples from I-25 well. 41
Figure 4.7 Examples of histograms of reflectance measurements of various huminite macerals on Yatağan coal samples. 44
Figure 4.8 Mineral contents of samples from cores I-18, I-23 and I-25 47
Figure 4.9 Diffractograms of samples #29 (a) and #12 (b) from core I-18, as well as of the fine fraction (∅ < 2 μm) of sample #12 (c), (Sme: smectite; Il: illite; Kln: kaolinite; Chl: chlorite). 49
Figure 4.10 SEM-EDX result of sample I-18/9 a, b. 51
Figure 4.11 SEM-EDX result of sample I-18/23 a, b. 51
Figure 4.12 SEM-EDX result of sample I-23/48 a, b. 52
Figure 4.13 SEM-EDX result of sample I-23/49 a, b. 52
Figure 4.14 SEM-EDX result of sample I-25/6 a, b. 53
Figure 4.15 SEM-EDX result of sample I-23/49 a, b. 53
Figure 4.16(a) Average contents (%) of trace elements of Yatağan coal and inorganic samples; (b) Average contents (%) of trace elements in Yatağan coal and inorganic samples. 58
Figure 5.1 The Yatağan coal projected on the DIN and ASTM rank classification scheme (from Taylor et al., 1998). 62
Figure 5.2 The Yatağan coal samples plotted on the ECE-UN (1998) classification scheme. 63
Figure 5.3 The Yatağan coal samples projected on the Van Krevelen (1993) diagram (blue, yellow, and red circles denote I-18, I-23, and I-25 samples, respectively)..... 64
Figure 5.4 The Yatağan coal samples plotted on the Mukhopadhyay (1989) ternary diagram (blue, yellow, and red circles denote I-18, I-23, and I-25 samples, respectively)..... 66
Figure 5.5 The TPI vs. GI plot (after Diessel, 1992, as modified by Kalaitzidis et al., 2004) of the Yatağan coal samples (blue, yellow and red circles denote I-18, I-23, and I-25 samples, respectively). 67

Figure 5.6 The GWI vs. VI diagram (after Calder et al., 1991, as modified by Kalaitzidis et al., 2004) for the studied lignite samples (blue, yellow and red circles denote I-18, I-23, and I-25 samples, respectively). 68
Figure 5.7 Comparison of the trace element contents (a: in wt%, b: in ppm) obtained from the P-XRF analysis of the Yatağan coal and clay samples..... 70
Figure 5.8 Correlation of Si and Al average contents 72
Figure 5.9 Correlation diagrams of ash with calcite, quartz, smectite and pyrite according to XRD results. 74
Figure 5.10 Classification of the studied samples using the Log(SiO_2/Al_2O_3) and Log(Fe_2O_3/K_2O) ratios (Herron, 1988). 78
Figure 5.11 Location of four boreholes (I-18, I-23, I-25 and B-22, the latter studied by Erecek, 2024) of the Yatağan coal field, and the cross-section constructed by projection of the boreholes along an arbitrary NNW-SSE profile. The topographic relief is drawn hypothetically taking the starting elevations (Z) of the boreholes and the river beds crossed into account. 81
Figure 5.12 Maceral group composition in volume %, on mineral matter-free basis (mmf) of the wells I-18, I-23, and I-25 from this study, and B-22 from Erecek (2024). 83
Figure 5.13 The correlation between mean corpohuminite and gelinite reflectance values. 84
Figure 5.14 Ash, volatile matter (VM), and sulphur contents of coal fields in the Muğla Basin. 86

LIST OF TABLES

Page

Table 1.1 Reserves and quality results in Yatağan Thermal Power Plant license areas (ETKB, 2024). 5

Table 4.1 The results of the proximate analysis of the I-18, I-23 and I-25 samples obtained from Yatağan Thermic Energy Production Inc. (VM: volatile matter; Cfix: fixed carbon; CV: calorific value; db: dry basis; daf: dry, ash-free basis; ar: as-received basis; maf: moist, ash-free basis) 29

Table 4.2 The results of the proximate analysis on the Yatağan coal samples (VM: volatile matter; Cfix: fixed carbon; CV: calorific value; db: dry basis; daf: dry, ash-free basis). 30

Table 4.3 Ultimate analysis results of Yatağan coal (daf: dry, ash-free basis, *: calculated by subtraction: O = 100-C-H-N-S). 32

Table 4.4 The maceral composition (in vol%, on a mineral matter-free basis) and the mineral matter (in vol%, on a whole-rock basis), as well as the mean random reflectance of the Yatağan coal samples from core I-18. 35

Table 4.5 The maceral composition (in vol.%, on a mineral matter-free basis) and the mineral matter (vol.%, on a whole-rock basis), as well as the mean random reflectance of the Yatağan coal samples from core I-23. 36

Table 4.6 The maceral composition (in vol.%, on a mineral matter-free basis) and the mineral matter (in vol.%, on a whole-rock basis), as well as the mean random reflectance of the Yatağan coal samples from core I-25. 37

Table 4.7 Mean random reflectance (in %) of some huminite macerals in the Yatağan lignite 45

Table 4.8 Mineralogical composition (in wt.% of the crystalline phases) of the Yatağan coal samples. 46

Table 4.9 The mineralogical composition of the lignite samples from cores I-18, I-23 and I-25 47

Table 4.10 The semi-quantitative composition (on wt.% of the crystalline phases) of the fine fraction (∅ < 2 μm) of two samples from I-18 core 48

Table 4.11 Results of SEM-EDX analyses of coal samples from borehole I-18, I-23, and I-25 50

Table 4.12 Results of PXRF analyses of coal samples from borehole I-18. 54
Table 4.13 Results of PXRF analyses of coal samples from borehole I-23. 55
Table 4.14 Results of PXRF analyses of coal samples from borehole I-25. 56
Table 4.15 The trace element composition of the coal (on average per core) and the inorganic samples from the Yatağan Field (DL: detection limit). 57
Table 4.16 Weighted content averages of trace elements in the coal samples examined within the scope of the study, and comparison of these values with world coals (from Swaine, 1990), and Clarke values for low-grade coals (from Ketris and Yudovich, 2009). 59
Table 4.17 Lithology of inorganic rock samples taken from coal roof, intercalations and floor. 61
Table 5.1 The maceral indices of the Yatağan lignite samples (for the calculation of A, B and C see Fig. 5.4; for TPI and GI see Fig. 5.5; for GWI and VI see Fig. 5.6)..... 65
Table 5.2 Trace element correlation matrix values of Yatağan coal deposit. 71
Table 5.3 Trace element correlation coefficients in the coal samples examined. 75
Table 5.4 Oxide contents (in wt.%) of the Yatağan samples. 77
Table 5.5 Slagging index parameters 79
Table 5.6 Correlation coefficients among the reflectance values of some huminite macerals from Yatağan coal samples. 84
Table 5. 7 Ash, volatile matter (VM), and fixed carbon (Cfix) yields, as well as sulphur content and calorific value (CV) of coal samples obtained from various lignite fields in the Muğla Basin (MTA, 2010). 86

CHAPTER ONE

INTRODUCTION

1.1 Coal Quality and Reserves in Türkiye

Despite the current worldwide agenda concerning the transition to green energy sources, fossil fuels still play an important role in covering an essential part of the global energy needs. In 2023, coal covered ca. 26.47% of the primary energy demand in the world, second only after oil (31.7%) (Ritchie and Rosado, 2020). Coal is not only an energy raw material for power generation but also finds applications in many other industrial applications or sectors, such as the manufacturing of paints, plastics, pharmaceuticals, cosmetics, iron/steel, aluminum, etc. (e.g., Schobert and Song, 2002; Giannouli et al., 2009; Zhang and Honaker, 2020; ETKB, 2024) (Fig. 1.1). Hence, studying and understanding the occurrence and feasibility of greenfield and brownfield coal deposits are still a national priority for countries like Türkiye, which has limited indigenous energy sources (ETKB, 2024).

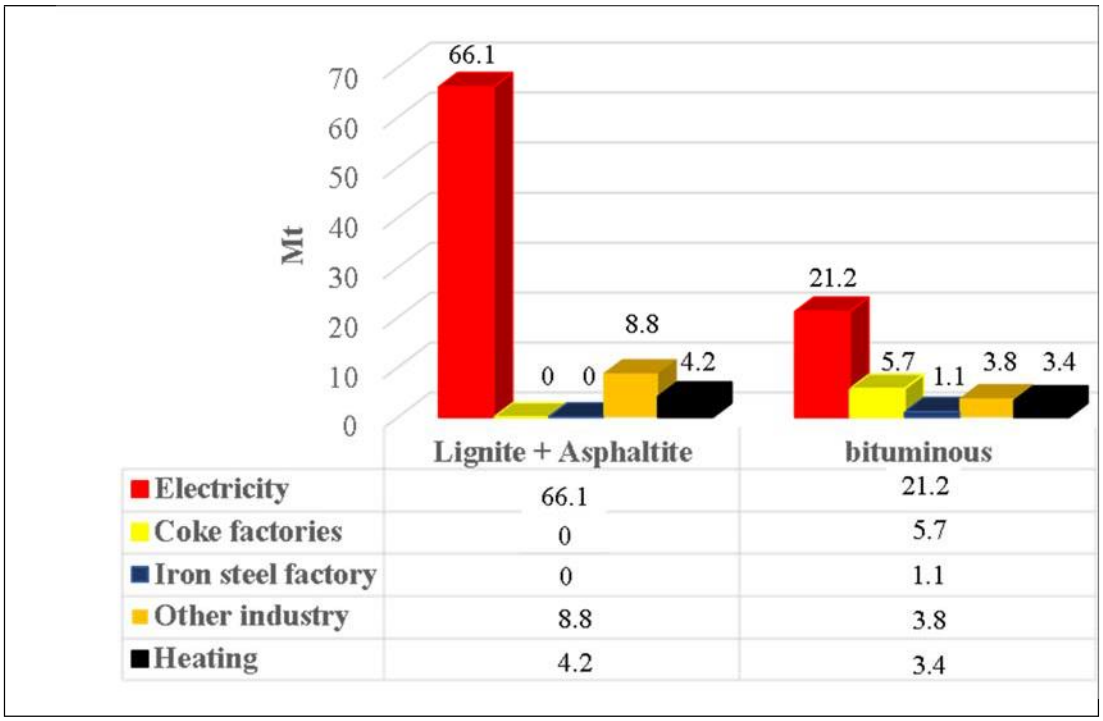

Figure 1.1 Distribution of Coal Consumption by Sectors in Türkiye for 2022 (ETKB, 2024).

Türkiye's total coal resources amount to approximately 20.84 Gt, 19.32 Gt of which is lignite and asphaltite (92.7%) and 1.52 Gt bituminous coal (7.3%). The gross calorific value of bituminous coal varies between 25.96-30.35 MJ/kg (on as-received basis). Although the gross calorific values of Turkish lignite resources vary between 4.19 and 17.58 MJ/kg, ca. 79% of the gross calorific values of the reserves are below 10.47 MJ/kg (on an as-received basis). In Türkiye, the Miocene and Pliocene formations contain a significant number of lignite deposits. Lignite deposits are rarely encountered in the Eocene-Oligocene formations (Fig.1.2). Eocene coal-bearing basins are mostly located in the central part of the Black Sea region (Bolu/Mengen-Merkeşler; Çorum/Alpagut-Dodurga) and another one (Yozgat/Sorgun) is located in the Central Türkiye (Gökmen et al., 1997; İnaner and Nakoman, 1997; Toprak, 2009) (Fig. 1.2). Eocene coals present (on average, as-received basis) low moisture (11.19%), moderate ash yield (28.18%), high total sulphur content (5.13%), fixed carbon yield (55%) and high calorific value (16.95 MJ/kg, ar) (İnaner and Nakoman, 1997; Karayiğit and Whateley 1997; Tuncalı et al., 2002; Besbelli, 2009 and Toprak, 2009). Oligocene and Oligocene/Miocene coal-bearing basins on the other hand are concentrated on the Thrace Peninsula (Edirne/Vize–Uzunköprü–Harmanlı; Tekirdağ/Malkara), and also in Southwestern Türkiye (Burdur/Tokça-Çardak; Denizli/Kale) and Central Türkiye (Ankara/Şereflikoçhisar) (Fig. 1.2). These coal-bearing formations located in northwestern Anatolia were formed in limnic-fluvial and paralic environments (Akgün and Akkiraz, 2005; Palmer et al., 2009). Although the total Oligocene coal reserves (1 Gt) are larger than the Eocene coals (Besbelli, 2009), they are of lower quality. On average, they have an ash yield of 25% (ar) and a moisture content of 32%. The net calorific value is 10.46 MJ/kg (ar) (İnaner and Nakoman, 1997; Karayiğit and Whateley, 1997; Tuncalı et al., 2002; Besbelli, 2009; Toprak, 2009). The most important part of the coal deposits was formed during the Neogene period, between Middle Miocene and Pliocene. Terrestrial conditions dominated in the region from the beginning of the Miocene onward. The formation mechanism of important coal deposits in Western Anatolia, such as Çanakkale/Çan, Manisa/Soma, Balıkesir/Bigadiç, Bursa/Orhaneli and Muğla/Yatağan, was generally driven through extensional tectonics (Ediger, 1960; Görür et al., 1997; Akkiraz et al., 2011).

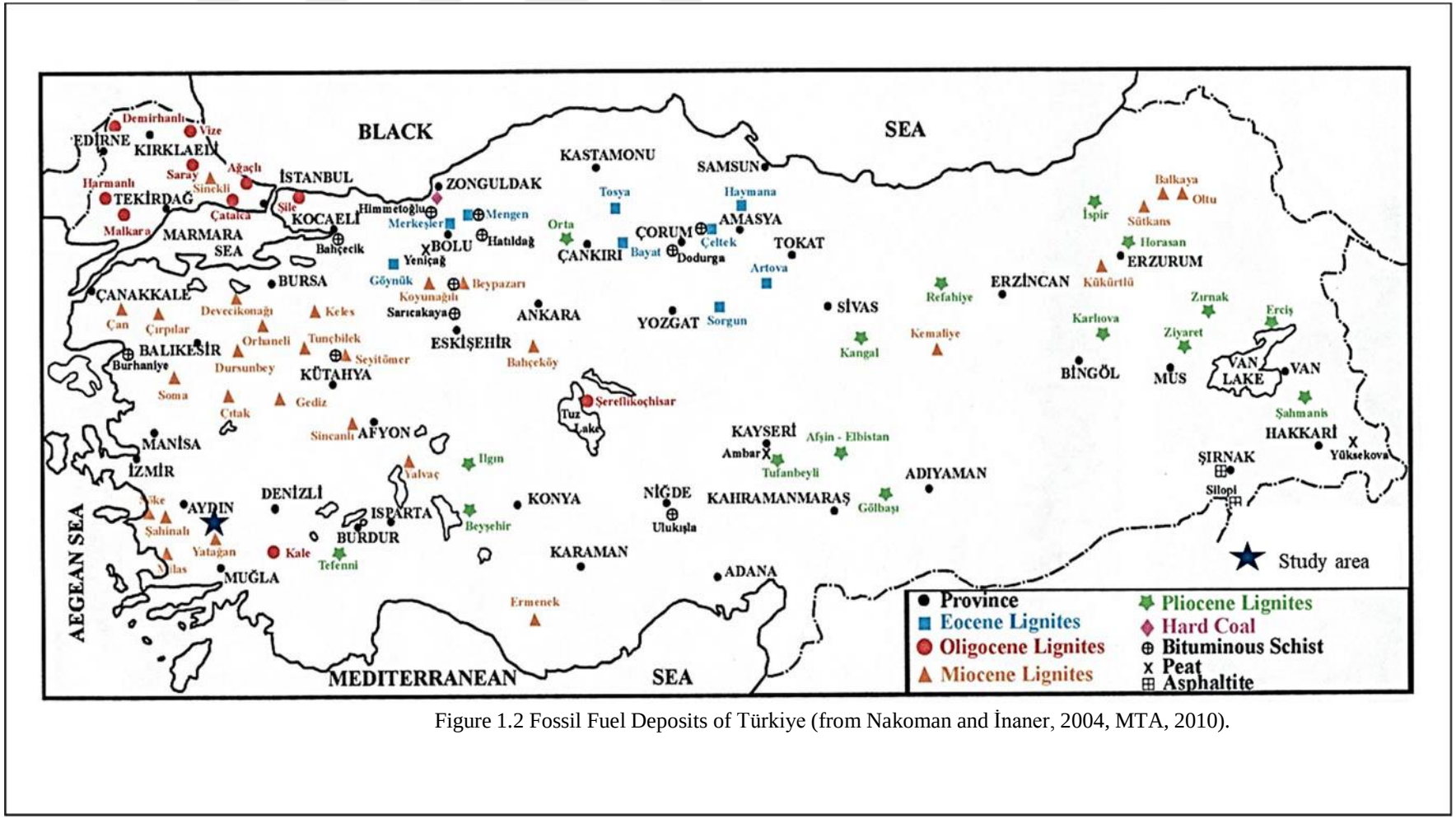

Figure 1.2 Fossil Fuel Deposits of Türkiye (from Nakoman and İnaner, 2004, MTA, 2010).

The coal-bearing basins in Eastern Anatolia region were formed by strike-slip faults (Adıyaman/Gölbaşı and Bingöl/Karlıova) or in intermontaine basin (Muş and Bitlis/ Adilceviz; Erzurum/Pasinler), and in the Central Türkiye they are "ova" (Kahramanmaraş/Afşin-Elbistan; Sivas/Kangal; Niğde/Ulukışla; Konya/Ilgın) or epirogenic (Çorum/Alpagut; Sivas/Şarkışla; Erzincan/Refahiye) (Şengör et al., 1984; Görür et al., 1997; Karayiğit and Whateley 1997; Akgün et al., 2007; Kayseri and Akgün, 2008; Besbelli, 2009; Toprak, 2009) (Fig. 1.2).

Western Anatolia, where the lignite deposit to be examined in this thesis is located, is the region where the most Miocene lignite deposits are found and mined in Türkiye. The seam thickness is also relatively higher in Western Anatolian lignite deposits compared to other regions of Türkiye. Most of the coal produced in western Anatolia is used for electricity generation in coal-fueled thermal power plants. As of December 2022, there were a total of 67 coal power plants in Türkiye with a total installed capacity of 115,188 MW: one fueled with asphaltite, 46 with lignite, 4 with bituminous coal and 16 with imported coal (ETKB, 2024) (Fig. 1.3). Low-calorific value coal in the Muğla-Yatağan lignite basin, where the study area is located, is similarly used to generate electricity in thermal power plants established to meet the needs of the national energy system.

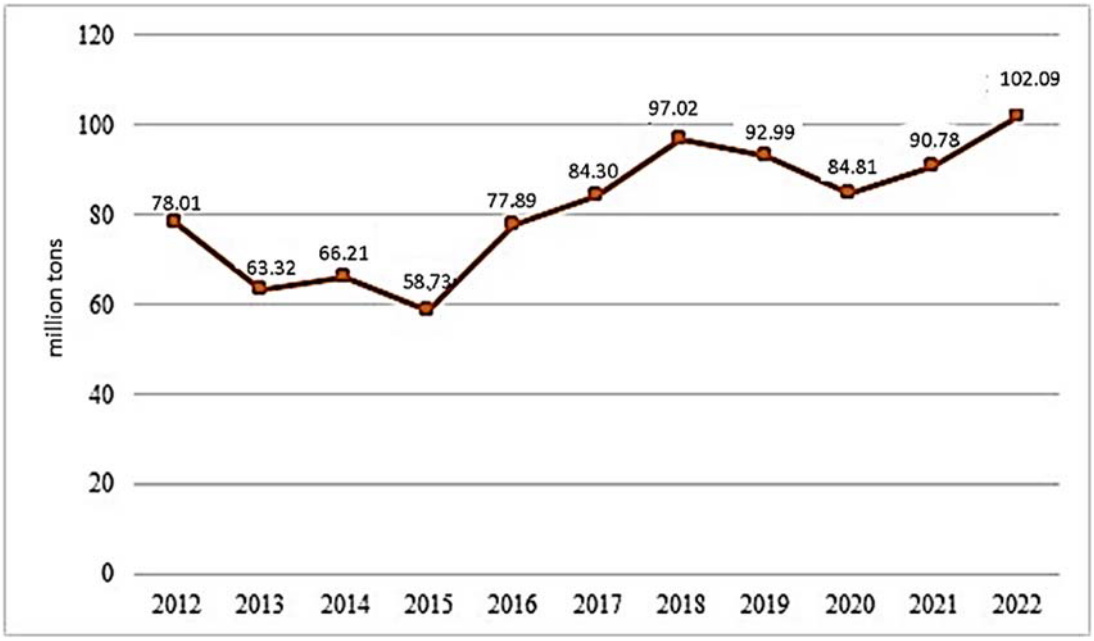

Figure 1.3 Lignite Production in Türkiye from 2012 to 2022 (ETKB, 2024).

Being one of those, Yatağan Thermal Power Plant is Türkiye's fifth largest thermal power plant. It has a total installed capacity of 630 MW with three units of 210 MW each, and an annual energy generation of 4096 GWh. An average of 30 Mm^3 of overburden wastes and 5.2 Mt of coal are mined annually. About 18 kt of coal are burned daily in the Yatağan Thermal Power Plant. There are open mining reserves in Eskihisar, Tınaz, Bağyaka, Yeşilbağçılar, Bayır-Salihpaşalar, and the lignite produced from these fields is used in the Yatağan Thermal Power Plant. Studies for new underground mining areas are ongoing in the Turgut, Hacıbayramlar and Salihpaşalar fields, where almost all of the coal is extracted from open pits (Table 1.1) (YTES, 2024).

Table 1.1 Reserves and quality results in Yatağan Thermal Power Plant license areas (ETKB, 2024).

Mining operation	Reserves (in Mt)	Moisture (%)	Ash (%, on as-received basis)	Calorific value (MJ/kg, on as-received basis)
Surface	51	38	27	9.25
Underground	110	30	23	11.11
Total	161			

Due to the decrease in the open-pit operating reserves needed by Yatağan Thermal Power Plant, the company runs exploration drilling activities in the licensed area in order to bring of newly discovered fields to the national economy. The coal produced will be used directly in the thermal power plant.

1.2 Bibliographic Review

In 1965, coal exploration studies began in the region by the Mineral Research and Exploration Institute (MTA) in partnership with the Otto-Gold Consulting Bureau (Germany). MTA started drilling operations in 1974 with the acquisition of 1/10.000 and 1/25.000 scale geological maps. Feasibility studies were completed in 1978. The Turkish Coal Enterprises (TKİ) initiated operational activities between 1980 and 1990. Otto-Gold Consulting Bureau carried out prospection work in 1965, and reported that

there are coal-bearing layers in the Turgut Formation in Bağyaka, noting they are economically not important (Gold, 1965).

Abdülselamoğlu (1965) made comparisons between the formations outcropping around Yatağan and stated that the Neogene formations in this region consist of conglomerate, sandstone and lacustrine limestones being deposited in terrestrial facies.

Becker-Platen (1970) studied the general geology and biostratigraphy in the region including Denizli and Muğla. In that study, the Cenozoic sedimentary rocks were distinguished lithostratigraphically. He argued that the Oligocene debris characterising freshwater, unconformably overlies the Burdigalian-Helvetic marine sediments, which are again overlain by Upper Miocene-Lower Pliocene terrestrial sediments. The researcher further stated that these units consist of Turgut Formation of lacustrine and fluvial origin, Sekköy Formation with lacustrine sediments, Yatağan Formation of terrestrial-fluvial origin and Milet Formation of lacustrine character.

Yücelay (1970) conducted the geological study of the coal-bearing formations around Eskihisar and suggested drilling at 29 locations due to positive results in some of the previous drillings. The author argued that there was a total coal reserve of over 45 Mt in the area.

Kavuşan (1974) studied the lignite deposits around Muğla-Yatağan-Eskihisar villages within the scope of his master's thesis. He studied the stratigraphy of the area, compiled the geological map and carried out palynological studies. He pointed out that the coals have limnic and autochthonous origin and their average thickness is 10 m. He also determined the moisture, calorific value and ash yield of the coals.

Becker-Platen et al. (1977) determined the radiometric age of the Neogene in Türkiye based on the vertebrate fossil data they collected, and evaluated it litho- and biostratigraphically.

Yiğitel and Ünal (1977) conducted prospection work and made suggestions for lignite basins under the covered areas in W and SW Anatolia.

Nakoman (1978) carried out palynological and economic geological researches in a wide area including Muğla and its surroundings.

Leflef and Hakyemez (1979) prepared a report for the Geology Department of the General Directorate of MTA, focusing on the sedimentological and palaeogeographic study of the Tertiary basins around Muğla. They distinguished sediments and formations such as alluvial fans at different locations in the basin, meandering river deposits, lacustrine sediments, sediments formed in a coastal environment, mire and lignite formations between Oligocene and Quaternary.

Atalay (1980) studied the stratigraphy of the terrestrial Neogene around Yatağan. In this region, he distinguished two formations (named Eskihisar and Yatağan) consisting of stream and lake sediments. In his study, it was possible to establish a relationship between some important vertebrate fossil findings in Neogene sediments and fossils found in previously discovered beds in Türkiye, Asia and the Balkans.

Gökmen (1980) made a 1/10 000 scale map of the Yatağan Eskihisar region. Based on the findings of 170 exploration drillings, he estimated the reserves of the coalfield. In addition, chemical properties such as moisture, ash, volatile matter, fixed carbon, total sulphur and calorific value were determined in the coal samples studied.

Gökçen (1982) examined the Neogene sequence of Denizli and Muğla regions in terms of lithology, chronology and ostracod biostratigraphy and made the environmental and palaeogeographic interpretation of this region.

Kasap and Ünal (1987) determined the stratigraphic sequence in the Neogene Muğla lignite in Eskihisar Sector. From the bottom to the top, a lithostratigraphic succession of metamorphic schists, crystallized limestones, Turgut Formation, lignite seam, Sekköy Formation and slope debris are reported.

Bürküt (1988) studied the geochemical and thermal properties of some Tertiary coal formations in Western Anatolia. Elemental analysis showed that these coals are of lignite and sub-bituminous rank. Data on coking and briquetting properties of these coals, technical, trace element and ash analyses and thermogravimetric and differential thermal analyses were also presented.

Nakoman and İnaner (1990) calculated the lignite reserves, although of low calorific value, in southwestern Türkiye.

Ulusoy (1990) studied the slope stability in Yatağan Eskihisar Open Pit and examined the Neogene sedimentary rocks in this region. In addition to the sediments representing the Sekköy Formation, he distinguished a detritic facies at the basin margins and a transition zone between the Yatağan Formation and these facies.

Ünal (1991) calculated the lignite reserves in the Turgut Field of Yatağan. According to the author's calculations, nearly 136 Mt proven reserves were identified. In addition, the technical properties of the coal were also determined.

Atalay (1993) studied the health issues and economics of uranium in the coals in Yatağan. He conducted natural radiation measurements in nearby villages and stated that no harmful effects due to radiation were encountered in the area. He also proved that the radiation was within normal limits in the coal and the ash from Yatağan. He concluded that obtaining uranium from coal ash would be not economical due to various technical reasons.

İnaner (1994) conducted research on chemical properties, and made reserve calculations and feasibility analyses of lignite basins located in SW Anatolia.

Yamık et al. (1994) compared Yatağan and Kans-Acinsk lignite in Russia in terms of thermal resistance, radiation, paramagnetism and molecular structure.

Yamık et al. (1997) wrote an article on radiation measurements and evaluations of Yatağan lignite and the relevant ash.

Engin (1999) in his doctoral thesis, examining the geology and geochemistry of Yatağan lignite, determined the technical properties of Yatağan coal such as moisture, ash yield, volatile matter yield, upper and low calorific value, and evaluated inorganic components from an environmental, theoretical and economic perspective. He also determined the major element contents (C, H, O and S) and made a statistical evaluation by geochemical classification as a function of these compositions.

Querol et al. (1999) carried out a joint NATO and MTA project on the geology and quality of the coals in the Muğla Basin.

Karayiğit et al. (2000) studied major and trace element concentrations on feedstock samples taken from several coal-fired power plants in Türkiye (Çayırhan, Seyitömer, Tuncbilek, Orhaneli, Soma, Yatağan, Yenikoy, Elbistan, Kangal and Çatalağzı). They compared coal from these 10 locations presenting their mineral distribution, moisture, ash yield, total sulphur content. They proved that the contents of As, Co, Cu, Ga, Mn, Li, Sc, Sn, Ta and Tl and some REE are higher in some coals from these areas in comparison to most of the world coals.

Tuncalı et al. (2002) evaluated the coal quality, trace element distributions, etc. of all sites with samples taken from Tertiary coal fields in Türkiye.

GELİ (2005) (Southern Aegean Lignite Business Administration Directorate of TKI) reported briefly the geology, hydrogeology and slope stability, old excavations, drilling, production and stripping works and operating systems, especially of open pit fields.

Aşar (2006) determined the distributions of germanium, gallium, indium, selenium and tellurium in lignite deposits around Muğla-Milas. She stated that the trace element contents of the coal analyses on dry basis were generally within the world averages and only W-Mo-Ta and Co, Ni and U-Th values caught and exceeded the world averages at the upper limit in some samples.

Toprak (2009) studied the chemical, petrographical, thermal and structural properties of four coal samples from Türkiye (Çan, Saray, Tunçbilek, Yatağan). Ultimate (C, H, O, N, S) and proximate (volatile matter, fixed carbon, ash yield) analyses were completed. Petrographic analyses were discussed.

Tuncalı et al. (2010) explained the geology, chemical properties, and reserves of the lignite deposits in Türkiye in detail.

Büçkün (2013) studied the coal quality, mineralogical and maceral compositions of the Miocene Hüsamlar lignite in the Muğla-Milas Basin.

Oskay (2013) studied general characteristics and importance of the energy needs of Türkiye's coal deposits. He stated that the total coal reserves of the country reached 13 Gt and low rank coals (i.e., lignite and sub-bituminous) are dominant. He pointed out that the most important coal fields are Tertiary, especially Neogene coals, which are the most suitable coals for combustion in thermal power plants due to their high total reserves despite their high ash yields and low calorific values.

Özer et al. (2013) described the palynoflora of Kultak, Hüsamlar and Karacaağaç in the Muğla-Milas Basin. They found that thermophilous plants (*Engelhardtia*, Sapotaceae, Cyrillaceae, *Avicennia*, *Palmae* etc.) were dominant. They stated that the palaeoclimatic conditions in Europe and Türkiye were humid and warm subtropical in the Middle Burdigalian-Langian time interval.

Hoş-Çebi (2016) investigated the organic geochemical properties, depositional environment and palaeoclimatic conditions of the coal of the Ekizköy Field in the southeast of Milas district of Muğla province.

Bouchal et al. (2017), by analysing a palynological section of middle Miocene sediments from Eskihisar (Southwestern Anatolia), determined the biogeographic relationships of the palynoflora and assessed the palaeoenvironment. They analysed the algal, spore, and pollen species and concluded that two pollen zones reflect different stages of basin development. Based on the spores and pollen identified at the Tınaz sequence in the Yatağan sub-basin, Bouchal et al. (2017) described the studied region as a zone dominated by woody pollen, a transition zone with an increase in herbaceous pollen, and a zone with a high amount of herbaceous pollen.

Şengüler et al. (2017) determined the stratigraphical structure of the Neogene sequence in the light of data obtained from the coal exploration and research drillings carried out in the region around Aydın, Muğla and Denizli within the scope of the project carried out by the Energy Raw Materials Survey and Exploration Department of the General Directorate of MTA.

Yakupoğlu et al. (2017) studied the sedimentological and petrographic properties of sedimentary rocks in the Yatağan sub-basin. They classified and evaluated the formation environments of the rocks and determined that the sediments had formed in a basin characterised by alternating periods of river and lake activity.

Erecek (2020) carried out a petrographic and precise analytical preliminary study on samples from the B-22 borehole in the Muğla-Yatağan coal field. She (2024) evaluated mineralogical and geochemical data based on organic petrography, micro-Raman spectroscopy and X-Ray diffraction analyses contributing to the understanding of the molecular composition and structure of lignite.

Hacımustafaoğlu et al. (2023) measured reflectances of various huminite macerals in the lignite samples of the current study. The study concluded that the average reflectance values of ulminite B, corpohuminite and gelinite are quite similar, while values for ulminite A are substantially lower, noting a strong positive correlation between the average corpohuminite and gelinite values at $\alpha = 0.05$ significance level ($R^2 = 0.94$). It was suggested that it could be considered as an alternative measurement approach to be used for samples with low amounts of Ulminite B, emphasising, however, the need for further work on larger data sets from coals of various grades.

The latest contribution to the above bibliography is made by Hacımustafaoğlu et al. (2025). In the authors' work, the coal petrographical, mineralogical and geochemical evaluations of the findings in this current Ph.D. thesis are summarized and preliminary discussed.

1.3 The Study Area

The study area hosts a newly discovered coal field near the Yatağan Thermal Power Plant in the southwest of the Yatağan District of Muğla Province (Fig. 1.4). This field is located 28 km away from Muğla, in the northwest of the Bayır Sector and in the southeast of the Turgut Sector, near the Yatağan Thermal Power Plant. The Muğla-Yatağan lignite field is located in the Denizli Sheet on the 1/500.000 scale geological map of Türkiye and within the Aydın N20-a3, a4 sheets on the 1/25.000 scale map.

The Muğla Basin comprises the Yatağan and the Milas coalfields, based on their geomorphological characteristics (Fig. 1.4). Both sub-basins strike in a NW-SE direction. The Yatağan coal field in the east, where the study area is located, covers an area of about 132 km^2.

The Milas coalfield at the western part hosts the Ekizköy, Sekköy, Çakıralan, Hüsamlar and Alatepe coal deposits, whereas the Yatağan coal field located at the eastern part, hosts the Bayır, Tınaz, Bağyaka, Eskihisar, and Turgut coal deposits (Fig. 1.4). Open-pit mines operate in Eskihisar. The coals of Bağyaka, Tınaz, Sekköy, Ekizköy, Hüsamlar and Çakıralan coal fields and the Alatepe field are extracted by both open pit and underground mining methods.

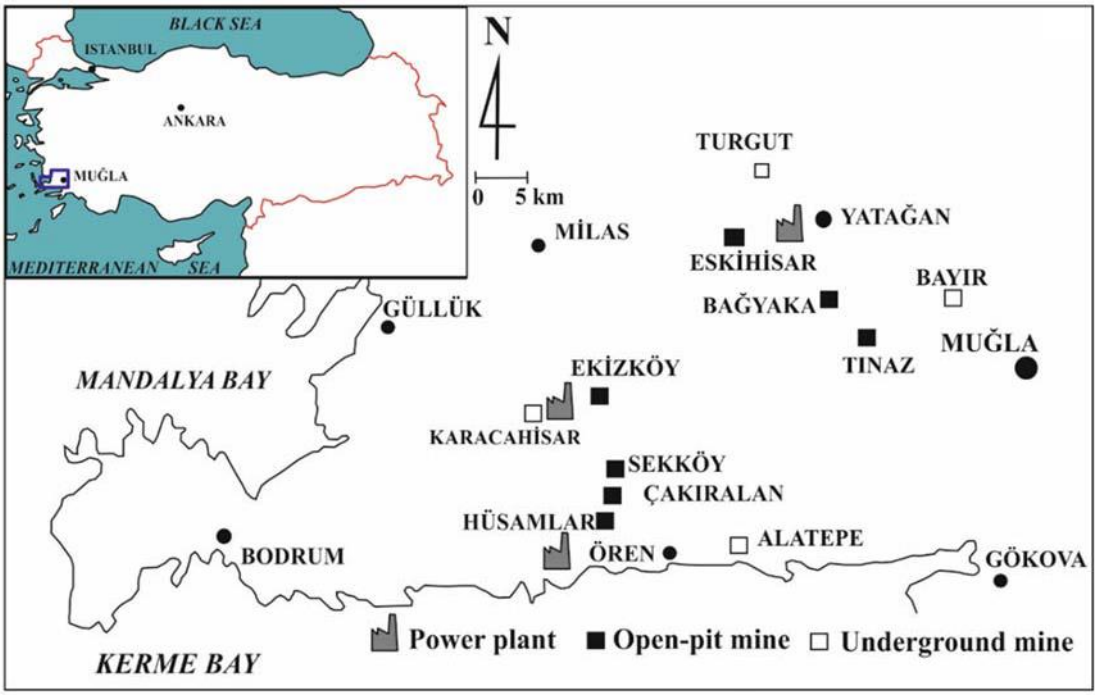

Figure 1.4 Major lignite fields in the Muğla Basin (İnaner et al., 2008).

The study area and its surroundings are influenced by the Mediterranean climate, where the summers are hot and dry, and the winters are mild and rainy. Although rainfall rates vary from year to year, high rainfall occurs during November-December and February-March. The coldest months are January and February. The hottest months are July and August. December receives the most rainfall and September the least. Due to the influence of climate and soil structure, the natural plant community

is quite rich in diversity. The vegetation is typical for the Mediterranean climate. The temperature effect of the summer months and the mild effect of the winter months have positively affected the development of vegetation (Algan, 2023).

Because drought is so pronounced, maquis vegetation being characteristic of the Mediterranean climate, prevails. Since the temperature is lower at higher altitudes, these areas are covered with coniferous forests. Herbaceous plants such as sage and thyme, are abundant in areas with calcareous soil hosting large shrub communities. The vegetation in the study area consists of pine trees (red, rock and radiata), juniper, cedar and oak, which together form forests. Other vegetation includes olive, plane and poplar trees, as well as thyme and blackberries (Algan, 2023).

The main elements of livelihood in the region consist of marble quarrying, coal mining, energy generation, agriculture, forestry, animal husbandry and transport, the latter as the region serves as a bridge to some touristic districts.

1.4 Aim of the Study

Coal in the Muğla Yatağan Lignite Basin, located in SW Anatolia, is operated by the private sector through open and underground mining methods and is mostly used in thermal power plants. Due to the decrease in coal reserves suitable for open-pit mining in the Muğla Basin, coal exploration and drilling activities are ongoing.

From the last drilling campaign (2019) conducted by the Yatağan Mine Directorate, coal cores taken from three boreholes (I-18, I-23, and I-25), were allowed to be sampled and examined for the current study. The objectives of the study are to examine the samples for their mineralogical, petrographical and geochemical compositions with the aim to reconstruct the palaeoenvironmental conditions and factors, which have affected the coal deposit formation.

Palaeoenvironmental conditions affecting coal formation will be revealed in the light of the obtained data. This improves the understanding of the coal formation in the Muğla Basin and in other basins in Türkiye.

CHAPTER TWO
GEOLOGICAL SETTING

2.1 Tectonic Development of Muğla Basin

The last tectonic deformation phase in Türkiye was the collision of the Anatolian and Arabian Plates in the Middle Miocene (Şengör, 1979; Şengör et al., 1985). The subsequent "neotectonic" phase, which is still ongoing, formed the North and East Anatolian Faults.

The Anatolian Plate is moving westwards along these two strike-slip faults, which formed as a result of its collision with the Arabian Plate. Under this influence, the Central Anatolian plain, which developed in the eastern part of the Anatolian Plate, is also moving westward. These wide plains were formed from thick Neogene sediments deposited under lacustrine-continental conditions. The Aegean graben system in Western Anatolia developed in the same time period, and terrestrial sedimentary basins were formed within the approximately E-W trending graben system (Fig. 2.1).

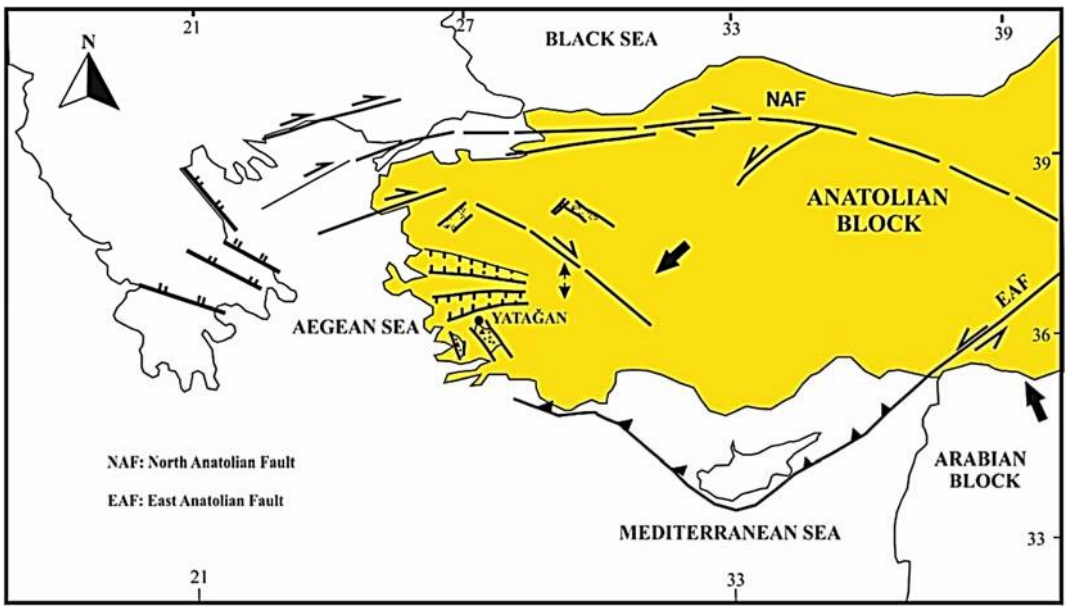

Figure 2.1 Present tectonic setting of the Aegean extensional province and related graben systems in Western Anatolia (from Yağmurlu, 2000).

The Muğla Basin is very complex in terms of fault tectonics due to its graben system. The tectonic activity during the Miocene period has significantly affected the formation of the basin, in which the study area is located. No significant folding has occurred in the basin, but many fault systems have developed. Faults are distinguished in two groups: pre-Neogene and post-Neogene faults. Pre-Neogene faults have caused the development of the depressions filled in with Neogene sediments (Fig. 2.1). The boundaries of the metamorphic basement rocks surrounding the basin are considered as the graben boundaries.

An angular unconformity is present between the metamorphic basement rocks and the sedimentary rocks of Cenozoic age in the study area. The borders of the basement rocks surrounding the basin are covered by young Neogene sediments and slope debris, which make them difficult to see clearly (Fig. 2.2).

With few exceptions, the faults affecting the Neogene units in the study area are NW-SE trending dip-slip normal (gravity) faults. Faults within the Neogene series are difficult to trace and follow. The sections where the faults in the Neogene can be best observed, are the fault mirrors in the open-pit coal fields located in the west of the study area (Engin, 1999).

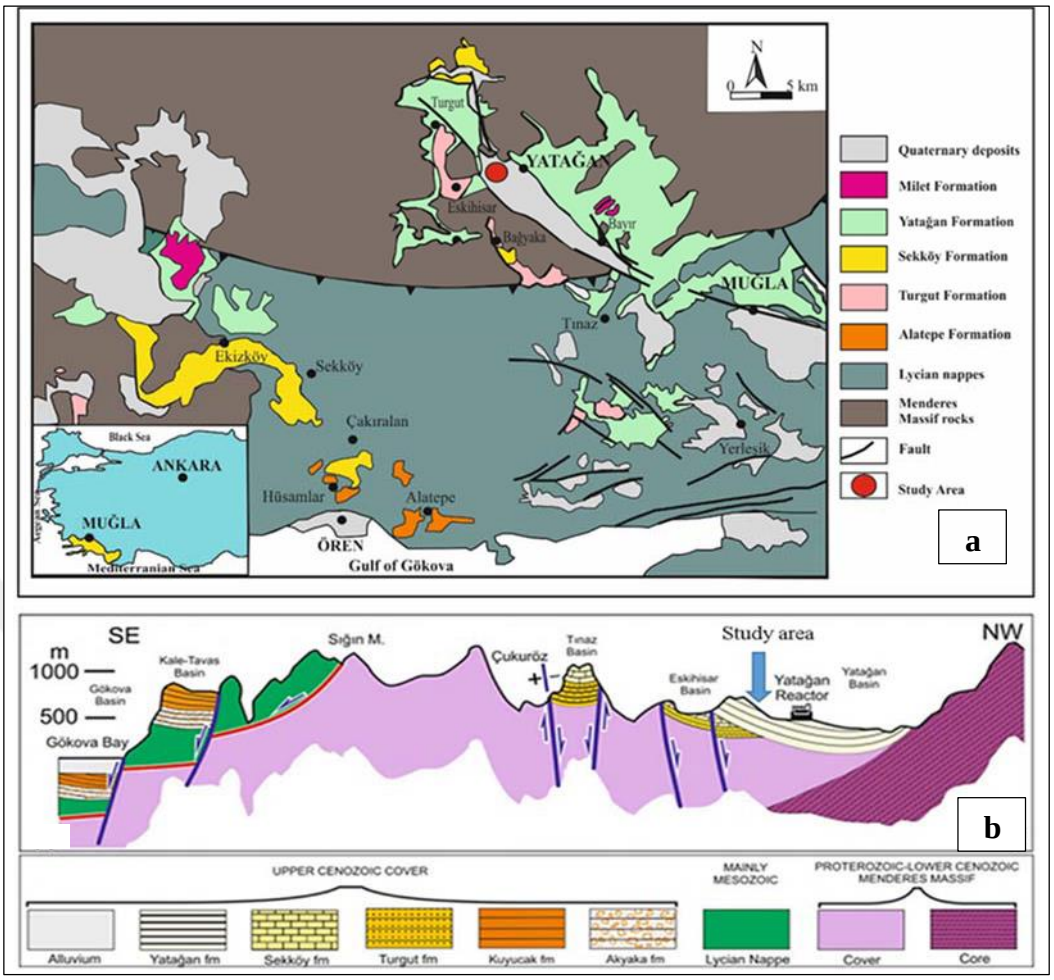

Figure 2.2(a) Geological map of the Miocene Muğla Basin, SW Türkiye (after Querol et al., 1999), and Geological cross-section of the Muğla and Gökova Gulf region. (b) Cross-section of the Muğla Basin (vertical scale is exaggerated), (from Gürer et al., 2013).

The basement of the Muğla Basin is formed by gneiss, schist and marble of the Menderes Massif and the carbonate rocks of the Lycian Nappes. To the north, it is made of metamorphic rocks (schist, gneiss, amphibolite, and marble). One of the two younger series in the basin, the marine Alatepe Unit, that belongs to the Kale-Tavas foredeep, is found in the south of the study area; it represents the southward-moving Lycian Nappes (Göktaş, 1982). The second one unconformably overlying the Alatepe Unit, is in the north. Gökmen (1975), Yiğitel (1979), Atalay (1980), and Göktaş (1982) have previously proposed a four-fold stratigraphy in the region for this second series, made from bottom to top (Fig. 2.3): the Turgut Unit (mainly fluvial-granied sediments), Sekköy Unit (lacustrine marlstone), Yatağan Unit (alluvial coarse clastics) and Milet Unit (mainly freshwater limestones) (Büçkün, 2013).

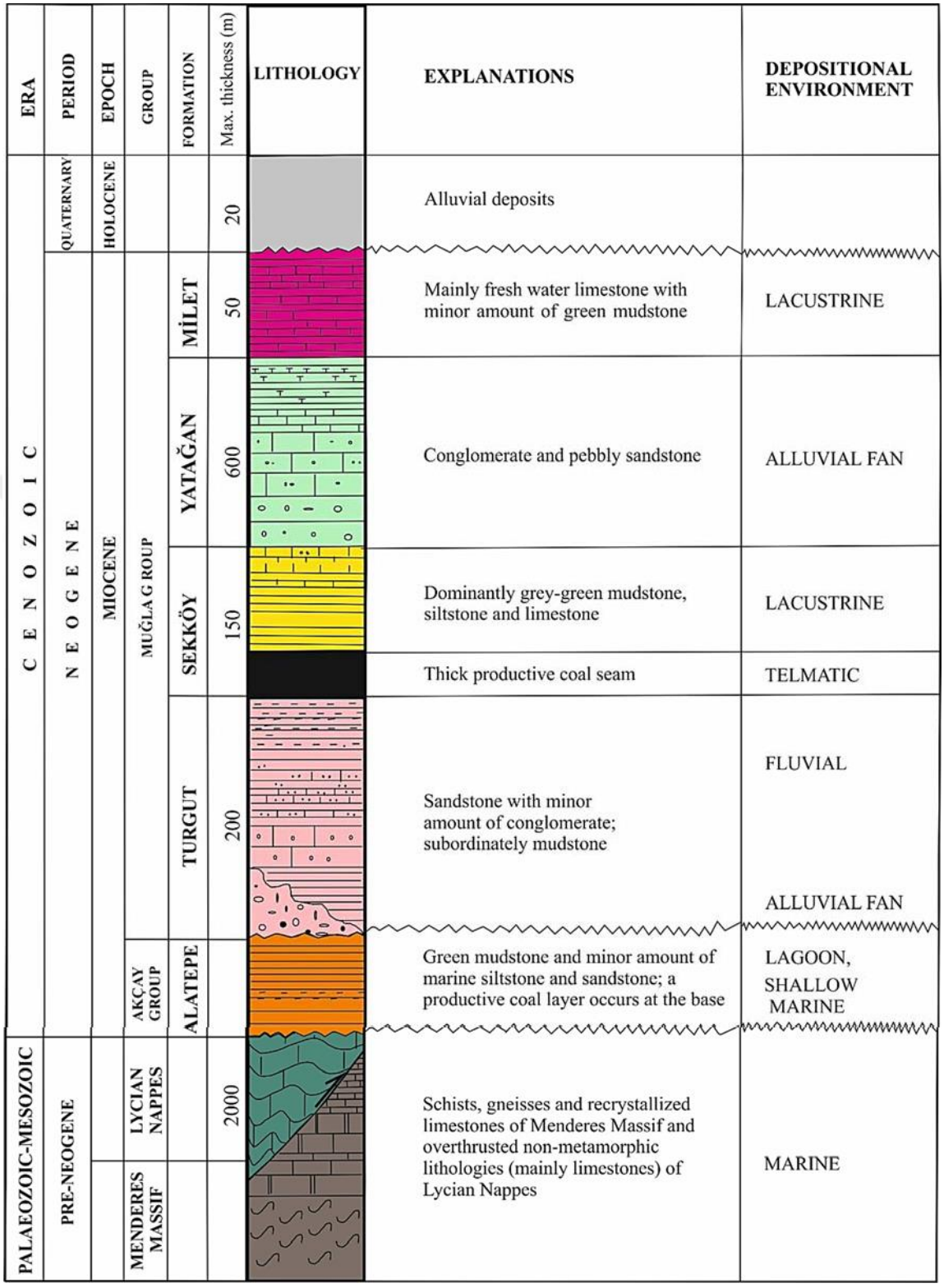

Figure 2.3 Lithostratigraphic column of Muğla Basin (modified from Sun and Karaca, 2000).

2.2 The Yatağan Area

The Yatağan sub-basin is located in the east of the Muğla Basin. The study area is a newly discovered coalfield between Şahinler and Bozüyük, in the southwest of Yatağan district of Muğla Province. This field is located 28 km away from Muğla, in the northwest of the Bayır Sector and in the southeast of the Turgut Sector, near the Yatağan Thermal Power Plant (Fig. 2.4).

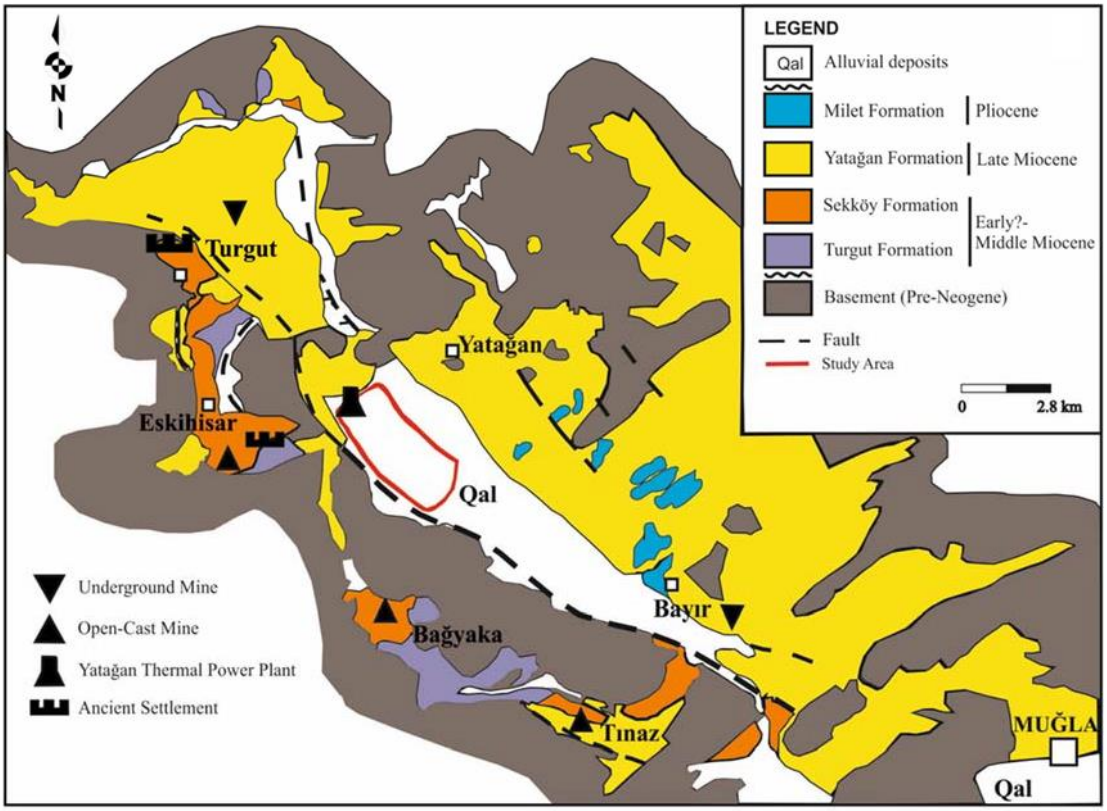

Figure 2.4 Geological map of the Yatağan Basin (Ünal, 1989; Bulut et al., 2001).

2.2.1 Pre-Neogene Rocks

In the Yatağan region, the Pre-Neogene formations represent the basement, consisting of Palaeozoic gneisses and schists, along with Mesozoic marbles. The thickness of the Triassic-Upper Cretaceous marble reaches up to 2000 m (Fig. 2.5).

2.2.2 Neogene Formations

Neogene is represented by Turgut, Sekköy and Yatağan formations, which unconformably overlay the Palaeozoic and Mesozoic basement rocks.

2.2.2.1 Turgut Formation

Among the Neogene deposits outcropping in the region, the lowest strata constitute the Turgut Formation, which is around 200 m in thickness. The sedimentary units underlying the main productive coal seam at the study site consist of conglomerate, claystone, siltstone, sandstone and gravels. Where the basement is close to the depositional area, the formation consists of gravels, boulders, and abundant micaceous sand with variable scale crossbedding, probably originating from unidirectional fluvial currents (Querol et al., 1999).

2.2.2.2 Sekköy Formation

The Sekköy Formation is conformable with the Late Miocene Yatağan Formation above and the Early-Middle Miocene aged Turgut Formation beneath; coal seams are included in the lower segment of the formation (Yiğitel, 1979). It overlies lignite layers ~20 m thick and is represented by a stack of grayish and olive green, compact marlstone at the bottom and a laminated marlstone, thin limestone and claystone succession towards the top. This formation presents detrital facies at the basin margins with limestone and conglomerate and transitional facies with a sequence of poorly consolidated claystone and siltstone interbedded with the Yatağan Formation (Querol et al., 1999). The depositional environment of the Sekköy Formation was lacustrine (Atalay, 1980).

2.2.2.3 Yatağan Formation

Yatağan Formation is Upper Miocene in age and its dominant lithology is reddish brown, medium- and coarse-grained sandstone with an approximately 600 m thickness. The Sekköy Formation underlies the Yatağan Formation and the Milet Formation, and conformably overlies the Yatağan Formation (Fig. 2.5). The upper

segment is generally represented by coarse-grained alluvial deposits and the lower segment by yellow sandstone and siltstone gradually covering the marlstone of the Sekkoy Formation (Querol et al., 1999). Mammalian fossils are abundant in the Yatağan Formation (Querol et al., 1999).

2.2.2.4 Milet Formation

The lower boundary of the Milet Formation is comformable with the underlying Yatağan Formation. The upper boundary is unconformable with the overlying Quaternary deposits, followed by a 1-2 m thick siltstone with lignite interlayers at the base (Querol et al., 1999). The formation thickness is approximately 50 m. Atalay (1980) found gastropod and mammalian fossils in the limestones and stated that the formation was a result of the uplift of lake environments.

2.2.3 Quaternary Formations

Quaternary deposits in the area consist of sand, clay and poorly graded pebble and cover the Neogene sediments.

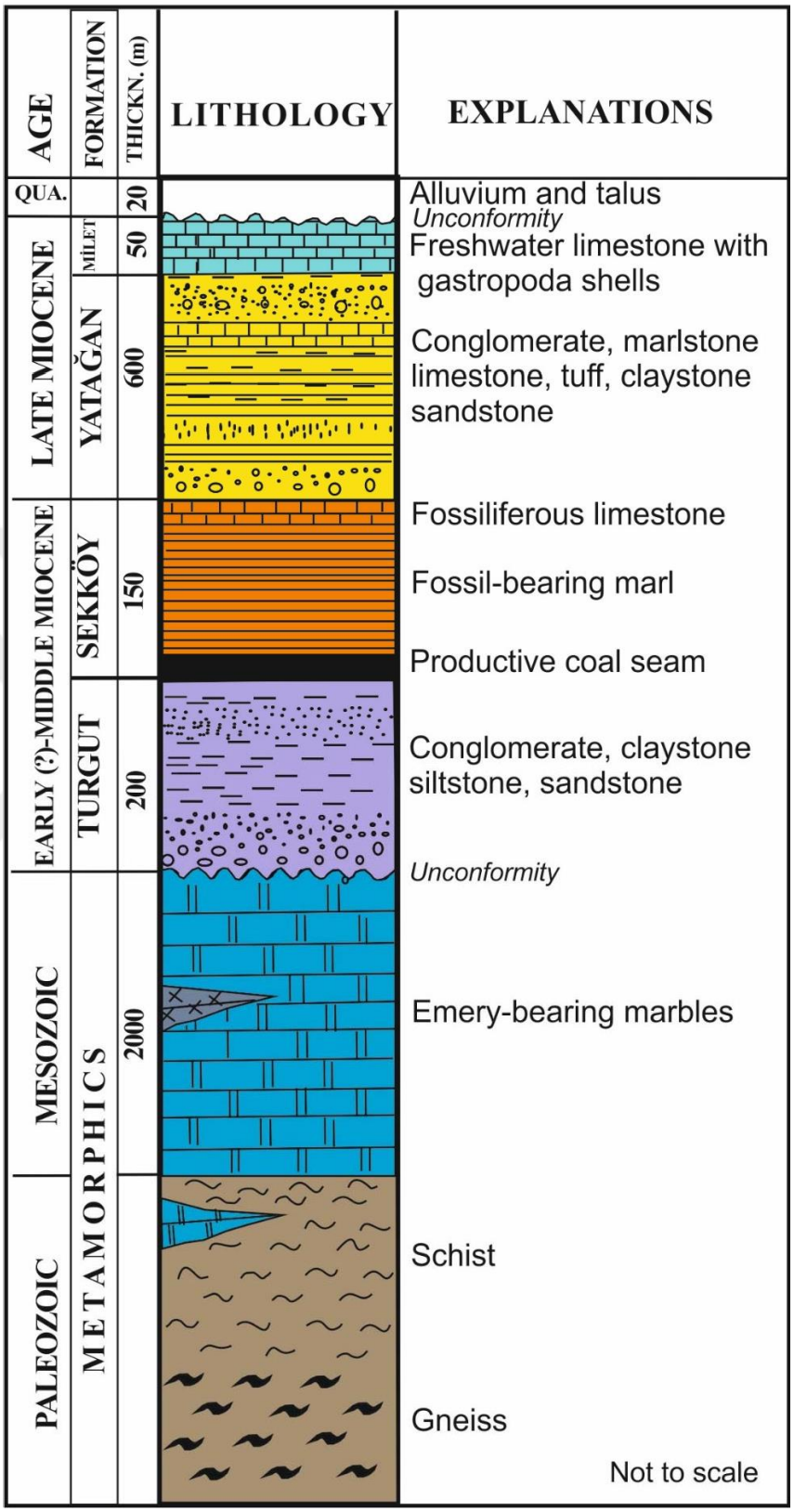

Figure 2.5 Generalized stratigraphic column of Muğla-Yatağan Basin (from Gürsoy et al., 1993, and İnaner, 1994).

CHAPTER THREE
MATERIALS AND METHODS

The study was carried out in two phases: field and laboratory. The flow chart of the work is given in Figure 3.1.

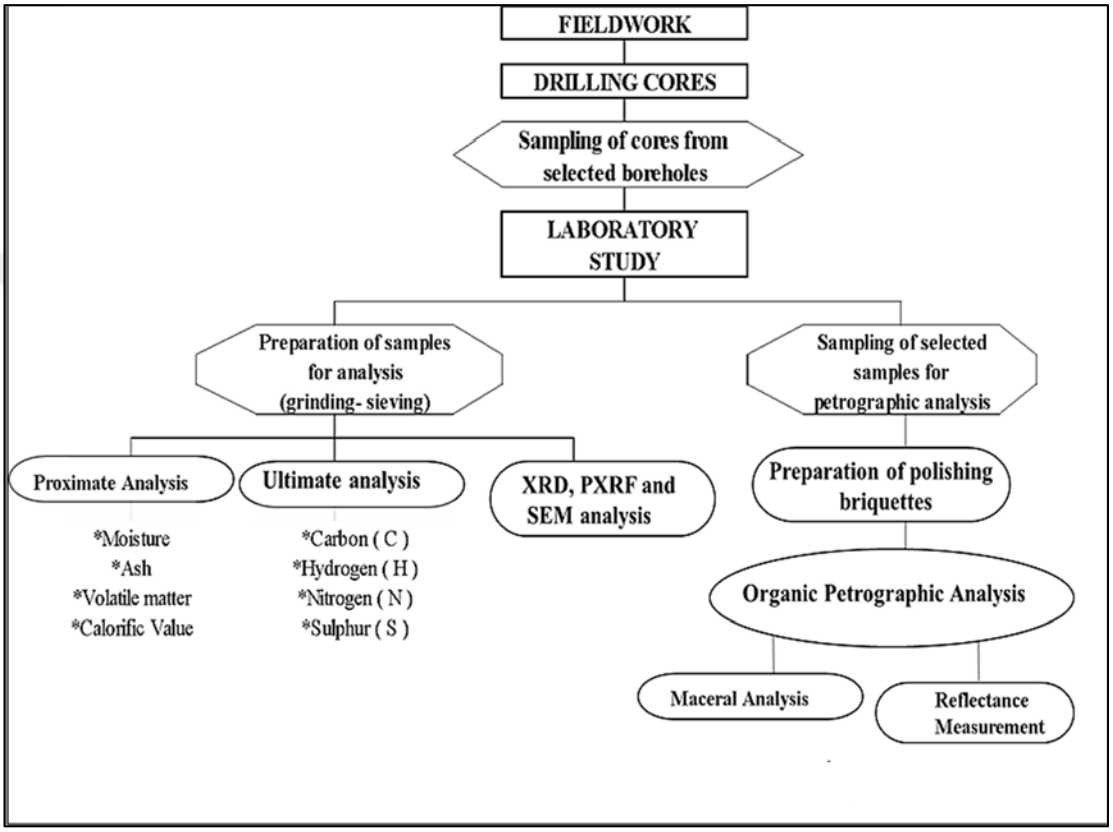

Figure 3.1 Flowchart of the methodology applied in the study on Yatağan coal samples.

3.1 Field Work

During the fieldwork, the existing geological map was verified, and macroscopic observations on the outcropping formations were made. Thirty-nine lignite core samples were also taken from the most recent drillings (I-18, I-23, and I-25) near the Yatağan Thermal Power Plant to represent the study area. As part of these studies, the stratigraphic position of the coal seam was determined in some of the exploration boreholes drilled by the Yatağan Thermal Power Plant Mining Directorate (Fig. 3.2, App. I). Coal samples were collected from drilling cores, taking into account their depth. In total, 19 samples were taken from core #I-18 where approximately 18.8 m of coal was cut; three of the samples were inorganic. From core #I-23, 11 samples were taken, in which approximately 11 m of coal seam was cut; one of these samples was inorganic. And finally, 9 samples were obtained from core #I-25, out of which 3 were inorganic. The coal thickness at the I-25 site is about 14 m.

Finally, as part of the field study, some of the boreholes drilled by the Yatağan Thermal Power Plant Mining Directorate were examined on-site, and samples were collected for laboratory analysis.

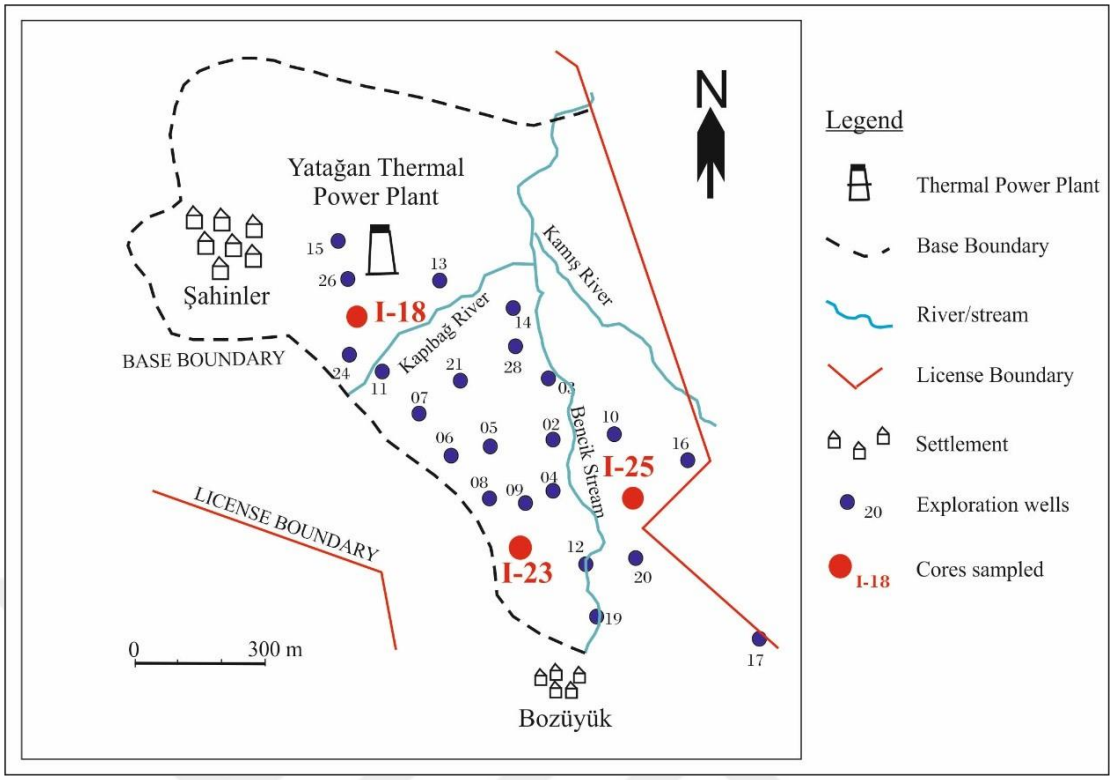

Figure 3.2 Sketch map of the drilling sites within the Yatağan Thermal Energy Mining Directorate license area.

The samples were properly prepared for proximate and petrographic analyses. Each sample was milled with an agate mortar and passed through the 1 mm aperture sieve. Bed moisture could not be determined because the samples were stored in the core boxes for a long time. To remove the residual moisture, the samples were dried for 4 hours at 105°C before the analyses. Afterwards, the samples were placed in a desiccator. Bed moisture along volatile matter yield, sulphur content and calorific values were kindly provided by the Mining Directorate of the Yatağan Thermal Power Plant. As the original sampling scheme of the company was different from that in the current study, in ten samples, the ash and the volatile matter yields were determined at Dokuz Eylül University, Department of Geological Engineering. Ultimate analysis was conducted on all (28) the bulk coal samples, using a Carlo Erba EAGER 200 C, H, N, S Automatic Analyser calibrated against the AgroMAT CP-1 standard (certified reference material, SCP Science). The analysis was performed at the Laboratory of Instrumental Analysis of School of Natural Sciences, University of Patras.

For coal petrographic analyses, polished blocks of coal samples were prepared after grinding to Ø < 1 mm, in accordance with the ISO 7404-2 (2009) standard. They were prepared in the Organic Petrography Laboratory of Dokuz Eylül University, Department of Geological Engineering. Polishing of the sections was performed using a Struers LaboForce-50 equipment (App. II). The samples are then examined under a LEICA DM 4500 P coal petrography microscope installed at the Organic Petrography Laboratory, Department of Geological Engineering, Dokuz Eylül University (App. II).

The maceral analysis was performed in oil immersion, under incident white light and blue-light excitation at maceral-group/sub-group level (ISO 7404-3, 2009). The microscope is equipped with the Hilgers FOSSIL MOT software. The maceral nomenclature applied is this of ICCP System 1994 (ICCP, 1998; Sýkorová et al., 2005; Pickel et al., 2017). Reflectance measurements were mainly performed according to ISO 7404-5 (2009) on Ulminite B macerals. Additional reflectance measurements were also performed on Ulminite A, Gelinite and Corpohuminite for inquiry of an alternative complementary method for samples bearing low levels of Ulminite B. For the maceral analysis, a minimum of at least 500 points (on an area of ~4 cm²) in each sample were determined. Reflectance was measured on a minimum of 150 points for each sample.

X-ray diffraction (XRD) analysis was conducted at the X-Ray Laboratory of the Department of Geological Engineering, Dokuz Eylül University, using a Rigaku MiniFlex 600 diffractometer (App. II). The XRD measurements were performed on randomly oriented grains using CuKα radiation (k=1.542 Å). The analytical conditions were set as 33 kV and 15 mA, scanning 2-65° of 2θ with a step size of 2°/min. The crystalline phase identification was carried out using the PDXL2 software package (Rigaku). Two out of the seven inorganic samples (#12 and #29) were subjected to clay separation by centrifugation, separation in three phases (dried under ambient conditions, saturated by holding in a desiccator containing ethylene glycol at 60ºC and heated in an oven at 550ºC for 2 hours) and XRD analysis was conducted in the range 4-40° 2θ. The clay mineral content of each sample was semi-quantitatively evaluated based on the patterns obtained.

Additionally, selected 29 dried coal samples were powdered (∅ <50 μm) and subjected to XRD analysis *via* a Bruker D8 X-ray diffractometer outfitted with a LynxEye® detector, which is installed at the Department of Geology, University of Patras. The scanning step was 0.015° and the time step was 1 s. EVA® and Rietveld-based Topas® software were employed for the qualitative and semi-quantitative determination of the phases, respectively. The technique introduced by Siavalas et al. (2009) was applied for the semi-quantitative determination. As features of the poorly crystalline minerals generally differ from the ones exemplified in the database, the calculated weight percentages may only be deemed as semi-quantitative values.

Selected polished blocks from four coal samples (I-18/9, I-23/48, I-25/4 and I-25/6) from three drill holes were examined under the SEM-EDX microscope with FEI QUANTA 250 FEG-EDX Detector (Oxford Aztec) at Izmir Institute of Technology, Integrated Research Centers (IZTECH-IRC) to identify possible accessory mineral phases and to better understand their elemental composition (App. II).

A set of XRF analyses were carried out at Torbalı Vocational School of the Dokuz Eylül University, using an Olympus Delta Premium DP-6000 portable X-ray fluorescence (PXRF) device with a 4W X-ray tube, 156.5 hrs (App. II). Operating conditions were set to 22 kV and 51 mA. Analyses were performed on samples taken from the cores. Measurements were taken by placing the instrument directly on the surface of each sample. Care has been taken to ensure that there is no visible residue on the surface of the samples. Three measurements have been made on each sample, and the mean value was calculated.

Thin sections from seven inorganic samples (I-18/12, I-18/29, I-18/32, I-18/50, I-25/1, I-25/8 and I-25/9) taken from the roof, intercalation and floor of the coal seam, were examined under an Olympus Bx41TF optical microscope at the DEU Torbalı Vocational School (App. II).

CHAPTER FOUR
RESULTS

4.1 Lithological Features

In borehole I-18, an 18.8-m-thick coal seam is cored between 535 m and 553.8 m beneath the surface, intersected with inorganic layers up to 1 m thick (Fig. 4.1). The coal seam overlays clayey-silty limestone and underlies marlstone. In borehole I-23, samples were taken from the coal seam between 291.3 m and 302.3 m (Fig. 4.2). The 11-m-long coal seam displays intercalations of gray claystone and siltstone at the bottom and marlstone at the top. In borehole I-25, samples were taken from a 14-m-long interlayered coal seam at depths between 473.9 m and 487.9 m (Fig. 4.3). Gray claystone and limestone intercalate at the floor and marlstone at the roof of the seam.

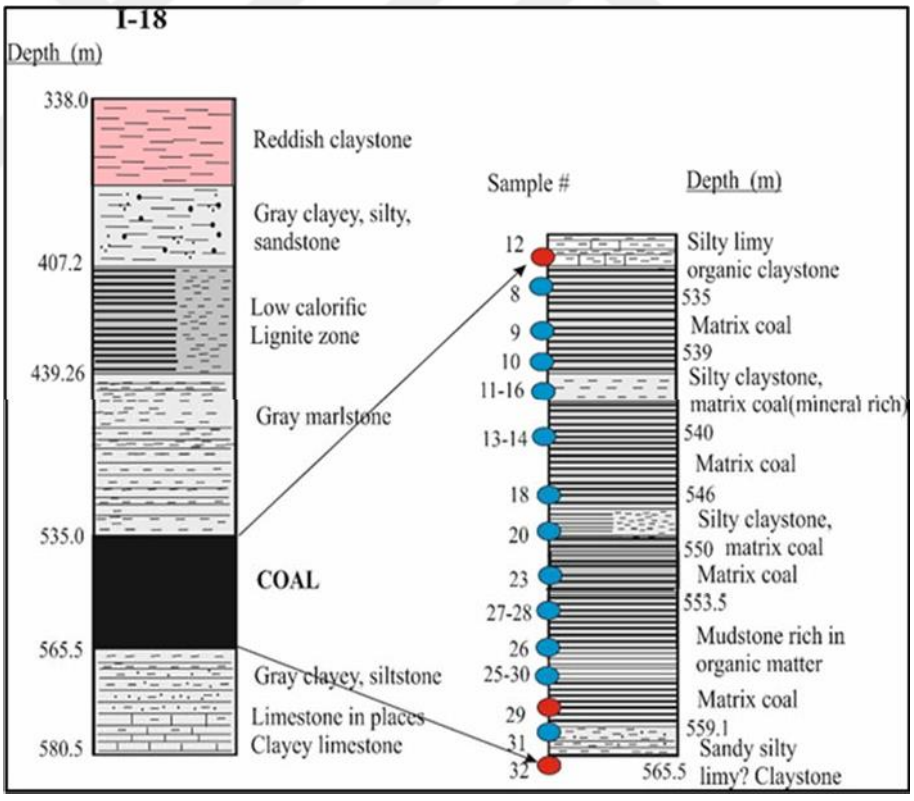

Figure 4.1 The I-18 borehole profile (the red circles correspond to inorganic, the blue ones to coal samples).

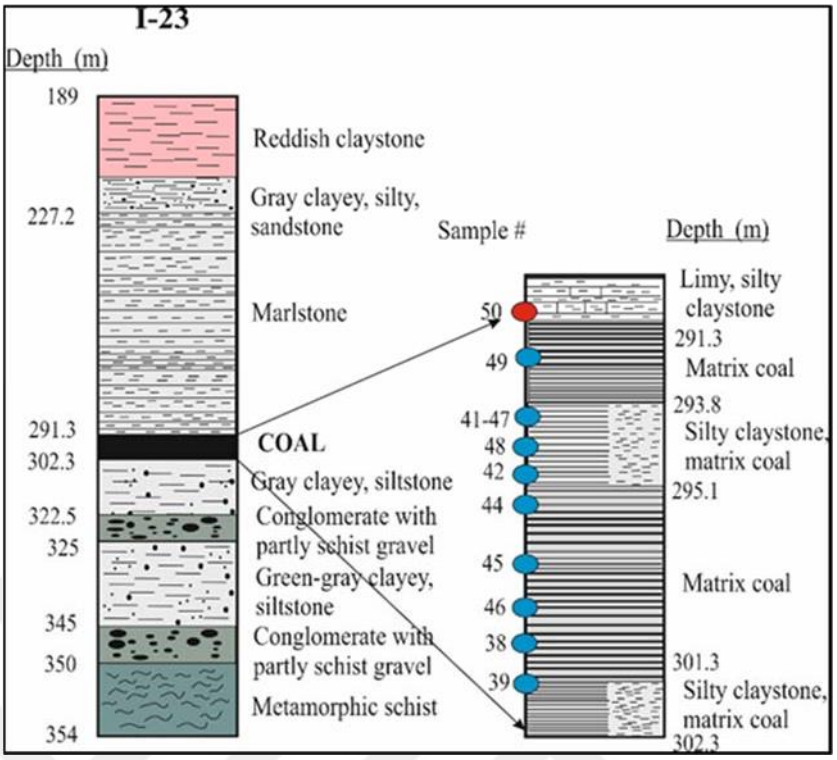

Figure 4.2 The I-23 borehole profile (the red circles correspond to inorganic, the blue ones to coal samples).

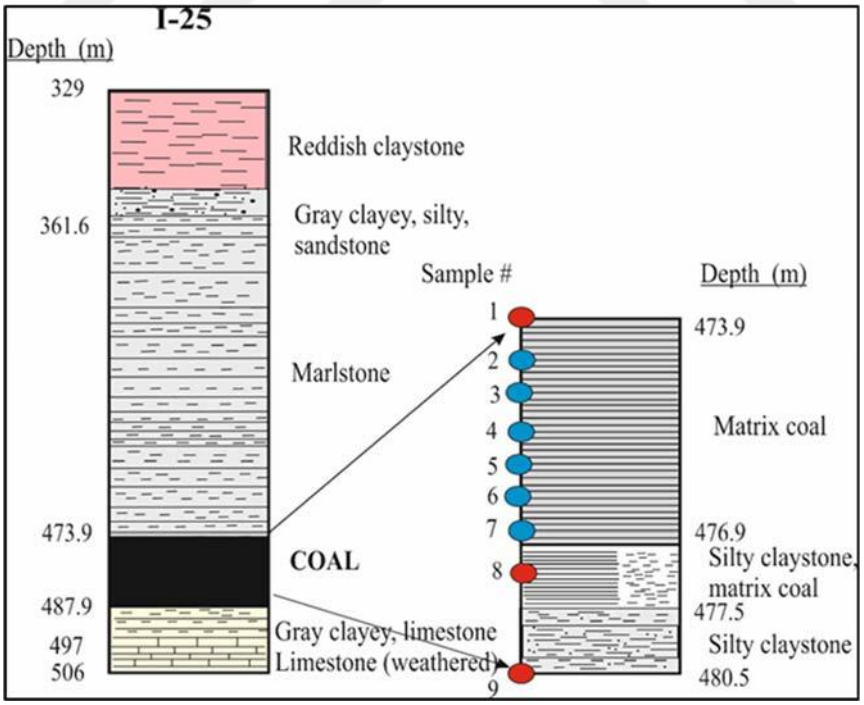

Figure 4.3 The I-25 borehole profile (the red circles correspond to inorganic, the blue ones to coal samples).

4.2 Laboratory Determinations

4.2.1 Proximate Analysis

The results of the proximate analysis provided by the company for the studied cores (I-18, I-23, I-25) are presented in Table 4.1.

Table 4. 1The results of the proximate analysis of the I-18, I-23 and I-25 samples obtained from Yatağan Thermic Energy Production Inc. (VM: volatile matter; Cfix: fixed carbon; CV: calorific value; db: dry basis; daf: dry, ash-free basis; ar: as-received basis; maf: moist, ash-free basis).

Core	Depth beneath surface (m)	Moisture (%, ar)	Ash (%, db)	VM (%, daf)	Cfix (%, daf)	Sulphur (%, ar)	CV (MJ/kg, maf)
I-18	535-539	35.50	33.16	61.73	38.27	2.64	12.38
	539-540	27.40	60.96	73.01	26.99	1.24	6.05
	540-546	35.76	33.86	59.28	40.72	2.62	12.66
	547-550	35.75	31.44	55.41	44.59	2.35	13.10
	550-553.8	36.25	25.71	57.50	42.50	2.58	14.20
I-23	291.3-293.8	35.95	30.88	62.30	37.70	2.45	12.93
	293.8-295.1	27.40	57.81	71.79	28.21	0.00	6.82
	295.1-301.3	36.70	29.70	58.38	41.62	2.85	15.44
	301.3-302.3	28.02	41.04	50.78	49.22	2.30	9.20
I-25	473.9-477.4	33.37	31.67				12.23
	477.8-479.25	34.10	42.91				7.44

The I-18 samples display bed moisture ranging between 35.50 and 36.25% (ar, as received basis), ash yield between 25.71 and 33.86% (db, on dry basis), volatile matter yield between 55.41 and 61.73% (daf, dry, ash-free basis), sulphur content between 2.35 and 2.64% (ar) and gross calorific value between 12.38 and 14.20 MJ/kg (maf, moist, ash-free basis). In the I-23 samples, moisture ranges between 28.02 and 36.70% (ar), ash yield between 29.70 and 41.04% (db), volatile matter yield between 50.78 and 62.30% (daf), sulphur content up to 2.85% (ar) and gross calorific value between 9.20 and 15.44 MJ/kg (maf). The I-25 samples have moisture ranging between 33.37 and 34.10%, ash yield between 31.67 and 42.91% (db), and gross calorific value between 7.44 and 12.23 MJ/kg (maf).

Overall, the Yatağan coal displays bed moisture between 28.02 and 36.70%, and ash yield between 25.71 and 42.91% (db). The sulphur content varies from 2.30 to 2.85% (ar), and the volatile matter yield between 50.78 and 62.30% (daf). The gross calorific values ranges from 7.44-15.44 MJ/kg (maf). The samples obtained at depths between 539 and 540 m at I-18 drilling site and between 293.8 m and 295.1 m at I-23 (Table 4.1, Fig. 4.1) display ash values >50% (db); thus, they are considered as partings. Taking into account the analytical results of all the samples analysed by the company, the average total moisture of the Yatağan coal is 34.60%; the ash yield 33.37% (db); the volatile matter yield 57.91% (daf); the fixed carbon yield 42.09% (daf); the total sulphur content 2.54% (ar); and the calorific value 12.18 MJ/kg (maf).

In the current study, bed moisture could not be determined due to the long storage period of the samples. The results of the proximate analysis of 10 samples selected in this study are given in Table 4.2.

Table 4.2 The results of the proximate analysis on the Yatağan coal samples (VM: volatile matter; Cfix: fixed carbon; CV: calorific value; db: dry basis; daf: dry, ash-free basis).

Core	Sample #	Ash (%, db)	VM (%, daf)	Cfix (%, daf)
I-18	8	8.63	51.78	48.22
	13	18.27	48.51	51.49
	16	18.99	49.55	50.45
I-23	38	49.98	38.94	61.06
	44	23.09	52.50	47.50
	46	12.56	52.14	47.86
	49	18.45	43.40	56.60
I-25	2	8.55	43.07	56.93
	4	44.94	52.06	47.94
	7	30.92	48.19	51.81

The ash yield of Yatağan coal samples varies from 8.55% to 44.93% (db) (#38 was excluded as the ash yield is approximately 50%), while the volatile matter yield ranges from 43.1 to 52.5% (daf).

Fixed carbon yield shows the opposite relation increasing with increasing coal rank. The fixed carbon yield is the solid residue remaining after heating the coal in a lack of oxygen. The fixed carbon yield (ar) is a value determined via subtraction of the sum of moisture, volatile matter, and ash yields from 100%. The fixed carbon yields for the studied coal samples in this work vary between 47.50% and 61.06% (daf).

4.2.2. Ultimate Analysis

The major elements of coal are carbon (C), hydrogen (H) and oxygen (O), whereas sulphur (S) and nitrogen (N) are minor. The contents of the elements are determined via ultimate analysis (Table 4.3).

Carbon in coals derives from both the organic and the inorganic matter. The carbon content of Yatağan coal samples ranges from 37.48 to 52.81 wt% (daf) with an average of 47.18 wt%.

Hydrogen which can derive from the organic compounds, as well as the inherent moisture and the breakdown of clay minerals contained in coal, is released during combustion as water vapor (Thomas, 1992). The hydrogen content of Yatağan coal samples ranges from 4 to 5.18 wt% (daf) with 4.5 wt%, on average.

Nitrogen is almost exclusively found in the organic matter in coal (Thomas, 1992; Büçkün, 2013). The original source of nitrogen is both plant and animal proteins (Kaye and Hart, 1997). The nitrogen content of Yatağan coal samples ranges from 1.06 to 1.71 wt% (daf) with an average of 1.32 wt%.

Sulphur is contained in coal in three forms: organic sulphur, inorganic sulphide phases (e.g., pyrite, marcasite etc.) and inorganic sulphates (e.g., Na_2SO_4, $CaSO_4$) (Speight, 2005; Reddy et al., 2018). The total sulphur content of lignite samples from the study area ranges from 2.59 to 6.79 wt% (daf), with an average of 4.48%.

The oxygen content is determined in the laboratory but calculated by subtraction of the sum of the rest elements from 100% (Table 4.3).

Table 4.3 Ultimate analysis results of Yatağan coal (daf: dry, ash-free basis, *: calculated by subtraction: O = 100-C-H-N-S).

Core	Sample #	C	H	N	S	O	H/C	O/C
		wt.%, daf					atomic ratio	
I-18	8	51.09	4.78	1.25	4.77	38.11	1.12	0.56
	9	52.19	4.76	1.35	5.26	36.44	1.09	0.52
	10	51.09	4.41	1.14	5.22	38.14	1.04	0.56
	11	43.74	4.29	1.17	5.26	45.54	1.18	0.78
	13	43.77	4.20	1.14	5.22	45.67	1.15	0.78
	14	44.53	4.22	1.10	6.79	43.36	1.14	0.73
	16	45.36	4.40	1.32	4.89	44.03	1.16	0.73
	18	44.63	4.41	1.21	4.21	45.54	1.19	0.77
	20	45.52	4.24	1.37	4.95	43.92	1.12	0.72
	23	48.95	4.61	1.64	3.77	41.03	1.13	0.63
	25	43.73	4.00	1.17	5.63	45.47	1.10	0.78
	26	46.72	4.51	1.59	4.40	42.78	1.16	0.69
	28	47.87	4.68	1.54	3.32	42.59	1.17	0.67
	30	46.62	4.49	1.34	2.59	44.96	1.15	0.72
	31	48.96	4.51	1.06	3.76	41.71	1.11	0.64
I-23	41	48.52	4.72	1.44	4.57	40.75	1.17	0.63
	44	42.23	4.18	1.17	3.69	48.73	1.19	0.87
	45	47.56	4.57	1.19	4.25	42.43	1.15	0.67
	46	49.72	4.96	1.47	4.36	39.49	1.20	0.60
	47	48.06	4.60	1.34	4.77	41.23	1.15	0.64
	48	44.69	4.45	1.29	3.88	45.69	1.20	0.77
	49	51.40	5.18	1.33	2.82	39.27	1.21	0.57
I-25	3	52.81	4.96	1.71	4.41	36.11	1.13	0.51
	5	52.19	4.90	1.61	4.96	36.34	1.13	0.52

4.2.3 Coal Petrography

Coal petrography offers a special tool to examine organic matter and has unique application fields. The aims, applications, and framework methods of coal petrography can be briefly summarized in the following lines by Gonçalves et al. (2024).

"Organic petrology is a field of Earth Sciences that uses petrographic methods, usually in combination with geochemical techniques, to study the organic matter (OM) present either in coal or being finely dispersed in sedimentary rocks (dispersed organic matter, DOM). Traditional organic petrology methods are performed using optical microscopy in both incident (reflected) and transmitted white light, combined with epi-fluorescence. The individual organic components observed in reflected light are referred to as macerals and are grouped into three major maceral groups

(huminite/vitrinite, inertinite and liptinite; ICCP, 1998, 2001; Sýkorová et al., 2005; Pickel et al., 2017)".

Below a brief information on the characteristics and the origin of the above mentioned maceral groups is provided.

4.2.3.1 Definitions of the Maceral Groups

Coal is composed of organic material of variable properties and origin. The characteristics of coal change according to the degree of diagenesis, also called coalification. While it is possible to identify the plant parts that make up peat, this becomes difficult or even impossible in the course of coalification. When examined under the naked eye, the coal appears consisting of bands of different brightness and texture called lithotypes (Taylor et al., 1998). When examined under an organic-petrography microscope, the smallest organic components are called macerals. Just as minerals come together to form rocks, macerals also form coal. In other words, the smallest organic components of coal, recognizable under the microscope, are the macerals. Since macerals derive from various plant parts, their morphological structures and physical and chemical properties differ from one another. The components and ratios of macerals obtained from coal petrography studies provide important information about the conditions of coal formation and the depositional environment, as well as the source of organic matter (Diessel, 1986).

The macerals vary in their chemical and physical properties. The macerals do not have a specific crystal structure; as they are of organic composition, they are amorphous. They can be distinguished under a microscope using parameters such as colour, reflectance, shape and relief. The macerals are distinguished into three main groups (App. III): huminite/vitrinite, liptinite and inertinite (Stach et al., 1982; Taylor et al., 1998).

4.2.3.1 a Huminite/Vitrinite Group

According to Sýkorová et al. (2005), the vitrinite group minerals in high-rank coal are the counterparts of the huminite group macerals in lignite (low-rank coal) (App. III). During coalification, the cellulose and the hemicellulose of terrestrial plant residues undergoes humification and gelification to form first huminite and then vitrinite at more advanced levels of coalification (rank).

Huminite macerals derive from the cell walls and cell filling of the plants and consist of cellulose, hemicellulose, lignin and tannin that make up the roots, stems and leaves of plants. Depending on the degradation processes (degree of humification and gelification) and the level of coalification, cell structures may be preserved at different levels. In Tertiary coals of the Northern Hemisphere, huminite is the main component, and its amount can exceed 90 vol.% (Sýkorová et al., 2005).

4.2.3.1 b Inertinite Group

Inertinite macerals originate from stems, branches, roots of large plants such as vitrinite/huminite, which underwent partial oxidation called fusinitization. The degree and form of preservation of the cell structures varies depending on their origin and the conditions to which they were exposed on the surface of the palaeomire. Their colour under incident white light varies from grey, greyish white to yellowish white. Compared to other maceral groups, they are characterised by high carbon, low hydrogen and oxygen contents (Van Krevelen, 1993). The carbon content depends on the origin of the maceral and the redox/drying processes to which the inertinite was subjected during peatification (ICCP, 2001) (App. III).

4.2.3.1 c Liptinite Group

Liptinite group macerals mainly originate from hydrogen-rich parts of plants such as spores, pollen, resins, waxes and oils. Under incident white light, their colour is dark grey-black, and they show a very strong fluorescence in greenish-yellow to yellow colours. Fluorescence intensity decreases with increasing coalification (Taylor et al., 1998). The reflectance value of the liptinite macerals increases with coalification/thermal maturity up to about 1.3%, but at higher rank, liptinite maceral

cannot maintain their stability (Pickel et al., 2017). The reflectance is lower than that of inertinite and huminite/vitrinite. It is the richest maceral group in terms of hydrogen and volatile matter. Due to their high hydrogen content, liptinite-rich coals can be utilised as a source of liquid hydrocarbons. Liptinite group macerals are easily distinguished from other maceral groups by their fluorescence under blue-light or ultraviolet excitation (Pickel et al., 2017) (App. III).

4.2.3.2 Maceral Composition of Yatağan Coal

Tables 4.4, 4.5, and 4.6 present the contents (in volume percentages) of the macerals and the mineral matter of each sample examined, as well as the reflectance values.

Table 4.4 The maceral composition (in vol.%, on a mineral matter-free basis) and the mineral matter (in vol.%, on a whole-rock basis) as well as the mean random reflectance of the Yatağan coal samples from core I-18.

Sample / Maceral	I-18/8	I-18/9	I-18/10	I-18/11	I-18/13	I-18/14	I-18/16	I-18/26	I-18/27	I-18/31
	in vol.%, on mineral matter-free basis									
Textinite	23.1	1.1	3.3	9.1	2.2	2.3	7.8	15.6	3.2	11.4
Ulminite	12.1	25.3	19.8	11.4	15.4	25.8	2.6	11.1	29.8	14.8
Telohuminite	***35.2***	***26.4***	***23.1***	***20.5***	***17.6***	***28.1***	***10.4***	***26.7***	***33***	***26.2***
Attrinite	9.9	1.1	9.9	10.2	11		35.1	14.4	3.2	20.5
Densinite	26.4	48.3	19.8	17.1	53.8	37.1	9.1	28.9	43.5	19.3
Detrohuminite	***36.3***	***49.4***	***29.7***	***27.3***	***64.8***	***37.1***	***44.2***	***43.3***	***46.7***	***29.8***
Gelinite	11	12.1	25.2	23.8	8.8	16.9	13	8.9	13.8	13.6
Corpohuminite	11	8.8	16.5	18.2	8.8	11.2	24.6	12.3	4.3	9.1
Gelohuminite	***22***	***20.9***	***41.7***	***42***	***17.6***	***28.1***	***37.6***	***21.2***	***18.1***	***22.7***
HUMINITE	**93.5**	**96.7**	**94.5**	**89.8**	**100.0**	**93.3**	**92.2**	**91.2**	**97.8**	**78.7**
Fusinite							1.3			
Semifusinite										
Funginite	3.3	2.2	1.1	1.1		3.4	2.6	2.2		2.3
Inertodetrinite			1.1	1.1			1.3	1.1		2.3
INERTINITE	**3.3**	**2.2**	**2.2**	**2.2**		**3.4**	**5.2**	**3.3**		**4.6**
Sporinite								1.1	1.1	
Cutinite				1.1		1.1				1.1
Resinite			1.1	2.3						
Alginite	1.1	1.1	1.1	2.3		2.2		1.1	1.1	2.3
Liptodetrinite	2.1		1.1	2.3			2.6	3.3		3.4
LIPTINITE	**3.2**	**1.1**	**3.3**	**8**		**3.3**	**2.6**	**5.5**	**2.2**	**6.8**
TOTAL ORGANICS	**100.0**	**100.0**	**100.0**	**100.0**	**100.0**	**100.0**	**100.0**	**100.0**	**100.0**	**100.0**

Table 4.4 continue

	in vol.%, on whole-rock basis									
MINERAL MATTER	**9.0**	**9.0**	**9.0**	**12.0**	**9.0**	**11.0**	**23.0**	**10.0**	**6.0**	**11.0**
Rr (%)	0.28	0.28	0.27	0.30	0.23	0.29	0.29	0.31	0.28	0.26
St. deviation	0.039	0.042	0.040	0.037	0.051	0.061	0.037	0.042	0.049	0.034

Table 4.5 The maceral composition (in vol.%, on a mineral matter-free basis) and the mineral matter (in vol.%, on a whole-rock basis) as well as the mean random reflectance of the Yatağan coal samples from core I-23.

Sample / Maceral	**I-23/38**	**I-23/41**	**I-23/42**	**I-23/44**	**I-23/45**	**I-23/46**	**I-23/49**
	in vol.%, on a mineral matter-free basis						
Textinite	2.7	7.1	5.9	4.8	12.3	4.8	4.8
Ulminite	4.2	12.9	33.7	19.3	16.7	27.8	34.4
Telohuminite	***6.9***	***20.0***	***39.6***	***24.1***	***29.0***	***32.6***	***39.2***
Attrinite	13.4	11.8	16.3	22.9	10.0	26.5	13.1
Densinite	50.2	34.1	17.4	25.3	21.2	16.9	22.6
Detrohuminite	***63.6***	***45.9***	***33.7***	***48.2***	***31.2***	***43.4***	***35.7***
Gelinite	9.4	7.1	8.1	8.4	10.0	6.0	4.8
Corpohuminite	6.8	14.1	9.3	12.1	13.3	6.0	8.3
Gelohuminite	***16.2***	***21.2***	***17.4***	***20.5***	***23.3***	***12.0***	***13.1***
HUMINITE	**86.7**	**87.1**	**90.7**	**92.8**	**83.5**	**88.0**	**88.0**
Fusinite				1.2	1.1		1.2
Semifusinite					2.2	1.2	
Funginite	1.3	3.5	2.3	1.2	3.3	3.6	2.4
Inertodetrinite	1.3	1.2			1.1	1.2	
INERTINITE	**2.6**	**4.7**	**2.3**	**2.4**	**7.7**	**6.0**	**3.6**
Sporinite	2.7			1.2			1.2
Cutinite	1.3		1.2		2.2	1.2	1.2
Resinite		1.2	2.3		3.3		2.4
Alginite	2.7	1.2	1.2		2.2	2.4	1.2
Liptodetrinite	4	5.8	2.3	3.6	1.1	2.4	2.4
LIPTINITE	**10.7**	**8.2**	**7**	**4.8**	**8.8**	**6**	**8.4**
TOTAL ORGANICS	**100.0**	**100.0**	**100.0**	**100.0**	**100.0**	**100.0**	**100.0**
	in vol.%, on whole-rock basis						
MINERAL MATTER	**25**	**15**	**14**	**17**	**10**	**17**	**16**
Rr (%)	0.30	0.27	0.27	0.27	0.33	0.31	0.26
Standard deviation	0.047	0.030	0.043	0.043	0.041	0.043	0.044

Table 4.6 The maceral composition (in vol.%, on a mineral matter-free basis) and the mineral matter (in vol.%, on a whole-rock basis) as well as the mean random reflectance of the Yatağan coal samples from core I-25.

Sample / Maceral	I-25/2	I-25/3	I-25/4	I-25/5	I-25/6	I-25/7
	in vol.%, on mineral matter-free basis					
Textinite	6.6	30.8	21.8	1.1	3.2	43.2
Ulminite	16.5	5.3	9	23.1	29.7	7.3
Telohuminite	***23.1***	***36.1***	***30.8***	***24.2***	***32.9***	***50.5***
Attrinite		4.2	10.3	1.1	2.1	7.4
Densinite	59.3	24.5	35.8	47.2	53.2	25.2
Detrohuminite	***59.3***	***28.7***	***46.1***	***48.3***	***55.3***	***32.6***
Gelinite	6.6	10.6	5.1	19.8	5.3	4.2
Corpohuminite	2.2	11.7	2.6	5.5	3.2	1.1
Gelohuminite	***8.8***	***22.3***	***7.7***	***25.3***	***8.5***	***5.3***
HUMINITE	**91.2**	**87.1**	**84.6**	**97.9**	**96.7**	**88.4**
Fusinite	2.2	1.1				
Semifusinite	1.1		1.3			
Funginite	2.2	1.1	1.3	1.1	1.1	1.1
Inertodetrinite		4.3	6.4			4.2
INERTINITE	**5.5**	**6.5**	**9**	**1.1**	**1.1**	**5.3**
Sporinite						
Cutinite					1.1	
Resinite						
Alginite	2.2	1.1		1.1	1.1	2.1
Liptodetrinite	1.1	5.3	6.4			4.2
LIPTINITE	**3.3**	**6.4**	**6.4**	**1.1**	**2.2**	**6.3**
TOTAL ORGANICS	**100.0**	**100.0**	**100.0**	**100.0**	**100.0**	**100.0**
	in vol.%, on whole-rock basis					
MINERAL MATTER	**9.0**	**6.0**	**22.0**	**9.0**	**6.0**	**5.0**
Rr (%)	0.25	0.28	0.24	0.28	0.24	0.25
Standard deviation	0.045	0.064	0.030	0.039	0.039	0.030

According to the results of the maceral analysis of 10 samples from I-18 well, the dominant huminite maceral group in the coals varies between 71-92 vol% (average 83.5%). It is observed that densinite maceral (7-49 vol%) belonging to the

detrohuminite subgroup, is the most dominant maceral (Table 4.4). Densinite belonging to detrohuminite, which is the second dominant sub-maceral group of the huminite group and represents the clastic huminite maceral, was identified in all samples. Attrinite (1-27 vol.%), another maceral of detrohuminite subgroup, presents lower values compared to densinite. Densinite consists of fine huminite fragments cemented with amorphous humic matter. It is formed through the gelification of attrinite during coalification, i.e., during the biochemical gelification and extensive degradation of the parenchyma and woody tissues of stems and leaves made of cellulose and lignin during the peat stage. It is abundant in low-rank Tertiary coals. Densinite has poor briquetting properties because it is rigid and does not interact with other coal grains during briquetting. On the other hand, it is easy to grind (Sýkorová et al., 2005). The abundance of detrohumite macerals in coal indicates the presence of herbaceous plants on the palaeomire surface. In addition, mires with high water table facilitate the decomposition and dispersion of organic matter, so that the maceral composition is rich in detrohuminite (Petersen and Nielsen, 1995). Coals containing fragmented macerals such as attrinite and densinite, might be interpreted as coal transported within the depositional environment, namely as hypo-autochthon peat accumulations (Stach et al., 1982).

Apart from densinite, ulminite and gelinite are also present in significant amounts, and attrinite, textinite and corpohuminite were encountered in lesser proportions. The gelohuminite content is relatively lower in the total composition of huminite (16-38 vol%) and consists of gelinite and corpohuminite macerals. The gelinite content in the studied coal varies between 8-23 vol%. Corpohuminite, which ranges between 4-19 vol%, derives from woody fragments and alteration processes in environments with high water levels.

In addition, liptinite is present in 1-7 vol% (average 3.2%) and inertinite in 2-4 vol% (average 2.3%). Among the liptinite, resinite, alginite and liptodetrinite (1-3%) are clearly visible in fluorescent mode. Sporinite and cutinite contents are very low in the analysed samples (Table 4.4-6). The inertinite content is lower than the liptinite one (2-4%) and is mainly represented by funginite with a proportion ranging from 1-3 vol% and inertodetrinite maceral ranging from 1-2% (Fig. 4.4-6).

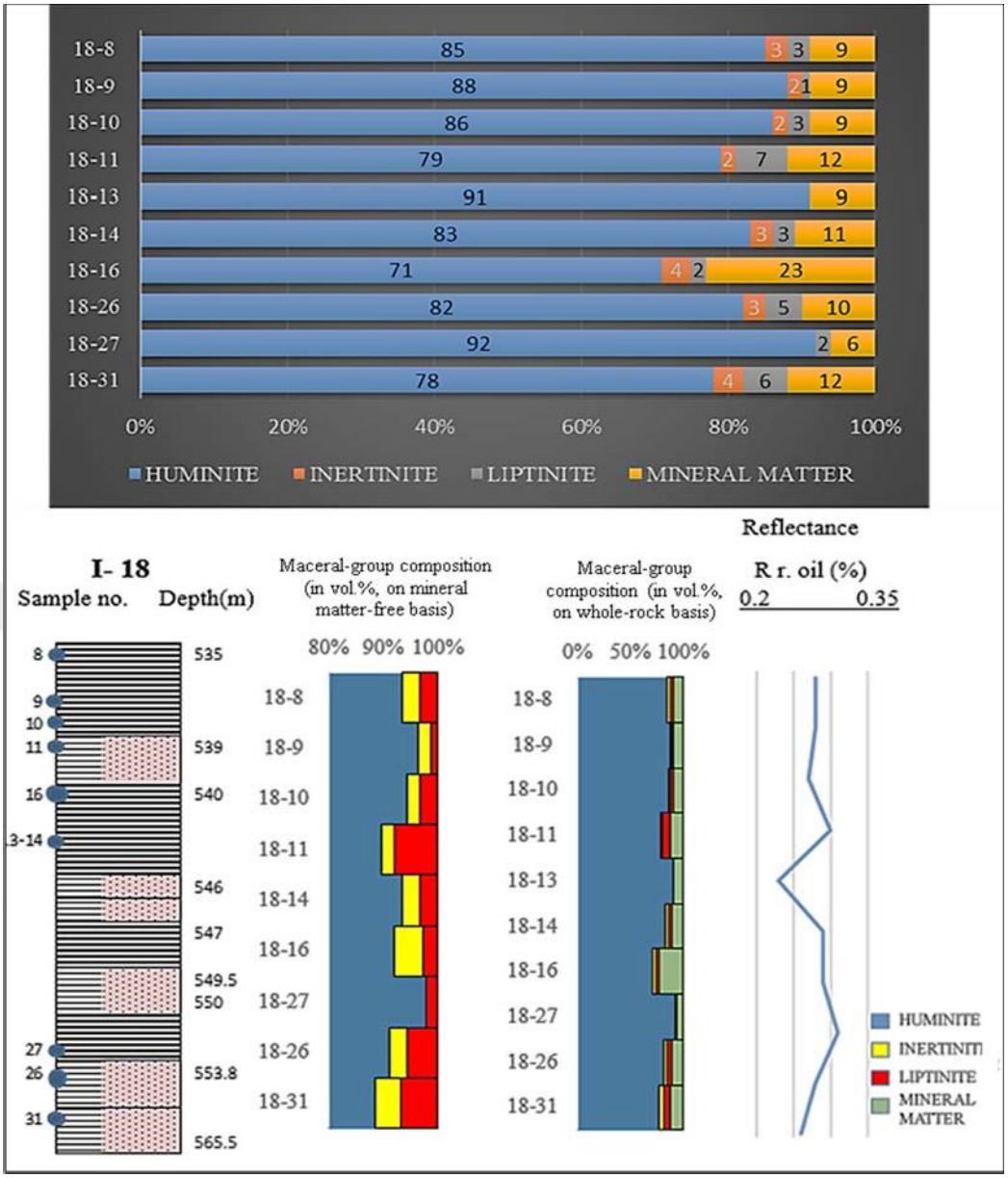

Figure 4.4 Maceral group composition and reflectance values of the samples from I-18 well.

According to the results of the mineral analysis of the 7 coal samples from the borehole I-23, the huminite group is dominant (65-78 vol%) (Table 4.5). Densinite (14-38%), ulminite (3-29%) and corpohuminite (5-12%) macerals are more common than atrinite (9-22%), textinite (2-11%) and gelite (4-9%). Liptinite content ranges from 4% to 8% and inertinite from 2% to 7%. Funginite and inertodetrinite are common, while other inertinite macerals are rare (Fig. 4.5).

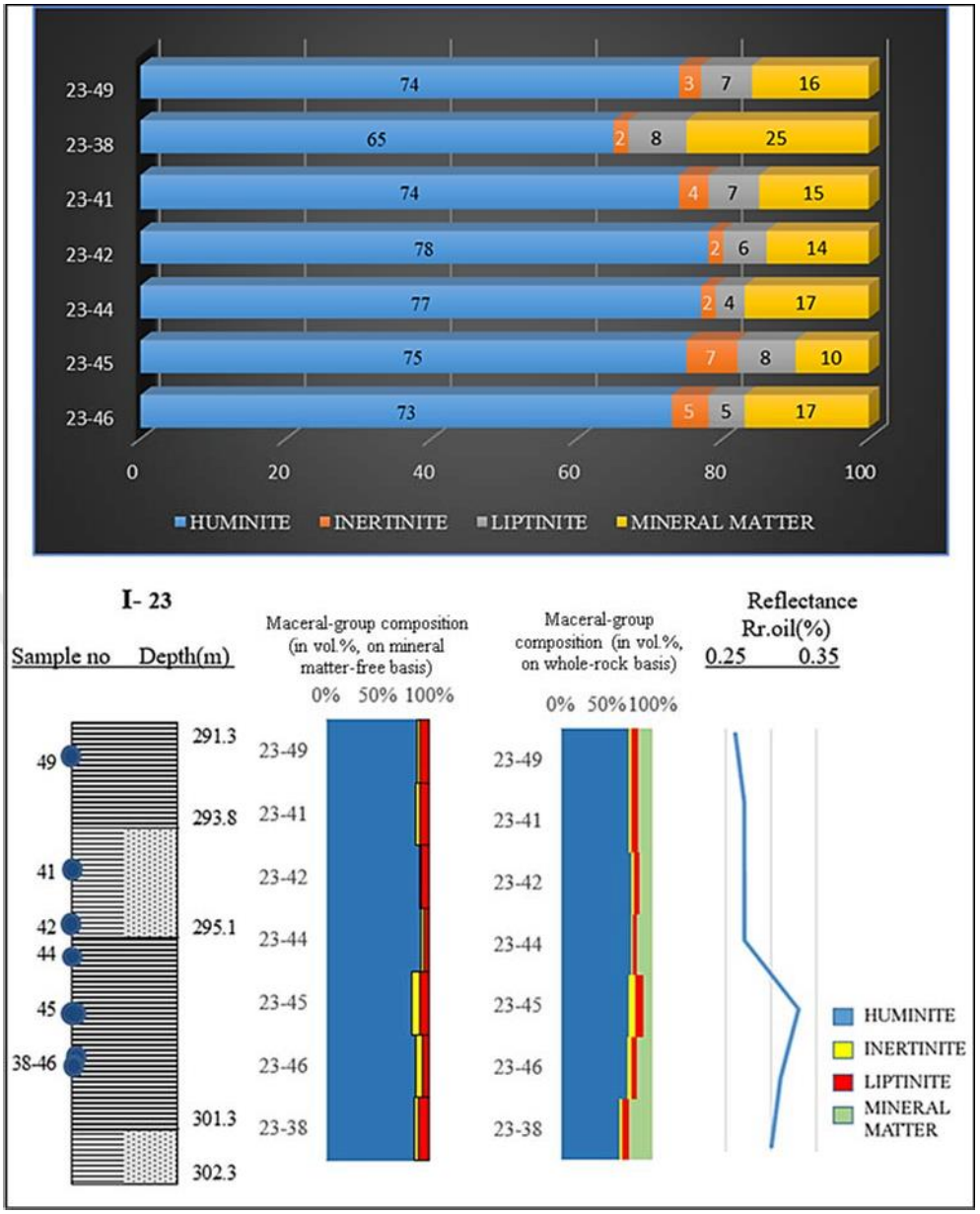

Figure 4.5 Maceral group composition and reflectance values of the samples from I-23 well.

According to the results of the maceral analysis of 6 coal samples obtained from borehole I-25, the dominant maceral group is huminite (66-91 vol%) (Table 4.6). According to the abundance percentages, it can be listed as densinite (23-54%) maceral belonging to detrohuminite sub-group, ulminite (5-28%) maceral belonging to telohuminite subgroup and gelinite (4-18%) maceral belonging to gelohuminite subgroup. Liptinite, mainly alginite (1-2%) and liptodetrinite (1-5%), was observed at

low contents. The inertinite maceral group is represented by inertodetrinite (4-5%) and funginite (1-2%) (Fig. 4.6).

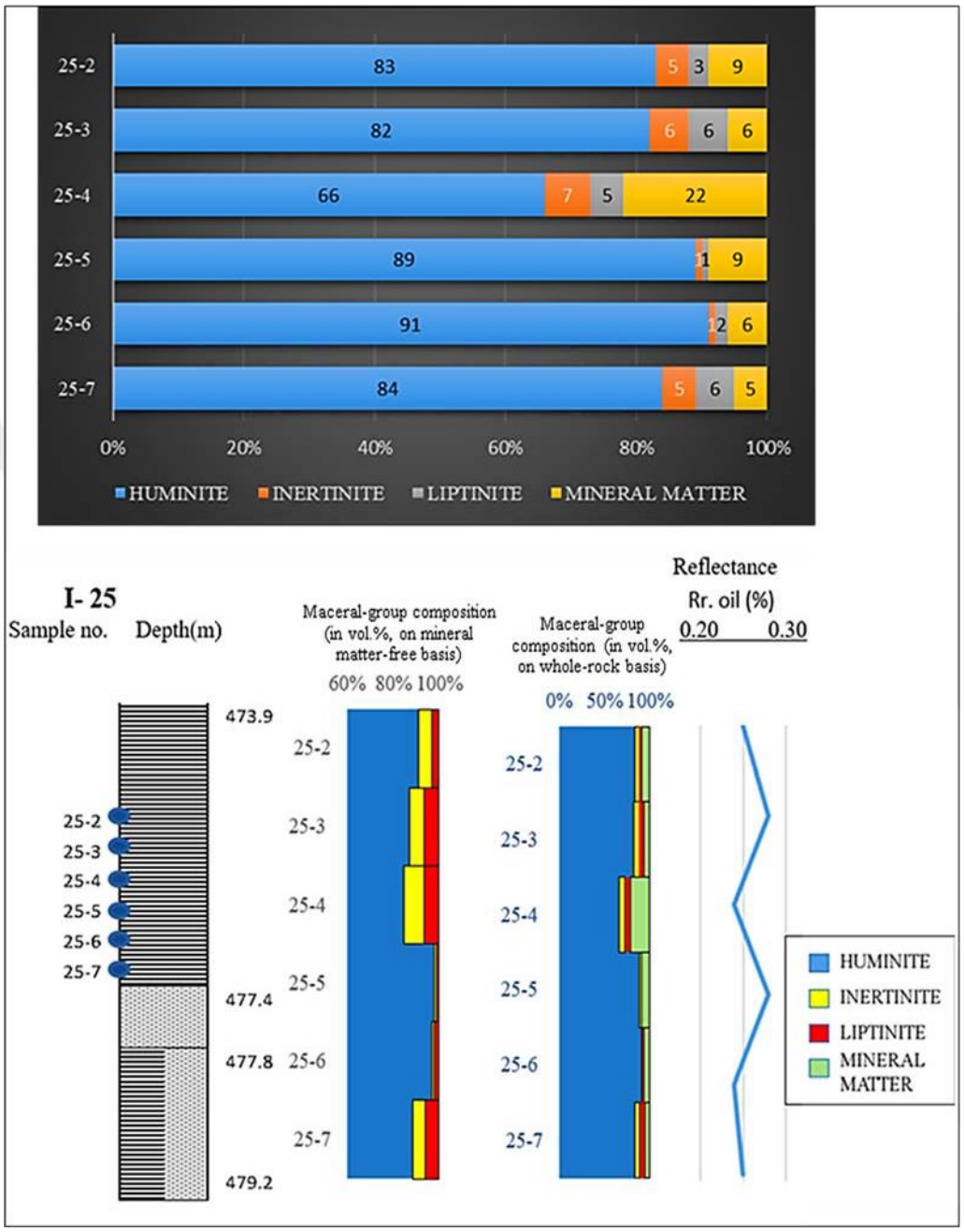

Figure 4.6 Maceral group composition and reflectance values of the samples from I-25 well.

The maceral analysis of all the samples reveals the predominance of the huminite macerals (> 78.7 vol.%, on a mineral matter-free basis, mmf). Mostly, detrohuminite dominates (27.3-64.8 vol.%), with densinite prevailing (9.1-59.3 vol.%) over attrinite

(up to 35 vol.%). Photomicrographs of the macerals contained in the Yatağan coal are presented in Appendix IV.

Textinite and ulminite are contained in significant amounts, whereas gelinite and corpohuminite are in lesser proportions. The gelohuminite subgroup content is relatively low (5.3-42%). Gelinite ranges from 4.2-25.2% and corpohuminite reaches values up to 24.6%. In general, the gelohuminite subgroup (5.3-42%) displays lower values than the telohuminite subgroup (6.9-50.5%).

Liptinite varies up to 10.7% (mean: 5%) and inertinite up to 9.0% (mean: 4%). Sporinite, cutinite, resinite and alginite occur at very low amounts. Liptodetrinite is the most abundant of the liptinite macerals with values reaching 6.4 vol.%. Inertinite content is lower than liptinite content, the latter being mainly represented by funginite (up to 3.6%) and inertodetrinite (up to 6.4%).

The mineral matter content varies between 5 and 25 vol.%, on whole-rock basis. Framboidal pyrite is common in all samples pointing to a syngenetic formation. Epigenetic pyrite is observed in cleats and cracks as infillings. Carbonates derived from fossil shells, are also identified in the examined samples.

4.2.3.3 Huminite Reflectance

Vitrinite/huminite reflectance values are one of the most reliable parameters used to determine the degree of coalification. Among the maceral groups contained in coals, only the brightness of the huminite/vitrinite macerals shows a relatively regular change by increasing rank compared to the inertinite and liptinite ones in parallel (Stach et al., 1982; Karayiğit, 1983). The reflectance value (Ro) is related to the aromaticity of the organic components and increases with the advance of coalification, i.e. by increasing rank (Suárez-Ruiz et al., 2012). The chemical change in the structure of huminite due to increasing temperature causes an increase in the reflectance. For this reason, Rr values obtained as a result of reflectance measurements are used as maturity

parameters (Stach et al., 1982; Taylor et al., 1998). For lignite, these reflectance measurements are carried out on ulminite B macerals (ISO 7404-5, 2009).

The random huminite reflectance values of the examined Yatağan coal samples range from 0.23% to 0.33% and the standard deviations from ±0.039-0.064% (Tables 4.4-6, App. V); the mean Rr of the samples is 0.28%.

Reflectance values provide an idea of the coalification degree of a coal, directly revealing their past diagenetic history, mainly the heat to which it was exposed (Stach, 1982; Ward, 1984). In addition to the ulminite-B reflectance measurements, the reflectance of ulminite A, corpohuminite, and gelinite was measured in six selected coal samples to shed light on their interrelationship (Fig. 4.7). This was done in order to inquire availability of alternative reflectance measurements in the lack of sufficient amounts of ulminite B macerals.

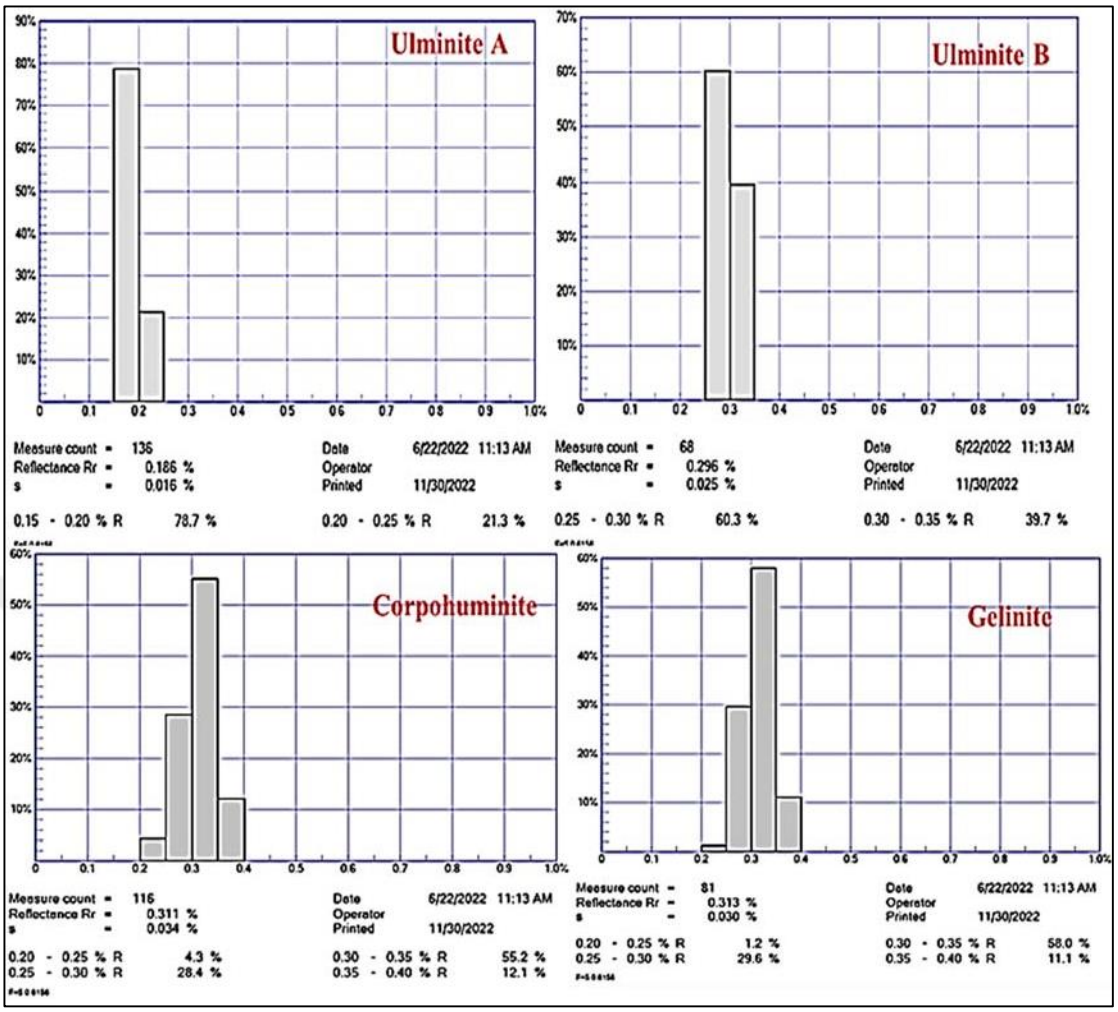

Figure 4.7 Examples of histograms of reflectance measurements of various huminite macerals on Yatağan coal samples.

Samples 9 and 21 from core I/18, samples 39 and 48 from core I/23 and samples 2 and 6 from core I/25 contain ulminite A and B, corpohuminite and gelinite macerals and 400 reflectance measurements were made on each polished block. Table 4.9 shows the results of the reflectance measurement of the above mentioned samples.

Table 4.7 Mean random reflectance (in %) of some huminite macerals in the Yatağan lignite.

Sample #	Ulminite-A	Ulminite-B	Corpohuminite	Gelinite
I/18-9	0.19	0.33	0.28	0.29
I/18-21	0.19	0.30	0.31	0.32
I/23-39	0.21	0.29	0.30	0.31
I/23-48	0.21	0.30	0.31	0.32
I/25-2	0.20	0.30	0.28	0.29
I/25-6	0.21	0.28	0.27	0.26

4.2.4 Mineralogical Composition

Table 4.8 presents the mineralogical composition of the studied samples. The accuracy of the semi-quantitative mineralogical analysis is high as the GOF parameter varies between 1.11 and 1.33, indicating that a good fit is achieved (Bish and Post, 1993).

Rietveld-based TOPAS software was used for semi-quantitative determination of the minerals by applying the method previously described in detail by Siavalas et al. (2009). As features of the poorly crystalline minerals generally differ from the ones exemplified in the database, the calculated weight percentages may only be considered as semi-quantitative values.

The dominant mineral phases identified are smectite, illite/mica, quartz, and pyrite. Aragonite is contained only in sample I-25/4; calcite is not identified in the samples from I-23 core; gypsum is traced in two samples only. Smectite exists in most samples in values strongly varying between 36.7 and 97.8 wt% of the crystalline phases. The illite/mica and the kaolinite/chlorite contents range up to 96.5% and 63.6%, respectively; quartz varies from 0.4-23.8%, and calcite reaches 85% in sample I-25/4.

Table 4.8 Mineralogical composition (in wt.% of the crystalline phases) of the Yatağan coal samples.

Core	Sample #	Aragonite	Calcite	Bassanite	Gypsum	Quartz	Chlorite	Kaolinite	Illite/Mica	Smectite	Pyrite
I-18	**8**		1.8							95.6	2.6
	9					1.0				94.7	4.3
	10					5.8				88.1	6.1
	11					2.4	0.5		96.5		0.7
	13					0.5		3.2	95.2		1.1
	14					2.0			92.7		5.3
	16		0.5							98.5	1.0
	18		7.2			7.0	7.9		9.7	64.5	3.8
	20		1.6			3.3	6.0		0.2	74.2	14.7
	23			0.7		2.1	1.9	5.6		84.2	5.4
	25			7.1		2.9	2.6	6.4		70.3	10.8
	26					9.2				78.3	12.5
	27		0.5			1.4				90.8	7.3
	28					3.8	2.7			84.5	8.9
	30					7.7	11.2			76.0	5.1
	31					2.6				86.5	10.8
I-23	**38**					5.5	4.4		88.3	1.3	0.5
	39					5.0	8.9		34.8	46.2	5.1
	41					2.1				92.6	5.4
	42				2.1	5.2	11.0		43.2	36.7	1.8
	44					4.9	5.8	12.0	24.1	50.3	3.0
	45					23.8	0.2	63.6			12.5
	46					1.8				92.9	5.3
	47					1.9				91.4	6.7
	48					8.6	7.4		0.1	77.1	6.8
	49					0.4				97.8	1.8
I-25	**3**		1.3			1.9				95.3	1.5
	4	11.9	85.3		1.8						1.0
	5					1.7				93.2	5.1

According to the analyses of the coal samples, pyrite is detected in all samples. The main carbonate mineral is calcite, while aragonite is identified in one sample only. Smectite and illite are detected in high amounts (Table 4.9, Fig. 4.8).

Table 4.9 The mineralogical composition of the lignite samples from cores I-18, I-23 and I-25.

Core #	Average mineral contents (%)									
	Pyrite	**Calcite**	**Smectite**	**Quartz**	**Chlorite**	**Illite/Mica**	**Bassanite**	**Aragonite**	**Gypsum**	**Kaolinite**
I-18	6.5	2.5	81	3.7	4.7	66	3.9	-	-	5.1
I-23	4.9	-	65	5.9	6.3	38	-	-	2.1	38
I-25	2.6	43	94	1.8	-	-	-	12	1.8	-

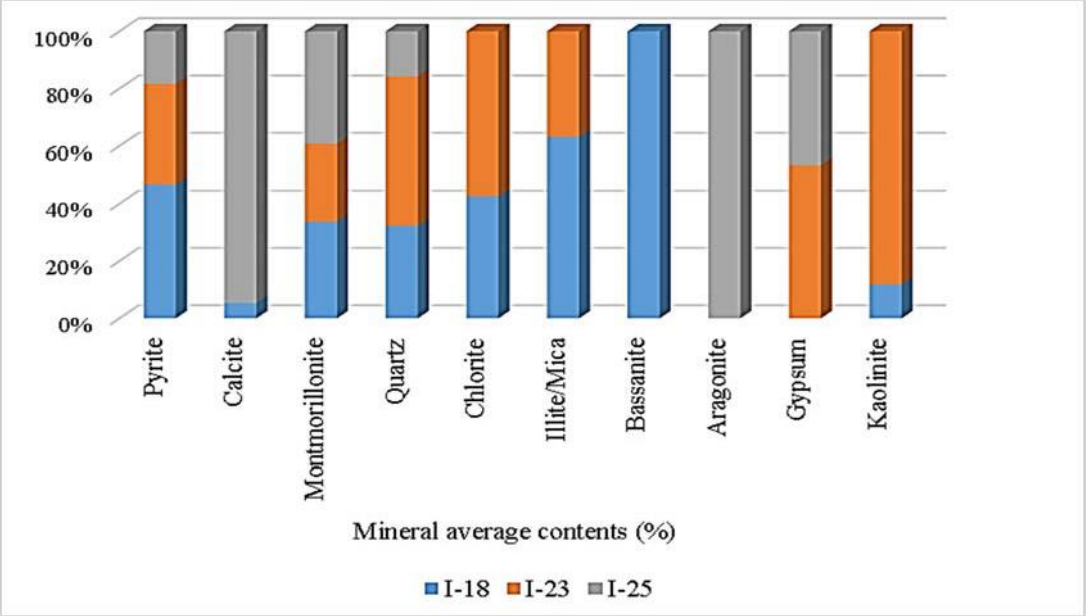

Figure 4.8 Mineral contents of samples from cores I-18, I-23 and I-25

4.2.4.1 Inorganic Sediments

The mineralogical contents of samples 12 and 29 from core I-18 were determined by X-ray diffraction on both the whole rock and on the clay fraction (Fig. 4.9; App. VI). Mica, clay minerals, quartz, feldspar, calcite and aragonite were identified in the samples. Table 4.10 shows the whole rock and clay fraction and semi-quantitative clay

fraction results for the two clay samples from core 18 (percentage of fraction with particle size less than 2 μm).

Table 4.10 The semi-quantitative composition (on wt.% of the crystalline phases) of the fine fraction (∅ < 2 μm) of two samples from I-18 core.

Core	Sample #	Illite	Smectite	Chlorite	Kaolinite
I-18	**12**	55.5-59.5	20.0-24.0	11.0-15.0	5.6-9.6
	29	58.0-62.0	0.5-2.5	-	38.0-42.0

The mineralogical composition of the fine fraction (∅ < 2 μm) of two selected samples from core I-18 (Fig. 4.9, Table 4.10) shows no significant differences between the mineralogical composition of both whole-rock samples and their fine fractions. In addition, the dominant clay minerals in the analysed fine fractions are smectite and illite. Kaolinite and chlorite are included in lesser amounts.

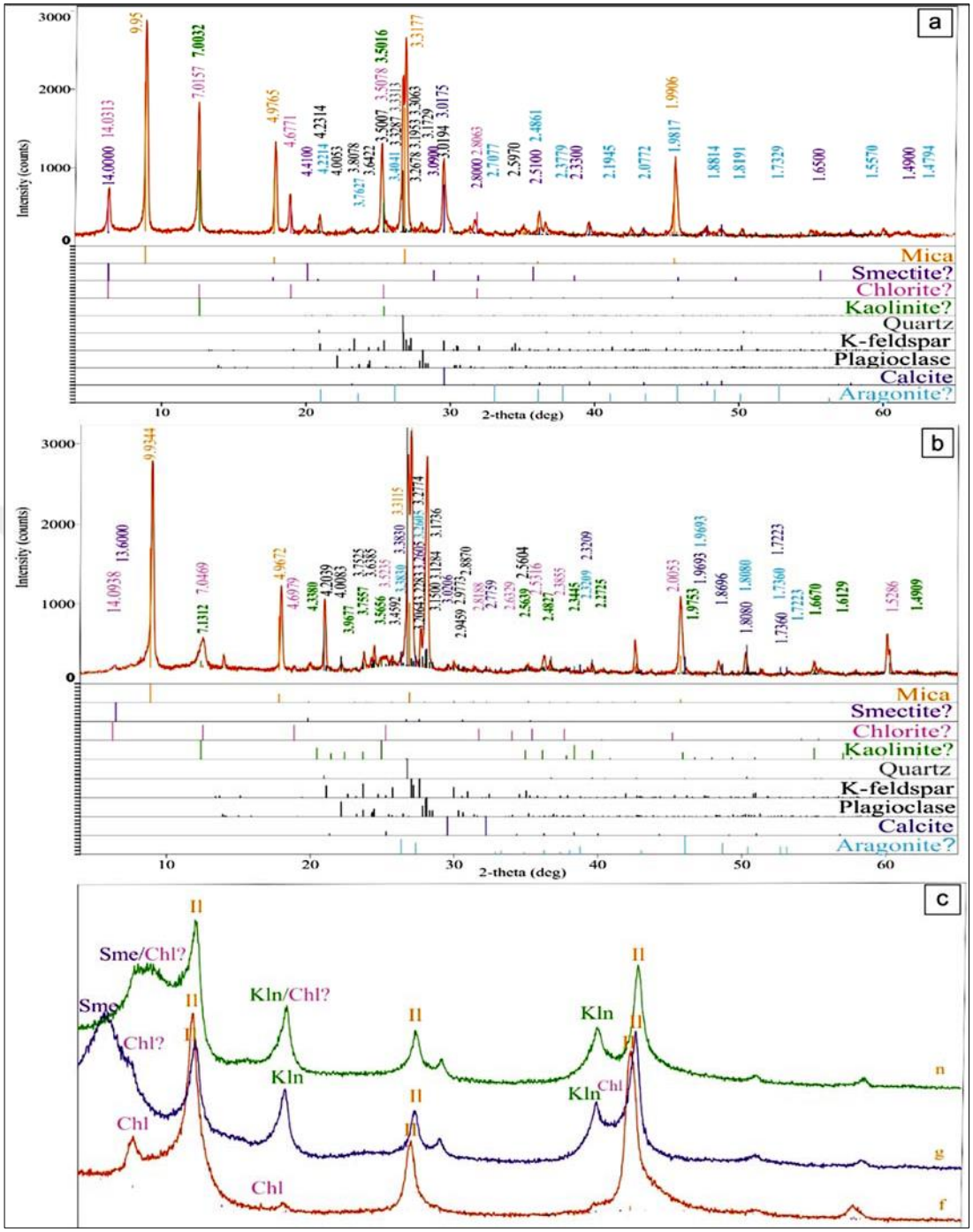

Figure 4.9 Diffractograms of samples #29 (a) and #12 (b) from core I-18, as well as of the fine fraction (∅ < 2 μm) of sample #12 (c), (Sme: smectite; Il: illite; Kln: kaolinite; Chl: chlorite).

4.2.5 SEM-EDX Analysis of Coal Samples

Samples I-18/9/23, I-23/48/49, and I-25/6/8 taken from the cores obtained from the Yatağan coal field were evaluated by SEM-EDX analysis (Table 4.11; App. VII).

Table 4.11 Results of SEM-EDX analyses of coal samples from borehole I-18, I-23, and I-25.

Sample code		Element (wt.%)												
		C	O	Na	Mg	Al	Si	S	Ca	Fe	P	K	Zn	Ti
I-18	#9-1	61.46	30.41	0.02	0.35	0.19	0.06	4.90	2.32	0.31				
	#9-2	68.40	25.20		0.26	0.18	0.04	3.95	1.96					
	#9-3	62.84	27.62	0.08	0.33	0.19	0.09	5.80	2.65	0.32	0.09			
	#9-4	26.22	14.98	0.23		0.57	0.06	27.83	1.38	28.30		0.10	0.34	
	#9-5	41.33	12.88	0.18	0.12	0.30	0.07	21.08	1.61	22.43				
	#9-6	63.86	30.28		0.33	0.47		3.70	1.36					
I-18	#23-1	61.73	29.08		0.38	0.60	0.31	4.00	2.75	1.16				
	#23-2	60.48	33.23	0.05	0.35	0.58	0.47	2.65	1.68	0.50				
	#23-3	60.11	33.21	0.00	0.33	0.51	0.35	2.83	2.03	0.63				
	#23-4	17.90	53.43	0.11	1.59	8.65	12.82	0.44	0.37	0.77		3.81		0.11
	#23-5	27.33	9.70					27.58	1.09	34.29				
	#23-6	61.48	33.81	0.02		0.34	0.36	0.19	2.13	1.52	0.15			
I-23	#48-1	58.38	22.14	0.11	0.18	0.53	0.73	8.39	1.16	8.19	0.07	0.05		0.06
	#48-2	60.49	32.52	0.05	0.35	1.22	2.19	1.42	1.26	0.27		0.16		0.06
	#48-3	61.76	28.38	0.05	0.29	0.67	1.19	3.83	1.40	2.29		0.09		0.06
	#48-4	47.52	14.47	0.13	0.04	0.14	0.24	20.09	0.48	16.90				
	#48-5	46.88	20.12	0.27	0.13	0.33	0.53	15.66	0.60	15.41		0.06		
	#48-6	69.48	27.58		0.21	0.25	0.26	1.24	0.89	0.10				
I-23	#49-1	62.49	31.21	0.10	0.29	0.75	1.34	1.90	1.47	0.33		0.10		0.03
	#49-2	55.22	34.57	0.10	0.37	1.48	2.81	2.63	1.46	1.10		0.19		0.08
	#49-3	56.90	31.60	0.09	0.45	2.13	4.10	1.96	1.84	0.51		0.31		0.10
	#49-4	39.68	10.90	0.51		0.22	0.18	25.05	0.49	22.98				
	#49-5	31.42	17.79	0.28	0.04	0.28	0.23	27.79	0.26	21.79		0.13		
	#49-6	67.63	26.09	0.34		0.64	0.57	2.74	1.69	0.23		0.03		0.04
I-25	#6-1	62.98	29.30	0.08	0.49	0.34	0.07	4.63	1.84	0.28				
	#6-2	63.40	28.01	0.02	0.43	0.31	0.25	5.02	1.40	1.17				
	#6-3	61.41	31.67	0.08	0.45	0.32	0.04	4.18	1.51	0.34				
	#6-4	31.63	12.30	0.61	0.07	0.13	0.09	28.47	0.34	26.37				
	#6-5	55.91	17.63	0.20	0.19	0.15	0.06	14.06	0.86	10.95				
	#6-6	41.80	35.70		0.09	0.12	20.17	1.37	0.35	0.39				
I-25	#8-1	62.47	28.66	0.05	0.47	0.24	0.17	5.37	2.13	0.45				
	#8-2	59.33	32.93	0.06	0.30	0.22	0.18	4.62	0.90	1.37	0.08			
	#8-3	65.27	23.46	0.04	0.35	0.23	0.09	7.14	2.37	1.05				
	#8-4	46.85	18.05	0.27	0.15	0.20	0.13	18.4	1.14	14.8				
	#8-5	44.40	6.68	0.12	0.07	0.24	0.09	25.84	0.28	22.28				
	#8-6	63.45	30.86	0.09	0.42	0.29	0.12	3.41	1.21	0.15				

Abundances of the main elements in the I-18/9 sample are as follows: C: 26.22–60.40 wt.%; O: 12.88–30.28 wt.%; Fe: 22.43–28.30 wt.%; S: 3.70–27.83 wt.%; Ca: 1.36–2.65 wt.% (Fig. 4.10, Table 4.11).

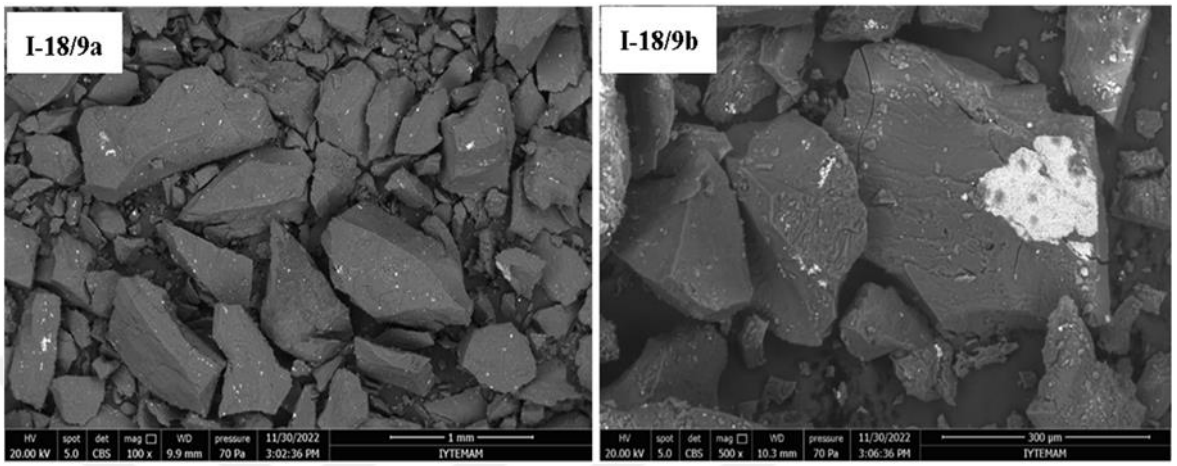

Figure 4.10 SEM-EDX result of sample I-18/9 a, b.

In sample I-18/23, the main elements contents are as follows: C, 17.90–71.63 wt.%; O, 9.70–53.43 wt.%; Fe, 1.16–34.29 wt.%; S, 2.65–27.58 wt.%; and Ca, 1.09–2.75 wt.%. The wt.% of Si, K, Al (illite) and Mg were to be 12.82, 8.65, 3.81 and 1.59 wt. %, respectively (Fig. 4.11, Table 4.11).

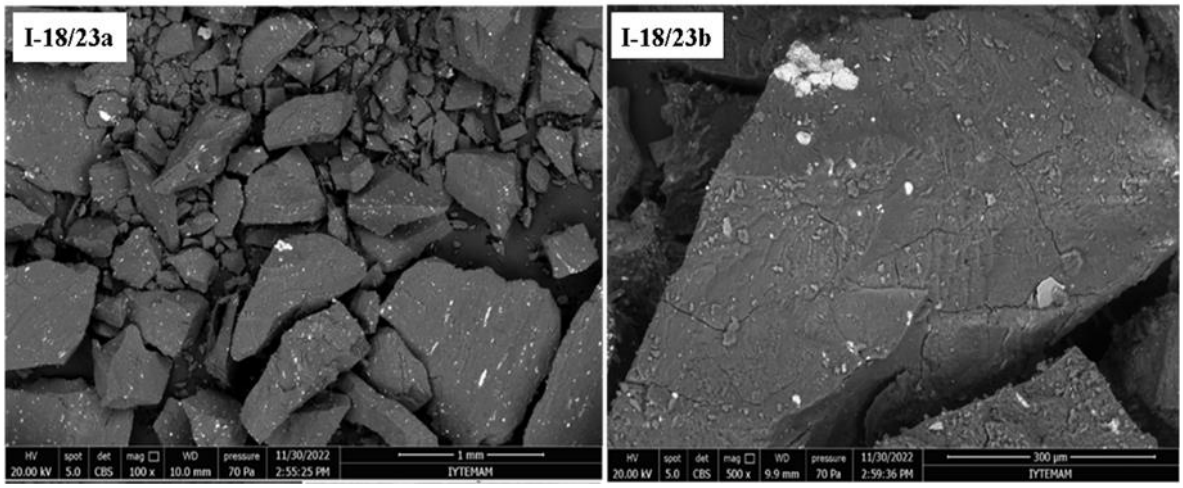

Figure 4.11 SEM-EDX result of sample I-18/23 a, b.

For the sample I-23/48, the main elemental abundances were found to be 46.88–69.48 wt.% C, 14.47–32.52 wt.% O, 2.29–16.90 wt.% Fe, 1.24–20.09 wt.% S and 1.16–1.40 wt.% Ca. The Si and Al wt.% values were found to be 1.19–2.1% and 1.22%, respectively (Fig. 4.12, Table 4.11).

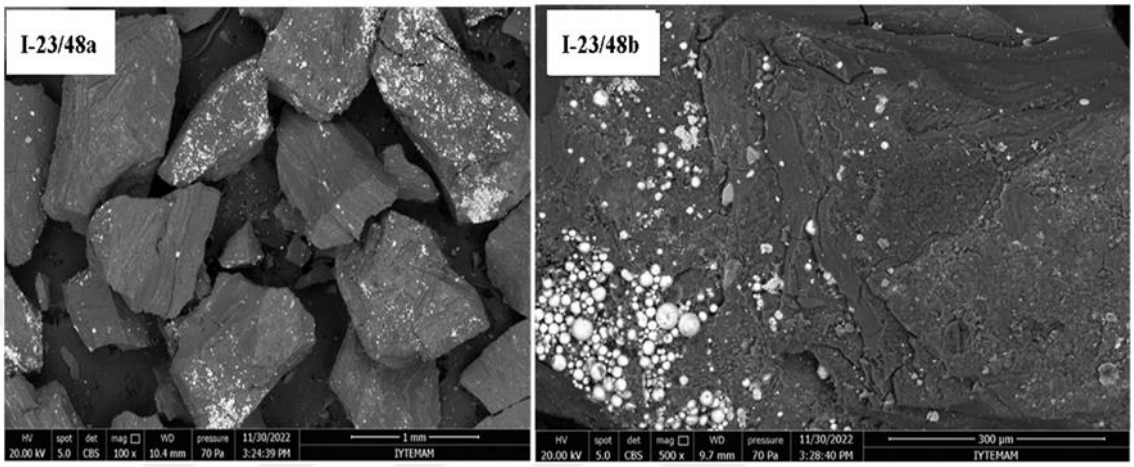

Figure 4.12 SEM-EDX result of sample I-23/48 a, b.

Sample I-23/49 shows main elemental values as follows: C: 31.42–67.63 wt.%; O: 10.90–34.57 wt.%; Fe: 1.10–22.98 wt.%; S: 1.90–27.79 wt.%; Ca: 1.46–1.84 wt.%. The wt.% values for Si and Al were found to be 1.34–4.10 and 1.48–2.43, respectively (Fig. 4.13, Table 4.11).

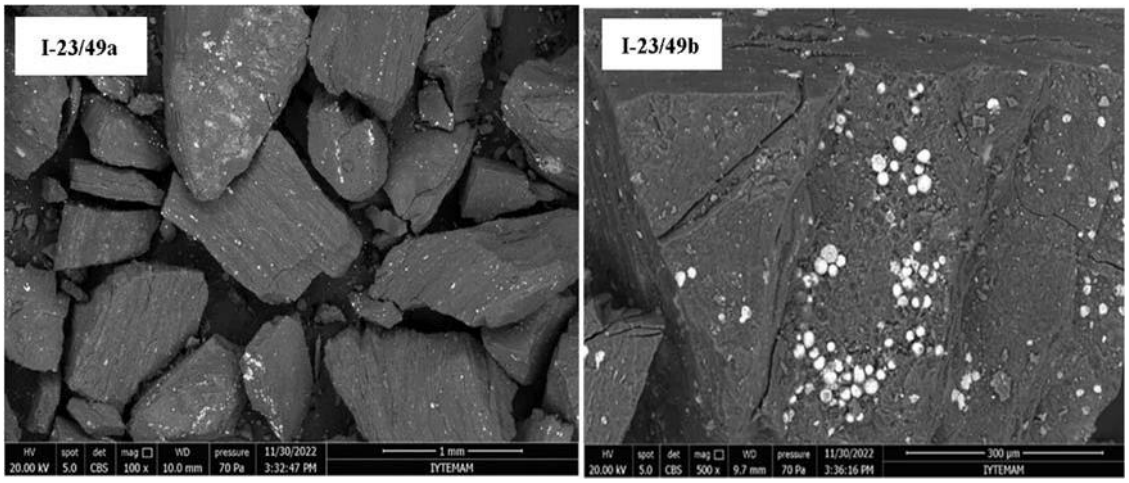

Figure 4.13 SEM-EDX result of sample I-23/49 a, b.

In the I-25/6 sample, abundance of the main elements are: C: 31.63–63.40 wt.%; O: 12.30–35.70 wt.%; Fe: 1.17–26.37 wt.%; S: 1.37–28.47 wt.%; and Ca: 1.40–1.84 wt.%. In one of the analysis, silicon (Si) value is detected to be 20.17 wt. % (Fig. 4.14, Table 4.11).

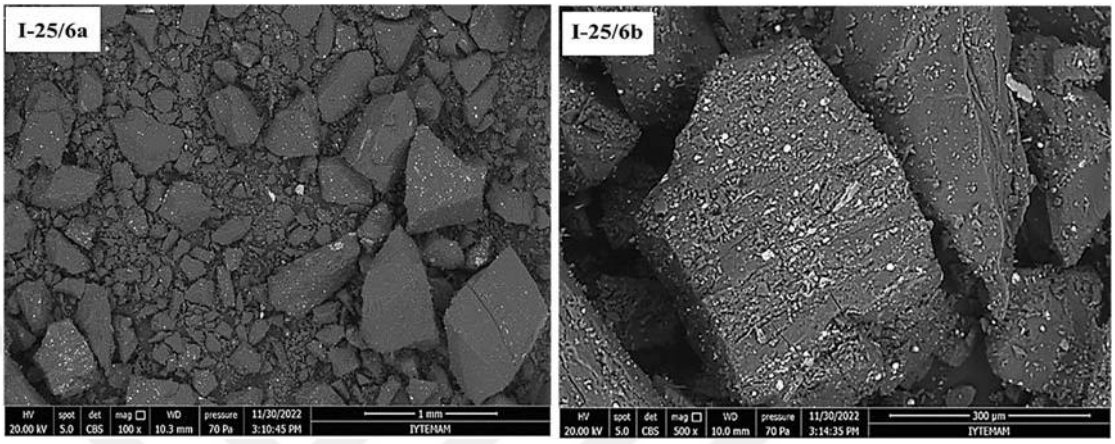

Figure 4.14 SEM-EDX result of sample I-25/6 a, b.

Main elemental abundances in sample I-25/8 present 44.40–65.27 wt.% C;6.68–32.93 wt.% O;1.05–22.28 wt.% Fe;3.41–25.84 wt.% S; and1.14–2.37 wt.% Ca (Fig. 4.15, Table 4.11).

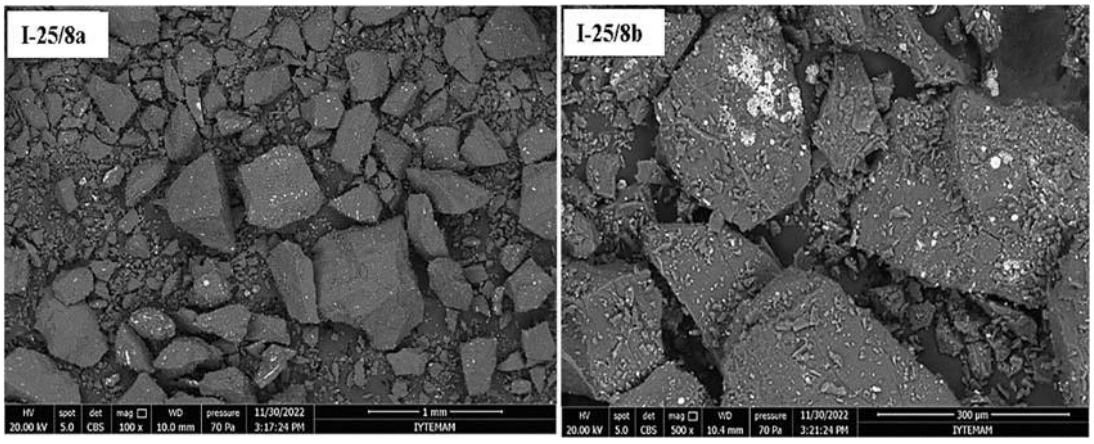

Figure 4.15 SEM-EDX result of sample I-23/49 a, b.

The results of the SEM-EDX analysis confirm that the coal samples contain pyrite (FeS_2), primarily in the form of framboidal pyrite, as well as quartz (SiO_2), clay minerals and fossil shells ($CaCO_3$).

4.2.6 PXRF Evaluation of Yatağan Coal And Inorganic Rock Samples

4.2.6.1 Trace Element Chemistry

The trace element contents of the coal samples from borehole I-18 are given in Table 4.12.

Table 4.12 Results of P-XRF analyses of coal samples from borehole I-18.

Element	DL	I-18/8	I-18/9	I-18/10	I-18/11	I-18/13	I-18/14	I-18/16	I-18/26	I-18/27	I-18/31
	all values in wt.%										
Si	0.025	3.1	3.7	2.4	3.5	5	5.5	0.9	0.8	1.0	0.8
Al	0.045	2.5	2.0	1.0	2.0	3.7	3.2	0.4	1.2	1.5	2.0
Fe	0.0005	3.9	4.5	1.3	0.8	1.0	3.5	0.5	1.9	2.4	2.7
Mg	0.3	<DL	1.5	1.2	<DL	1.1	0.8	0.02	0.011	0.045	0.008
Ca	0.001	3.05	3.12	2.97	2.60	2.9	2.58	0.025	0.012	<DL	0.044
K	0.002	<DL	0.1	0.1	0.3	0.2	0.45	0.043	0.058	0.083	0.2
Ti	0.0005	<DL	<DL	0.02	0.09	0.047	0.13	2.3	3.36	3.28	2.6
P	0.004	<DL	0.06	<DL	<DL	<DL	<DL	0.002	<DL	<DL	<DL
Mn	0.0003	<DL	0.004	0.002	0.003	0.003	0.004	0.01	0.004	0.006	0.005
	all values in mg/kg										
Ni	4	<DL	<DL	<DL	13	13	27	12	8	13	8
Cu	2	<DL	<DL	<DL	<DL	8	10	<DL	<DL	<DL	<DL
Zn	1	12	7	4	23	30	53	<DL	9	<DL	<DL
As	1	20	22	36	23	15	26	16	11	2	11
Se	1	<DL	<DL	<DL	2	2	13	25	23	24	24
Rb	1	2	2	10	22	14	18	30	32	27	10
Sr	1	857	101	104	130	106	109	<DL	<DL	<DL	<DL
Y	1	3	6	4	6	6	5	9	11	3	10
Zr	1	3	4	20	43	18	32	<DL	<DL	<DL	<DL
Nb	1	<DL	3	4	7	<DL	5	78	109	85	97
Mo	1	8	11	5	15	7	24	6	3	2	10
Ag	5	32	31	25	32	26	22	21	21		20
Cd	5	23	29	20	25	26	20	<DL	<DL	<DL	<DL
Ta	4	<DL	<DL	<DL	11	10	11	20	57	36	59
V	4	<DL	<DL	<DL	<DL	<DL	<DL	<DL	<DL	<DL	40
Cr	2	<DL	<DL	<DL	37	37	<DL	21	16	30	16
Th	2	13	7	8	13	<DL	<DL	<DL	<DL	<DL	<DL
Pb	1	<DL	<DL	<DL	5	4	<DL	6	<DL	<DL	5
U	1	28	27	18	51	20	38	47	5	4	13
Bi	1	<DL	12	9	<DL	<DL	<DL	<DL	<DL	<DL	10
Sb	1	20	17	18	<DL	<DL	<DL	55	20	6	34

The values of the trace elements Si, Al, Fe, Mg and Ca in the coal samples from core I-18 vary between 0.80-5.55 wt.%, 0.40-3.70 wt.%, 0.80-2.36 wt.%, 0.01-1.50 wt.% and 0.01-3.12 wt.%, respectively. Trace element values, U, As, Sr, and Ta vary between 4-51 ppm, 2-36 ppm, 101-857 ppm, and 10-59 ppm, respectively. The trace element contents of the coal samples from borehole I-23 are given in Table 4.13.

Table 4.13 Results of PXRF analyses of coal samples from borehole I-23.

Element	DL	I-23/38	I-23/41	I-23/42	I-23/44	I-23/45	I-23/46	I-23/49
	all values in wt.%							
Si	0.025	7.4	1.1	6.2	5.9	1.6	0.6	1.7
Al	0.045	4.13	0.72	3.5	3.9	0.8	0.5	0.7
Fe	0.0005	1.83	0.8	2.4	1.17	1.00	1	0.5
Mg	0.3	1.09	0.8	<DL	<DL	<DL	0.6	<DL
Ca	0.001	2.7	3.8	2.5	2.2	2.8	2.7	3.2
K	0.002	0.3	0.02	0.4	0.4	0.05	0.01	0.1
Ti	0.0005	0.2	0.02	0.17	0.07	0.03	<DL	<DL
P	0.004	0.02	0.03	0.03	<DL	0.01	0.02	0.02
Mn	0.0003	0.01	0.02	0.02	0.01	0.01	0.01	0.02
	all values in mg/kg							
Ni	4	50	<DL	70	<DL	10	<DL	<DL
Cu	2	40	<DL	46	<DL	<DL	<DL	<DL
Zn	1	11	10	160	17	17	4	20
As	1	33	23	38	25	44	47	30
Se	1	3	<DL	<DL	<DL	<DL	<DL	<DL
Rb	1	<DL	<DL	<DL	<DL	<DL	<DL	<DL
Sr	1	172	130	220	119	120	110	111
Y	1	49	18	71	22	21	21	16
Zr	1	62	4	44	17	20	10	8
Nb	1	13	<DL	21	5	9	3	7
Mo	1	19	<DL	20	3	7	2	9
Ag	5	17	26	25	26	30	28	33
Cd	5	19	24	<DL	18	20	25	18
Ta	4	<DL	<DL	<DL	<DL	<DL	<DL	<DL
V	4	119	80	133	99	<DL	<DL	<DL
U	1	18	6	50	9	11	18	12
Cr	2	48	<DL	53	<DL	<DL	<DL	<DL

The values of the trace elements Si, Al, Fe, Mg and Ca in the coal samples from core I-23 vary between 0.60-7.40 wt.%, 0.50-4.13 wt.%, 0.50-1.83 wt.%, 0.60-1.09

wt.% and 2.20-3.80 wt.%, respectively. The Th, U, Pb, Bi, and Sb contents were not determined because they were below the detection limit. Sr, Y, Zr and Cd values vary between 110-220 ppm, 16-71 ppm, 4-62 ppm, and 18-25 ppm, respectively. The trace element contents of the coal samples from borehole I-25 are given in Table 4.14.

Table 4.14 Results of PXRF analyses of coal samples from borehole I-25.

Element	DL	I-25/2	I-25/3	I-25/4	I-25/5	I-25/6
	all values in wt.%					
Si	0.025	0.3	0.3	0.4	0.6	0.3
Al	0.045	0.15	0.19	0.19	0.4	0.19
Fe	0.0005	0.48	0.37	0.42	0.97	0.17
Mg	0.3	0.41	0.72	1.18	0.6	1.29
Ca	0.001	2.03	1.89	22.5	2.15	4.84
K	0.002	<DL	0.007	<DL	0.002	0.009
Ti	0.0005	<DL	<DL	<DL	<DL	0.003
P	0.004	0.005	0.002	0.006	0.0008	0.004
Mn	0.0003	<DL	<DL	0.003	0.0009	0.002
	all values in mg/kg					
Ni	4	<DL	<DL	<DL	<DL	19
Cu	2	<DL	<DL	<DL	<DL	<DL
Zn	1	6	<DL	8	<DL	16
As	1	27	20	22	33	26
Se	1	<DL	<DL	3	<DL	<DL
Rb	1	3	2	<DL	3	6
Sr	1	84	80	372	92	112
Y	1	3	2	6	3	<DL
Zr	1	3	5	7	4	8
Nb	1	<DL	<DL	<DL	<DL	<DL
Mo	1	<DL	4	<DL	<DL	<DL
Ag	5	33	33	17	27	25
Cd	5	26	28	22	24	23
Bi	1	<DL	<DL	12	20	<DL
U	1	7	12	10	7	<DL
Th	2	12	15	<DL	<DL	<DL

The values of the trace elements Si, Al, Fe, Mg and Ca of the coal samples from core I-25 vary between 0.30-0.60 wt.%, 0.15-0.40 wt.%, 0.17-0.97 wt.%, 0.41-1.29 wt.% and 1.89-22.50 wt.%, respectively. The highest Ca content (22.50 wt.%) was found in sample I-25/4.

Trace element contents Cd, U, Sr, and As vary between 22-28 ppm, 7-12 ppm, 80-372 ppm, and 20-33 ppm, respectively.

The trace element contents of the coal samples are summarised in Table 4.15, and Figs. 4.16a,b. The average values of trace elements (except Si, Al, Fe, Mg and Ca) of the coal samples are below 1 wt%. The values determined for Si, Al, Fe, Mg and Ca vary between 3.75-5.64 wt.%, 2.45-3.46 wt.%, 0.48-2.36 wt.%, 0.84-1.05 wt.% and 2.60-6.68 wt.%, respectively. The trace element contents of the inorganic samples vary between 2.19-18 wt.% for Si, 2.6-6.7 wt.% for Al, 1.45-2.77 wt.% for Fe, 1.58-1.67 wt.% for Mg and 0.96-27.41 wt.% for Ca.

Table 4.15 The trace element composition of the coal (on average per core) and the inorganic samples from the Yatağan Field (DL: detection limit).

Element	DL	Coal samples (averages)			Inorganic samples						
		I-18	I-23	I-25	I-18/12	I-18/29	I-18/32	I-23/50	I-25/1	I-25/8	I-25/9
	all values in wt.%										
Si	0.025	4.35	5.64	3.75	9.13	18.00	7.80	2.19	5.67	2.39	3.65
Al	0.045	2.53	3.46	2.45	2.60	6.70	3.49	1.62	1.9	0.76	1.64
Fe	0.0005	1.88	2.36	0.48	1.99	2.77	1.45	1.92	1.74	0.56	1.35
Mg	0.3	0.99	1.05	0.84	1.67	<DL	1.58	<DL	1.87	<DL	1.19
Ca	0.001	3.75	2.60	6.68	27.16	0.96	22.41	27.41	24.93	35.68	32.46
K	0.002	0.36	0.47	0.23	0.47	2.43	0.50	0.06	0.35	0.18	0.29
Ti	0.0005	0.11	0.12	0.03	0.12	0.38	0.30	0.06	0.1	0.08	0.08
P	0.004	0.04	0.02	0.03	0.07	<DL	0.09	0.09	0.04	0.034	0.14
Mn	0.0003	0.024	0.007	0.008	0.07	0.02	0.02	0.08	0.05	0.03	0.04
	all values in mg/kg										
Ni	4	55	28	19	28	33	105	<DL	30	<DL	21
Cu	2	34	38	<DL	<DL	<DL	<DL	<DL	<DL	<DL	13
Zn	1	62	56	10	32	61	81	20	20	12	54
As	1	38	51	26	31	5	6	28	15	5	9
Se	1	3	4	2	<DL	<DL	<DL	3	<DL	<DL	<DL
Rb	1	25	38	40	27	128	46	7	18	6	21
Sr	1	147	102	148	313	115	325	682	117	<DL	750
Y	1	26	18	30	12	40	20	10	6	5	7
Zr	1	35	27	50	39	265	104	34	44	21	27
Nb	1	11	11	<DL	6	34	30	10	<DL	9	8
Mo	1	10	14	4	<DL	20	14	10	<DL	9	<DL
Ag	5	24	23	27	<DL	<DL	<DL	<DL	<DL	<DL	<DL
Cd	5	23	21	25	<DL	<DL	<DL	<DL	<DL	<DL	<DL

Table 4.15 continue

Ta	4	28	40	<DL	22	67	37	15	<DL	<DL	<DL
V	4	136	231	<DL	139	215	232	<DL	151	<DL	162
Cr	2	65	76	<DL	<DL	64	127	<DL	57	<DL	<DL
Th	2	16	<DL	13	14	39	<DL	<DL	<DL	<DL	<DL
Pb	1	9	17	<DL	8	<DL	<DL	6	<DL	<DL	<DL
U	1	32	17	8	<DL	8	<DL	10	<DL	<DL	<DL
Bi	1	<DL	<DL	16	<DL	<DL	<DL	<DL	<DL	<DL	<DL
Sb	1	11	<DL	19	<DL	<DL	<DL	<DL	<DL	<DL	<DL

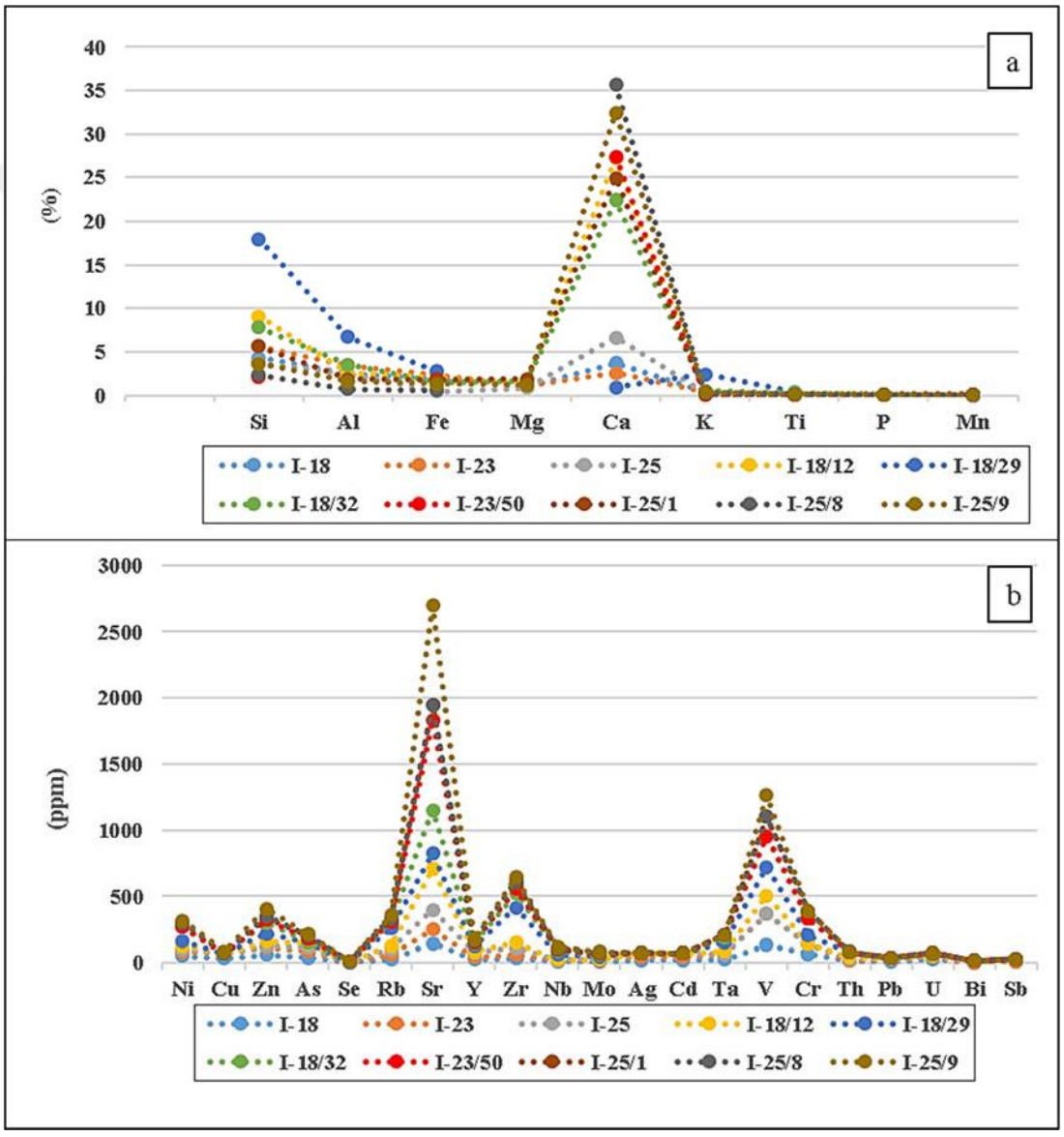

Figure 4.16(a) Average contents (%) of trace elements of Yatağan coal and inorganic samples; (b) Average contents (ppm) of trace elements in Yatağan coal and inorganic samples.

PXRF average trace element values of Yatağan samples were compared with world coal values reported by Swaine (1990). Highly enriched elements are shown in bold (Table 4.16)

Table 4.16 Weighted content averages of trace elements in the coal samples examined within the scope of the study, and comparison of these values with world coals (values for world coals are taken from Swaine, 1990), and Clarke values for low-grade coals (from Ketris and Yudovich, 2009).

Element(ppm)	World average	Clarke values	Yatağan coal ranges	CC
P	10-3000	200	200	1
Ti	10-2000	720	580	0.8
V	2-100	22	88	4.4
Cr	0.5-60	15	47	3.1
Mn	5-300	100	100	1
Co	0.5-30	4.2	7.2	1.7
Ni	0.5-50	9.0	31	3.4
Cu	0.5-50	15	21	1.4
Zn	5-300	18	25	1.4
Ga	1-20	5.5	4.2	0.8
As	0.5-80	7.6	28	3.7
Rb	2-50	10	18	1.8
Sr	15-500	120	152	1.3
Y	2-50	8.6	12	1.4
Cd	0.1-3	0.24	23	**96**
Mo	0.1-10	2.2	8	3.6
Sb	0.5-10	0.84	18	**21**
Pb	2-80	6.6	4	0.6
Th	0.5-10	3.3	12	3.6
U	0.5-10	2.9	21	**7.2**

Coefficient of concentration (CC) in coal samples are calculated to determine elemental enrichments. This calculation is based on the average elemental concentrations of low-grade coals divided by the corresponding Clarke values (Ketris and Yudovich, 2009; Dai et al., 2016). According to the classification method proposed by Dai et al. (2015), the concentration coefficients are distinguished into six categories: depletion (<0.5), normal (0.5~2), slight concentration (2~5), concentration (5~10), high concentration (10~100) and abnormal concentration (>100) (Wang et al., 2024). In the studied coal samples, Cd (CC=95), Sb (CC=21) and U (CC = 7.2) are the

enriched elements. Cadmium is of inorganic origin and can be associated with clay minerals and pyrite. Antimony (Sb) is associated with sulphides and organic matter in coals (Swaine 1990). It is thought to be largely associated with sulphides in the study area. Both organic and inorganic associations of U are common in coal, but mostly related to organic components (Swaine 1990; Finkelman 1995). Low amounts of U can also be found in clay minerals by adsorption. Uranium is also found in carbonate, silicate, oxide, vanadate, sulphate minerals (Swaine 1990). Slightly enriched elements are V (CC = 4.4), Cr (CC = 3.1), Ni (CC = 3.4), As (CC = 3.7), Mo (CC = 3.6) and Th (CC = 3.6), and the remaining elements are depleted (CC<0.5). Elemental enrichments in the study area are largely related to inorganic matter.

4.2.6.2 Petrographic Analysis of Inorganic Samples

In order to characterize the sedimentary rock samples, thin sections were prepared and petrographic examination was carried out. This analysis was carried out on seven samples from three boreholes (I-18, I-23 and I-25) in the study area (Figs. 4.1, 4.2, 4.3). The general distribution of the constituents was determined using a petrographic microscope, taking into account the average grain size in the thin sections of the samples. In the nomenclature, the most abundant grain size was determined as the main component of the rock.

Sample I-18/12 obtained from the coal roof, was classified as silt-bearing calcareous, muddy organic claystone. Sample I-18/29 taken from a coal parting, was classified as sandy, micaceous mudstone rich in organic matter (App. VII, Table 4.17).

Sample I-18/32, obtained from the floor of the coal seam, was classified as sandy-silty, calcareous claystone. Sample I-23/50 was as calcareous, silty claystone, taken from the coal roof (App. IV, Table 4.17).

Sample I-25/1 picked up from the coal roof, is a calcareous, silty claystone. Sample I-25/8 was classified as calcareous, silty claystone, taken from the coal intercalation.

Sample I-25/9 taken from the floor of the coal seam, is a calcareous, silty claystone (App. VII, Table 4.17).

Table 4.17 Lithology of inorganic rock samples taken from coal roof, intercalations and floor.

Sample no	Depth (m)	Location	Description
I-18/12	534.9	Roof	Silty, limy organic claystone
I-18/29	558.5	Intercalation	Fine-sandy mudstone, rich in organic matter
I-18/32	565.5	Floor	Sandy, silty calcareous claystone
I-23/50	291.3	Roof	Silty calcareous claystone
I-25/1	473.8	Roof	Silty calcareous claystone
I-25/8	477.5	Intercalation	Silty claystone
I-25/9	480.5	Floor	Silty claystone

CHAPTER FIVE
DISCUSSION

5.1 Coal Rank

As the bed moisture of the studied samples could not be determined due to the long storage time under ambient conditions, the bed moisture dataset provided by the company (Table 4.1) was considered for the rank assessment. It varies from 27.40-36.7%, pointing to a lignite to sub-bituminous coal C rank or Weich- to Mattbraunkohle according to the American and the German classification schemes (Taylor et al., 1998), respectively (Fig. 5.1).

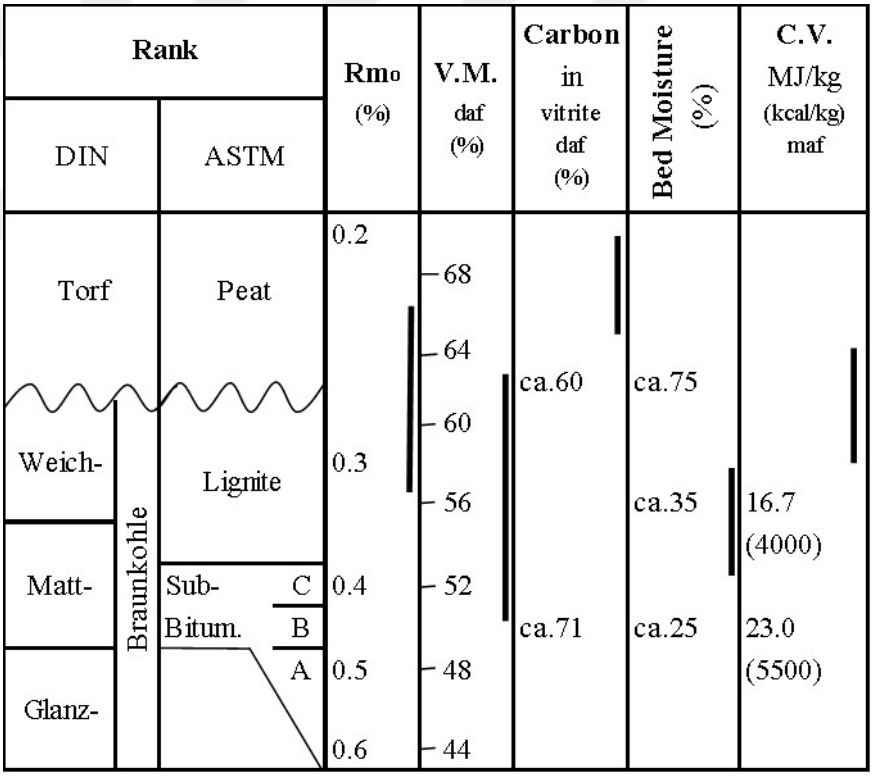

Figure 5.1 The Yatağan coal projected on the DIN and ASTM rank classification scheme (from Taylor et al., 1998).

The volatile matter yield is also considered a reliable rank parameter for low-rank coals. The volatile matter yield of the samples studied ranges between 50.78% and

62.30% (on a dry, ash-free basis; daf). The carbon content of the samples varies from 37.70% to 49.22% (on dry, ash-free basis; daf). The calorific value ranges from 7.44 MJ/kg to 15.44 MJ/kg (on moist, ash-free basis; maf). Considering the bed moisture and the volatile matter yield (Tables 4.1, 4.2), all the coal samples display a lignite and Weich- to Mattbraunkohle rank on the ASTM and DIN classification schemes, respectively (Taylor et al., 1998).

In the ECE-UN (1998) classification scheme, the Yatağan coal samples are humic, low-rank coal C or ortholignite, whereas the quality strongly varies from very low to high grade (Fig. 5.2).

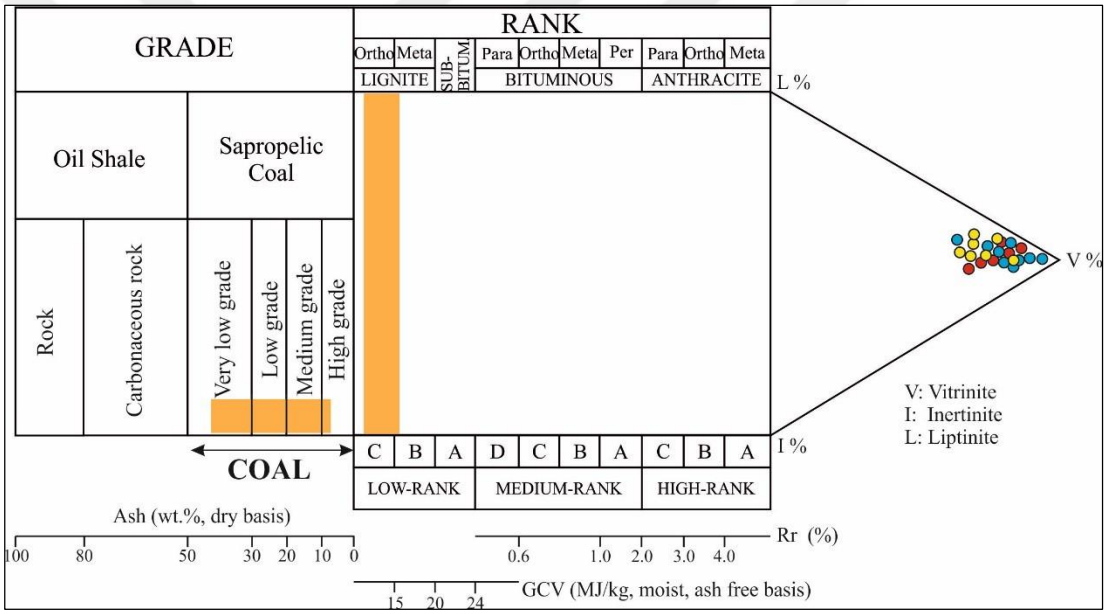

Figure 5.2 The Yatağan coal samples plotted on the ECE-UN (1998) classification scheme.

Noteworthy, the huminite reflectance displays strongly scattered values between 0.23 and 0.33% pointing to a lower rank (peat) for some of the samples. Of course, the huminite reflectance is not considered a suitable rank parameter for low-rank coals (Taylor et al., 1998). A possible reflectance suppression due to finely dispersed liptinite within the huminite (ulminite A) cannot be excluded for some samples, although the hydrogen content (Table 3) reasonably varies between 4 and 5% (daf), and no fluorescent ulminite (variety A) is identified under the microscope.

The O/C and H/C atomic ratios of the studied coal samples are presented in Table 4.3 and plotted on the Van Krevelen (1993) diagram (Fig. 5.3). The H/C atomic ratios vary between 1.04 and 1.21, and the O/C atomic ratio values between 0.51 and 0.87; they prove the humic origin and the low rank of the samples. The high O content, hence, the shift of the projected values to the peat area, might be due to the mineral matter contained.

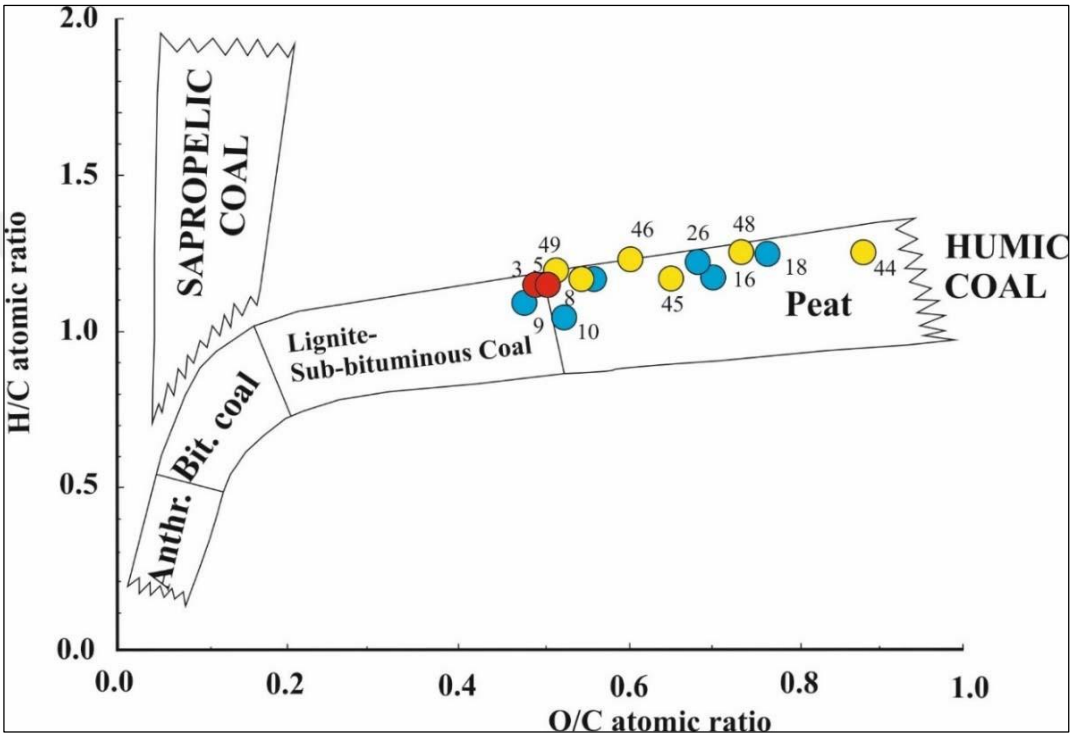

Figure 5. 3The Yatağan coal samples projected on the Van Krevelen (1993) diagram (blue, yellow, and red circles denote I-18, I-23, and I-25 samples, respectively).

Considering all the above results, the examined Yatağan samples are of ortholignite or low-rank C coal and qualitatively vary between high and very low-grade coals.

5.2 Depositional Environment

Several indices calculated from maceral contents (Table 5.1), and projected on certain facies diagrams, are commonly used to assess the palaeoenvironmental conditions during peat accumulation.

Table 5.1 The maceral indices of the Yatağan lignite samples (for the calculation of A, B and C see Fig. 5.4; for TPI and GI see Fig. 5.5; for GWI and VI see Fig. 5.6).

Core	Sample #	A	B	C	TPI	GI	GWI	VI
I-18	**8**	42	55	3	0.52	0.94	1.29	0.89
	9	33	65	2	0.04	5.92	2.88	0.52
	10	35	63	2	0.71	5.28	2.17	0.71
	11	35	63	2	0.74	3.26	2.37	0.66
	13	24	76	0	0.36	5.90	2.54	0.27
	14	23	74	3	0.60	16.20	2.76	0.72
	16	28	68	4	0.57	0.78	1.68	0.24
	26	36	61	3	0.81	2.00	1.49	0.56
	27	37	63	0	0.57	14.30	1.88	0.70
	31	33	63	4	0.65	2.60	1.20	0.56
I-23	**38**	17	80	3	0.18	3.78	5.00	0.14
	41	31	65	4	0.63	2.90	2.30	0.38
	42	48	50	2	1.17	2.81	0.92	1.06
	44	33	65	2	0.66	2.16	1.41	0.50
	45	42	51	7	1.03	2.04	1.43	0.86
	46	37	57	6	0.76	1.52	0.84	0.79
	49	48	49	3	1.21	3.28	1.05	0.97
I-25	**2**	25	70	5	0.36	3.13	3.28	0.42
	3	43	51	6	0.79	27.00	1.32	0.95
	4	32	59	9	0.68	1.80	1.75	0.54
	5	28	71	1	0.44	27.00	3.04	0.49
	6	36	63	1	0.58	13.80	1.85	0.58
	7	52	43	5	1.07	0.68	0.62	1.17

The ternary diagram introduced by Mukhopadhyay (1989), provides information regarding the dominant helophytic vegetation in the palaeomire, as well as the oxic/anoxic conditions during peat accumulation (Siavalas et al., 2009). The samples are scattered between apices A and B, closer to apex B (Fig. 5.4); this points to anoxic palaeoenvironmental conditions and intense bacterial activity in the palaeomire, where herbaceous peat-forming plants (e.g. reeds and sedges) were dominant.

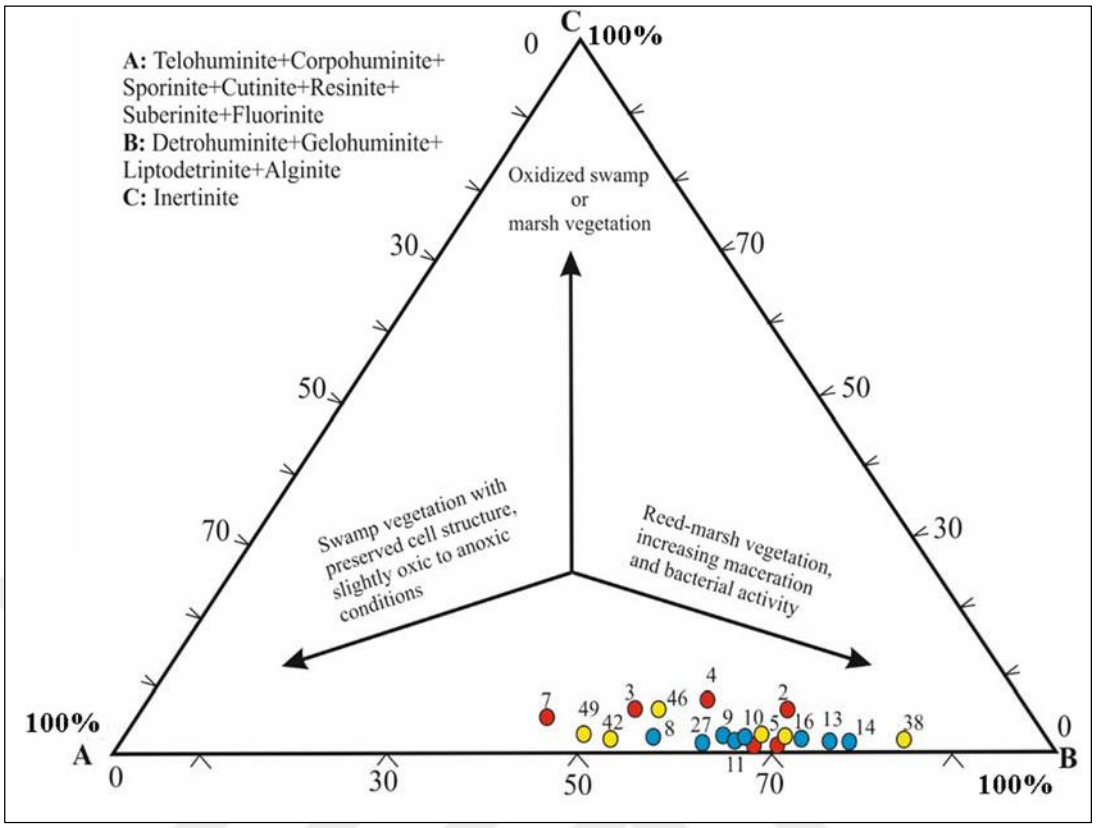

Figure 5.4 The Yatağan coal samples plotted on the Mukhopadhyay (1989) ternary diagram (blue, yellow, and red circles denote I-18, I-23, and I-25 samples, respectively).

The Gelification Index (GI) vs. Tissue Preservation Index (TPI) diagram proposed by Diessel (1992) and modified for Tertiary low-rank coals by Kalkreuth et al. (1991) and Kalaitzidis et al. (2004), is used to gain further insight into the peat-forming conditions. The GI values of the samples range from 0.68 to 27 and the TPI values from up to 1.21 (Table 5.1). In the GI *vs*. TPI facies diagram (Fig. 5.5), the examined samples fall in the upper left part of the diagram pointing to limnotelmatic conditions and herbaceous peat-forming plants (reeds and sedges).

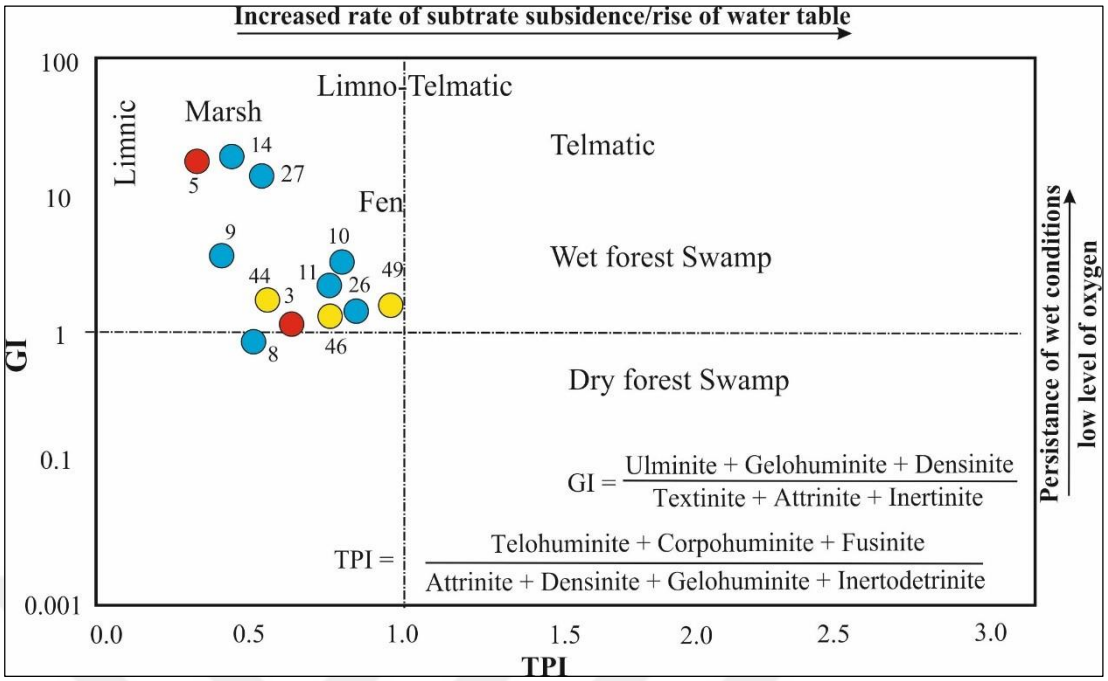

Figure 5.5 The TPI vs. GI plot (after Diessel, 1992, as modified by Kalaitzidis et al., 2004) of the Yatağan coal samples (blue, yellow and red circles denote I-18, I-23, and I-25 samples, respectively).

The Groundwater Influence Index (GWI) *vs.* Vegetation Index (VI) diagram introduced by Calder et al. (1991) and later modified by Kalaitzidis et al. (2004) for low-rank coals, is also used for reconstructing the depositional conditions. The calculated GWI and the VI values of the coal samples range from 0.62-5 and 0.14-1.17, respectively (Table 5.1). Plotting these values on the GWI *vs.* VI diagram (Fig. 5.6), it is also inferred that in the palaeomire limnotelmatic conditions dominated.

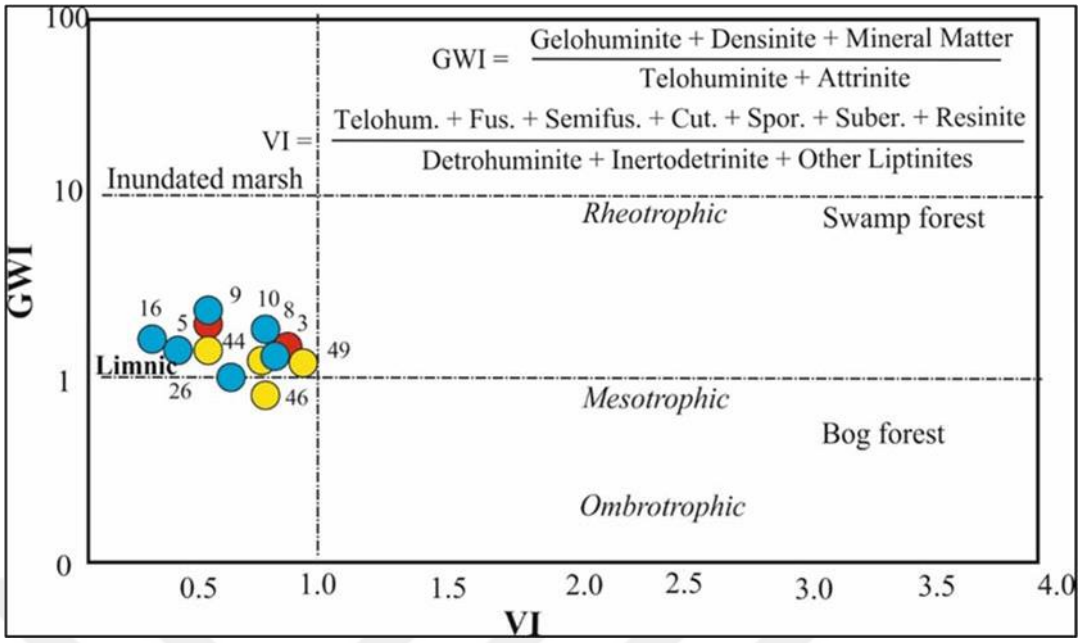

Figure 5.6 The GWI vs. VI diagram (after Calder et al., 1991, as modified by Kalaitzidis et al., 2004) for the studied lignite samples (blue, yellow and red circles denote I-18, I-23, and I-25 samples, respectively).

Additionally, the high framboidal pyrite content detected under the organic-petrography microscope also points to intense bacterial activity in the palaeomire, which destroyed the cellular tissues; hence, the samples have high detrohuminite contents (Table 4.9) and hence, display poor tissue preservation (low TPI; Table 5.1). Gastropods found in the coal beds and the intermediate marlstone in the lower parts of the studied core interval disclose an alkaline environment with flood events (İnci, 1998). Overall, a relatively high groundwater table (wet telmatic to limnotelmatic facies) and a moderate subsidence rate of the mire substrate prevailed during peat accumulation.

Quartz and clay minerals contained in the lignite point to the water input from the margins into the palaeomire. The abundance of syngenetic and framboidal pyrite grains in the coal samples indicates an increased activity of sulphate-reducing bacteria, probably associated with carbonate- and sulphate-rich waters in the depositional area during peat accumulation (Kuder et al., 1998; Teichmüller et al., 1998; Iordanidis and Georgakopoulos, 2003).

Illite/mica group minerals contained in samples obtained from boreholes I-18 and I-23 (Table 4.10) point to a provenance from weathered K-feldspars included in the basement rocks exposed on the basin margins. Chlorite might have been also transported along other clay minerals. The dominant minerals identified in the clay fraction (Table 4.10), were illite and smectite with lesser amounts of chlorite and kaolinite. Smectite is transformed to illite during burial diagenesis (Ünal, 2018). Although not identified in all samples, smectite (Table 4.10) also infers to the low rank of the coal. Furthermore, the occurrence of smectite along to chlorite and kaolinite indicates feldspar alteration under a hot and semi-dry climate (Millot, 1970; Koca, 2011).

5. 2 Inferences from The Mineral Matter

The amount of mineral matter in the analysed coals varies between 5 and 25 wt.% (Table 4.8). According to the results of the XRD analysis, the main minerals identified are quartz, pyrite, smectite (montmorillonite), illite, calcite, bassanite and aragonite. The mineral phases obtained from SEM-EDX analyses, and supporting the XRD results, are clay and carbonate minerals. According to the results of P-XRF analysis on the coal samples, the average values of the main elements except Si, Al, Fe, Mg and Ca, are below 1% (Fig. 5.6a,b). Trace elements accumulate in coal through plants and animals and through geological processes syngenetically in peat and epigenetically during coalification (Bouška et al., 2000; Singh et al., 2016). Depending on their occurrence (mobility), concentration and toxicity, trace elements have different effects on the environment (Finkelman, 1995; Dai et al., 2005) and therefore, the study of trace elements contributes to formulating and developing pollution control strategies in relation to coal combustion (Querol et al., 2001; Dai et al., 2005; Wang et al., 2008; Tang et al., 2009; Singh et al., 2016). Elements such as As, Be, Cd, Cr, Co, Cu, Pb, Mn, Hg, Mo, Ni, Sr, U, V and Zn, have harmful effects on the environment and the human health, especially when they are released into the atmosphere during coal combustion in thermal power plants (Singh et al., 2011, 2012, 2014; Singh and Singh, 2013). These elements are often associated with sulphide minerals such as pyrite. Thus, the removal (or at least content reduction) of sulphide minerals from coal prior to combustion in preparation plants, and the removal or conversion of sulphurous

flue gases after combustion contribute to reduce the environmental impacts. Moreover, the knowledge about the abundance of trace elements in coal is also important for geochemical comparisons (Ketris and Yudovich, 2009); most of them are hosted in silicate, carbonate and sulphate minerals in coal (Finkelman, 1995).

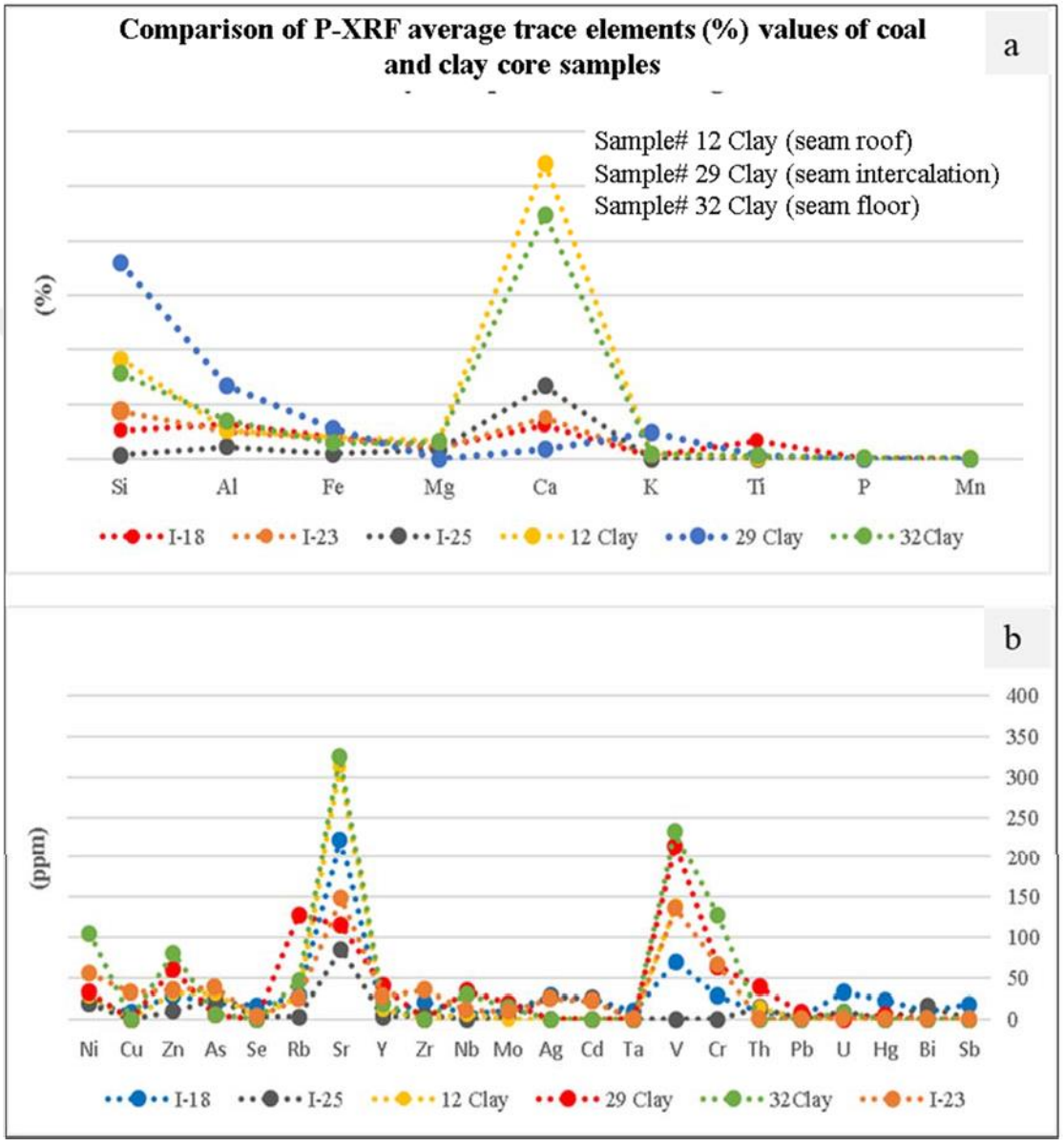

Figure 5.7 Comparison of the trace element contents (a: in wt%, b: in ppm) obtained from the P-XRF analysis of the Yatağan coal and clay samples.

The abundance of minerals identified in almost all samples, is confirmed by the alternating increase in inorganic content alongside the accumulation of organic matter during peat accumulation, as well as the occasional input of minerals through factors such as flooding or wind. The combination of regional, depositional, and palaeoenvironmental factors (e.g., marginal rock type, redox conditions, and climate) influence the mineral matter content of coal during peat accumulation and the subsequent coalification (e.g., subsurface fluid circulation and sediment diagenesis).

5.3.1 Correlation of Trace Element Contents in The Yatağan Lignite

The Pearson correlation coefficients (r) were calculated to determine the interrelations of the trace element values (Si, Al, Fe, Mg, Ca, K, Ti, and P) of the lignite samples (Table 5.2). The Pearson correlation coefficient (r) is a statistical parameter used as a measure of the strength of the relationship between two different variables in dataset.

Table 5.2 Trace element correlation matrix values of Yatağan coal deposit.

Element(%)	Si	Al	Fe	Mg	Ca	K	Ti	P	Mn	Ash (db)
Si	1	0.98	0.54	0.05	-0.31	0.87	-0.15	0.65	0.02	0.18
Al		1	0.58	0.02	-0.32	0.84	-0.18	0.74	0.06	0.05
Fe			1	-0.17	-0.24	0.50	-0.14	0.69	0.46	-0.28
Mg				1	0.50	-0.02	-0.37	-0.12	-0.13	0.55
Ca					1	-0.19	-0.28	-0.21	0.08	0.53
K						1	-0.18	0.65	-0.19	0.06
Ti							1	-0.27	-0.11	0.14
P								1	0.38	-0.34
Mn									1	-0.06
Ash										1

Examining the average concentrations of trace elements in coal samples reveals that there is no correlation between silicon (Si), and ash (see Table 5.2). Silicon shows a strong to moderate positive correlation with the minor elements Al, K and P, and a good one with Fe (r = 0.98, 0.87, and 0.65, respectively). There is no correlation with Mg, Ca and Ti. In general, the average Al content of the core samples from the three boreholes (I-18, I-23 and I-25) is 2.81%. A high positive correlation was also observed

between Al and Si, Fe, K and P, while no correlation was observed between Ca, Mg, Ti and ash. Since Si, Al and K are commonly found in clay minerals (Karayiğit, 2003; Karayiğit and Çelik, 2003), the positive correlation between Si and Al, Fe and K, may likely suggest a terrestrial detrital source, possibly the detritic clay mineral input in the environment (Fig. 5.8).

Aluminium is associated with clay minerals and also with feldspars (Boggs 2009). The very strong correlation between Al and Si (0.98; see Table 5.8), indicates the presence of detrital clays in the palaeomire. Moreover, the high positive correlation (r = 0.84) between Al and K is in good agreement with the presence of illite in the samples. Samples 9, 11 and 14 from core I/18 (Si content: 3.7%, 3.5% and 5.5%, respectively) and samples 38, 42 and 44 from core I/23 (Si content: 7.4%, 6.2% and 5.9%, respectively) demonstrate an increase in the supply of detrital quartz to the palaeomire (Tables 4.11, 4.12). This is evident from the increase in the Si/Al ratio observed in these samples.

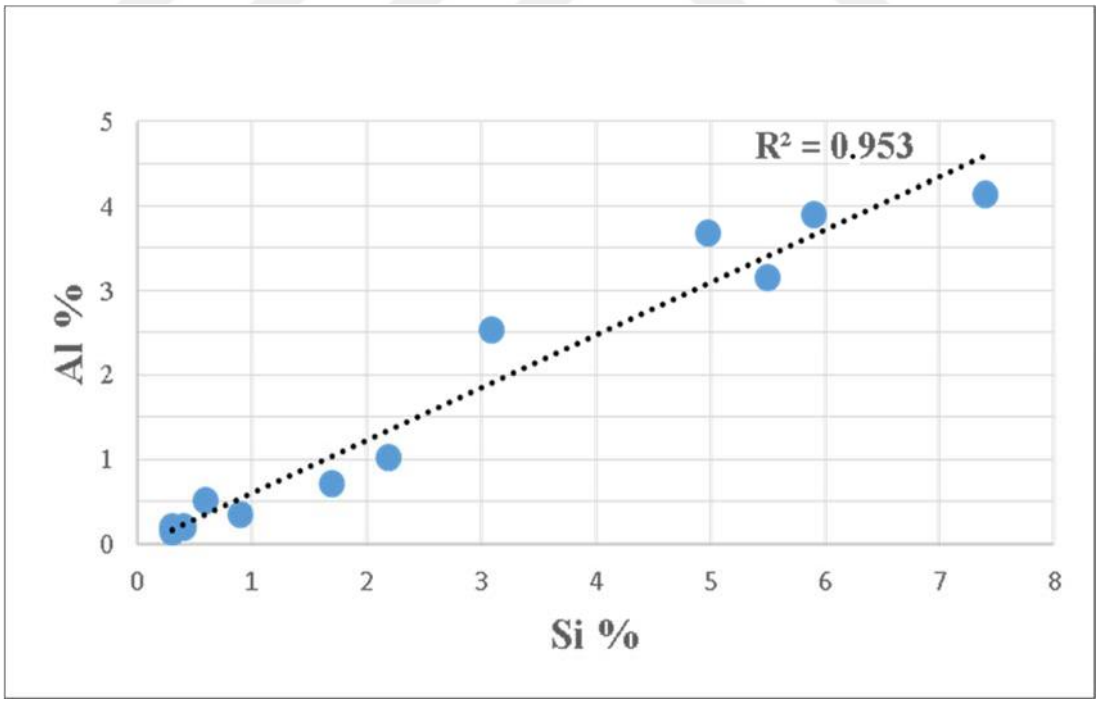

Figure 5.8 Correlation of Si and Al average contents

Iron, which has an average content of 1.57%, shows a higher average value in well I-23 than in the other wells (I-18 and I-25). A moderate positive correlation was observed between Fe and K, Al, Si, P, Mn (r = >0.5). No significant correlation was observed between Fe and Mg, Ca, Ti. Iron might be hosted both within the structure of clay minerals and as independent iron minerals. Iron-bearing phases are identified in the XRD diffractograms as clay minerals and pyrite (FeS_2) in all cores.

No significant relationship was found with other trace elements. Magnesium is generally affiliated with clay minerals and dolomite (Ünal, 2018). It may also originate from fossil shells. Calcium, with an average of 4.34%, has the highest value among the trace elements. The average of the I-25 core samples located in the south-east of the coal field, is 6.68%, which is higher than in other wells. Calcium shows a positive correlation with Mg and ash. Calcite, aragonite, and small amounts of bassanite and gypsum were encountered in the coal samples; the fossil shells may be considered the Ca source. Potassium was calculated to be 0.35%, on average, in the study area. Potassium showed a positive correlation with Al, Fe, Si, and P ($r \geq 0.5$). Potassium in coal is generally affiliated with silicate minerals (r=0.87). Sodium, K, and Al are usually associated with Al-Si-bearing phases (clay minerals, feldspar) and, rarely, with halite (Karayiğit et al., 2000a). The lack of halite mineral from the diffractograms suggests that K is predominantly related with clay minerals, and to a lesser extent with feldspars. Titanium, shows very weak negative to no correlation with Al, Si, Fe, Mg, Ca, K, P and Mn ($r \geq -0.37$). It also shows no significant correlation with ash (r = 0.14). Titanium is contained in clay minerals and micron-sized minerals such as augite, rutile, ilmenite, etc. (Calvert, 1976; Karayiğit and Whateley, 1997; Baba et al., 2008; Karayiğit, 2003). The overall average of P in the basin is 0.03 wt.%. Phosphorus showed moderately strong positive correlation with Si, Al, Fe, K and Mn in coal samples from the basin ($0.65 < r < 0.74$) and a weak negative correlation with ash value. Phosphorus is associated with nutrient-rich environments and is incorporated into organic matter-rich sediments at varying proportions. Apatite, another phosphate source, is typically found in individual grains but can also be present in monazite and calcite. However, monazite and apatite were not recognised in the diffractograms. Comparing the results of XRD analysis with the ash yield values it is evident that moderate correlation exists between the ash and the calcite, and ash and the quartz.

While smectite shows a moderately negative correlation, no correlation was observed between pyrite and ash (r=0.02) (Fig. 5.9).

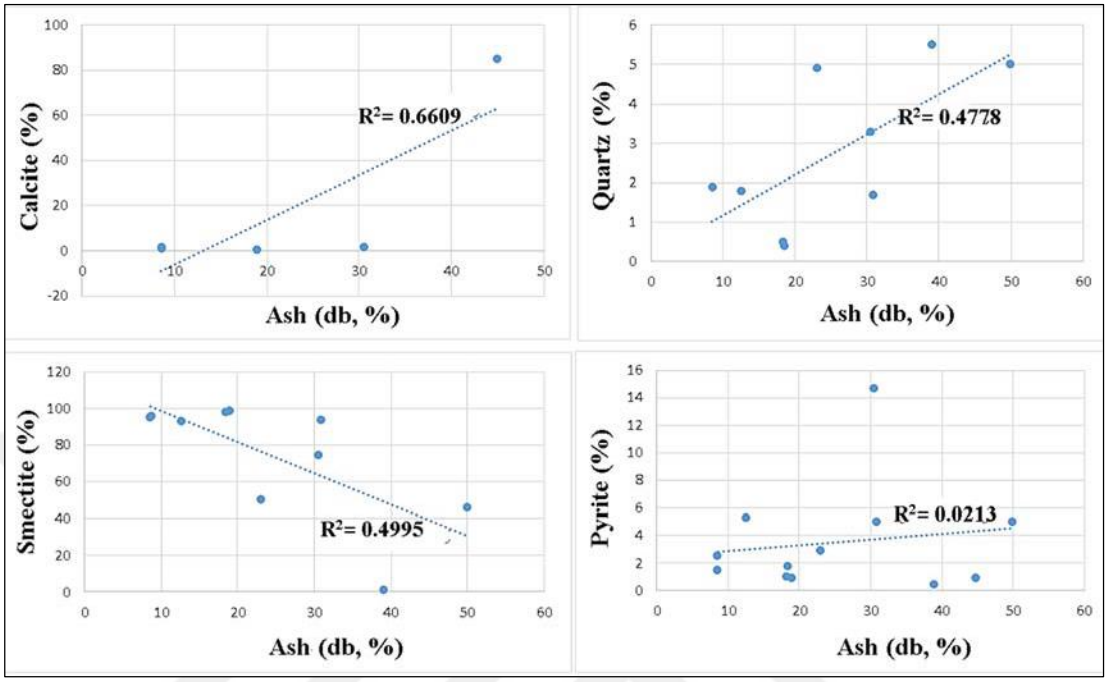

Figure 5.9 Correlation diagrams of ash with calcite, quartz, smectite and pyrite according to XRD results.

The contents of 21 other trace elements (Zn, Ni, As, Se, Rb, Sr, Y, Zr, Nb, Mo, Ag, Cd, Ta, V, Cr, Th, Pb, U, Hg, Bi and Sb) were evaluated through the Pearson correlation coefficient analysis (Table 5.3). The analysis revealed that V shows positive correlation with Ni, Zn, Cu, Rb, Zr, Cd, Y, Cu, Cr and Mo ($0.60<r<0.91$), and negative correlation with Se ($r=-0.53$). The concentration of V in Miocene lignite is interpreted to be related with clay minerals and organic matter (Querol et al. 1996; Finkelman and Gross 1999; Goodarzi 2002). Among clay minerals, it is contained particularly in illite (Finkelman 1980).

Table 5.3 Trace element (ppm) correlation coefficients in the coal samples examined.

Element (ppm)	Ni	Cu	Zn	As	Se	Rb	Sr	Y	Zr	Nb	Mo	Ag	Cd	Ta	V	Cr	Th	Pb	U	Hg	Bi	Sb
Ni	1	0.64	0.63	0.82	-0.50	0.54	0.72	0.74	0.50	-0.38	0.27	-0.53	-0.79	-0.45	0.61	0.72	-0.97	-0.50	0.03	-0.24	0.66	-0.02
Cu		1	0.53	0.30	-0.53	0.48	0.27	0.85	0.36	0.35	0.14	-0.46	-0.70	1.00	0.22	0.30						
Zn			1	0.48	-0.17	0.70	0.00	0.68	0.62	0.04	0.48	-0.18	-0.51	-0.63	0.60	0.64	0.20	-0.15	0.28		-0.28	-0.39
As				1	-0.53	0.43	0.00	0.57	0.58	-0.54	0.16	-0.12	-0.44	-0.49	0.74	0.82	0.30	0.35	0.41	0.89	0.26	-0.26
Se					1	-0.20	-0.03	-0.39	-0.13	0.93	-0.26	-0.14	-0.27	0.63	-0.53	-0.60	-0.92	0.34	-0.62	-0.10		0.38
Rb						1	-0.04	0.45	0.92	0.14	0.26	-0.63	-0.56	0.10	0.91	0.84	-0.29	0.37	-0.26	0.59	-0.35	0.28
Sr							1	0.00	-0.09	0.81	0.01	-0.01	-0.11	0.55	-0.08	0.00	0.49	-0.15	-0.12		-0.30	0.55
Y								1	0.52	-0.22	0.42	-0.33	-0.53	0.09	0.32	0.50	-0.68	-0.17	-0.23	0.21	-0.36	0.60
Zr									1	0.82	0.43	-0.43	-0.45	0.94	0.78	0.85	0.03	0.55	0.67		-0.68	0.23
Nb										1	-0.18	-0.41	-0.27	0.73	-0.29	-0.59	-0.76	0.28	-0.68	-0.36	0.19	0.19
Mo											1	-0.21	-0.17	-0.41	0.12	0.24	-0.02	0.26	0.31	0.34	0.53	0.14
Ag												1	0.56	-0.60	0.06	-0.12	-0.24	-0.27	0.33	0.69	0.08	-0.38
Cd													1	-0.56	0.31	-0.89	-0.16	0.84	-0.09		0.24	-0.22
Ta														1		-0.66	-0.86	0.39	-0.64	-0.43	0.78	-0.23
V															1	0.99						
Cr																1	0.88	-0.45	0.62	-0.35	-1.00	-0.25
Th																	1	0.47	0.76		-0.98	-0.75
Pb																		1	0.02	0.74		0.43
U																			1	0.62	-0.59	0.68
Hg																				1		0.52
Bi																					1	-0.57
Sb																						1

In the study area, the highest vanadium value of 133 ppm was analysed in sample I-23/40 (Table 4.12). It was not detected in samples from borehole I-25, which had a particularly high carbonate content, but was encountered in samples where detrital minerals were detected. It is estimated that V is related to clay minerals rather than organic matter. Nickel showed its lowest values in well I-25 and its highest values in wells I-23 and I-18, which are the richest in Si. Nickel, Cu, Zn, As, Rb, Sr Y, Zr, V, Bi and Cr show high positive correlation ($0.50<r<0.82$), while Ni, Se, Nb, Ag, Cd, Ta, Th and Hg show negative correlation ($-0.02<r<-0.97$). Nickel is found in coals, mostly in association with sulphides (Swaine, 1990, 1995). Nickel, Zn, Y, and Ta show a high positive correlation ($0.53 < r < 1.00$). Silver and Cd show a negative correlation ($-0.46 < r < -0.70$). The Zinc, which has the highest concentrations in cores numbered I-18 and I-23, such as Ni, Cu, Rb, and Y. It has a positive correlation with As, Zr, Mo, V, and Cr ($0.48 < r < 0.70$). A negative correlation has been detected with Se, Ag, Cd, Ta, Pb, Bi, and Sb ($-0.15 < r < -0.63$). Zinc is present in coal along sulphide minerals (e.g., pyrite, sphalerite), carbonates, and, rarely in clays (Karayiğit et al., 2000a; Goodarzi, 2002). Although its association with clays is rare, due to the fact that it offers relatively high values in detritic rather than in carbonates, it may be interpreted as being related to clays (Ünal, 2018). Arsenic shows positive correlation with Sb, Rb, Pb, Th, U, Co, Cu, Y, Zr, V, Cr, and Hg. Arsenic generally shows association with mineral matter (Ward et al., 1999; Dale et al., 1999; Kolker et al., 2000). The extremely low negative correlation observed between As and total sulphur in the examined samples ($r = -0.146$), and the lack of arsenopyrite in XRD and SEM analyses, indicates that the source of arsenic is likely clay minerals.

5.3.2 Characterization of inorganic rocks and inferences

In order to characterize the clastic sediments in the lignite seam roof, floor and the intercalations, three geochemical parameters, namely the SiO_2/Al_2O_3 ratio, the Fe_2O_3/K_2O ratio, and the Ca content (Herron, 1988) were calculated (Table 5.4).

Table 5.4 Oxide contents (in wt.%) of the Yatağan samples.

Core	**I-18**			**I-23**			**I-25**		
Sample #	**12**	**29**	**32**	**41**	**42**	**50**	**1**	**8**	**9**
SiO_2	19.53	38.50	16.68	2.42	13.26	3.64	12.13	5.11	7.81
Al_2O_3	4.91	12.66	6.59	1.36	6.61	3.06	3.59	1.44	3.10
Fe_2O_3	2.85	3.96	2.07	1.14	3.43	2.69	2.49	0.80	1.93
K_2O	0.56	2.93	0.60	0.02	0.48	0.07	0.42	0.22	0.35
log(Fe_2O_3/K_2O)	0.71	0.13	0.54	1.76	0.85	1.58	0.77	0.56	0.74
log(SiO_2/Al_2O_3)	0.60	0.48	0.40	0.25	0.30	0.08	0.53	0.55	0.40

In terrestrial sandstones and shales, the SiO_2/Al_2O_3 ratio distinguishes Si-rich quartz from Al-rich shale; other sand types have values between these two (Herron, 1998). The ratio of total iron (as Fe_2O_3) to K_2O distinguishes lithic sandstone (litharenite and sublitharenite) from feldspathic sandstone (arkose and subarcose), and very high Fe_2O_3/K_2O ratios indicate Fe-rich shales (e.g. pyritic, sideritic, haematitic), depending on the silica/alumina ratio (Herron, 1988). The Log (Fe_2O_3/K_2O) *vs.* Log (SiO_2/Al_2O_3) diagram of the sample dataset is given in Figure 5.10. The element contents of inorganic rock samples from the study area were determined in oxide form by P-XRF analysis, and their logarithmic ratios were entered into the classification scheme. The inorganic rock samples were identified as pyritic shale (Fe-rich shale) and shale.

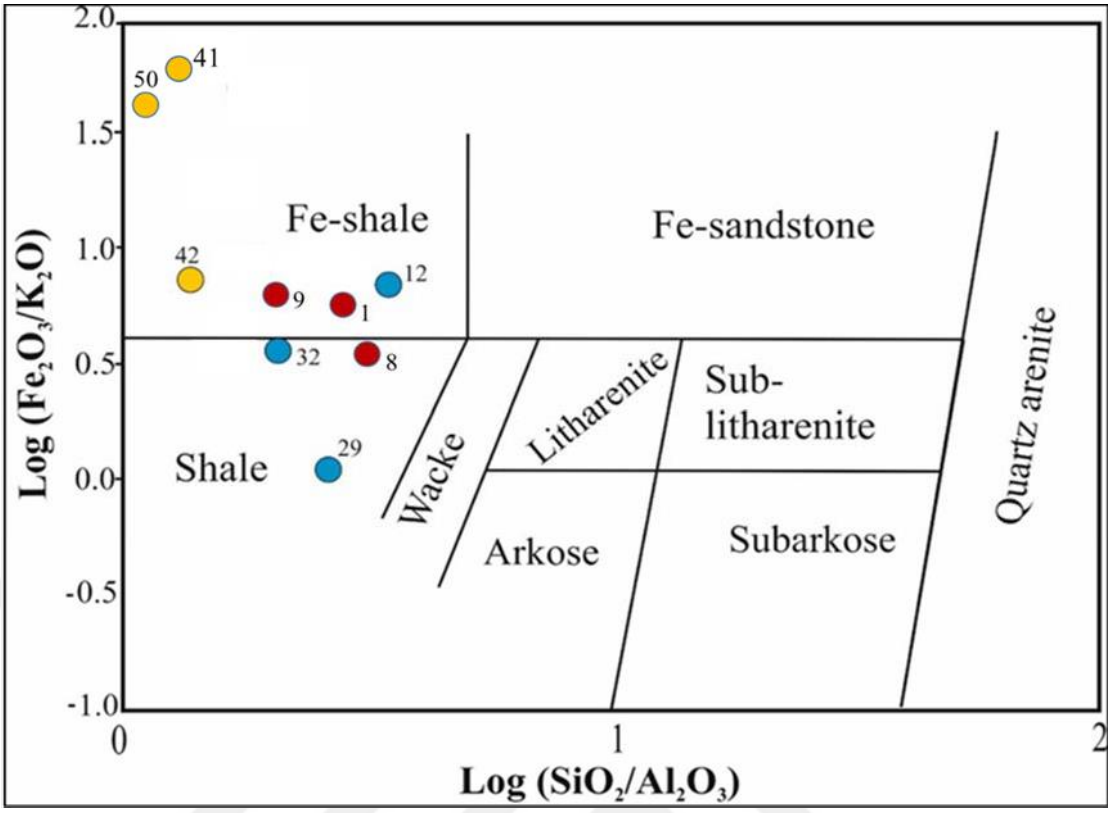

Figure 5.10 Classification of the studied samples using the Log(SiO_2/Al_2O_3) and Log(Fe_2O_3/K_2O) ratios (Herron, 1988).

The mineral matter content of the inorganic components and the coal is crucial for combustion. After combustion, a significant portion of these minerals remains in the ash (Gentzis and Goodarzi, 1997). Coal includes mainly carbonates and sulphides (mainly pyrite) as mineral matter components. Pyrite is primarily formed authigenically, occurring predominantly during the coalification (Querol et al., 1989; Kortenski and Kostova, 1996). It forms haematite (Fe_2O_3) as a result of combustion, which is a determinant for cindering problems. Similarly, lime (CaO) in the ash can be beneficial for binding S, but also it can cause slagging problems as the amount of lime in the ash increases. Clay minerals are another risk determinant for slagging. In addition, the mining of coal along the inorganic materials will increase this slagging tendency by degrading the coal quality. During coal combustion, some of the resulting ash deposits on the surfaces of the boiler tubes due to chemical reactions and physical processes (Zaid et al., 2019). Two types of high-temperature ash deposition are

slagging and fouling, and the difference between these two is the deposition mechanisms involved (Zaid et al., 2019): the former includes the formation of molten, partially fused or re-solidified deposits on surfaces exposed to radiant heat, whereas the latter is defined as the formation of high-temperature, bonded deposits on the surfaces of convective tubes.

Attig and Duzy (1969) developed a slagging and fouling indices, Rs, by multiplying the ratio of the sum of the basic (Fe_2O_3+CaO+MgO+K_2O+Na_2O) to the sum of the acidic oxides (SiO_2+Al_2O_3+TiO_2) in coal ash by the sulfur content of the coal (Table 5.5). The sintering temperatures of ashes with a base/acid ratio below 0.4 range between 950 and 1150°C. The Al_2O_3/SiO_2 ratio is the determining factor (Ural et al., 2002).

Table 5.5 Slagging index parameters

PARAMETER	GUIDELINES	I-18	I-23	I-25
Base/Acid ratio= (Fe_2O_3+CaO+MgO+Na_2O+K_2O)/ (SiO_2+Al_2O_3+TiO_2)	<0.4	0.69	0.49	0.89
Sulphur slagging= (Base/Acid ratio)* Sulphur%	<2.0	2.92	1.89	4.70
Iron Calcium=Fe_2O_3/CaO	<0.3	0.54	0.97	0.08
Alumina Silica ratio=Al_2O_3/SiO_2	<0.4	0.52	0.54	0.58

According to the above values, all the parameters related to slagging and fouling properties are elevated. The Iron/Calcium ratio is very low in only sample from I-25 drillhole. This very low value is affiliated with the presence of Ca bearing litologies in proximity of the samples. The low sulphur slagging ratio in samples from I-23 on the other hand, might be related to abundance of pyrite in the related samples.

Inorganic components and the mineral content of coal also have very important effects on self-combustion properties of coal. Low-rank coals with high moisture can lead to oxidation and overheating, which can cause spontaneous combustion. Coal

with a high ash yield has a lower oxidation potential. Substances such as lime, iron and soda in the ash accelerate oxidation, while silica and aluminium can slow it down (Didari, 1986; Ökten, 1988). Pyrite is present in coal in varying concentrations and is easily oxidised. When in contact with moist air, the resulting oxidation process generates heat, which can lead to overheating and spontaneous combustion.

A coal fire disaster creates thermal and dynamic hazards, including the risk of gas and dust explosions, production of greenhouse and toxic gases, deterioration in coal quality, loss of coal and loss of lives. Mining activities can be minimised by taking these risks into consideration and working in detail.

5.4 Evaluation ofthe Coal Petrography Data in relation with the Available Borehole Spatial Data.

The available drillhole data including the ones used in this work and the previous work on core B-22 by Erecek (2024), were marked on the location map, and then carefully assessed for the intersected coal seam depths and coal petrographic data obtained. A NNW-SSE oriented cross-section is constructed by projecting the available borehole data (Fig. 5.11).

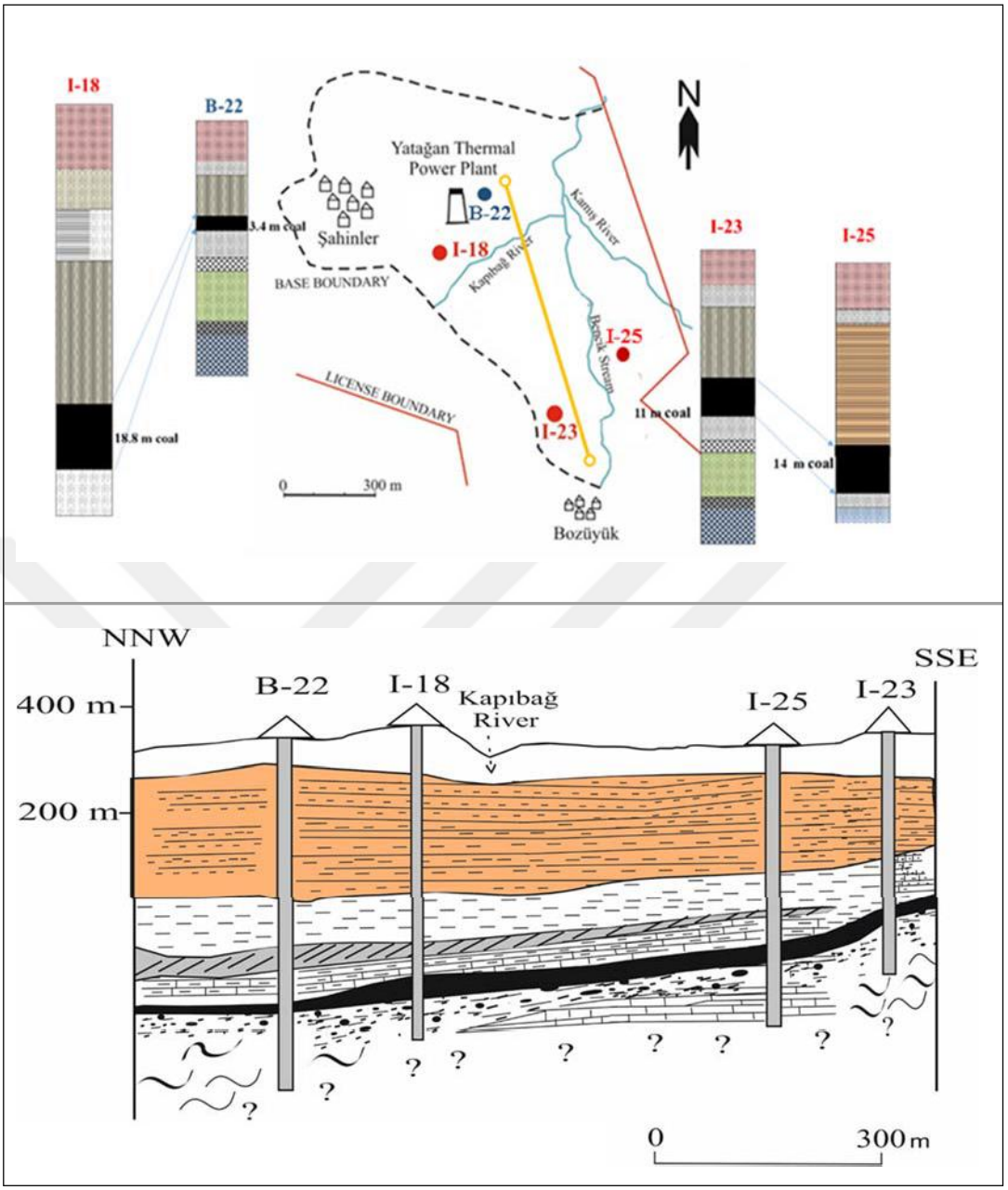

Figure 5.11 Location of four boreholes (I-18, I-23, I-25 and B-22, the latter studied by Erecek, 2024) of the Yatağan coal field, and the cross-section constructed by projection of the boreholes along an arbitrary NNW-SSE profile. The topographic relief is drawn hypothetically taking the starting elevations (Z) of the boreholes and the river beds crossed into account.

According to borehole data, coal core I-18 is the thickest (18.8 m) in the middle of the basin. In the B-22 drilling, a 3.4-m-thick coal seam was reached at a depth of 575 m. The basement rocks (schist) were reached at a depth of 594 meters, making it the deepest drilling in the field compared to other drillings. Drilling I-23 reached the coal seam at a depth of 291.3 m and basement rocks (schist) at a depth of 354 m. Compared

to other boreholes, it has been determined that the coal seam and bedrock are located at an elevation approximately 200 m higher. This situation may be related to the the plunge of the coal seam towards northeast, which is also supported by the cross-section drawn along the NNW-SSE profile (Fig. 5.11). However, as no other data obtained from other completed boreholes in the coal field is available in this study, no further conclusions will be made.

When the data obtained from the petrographic analysis were compared, no significant difference is encountered between the data obtained from individual coal samples from different depths (Fig. 5.12; Table 4.4-6). This similarity suggests that all samples studied represent a single coal seam despite the differences in sampling depths, and supports the above correlative interpretation of the available coal borehole data.

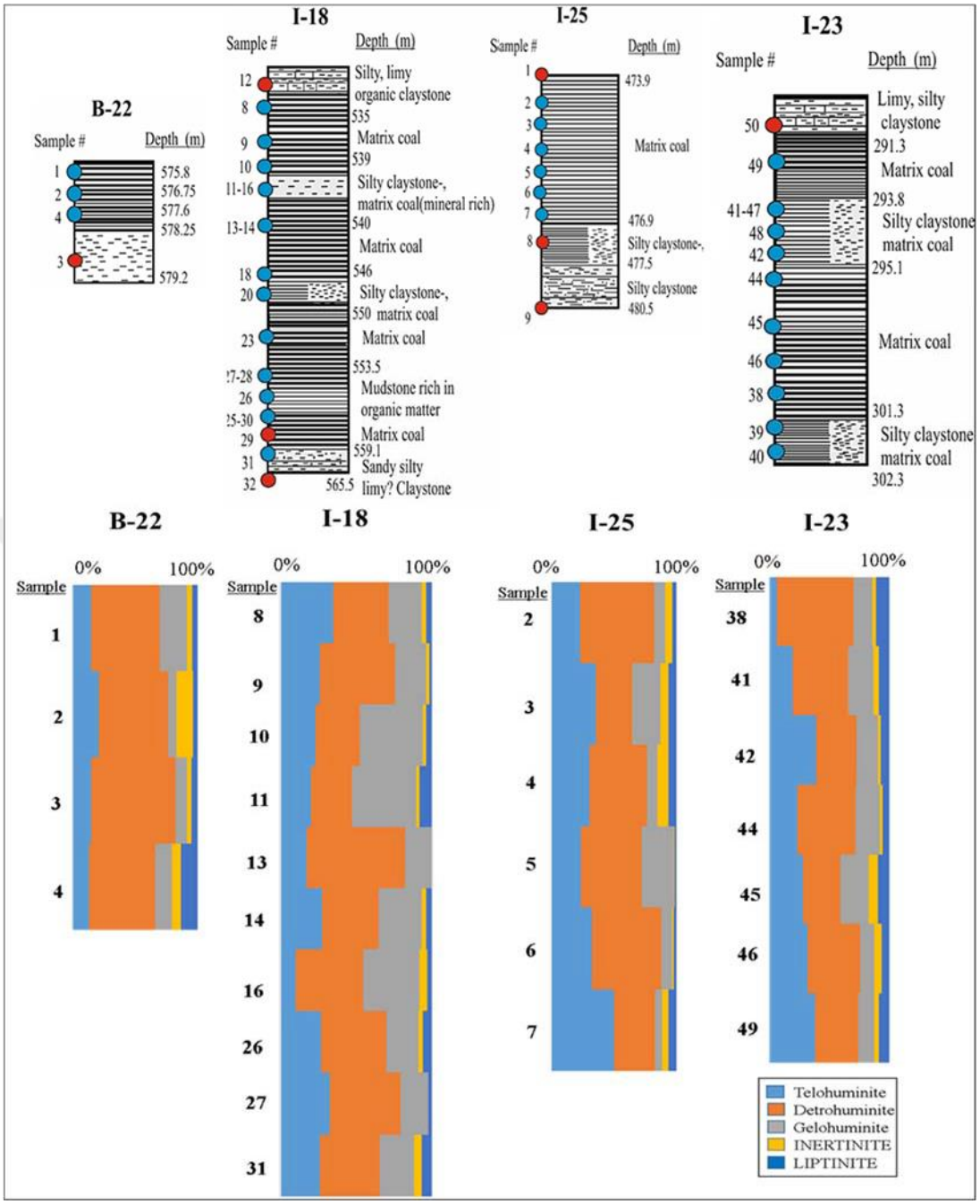

Figure 5.12 Maceral group composition in volume %, on mineral matter-free basis (mmf) of the wells I-18, I-23, and I-25 from this study, and B-22 from Erecek (2024).

5.5 Comparison of Reflectance Measurements between Huminite Macerals

Additional reflectance measurements on huminite macerals other than ulminite B, are made searching for an alternative approach to reflectance values for coals significantly low in ulminite B, has shown that the mean reflectance values of ulminite B, corpohuminite, and gelinite are quite similar (Table 4.9). The values of ulminite A are substantially lower. Furthermore, a strong positive correlation was found between the mean corpohuminite and gelinite values ($R^2 = 0.94$) at the $\alpha = 0.05$ significance level (Table 5.6, Fig. 5.13).

Table 5.6 Correlation coefficients among the reflectance values of some huminite macerals from Yatağan coal samples.

	Ulminite-A	Ulminite-B	Corpohuminite	Gelinite
Ulminite-A	1			
Ulminite-B	-0.499	1		
Corpohuminite	0.030	0.039	1	
Gelinite	-0.145	0.234	0.967	1

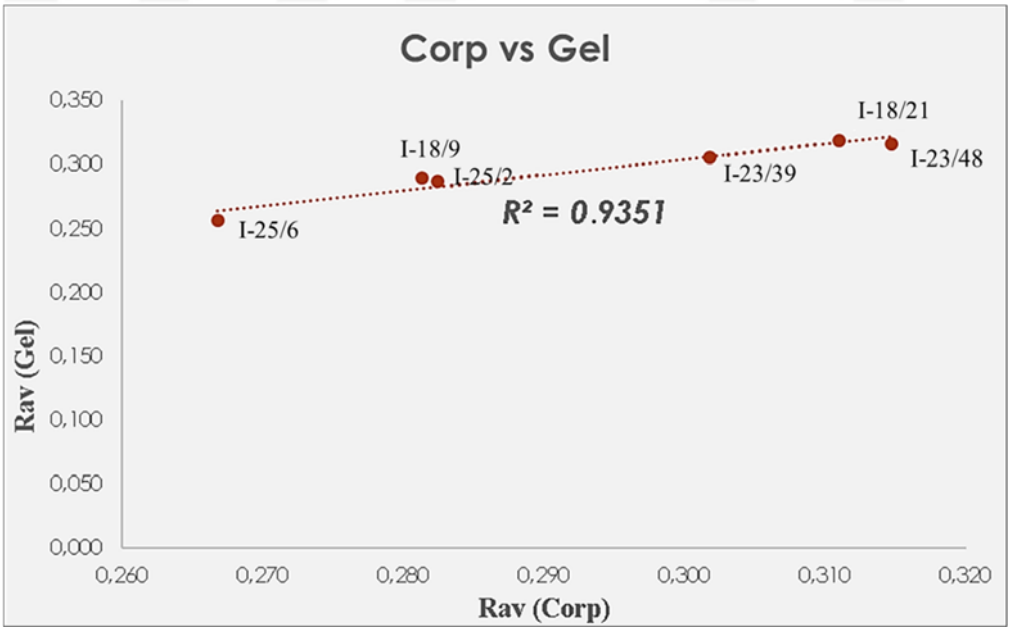

Figure 5.13 The correlation between mean corpohuminite and gelinite reflectance values.

The data and the above statistical analysis, despite the small number of samples examined, encourages further alternative measurement trials for samples poor in ulminite B for investigation using larger data sets from coals of different rank.

5.6 Comparison to other coal fields in the Muğla Basin

The Yatağan coal can be compared with other coals (Alatepe, Bağyaka, Bayır, Çakıralan, Ekizköy, Eskihisar, Hüsamlar, Sekköy, and Tınaz) in the Miocene Muğla Basin in terms of petrographic, mineralogical, and geochemical characteristics. According to the results of the study conducted by Querol et al. (1999), the coal in the basin is characterised by a high huminite content, particularly gelinite. In the Hüsamlar coal field, Büçkün et al. (2015) found that the coal has a very high huminite content and belongs mainly to the telohuminite and detrohuminite macerals subgroups. The Yatağan coal is also characterised by a high huminite content, particularly detrohuminite. During the Early-Middle Miocene, the palaeoenvironmental conditions in the Muğla Basin favoured the development of several topogenous mires (fens) on the fluvial sediments of Turgut Formation (Fig. 2.3). Surface and groundwater supplied the fens with water, transporting clastic input, which provided detritic minerals like quartz, calcite and clay minerals from the basin margins into the palaeomires (Querol et al., 1999).

The limnotelmatic conditions dominated at several places of the broad basin and resulted in the formation of peatlands; hence, coal deposits between 7 and 13 m thick were formed, except the 1.7-m-thick Alatepe coal deposit (Tuncalı et al., 2002). The coal in the Muğla Basin yields ash ranging between 15% and 32% (db), except for the Alatepe coalfield, which displays an ash yield of only 15% (Tuncalı et al., 2002; Table 5.7; Fig. 5.14). The coal seams in the basin is of low-rank C (lignite), displaying random huminite reflectance values between 0.23 and 0.34%, with the exception of Alatepe coal which reveals 0.47% (Tuncalı et al., 2002).

Table 5. 7 Ash, volatile matter (VM), and fixed carbon (Cfix) yields, as well as sulphur content and calorific value (CV) of coal samples obtained from various lignite fields in the Muğla Basin (MTA, 2010).

Basin	Coal field	Ash (%, db)	VM (%, daf)	Sulphur (%, db)	CV (MJ/kg, daf)
Milas	Sekköy	24.87	65.07	4.14	23.0
	Ekizköy	23.37	63.49	5.02	22.2
	Hüsamlar	20.06	57.03	4.20	23.5
	Alatepe	15.07	51.62	5.63	26.2
Yatağan	Eskihisar	23.31	58.44	2.89	24.2
	Tınaz	31.20	60.17	3.47	23.4
	Bağyaka	31.04	63.88	3.10	21.4
	Bayır	32.42	63.26	5.30	21.7
	this study	20.49	49.02	3.78	nd

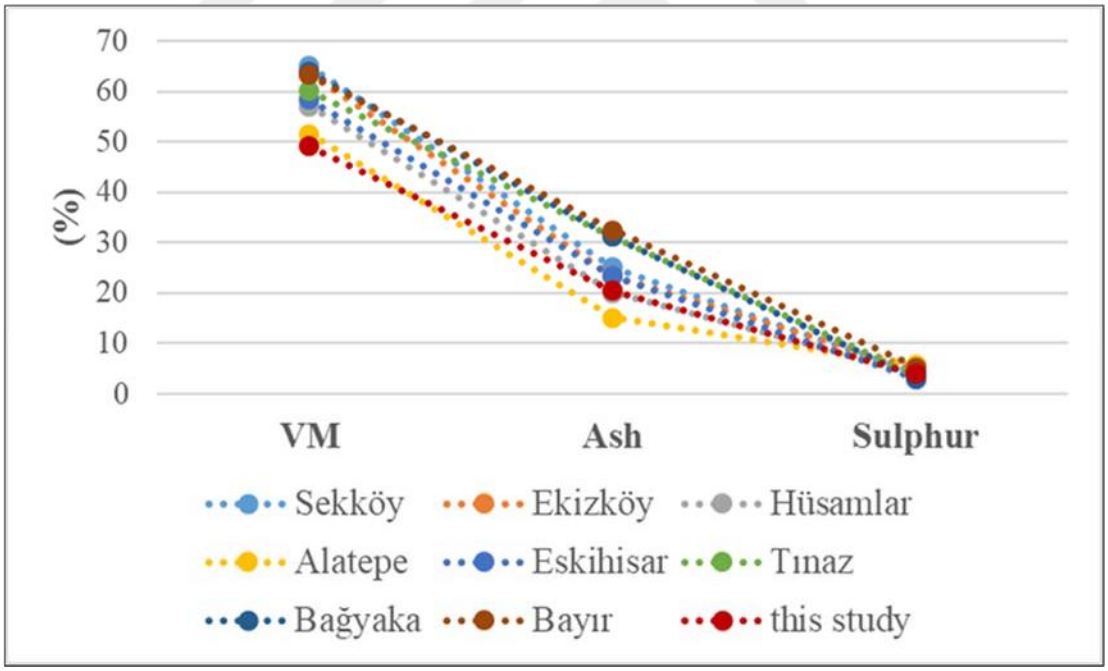

Figure 5.14 Ash, volatile matter (VM), and sulphur contents of coal fields in the Muğla Basin.

The Muğla coals, in general, display high ash yield (16-56%, db) and sulphur content (2.1-5.7%, db), and are characterised by high huminite content, mainly gelinite (Querol et al., 1999; Büçkün et al., 2015). Saturation and aromatic biomarker data from

Middle Miocene coals in the Ekizköy (Muğla-Milas) region indicate that the coals were deposited in a lacustrine environment under suboxic conditions and derived from terrestrial organic matter (Hoş-Çebi, 2024). The climate was probably humid and warm.

The fossil record of the mid-late Middle Miocene coal deposits also points to a freshwater lacustrine environment and warm, temperate climatic conditions (Yılmaz et al., 2020).

Querol et al. (1999) noted that the main mineral impurity in the Sekköy and Ekizköy lignite deposits is calcite. In other lignite samples, such as those from the Yatağan coalfield, clay minerals and quartz are included. Traces of aragonite, along with small amounts of pyrite, opal and gypsum, are also identified. The researchers suggested that the differentiation of these two lignite types resulted from the simultaneous development of high detrital input and carbonate-rich lakes/peatlands.

Summing up, the Yatağan lignite shows genetic similarities with other lignite deposits in Muğla Basin and several other Tertiary lignite deposits of Türkiye (Gürdal and Bozcu, 2011; Karayiğit et al., 2015)

CHAPTER SIX
CONCLUSION

This study is based on samples taken from three coal exploration boreholes (I-18, I-23 and I-25), which are located near the Yatağan Thermal Power Plant in Muğla Province. In this context, organic petrographic analyses are performed to reconstruct the depositional palaeoenvironment. The mineralogical and elemental compositions of coal, floor, roof and intercalation samples are also determined using XRD and P-XRF analyses. The main results can be summarised as follows:

The average total moisture of the coal is 35%; the ash yield 33% (db); the volatile matter yield 58% (daf); the fixed carbon content 42% (daf); the total sulphur content 2.5% (ar); and the gross calorific value as 12.18 MJ/kg (maf). These values indicate a rank between peat and lignite.

When coal samples are examined under a microscope, the predominance of huminite maceral (>78.7 vol%, mmf) is obvious. Liptinite group is up to 10.7% (average: 5%) and inertinite is up to 9.0% (average: 4%). The mean random huminite reflectance varies between 0.23 and 0.33%. Based on these values, the Yatağan coal is classified as lignite according to the ASTM, and as soft brown coal with respect to the German DIN classification. In the ECE-UN (1998) classification scheme, the humic Yatağan coal is of low-rank C or ortholignite, and the quality varies greatly from very low to high grade. The low huminite reflectance also confirms the low rank.

The palaeoenvironmental setting was a topogenous mire (fen) supplied with surface and groundwater. The surface water washed out and transported dissolved ions and inorganic clastic material, mainly clay minerals and quartz, from the margins of the basin into the palaeomire, resulting in medium to high ash yields. The peat-forming vegetation comprised mainly herbaceous plants (reeds, sedges), and the bacterial activity in the palaeomire was intense. In general, the groundwater table was relatively high, and wet telmatic to limnotelmatic conditions and a moderate mire-substrate subsidence prevailed during peat accumulation.

The high mineral content of the lignite increases the tendency for boiler fouling and slagging in pulverised coal combustion systems. The Yatağan lignite displays high risk for boiler fouling and slagging.

Reflectance measurements performed on Yatağan coal samples, including ulminite A and B, as well as gelinite and corpohuminite maceralshas revealed that the average reflectance values for ulminite B, copohuminite and gelinite were quite similar, while the values for ulminite A were essentially lower. These findings suggest that, despite the small number of samples examined, this could be an additional alternative measurement method applicable to samples poor in ulminite B.

The samples from the Yatağan coal deposit under investigation has shown similarities with other coal deposits in the Muğla Basin in terms of their petrological, mineralogical and palaeoenvironmental conditions.

REFERENCES

Abdülselamoğlu, Ş., (1965). Muğla-Yatağan çevresinde görülen jeolojik formasyonların korelasyonları hakkında rapor: Maden Tetkik Arama Enst., Rap. no., 3497 Ankara.

Algan, Ö., (2023) *Yatağan Ovası ve Yakın Çevresi (Muğla) Jeomorfolojisi Ve Doğal Ortam İnsan İlişkileri.* Yüksek Lisans Tezi, Afyon Kocatepe Universitesi, Afyon.

Aşar, Z., (2006). *Ankara Üniversitesi Fen Bilimleri Enstitüsü Yüksek Lisans Tezi İleri Teknoloji Elementlerinin (Ga-Ge-Se-Te) Bazı Kömür Yataklarındaki Konsantrasyonlarının Araştırılması.* Yüksek Lisans Tezi, Ankara Üniversitesi, Ankara.

Atalay, Z., (1980). Muğla-Yatağan ve yakın dolayı karasal Neojeninin stratigrafi araştırması. *Türkiye Jeoloji Bülteni*, 23, 1, 93-99, Ankara.

Atalay, Y., (1993). Yatağan linyitlerindeki uranyumun sağlık ve ekonomik yönünden incelenmesi M.T.A. *Doğal kaynaklar ve Ekonomi Bülteni* sayı.2

Attig, R.C.,& Duzy, A. F., (1969) American Power Conf., Dlinois Ins. of Tech.

Baba, A., Save, D., Gündüz, O., Gürdal, G., Bozcu, M., Sülün, S., et al., (2008). Çan Kömür Havzasındaki madencilik faaliyetlerinin tıbbı jeoloji açısından değerlendirilmesi. ÇAYDAG-106Y041 nolu proje raporu, 479 s.

Becker-Platen, J.D., (1970). Lithostratigraphische Untersuhungen in Kanazoikum SüdwestAnatoliens (Kanozoikum und Braunkohlen der Türkei-2) Geologische Jb., 97, 244, Hannover.

Boggs, Jr. S. (2009). Petrology of sedimentary rocks. Cambridge University Press, UK, 2nd edition, 600 p.

Bouška, V., Pešek, J., & Sýkorová, I. (2000). Probable modes of occurrence of chemical elements in coal. Acta Montana Serie B, Fuel, Carbon, Mineral Processing, Praha 10 (117), 53–90.

Büçkün, Z. (2013). *Coal Quality of the Miocene Muğla-Hüsamlar Lignite*. Master's Thesis, Dokuz Eylül University, İzmir.

Büçkün, Z., İnaner, H., Oskay, R.G. & Christanis, K. (2015). Palaeoenvironmental reconstruction of Hüsamlar coal seam, SW Türkiye. Journal of Earth System Science 124(4):729-746. DOI:10.1007/s12040-015-0573-x

Bürküt, Y. (1998). Türkiye linyitlerinin jeokimyasal ve termik etüdü İ.T.Ü. Maden Fakültesi İstanbul.

Calvert, S.E. (1976). The mineralogy and geochemistry of near shore sediments. In: Riley JP, Chester R (Eds.). *Chemical oceanography*, Academic Press, London, pp.187280.

Casagrande, D.J. (1987). Sulphur in peat and coal. Coal and coal-bearing strata: recent advances, ed Scott AC, *Geological Society Special Publication*, pp. 87-105.

Dai, S., Ren, D., Tang, Y., Yue, M. & Hao, L. (2005). Concentration and distribution of elements in Late Permian coals from western Guizhou Province, China.

Dai, S., Seredin, V.V., Ward, C.R., Hower, J.C., Xing, Y., Zhang, et al. (2015). Enrichment of U–Se–Mo–Re–V in coals preserved within marine carbonate successions: Geochemical and mineralogical data from the Late Permian Guiding Coalfield, Guizhou, China. Mineralium Deposita 2015, 50, 159–186.

Dai, S., Graham, I.T. & Ward, C.R. (2016). A review of anomalous rare earth elements and yttrium in coal. *Inernational Journal of Coal Geology,* 2016, 159, 82–95.

Dale, L.S., Chapman, J.F., Buchanan, S.J. & Lavrencic, S.A. (1999). Mechanisms for trace element partitioning in Australian Coals, Project 4.2, Final Report, Cooperative Research Centre for Black Coal Utilisation.

Didari, V. (1986). Yeraltı ocaklarında kömürün kendiliğinden yanması ve risk indeksleri. *Madencilik,* cilt 25, ss.31-32, 1986.

Ediger, V.Ş., Berk, I. & Kösebalaban, A. (2014). Lignite resources of Türkiye: Geology, reserves, and exploration history, *International Journal of Coal Geology* 132, 13–22.

Electricity Generation Co. Inc. (EÜAŞ) (2014). Annual Report of 2013, Ankara, 81 pp (http://www.euas.gov.tr/Sayfalar/YillikRaporlar.aspx).

Engin, H. (1999). *Muğla-Yatağan linyitlerinin jeolojisi ve jeokimyası*. Doktora Tezi, İstanbul Üniversitesi, İstanbul.

Erecek, B. (2020). *Muğla-Yatağan Güneybatısında Yer Alan (Şahinler-Bozüyük Arası) Linyit Sahasının Kömür Petrografisinin İncelenmesi.* Bitirme Tezi, Dokuz Eylül Üniversitesi, İzmir.

Erecek, B. (2024). *Investigation of the Petrographic, Mineralogical and Geochemical Composition of the Coal from the Current Muğla-Yatağan Coal Fıeld Drilling Data.* Master's thesis, Dokuz Eylül University, İzmir.

ETKB (Enerji ve Tabii Kaynaklar Bakanlığı), (2017). Dünya ve Türkiye Enerji ve Tabii Kaynaklar görünümü, 2024.

Finkelman, R.B. (1980). *Modes of occurrence of trace elements in coal*. PhD Thesis, University of Maryland, 301 pp.

Finkelman, R.B. (1995). Modes of occurrences of environmentally-sensitive trace elements in coal. In: Environmental Aspects of Trace Elements in Coal. Swaine, D.J., Goodarzi, F. (eds), The Netherlands: Kluwer Academic Publishers, pp. 24-44.

Finkelman, R.B. & Gross, P.M.K. (1999). The types of data needed for assessing the environmental and human health impacts of coal. *International Journal of Coal Geology*, 40: 91-101.

Gentzis, T. & Goodarzi, F. (1997).Trace Element Geochemistry of Brackish-Water Coals in the Central Alberta Plains, Canada, *Energy Sources*, Vol.19, Pages 493-505.

Gonçalves, P.A., Kus, J., Hackley, P.C., Borrego, A.G., Hámor-Vidó, M., Kalkreuth, W., et al. (2024). The petrology of dispersed organic matter in sedimentary rocks: Review and update. *International Coal Geology Reviews*, 294: 104604, https://doi.org/10.1016/j.coal.2024.104604.

Goodarzi, F. (2002). Mineralogy, elemental composition and modes of occurrence of elements in Canadian feed-coals. Fuel, 81: 1199-1213.

Gold, O. (1965). Linyit Etüdü (Jeoloji), Cilt II, MTA Publish, Ankara.

Gökçen, N. (1982). Denizli ve Muğla çevresi neojen istifinin ostrokod biostratigrafisi, *Yerbilimleri*, sayı.9, sayfa.111-131 Ankara.

Gökmen, V. (1980). *Muğla Yatağan-Eskihisar bölgesi linyit yatakları jeolojisi, sondaj ve sonuçları*, İ.Ü.F.F. mineroloji ve petrografi kürsüsü diploma çalışması

Gökmen, V., Memikoğlu, O., Dağlı M., Öz, D. & Tuncalı, E. (1993). Lignite Inventory of Türkiye. Mineral Research and Exploration Directorate Publ., Ankara.

Göktaş, F. (1982). Muğla Bölgesi civarı Senezoik yaşlı sedimanter kayaçların sedimantolojik ve paleocoğrafik incelenmesi. *MTA Rapor no*. 519, 84p.

Güney Ege Linyit İşletmesi (GELİ), (2005). Türkiye Kömür İşletmeleri Genel Müdürlüğü Güney Ege Linyitleri İşletmesi Müessesesi Müdürlüğü Haziran 2005 raporu.

Gürdal, G. & Bozcu, M. (2011). Petrographic characteristics and depositional environment of Miocene Çan coals, Çanakkale-Türkiye, January 2011, *International Journal of Coal Geology* 85(1):143-160

Gürer, Ö.F., Sangu, E., Özburan, M., Gürbüz, A. & Sarıca Filoreau N. (2013). Complex basin evolution in the Gökova Region: implications on the Late Cenozoic tectonics of southwest Türkiye. *International Journal of Earth Science* 102, 2199-222. doi: 10.1007/s00531- 013-0909-1

Gürsoy, E.M., Ünal, D., Tan, T., Sun, S., Karahan, C., Aydın, H., et al. (1993). Coal Inventory. *MTA Aegean Region Directorate Report*, Izmir (in Turkish).

Hacımustafaoğlu, I., Akbulut, M., İnaner, H. & Christanis, K. (2023). Şahinler–Bozüyük Linyit Yatağının (Muğla-Yatağan, GB Türkiye) Jeolojik Konumu ve Hüminit Yansıtmalarının Ölçümü [Conference presentation abstract]. Seventy-fifth Geological Congress of Türkiye with International Participation, Ankara, Türkiye. https://www.jmo.org.tr/resimler/ekler/24f25904af8a59f_ek.pdf

Hacımustafaoğlu, I., Akbulut, M., İnaner, H. & Christanis, K. (2025). Preliminary petrological, mineralogical, and geochemical evaluation of a newly discovered lignite field in Yatağan, Muğla (SW Türkiye). *Turkish Journal of Earth Sciences*, 34: 734-753.

Helvacı, C. & Yağmurlu, F. (1995). Geological setting and economic potential of the lignite and evaporite-bearing Neogene basins of western Anatolia, Türkiye. *Israel Earth Sciences*, 44: 91-105.

Hoş-Çebi, F. (2016). Organic Geochemistry and Paleoclimate Conditions of the Early-Middle Miocene Coals at the Ekizköy (Muğla-Milas). *Journal of Geological Engineering* 40(2), 209-226, ISSN1016-9172, 2016 Research Article

International Committee for Coal Petrology (ICCP), (1998). The new vitrinite classification (ICCP System 1994). *Fuel*, 77: 349-358.

International Committee for Coal Petrology (ICCP), (2001). The new inertinite classification (ICCP System 1994). *Fuel*, 80: 459-471.

International Organization for Standardization (ISO) 7404-2 (2009). Methods for the Petrographic Analysis of Bituminous Coal and Anthracite — Part 2: Method for Preparing Coal Samples, Geneva, Switzerland.

International Organization for Standardization (ISO) 7404-3 (2009). Methods for the Petrographic Analysis of Coals — Part 3: Method of Determining Maceral Group Composition. International Organization for Standardization, Geneva, Switzerland.

International Organization for Standardization (ISO) 7404-5, (2004). Methods for the Petrographic Analysis of Bituminous Coal and Anthracite — Part 5: Method of Determining Microscopically the Reflectance of Vitrinite, International Organization for Standardization, Geneva, Switzerland.

Iordanidis, A. & Georgakopoulos, A. (2003). Pliocene lignites from Apofysis mine, Amynteo basin, Northwestern Greece: petrographical characteristics and depositional environment. *International Journal of Coal Geology* 54, 57-68. doi:10.1016/S0166-5162(03)0009-3.

İnaner, H. (1994). *Evaluation of lignite deposits of Southwestern Türkiye*. PhD. Thesis, Dokuz Eylul University, İzmir (in Turkish with English abstract).

İnaner, H. & Nakoman E. (1997). Turkish lignite deposits. In Gayer, R., Pesek, J.(eds), European Coal Geology and Technology. Geol. Soc. London, Spec. Publ., 125,77-99.

İnaner, H. & Nakoman, E. (2001a). Importance of lignite deposits in Türkiye's energy policy and measures taken for environmental protection. *Int. Acta Univ. Carolinae-Geologica*, 45: 27–31.

İnaner, H. & Nakoman, E. (2001b). Obtaining various results in coal reserve estimations on Husamlar deposit. International Earth Sciences Colloquium on the Aegean Region, (IESCA 2000), Proceedings, Izmir-Türkiye, pp. 143–150.

Karayiğit, A.İ. & Whateley, M.K.G. (1997). Properties of a lacustrine subbituminous (k1) seam, with special reference to the contact metamorphism, Soma Türkiye. *International Journal of Coal Geology*, 34: 131-155.

Karayiğit, A.İ., Gayer, R.A., Querol, X. & Onocak, T. (2000 a). Contents of major and trace elements in feed coals from Turkish coal-fired power plants, *International Journal of Coal Geology*, 44 (2): 169-184.

Karayiğit, A.İ., Spears, D.A. & Booth, C.A. (2000b). Antimony and arsenic anomalies in the coal seams from the Gokler Coalfield, Gediz, Türkiye. *International Journal of Coal Geology*, 44 (1): 1 -17.

Karayiğit, A.İ., Spears, D.A., & Booth, C.A. (2000c). Distribution of environmental sensitive trace elements in the Eocene Sorgun coals, Gediz, Türkiye, *International Journal of Coal Geology*, 42 (4): 297- 314.

Karayiğit, A.İ. (2003). Mineralogy and trace element contents of the Upper Carboniferous Coals from the Asma-Dilaver and Gelik Mines in Zonguldak, Türkiye. *Energy Sources*, 25 (7): 689-702.

Karayiğit, A.İ. & Çelik, Y. (2003). Mineral matter and trace elements in Miocene Coals of the Tunçbilek-Domanik Basin, Kutahya, Türkiye. *Energy Sources*, 25 (4): 339- 355.

Kavuşan, G. (1974). *Muğla ili Yatağan ilçesi Eskihisar köyü civarı linyitlerinin etüdü.* Yüksek Lisans Tezi, 94s., Ankara Üniversitesi.

Kaye, J.P. & Hart, S.C. (1997). Competition for nitrogen between plants and soil microorganisms. *Trends Ecol Evol*., 12: 139–143.

Kavuşan, G. (1974). *Muğla ili Yatağan ilçesi Eskihisar köyü civarı linyitlerinin etüdü.* Yüksek Lisans tezi, 94s., Ankara Üniversitesi.

Kayseri, M.S. (2010). *Oligo-Miocene palynology, palaeobotany, vertebrate, marine faunas, palaeoclimatology and palaeovegetation of the Ören Basin (North of the Gökova Gulf), Western Anatolia*. PhD Thesis, Dokuz Eylül University, İzmir.

Kırhan, Ş., İnaner, H., Nakoman, E. & Karayiğit, A.İ. (2007). Economics Planning and Policy. *Energy sources*, Part B-2 (1): 85-91.

Kolker, A., Huggins, F.E., Palmer, C.A., Shah, N., Crowley, S.S., Huffman, G.P., et al. (2000). Modes of occurrence of arsenic in four US coals. *Fuel Processing Technology*, 63: 167-178.

Kortenski, J. & Kostova, I. (1996). Occurrence and morphology of pyrite in Bulgarian coals. *International Journal of Coal Geology*, 29: 273-290.

Leflef, D. & Hakyemez, Y. (1979). Muğla ve civarı Tersiyer havzalarının sedimantolojik ve paleocografik etüdüne ilişkin ön rapor. 13s. MTA Arşiv No: 6562, Ankara

Maden Tetkik ve Arama Genel Müdürlüğü (2010). General Directorate of Mineral Research and Exploration, Inventory of Turkish lignites. Ankara: MTA Publication (in Turkish).

Mukhopadhyay, P. (1989). Organic petrography and organic geochemistry of Tertiary coals from Texas in relation to depositional environment and hydrocarbon generation. *Report of Investigations. Bureau of Economic Geol.*, Texas. 118 pp.

Nakoman, E. & İnaner, H. (1990). Lignite deposits of southwestern Türkiye, Dokuz Eylül Üniversitesi Mühendislik Fakültesi Jeoloji Mühendisliği Bölümü, İzmir

Ökten, G. (1988). Kömürün kendiliğinden yanması ve önlenmesi için alınacak tedbirler. *Kömür Kimyası ve Teknolojisi*, O. Kural (Editör), İstanbul, s.103-113.

Petersen, H.I. & Nielsen, L.H. (1995). Controls on peat accumulation and depositional environments of a coal-bearing coastal plain succession of a pull-apart basin; a petrographic, geochemical and sedimentological study, Lower Jurassic, Denmark. *International Journal of Coal Geology*, 27: 99-129.

Reddy, B.R. & Vinu, R. (2018). Feedstock Characterization for Pyrolysis and Gasification. In: S. De et al. (eds.), *Coal and BiomassGasification, Energy, Environment, and Sustainability*, 35-36. http://doi.org/10.1007/978-981-10-7335-9_1

Querol, X., Alastuey, A., Plana, F., Lopez-Soler, A., Tuncali, E., Toprak, S., et al. (1999). Coal geology and coal quality of the Miocene Mugla basin, southwestern Anatolia, Türkiye. *International Journal of Coal Geology*, 41(4): 311-332.

Siavalas, G., Linou, M., Chatziapostolou, A., Kalaitzidis, S., Papaefthymiou, H. & Christanis, K. (2009). Palaeoenvironment of Seam I in the Marathousa Lignite Mine, Megalopolis Basin (Southern Greece). *International Journal of Coal Geology*, 78: 233-248.

Singh, P.K., Rajak, P.K., Singh, M.P.,Singh, V.K. & Naik, A.S. (2016). Geochemistry of Kasnau-Matasukh lignites, Nagaur Basin, Rajatshan (India). *International Journal of Coal Science Technology*, 3(2): 104-122. DOI 10.1007/s40789-016-0135-0.

Speight, J.G. (2005). Handbook of coal analysis. *Wiley Interscience*, New Jersey.

Suárez-Ruiz, I., Flores, D., Filho, J.G.M. & Hackley, P.C. (2012). Review and update of the applications of organic petrology: Part 1, geological applications. *International Journal of Coal Geology*, 99: 54-112. https://doi.org/10.1016/j.coal.2012.02.004.

Swaine, D.J. (1990). Trace Elements in Coal. Butterwarh, London, 278 pp.

Swaine, D.J. (1995). The contents and some related aspects of trace elements in coals. In: Environmental Aspects of Trace Elements in Coal. Swaine, D.J., Goodarzi, F. (Eds.). *Kluwer Academic Publishers*, Dordrecht, pp. 5-23.

Sýkorová, I., Pickel, W., Christanis, K., Wolf, M., Taylor, G.H. & Flores, D. (2005). Classification of huminite — ICCP System 1994. *International Journal of Coal Geology*, 62:, 85–106

Şengüler, İ. (2017). Lignite exploration in Türkiye: New projects and new reserves.27th Annual Int. Pittsburgh Coal Conf. (October 11-14,2010, İstanbul).

Şengüler, İ. & Aydın, H. (2017). Akçay Vadisi (Aydın, Muğla, Denizli) Ve Civarının Jeolojisi, *Doğal Kaynaklar ve Ekonomi Bülteni*, 24: 1-6

Taylor, G.H., Teichmüller, M., Davis, A., Diessel, C.F.K., Littke, R. & Robert, P. (1998). Organic Petrology. Gebrüder Borntraeger, Berlin-Stuttgart.

Teichmüller, M. & Teichmüller, R. (1982). The geological basis of coal formation, In: Stach, E., et al. (Ed.), *Stach's Textbook of Coal Petrology*, 3rd. Borntraeger, Berlin, pp. 5-86.

Thomas, L.J. (1992). Handbook of Practical Coal Geology (Geological Society of London Handbook Series) ISBN 10: 0471935573 / ISBN 13: 9780471935575.

TKİ (General Directorate of Turkish Coal Enterprises), (2011). 2010 Linyit Sektörü Raporu (2010 Sectoral Report of Türkiye). TKİ Publications, Ankara.

Toprak, S. (2009). Petrographic properties of major coal seams in Türkiye and their formation. *International Journal of Coal Geology,* 78(4): 263-275.

Tuncalı, E., Çiftçi, B., Yavuz, N., Toprak, S., Koker, A., Aycık, H., et al. (2002). Chemical and technological properties of Turkish Tertiary coals, Ankara: MTA publication.

Ulusoy, R. (1990). Yatağan (Muğla) Eskihisar açık işletmesi şev stabilitesi etüdü raporu, Türkiye Kömür İşletmeleri. Güney Ege Linyitleri İşletmesi (GELİ).

Ural, S., Yıldırım, M. & Anıl, M. (2002). Kömürün mineral madde içeriğinin toz kömür yakma sistemindeki rolü. Proceedings of the 13th *Turkish Coal Congress*, Zonguldak, Türkiye

Ünal, D. (1991). Muğla Yatağan- Turgut sahalarındaki linyitlerin rezervi ve kalitesinin hesabı, Güney Ege Linyit İşletmesi raporu.

Ünal, N. (2018). *Şarkikaraağaç (Isparta) kömürlerinin organik jeokimyası ve iz element dağılımı.* Doktora Tezi, Akdeniz Üniversitesi, Antalya.

Wang, J., Yamada, O., Zhang, Z.G., Suzuki, Y. & Sakanishi, K. (2008). Statistical analysis of concentrations of trace elements in a wide diversity of coals and its implications for understanding elemental modes of occurrence. *Fuel*, 87: 2211-2222.

Wang, Y., Wang, W., Wang, W. & Duan, P. (2024). Geochemical Characteristics and Sedimentary Palaeoenvironment of the Coal-Bearing Strata in the Xishanyao Formation: A Case Study of the Yihua Coal Mine in the Zhundong Coalfield, Xinjiang. *Minerals* 2024, 14, 461. http://doi.org/10.3390/min14050461

Yağmurlu, F., İnaner, H., Nakoman, E. & İnci, U. (2004). Age, Tectonic Setting and Quality Distribution of The Neogene Lignite Deposits of Western Anatolia. *Geologica Belgica*, 7(3-4): 251-258.

Yakupoğlu, T. (2001). *Muğla-Yatağan Bölgesi'ndeki Neojen Yaşlı Sedimanter Kayaçların Kil Sedimantolojisi ve Sedimanter Petrografik İncelenmesi*. Doktora Tezi, Hacettepe Üniversitesi, Ankara.

Yakupoğlu, T. & Bayhan, E. (2017). Yatağan Havzasındaki (Muğla / GB Türkiye) Neojen Yaşlı Sedimanter Kayaçların Sedimantolojik ve Petrografik Özellikleri, Yüzüncü Yıl Üniversitesi Fen Bilimleri Enstitüsü Dergisi. *Journal of the Institute of Natural & Applied Sciences,* 22(2): 120-131.

Yiğitel, I. (1979). Güneybatı Anadolu kömür aramaları genel prospeksiyon raporu. MTA Rapor No. 6180 (yayınlanmamıştır).

Yücelay, A. (1979). Muğla ili Yatağan Eskihisar civarındaki kömürlü sahasının jeolojik etüdü, M.T. A. *rapor no*.4436 Ankara.

Zaid, M.Z.S.M., Wahid, M.A., Mailah, M., Mazlan, M.A. & Saat, A. (2019). Coal combustion analysis tool in coal fired power plant for slagging and fouling guidelines. AIP Conf. Proc. 2062,020028 (2019) http://doi.org/10.1063/1.5086575

APPENDICES

Appendix I: Drilling and core sampling in the Yatağan lignite field

Appendix II: Laboratory studies

Appendix III: Characterisation of Macerals in Coal

Appendix IV: Photomicrographs of the Yatağan lignite

Appendix V: Histograms of the Reflectance Measurements

Appendix VI: XRD Analysis

Appendix VII: SEM-EDX Analysis

Appendix VIII: Petrographic analysis of inorganic samples

APPENDIX I: Drilling and core sampling in the Yatağan lignite field



Drilling work in the Yatağan coal field.



Core samples in the storage of the Yatağan Mining Directorate.



Sampling from core boxes of boreholes I-18, I-23 and I-25.







Core sample boxes in the storage of the Yatağan Mining Directorate.

APPENDIX II: Laboratory studies



The prepared block samples were polished using the Struers LaboForce-50 Device at the Organic Petrography Laboratory, Department of Geological Engineering, Dokuz Eylül University







Maceral analysis of samples under the LEICA DM 4500 P brand microscope at the Organic Petrography Laboratory, Department of Geological Engineering, Dokuz Eylül University



Sample preparation by pipetting for XRD and Rigaku-MiniFlex 600 benchtop X-Ray diffractometer at the X-Ray Laboratory of the Department of Geological Engineering, Dokuz Eylül University



The SEM-EDX (Scanning Electron Microscope) at the Izmir Institute of Technology, Integrated Research Centers (IZTECH-IRC)

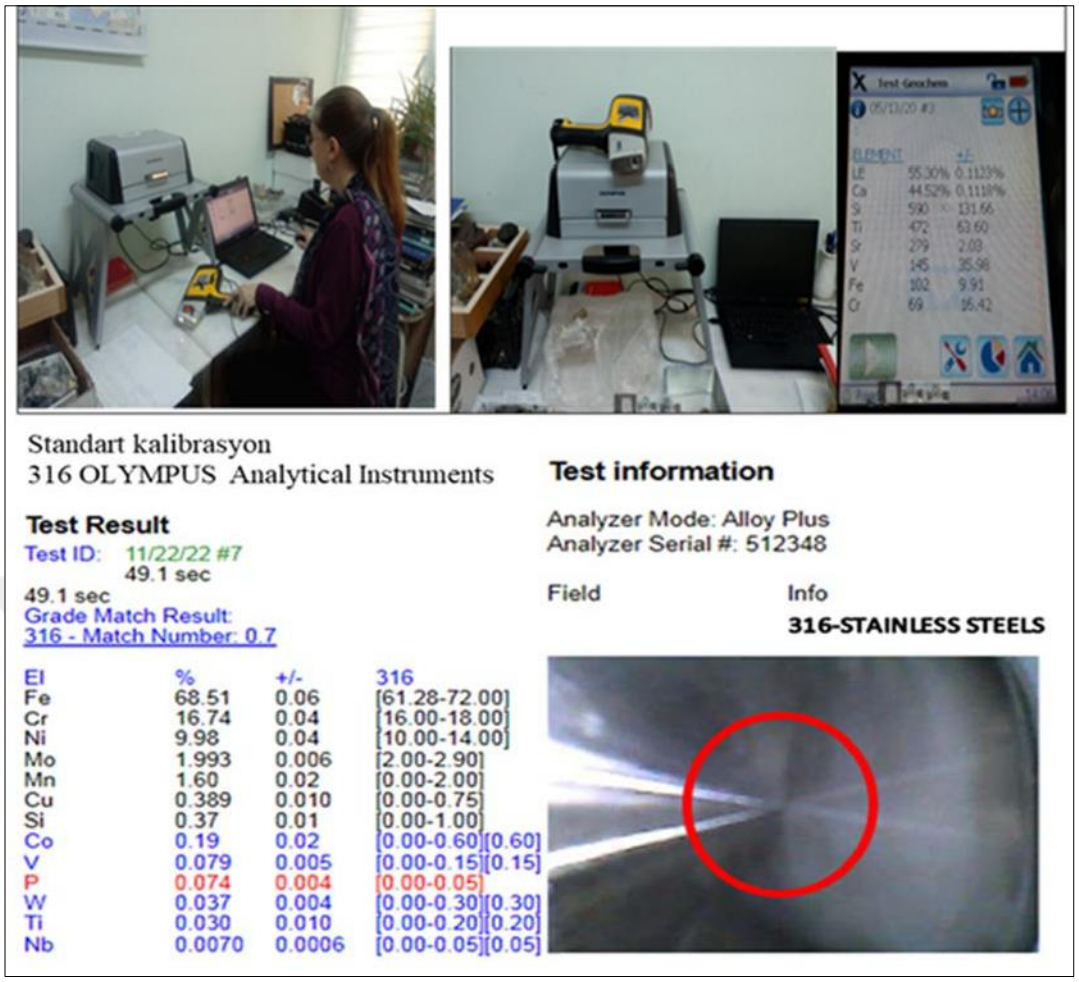

Standart kalibrasyon
316 OLYMPUS Analytical Instruments

Test Result

Test ID: 11/22/22 #7
49.1 sec
49.1 sec
Grade Match Result:
316 - Match Number: 0.7

El	%	+/-	316
Fe	68.51	0.06	[61.28-72.00]
Cr	16.74	0.04	[16.00-18.00]
Ni	9.98	0.04	[10.00-14.00]
Mo	1.993	0.006	[2.00-2.90]
Mn	1.60	0.02	[0.00-2.00]
Cu	0.389	0.010	[0.00-0.75]
Si	0.37	0.01	[0.00-1.00]
Co	0.19	0.02	[0.00-0.60][0.60]
V	0.079	0.005	[0.00-0.15][0.15]
P	0.074	0.004	[0.00-0.05]
W	0.037	0.004	[0.00-0.30][0.30]
Ti	0.030	0.010	[0.00-0.20][0.20]
Nb	0.0070	0.0006	[0.00-0.05][0.05]

Test information

Analyzer Mode: Alloy Plus
Analyzer Serial #: 512348

Field Info
316-STAINLESS STEELS

Portable-XRF Measuring Device (standard calibration)

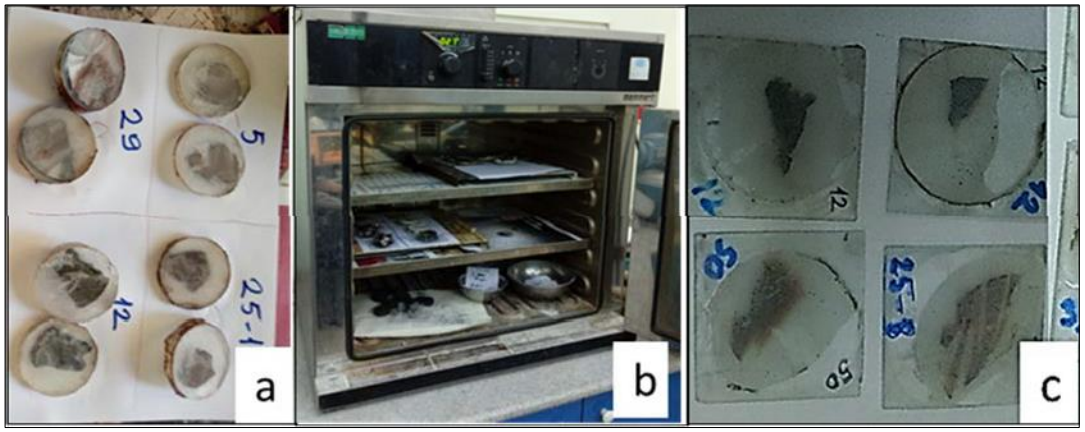

(a): Blocks prepared from inorganic samples at Torbalı Vocational School of the Dokuz Eylül University, (b): drying of block samples in the oven, (c): preparation of thin sections from the inorganic samples.

APPENDIX III: Characterization of Macerals in Coal

Maceral Group	Maceral Sub-Group	Maceral	Description	Origin
HUMINITE	Telohuminite	Textinite A-B	Cell walls either of isolated - but intact individual - cells or within tissues	From the cell walls of parenchymatous and woody tissues of roots, stems and barks, rarely also from leaves; composed of celhulose and lignin
		Ulminite A-B	Cell filling; partly or fully gelified tissues	From the parenchymatous and woody tissues of roots, stems, barks and leaves; composed of celhulose and lignin, originating from herbaceous and arborescent plants
	Detrohuminite	Attrinite	Mixture of fine non-gelified amorphous humirite particles (<10 µm) of various shape	From fragmentation of the parenchymatous plant tissues or gelified macerals
		Densinite	Mixture of fine humirite particles (<10 µm) of various shape cemented by amorphous dense humiritic (gel)substance	From the cementation in the progress of gelification, of fine humirite particles (<10 µm), namely attrinite
	Gelohuminite	Gelinite	Homogeneous and structureless infillings of cracks and other voids	From humic amorphous substance (gel) generated during peatification
		Corpohuminite	Homogeneous and discrete bodies representing cell infillings	From tannin-rich cell excretions, deposited in cortical cells, in parenchymatous or medullary- ray cells and especially in cork tissues

The huminite macerals (Sýkorová et al., 2005).

Maceral Group	Maceral	Description	Origin
INERTINITE	**Fusinite**	Well preserved cellular structure of at least one complete cell of parenchyma, collenchyma, or sclerenchyma	From ligno-cellulosic cell walls that 'survived' during fusinitization (= weak oxidation)
	Semifusinite	Displays intermediate reflectance and structure between telohuminite/vitrinite and fusinite in the same sample	From parenchymatous and xylem tissues of stems, herbaceous plants and leaves, which are composed of cellulose and lignin. It is formed in the peat stage by weak humification, dehydration and redox processes
	Funginite	Single or multi-celled fungal spores, sclerotia, hyphae and mycelia (stomata, mycorrhiza), and other fungal remains	From fungal spores, sclerotia, mycelia and other fungal tissue
	Secretinite	Commonly round, vesicled to non-vesicled, equant to elongate bodies without obvious plant structure	Not completely clear; commonly considered to be an oxidation product of resin but it may originate from humic gels that formed in secretory ducts of medullosan seed ferns and to a lesser extent in cells or ducts of other vascular plants
	Macrinite	Amorphous matrix or discrete, structureless bodies of variable shapes, which are commonly elongated when viewed perpendicular to bedding	From flocculated humic substances, which underwent dehydration and redox processes at an early stage of peatification due to temporary lowered groundwater table; or a metabolic product of fungi and bacteria; isolated aggregates may originate from coprolites
	Micrinite	Very small rounded grains (∅ < 2 μm) occurring close to liptinite macerals	Secondary maceral generated during coalification
	Inertodetrinite	Discrete small inertinite fragments of varying shape can no longer be assigned with certainty to one or other maceral of the inertinite group	From other inertinite macerals

The inertinite macerals (ICCP, 1998)

Maceral Group	Maceral	Description	Origin
LIPTINITE	Cutinite	Constituent formed from cuticles of leaves and stems	From cuticles, which form protective waxy layers of cormophyte epidermal cells in leaves and stems
	Suberinite	Cell walls filled with corpohuminitewhich differ from humotelinite by virtue of their liptinitic character and are derived from suberized cell walls	From suberized cell walls, particularly in bark and root (periderm)
	Sporinite	Outer cell walls of plant spores and polen	From outer membranes (exines and perines) of plant spores and pollen
	Resinite	Discrete bodies of varying shape (round, oval, rod-like) or occur as diffuse impregnations; it can also fill in cell lumens of textinite/telinite; fluorinite displays greenish fluorescence colour	From resin and copal being cell excretions in different parts of plants (bark, wood, leaves, etc.); fluorinite is a resinite type deriving from
	Liptodetrinite	Small particles of liptinite macerals; can no longer be assigned with certainty to one or other maceral of the liptinite group	From macerals of liptinite group through mechanical fragmentation or chemicalmicrobiological fractionation
	Chlorophyllinite	Particles with characteristic blood-red fluorescence; after short time of irradiation red colour disappears	From chlorophyll-rich particles
	Bituminite	Fine-granular ground mass or laminae, irregular streaks, wisps, pods, bands and elongated lenses with vein-like appearance, fine disseminations as seen in perpendicular sections or as more homogenous, diffuse, equidimensional particles of various shapes in horizontal sections	From algae, faunal plankton, bacterial bodies and bodies of higher animals (fish, crayfish etc.); it is a degradation product formed under predominantly anoxic to uboxic conditions

The liptinite macerals (Pickel et al., 2017)

APPENDIX IV: Photomicrographs of the Yatağan lignite

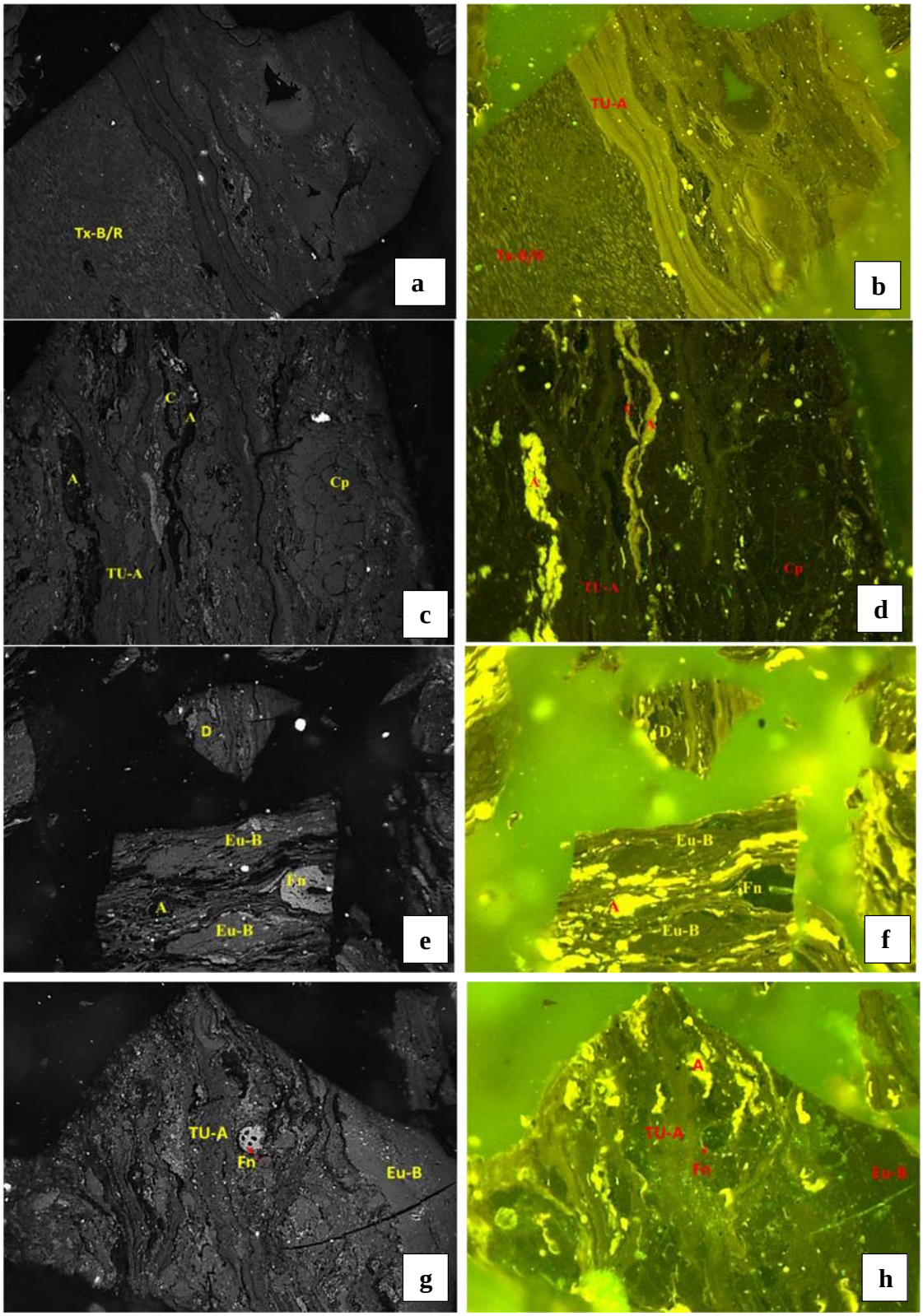

Photomicrographs of sample #I/25-6 under incident white light (a, c, e, g) and blue-light excitation (b, d, f, h), oil immersion, 500X total magnification. The length of each photomicrograph is 230 μm and the hight 173 μm.

a and b. Tx-B: Textinite B impregnated with Resinite (R); TU-A: Texto Ulminite A;

c and d. TU-A: Texto Ulminite A; A: Alginite; Cp: Corpohuminite; C: Cutinite;

e and f. Eu-B: Eu Ulminite B; A: Alginite; Fn: Funginite; D: Densinite;

g and h. TU-A: Texto Ulminite; A: Alginite; Cp: Corpohuminite; C: Cutinite; Fn: Funginite.

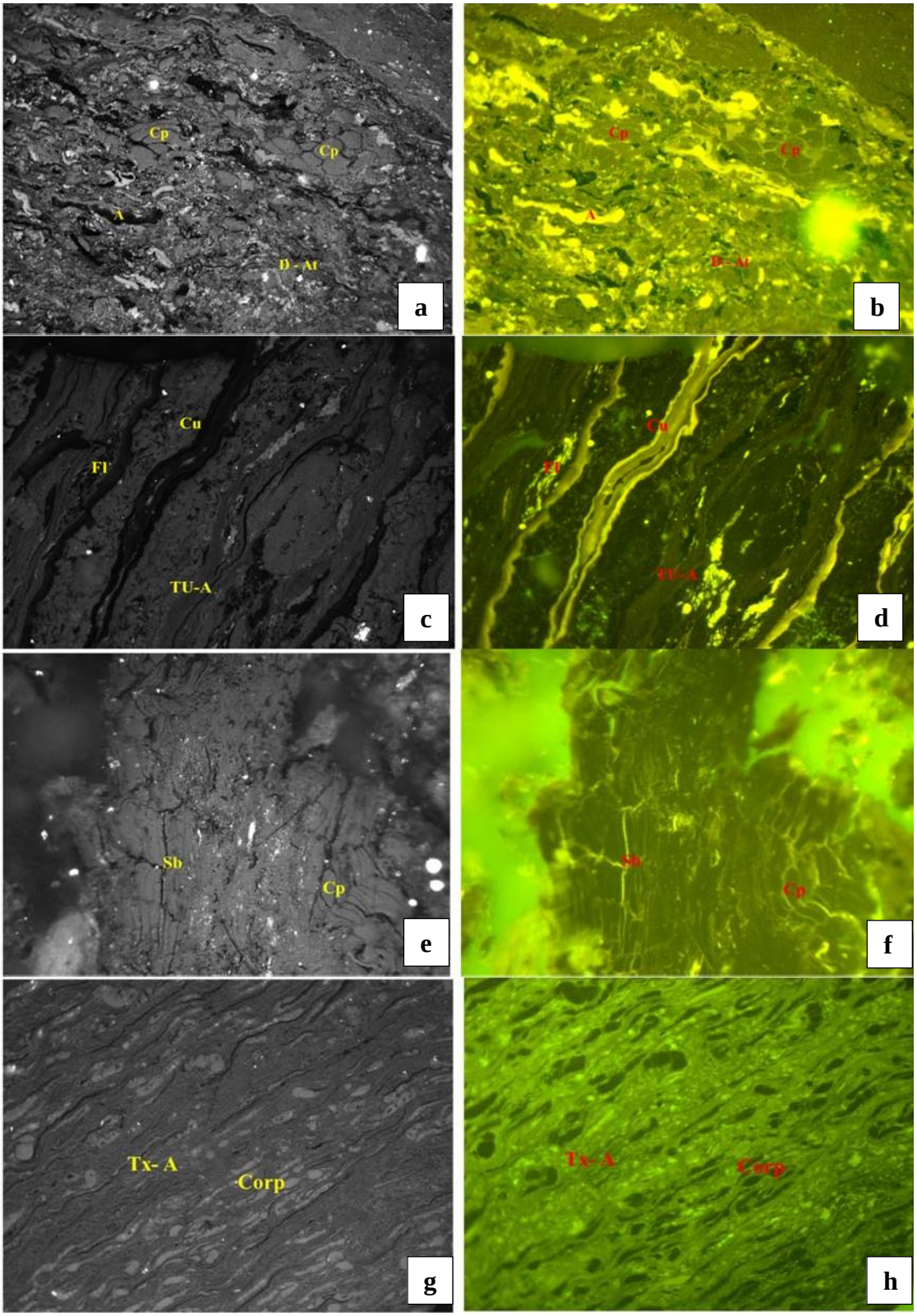
Cp
Cp
A
D - At
a
Cp
Cp
A
D - At
b
Cu
Fl
TU-A
c
Cu
Fl
TU-A
d
Sb
Cp
e
Sb
Cp
f
Tx- A
Corp
g
Tx- A
Corp
h

Photomicrographs of sample #I/18-10 under incident white light and blue-light excitation, oil immersion, 500X total magnification.

2. Sample I/18-10: macerals under incident white light (a, c, e, g) and blue-light excitation (b, d, f, h) at 500x magnification. Each photograph is 230 μm long and 173 μm high.

a. and b. Densinite; D- Attrinite;At, Alginite; A, Corpohuminite; Cp.

c. and d. Texto Ulminite; TU-A, Fluorinite; Fl, Cutinite; C.

e. and f. Corpohuminite; Cp, Suberinite.

g. and h. Texto Ulminite; TU-A, Corpohuminite; Cp.

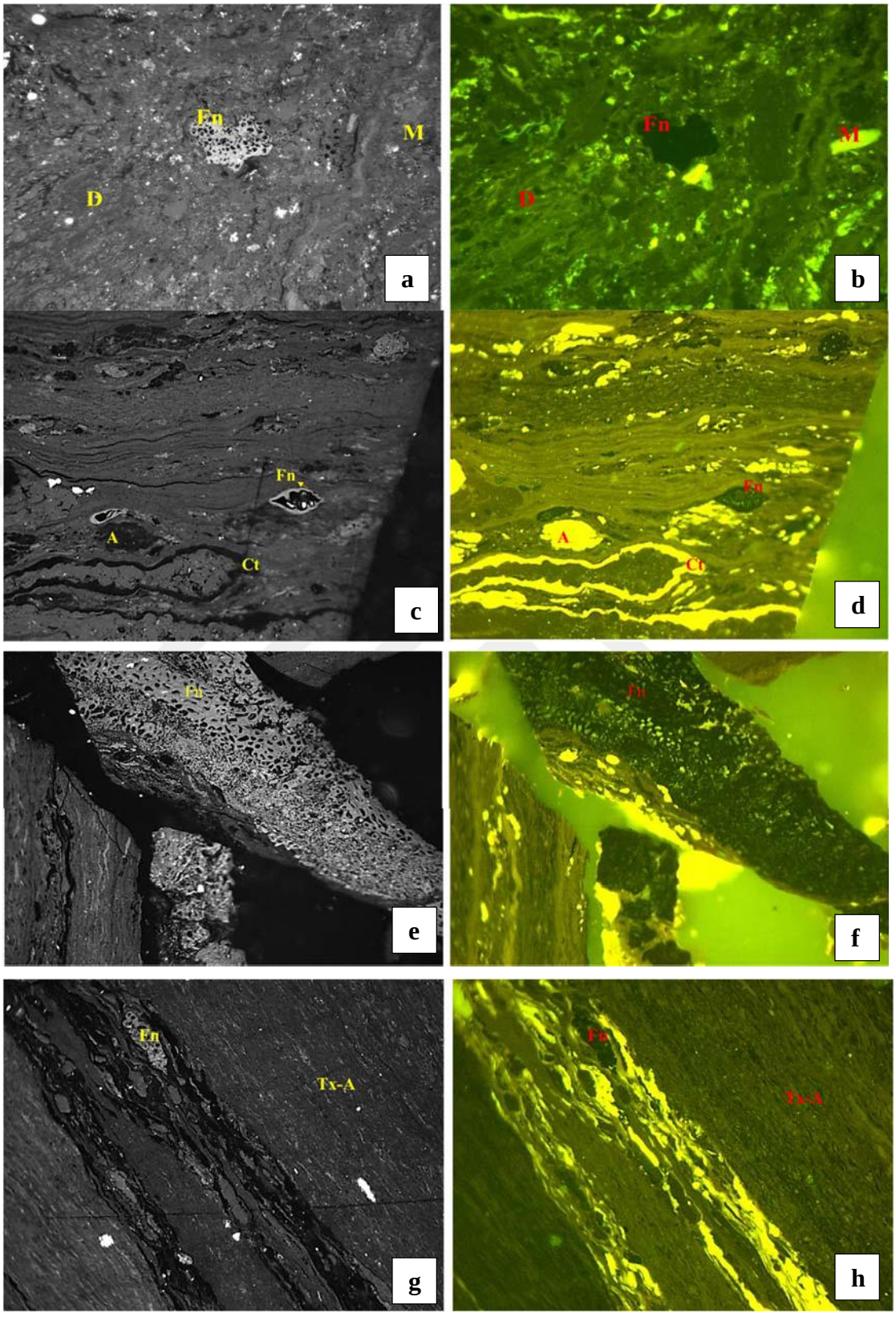
Fn
M
D
a
Fn
M
D
b
Fn
A
Ct
c
Fn
A
Ct
d
Fn
e
Fn
f
Fn
Tx-A
g
Fn
Tx-A
h

Photomicrographs of sample #I/18-13 under incident white light and blue-light excitation, oil immersion, 500X total magnification.

3. Sample I/18-13: macerals under incident white light (a, c, e, g) and blue-light excitation (b, d, f, h) at 500x magnification. Each photograph is 230 μm long and 173 μm high.

a. and b. Densinite; D, Funginite; Fn, Mineral; M.

c. and d. Cutinite; C, Alginite; A, Funginite; Fn, .

e. and f. Funginite colony; Fn.

g. and h. Textinite-A; Tx-A, Funginite; Fn.

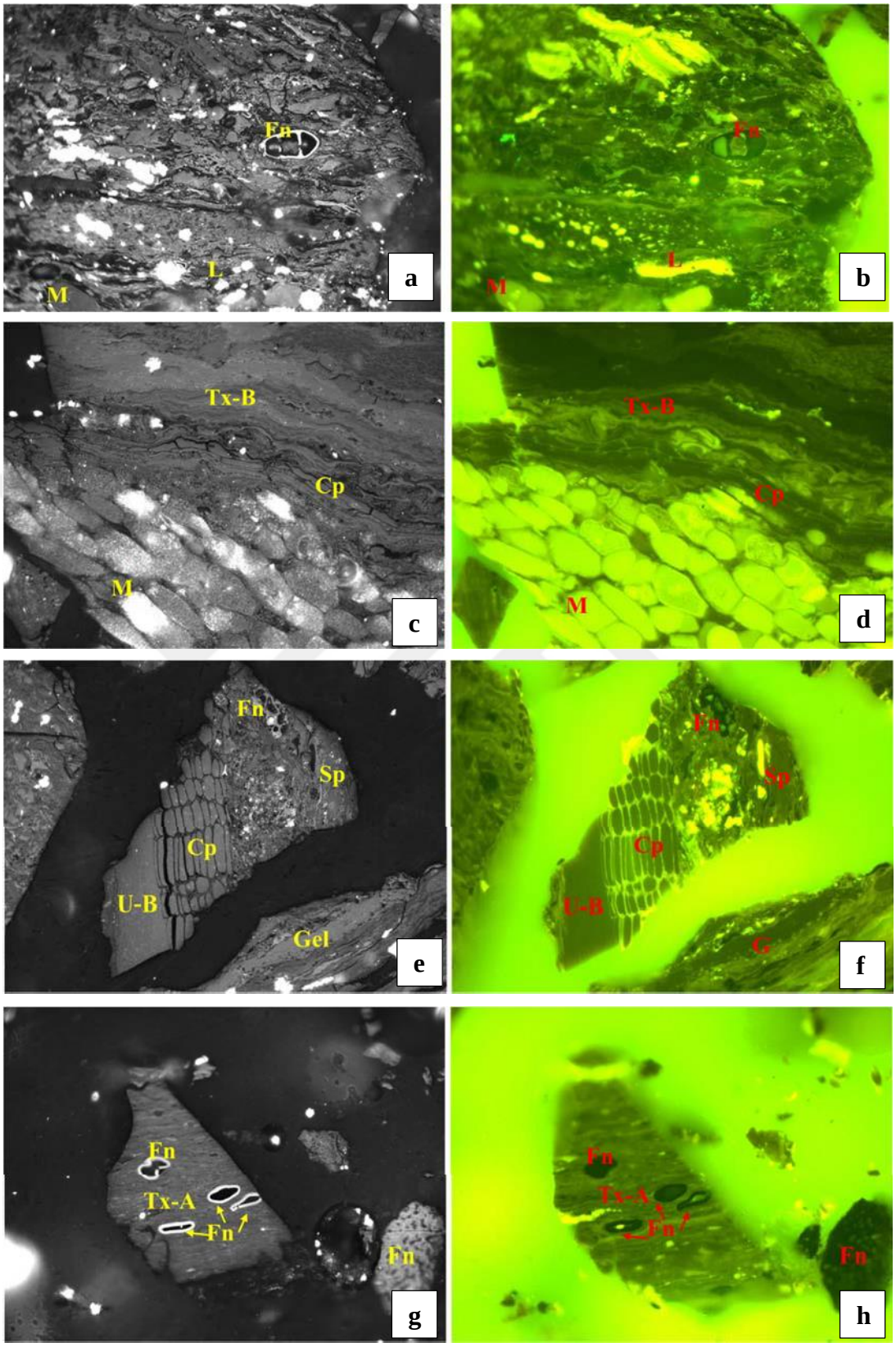

Photomicrographs of sample #I/23-44 under incident white light and blue-light excitation, oil immersion, 500X total magnification.

4. Sample I/23-44: macerals under incident white light (a, c, e, g) and blue-light excitation (b, d, f, h) at 500x magnification. Each photograph is 230 μm long and 173 μm high.

a. and b. Liptinite; D, Funginite; Fn, Mineral; M.

c. and d. Textinite-B; Tx-B, Corpohuminite; Cp, Mineral; M .

e. and f. Ulminite-B; Tx-B, Corpohuminite; Cp, Funginite; Fn, Gelinite; Gel, Sporinite; Sp.

g. and h. Textinite-A; Tx-A, Funginite; Fn.

APPENDIX V: Histograms of the reflectance measurements

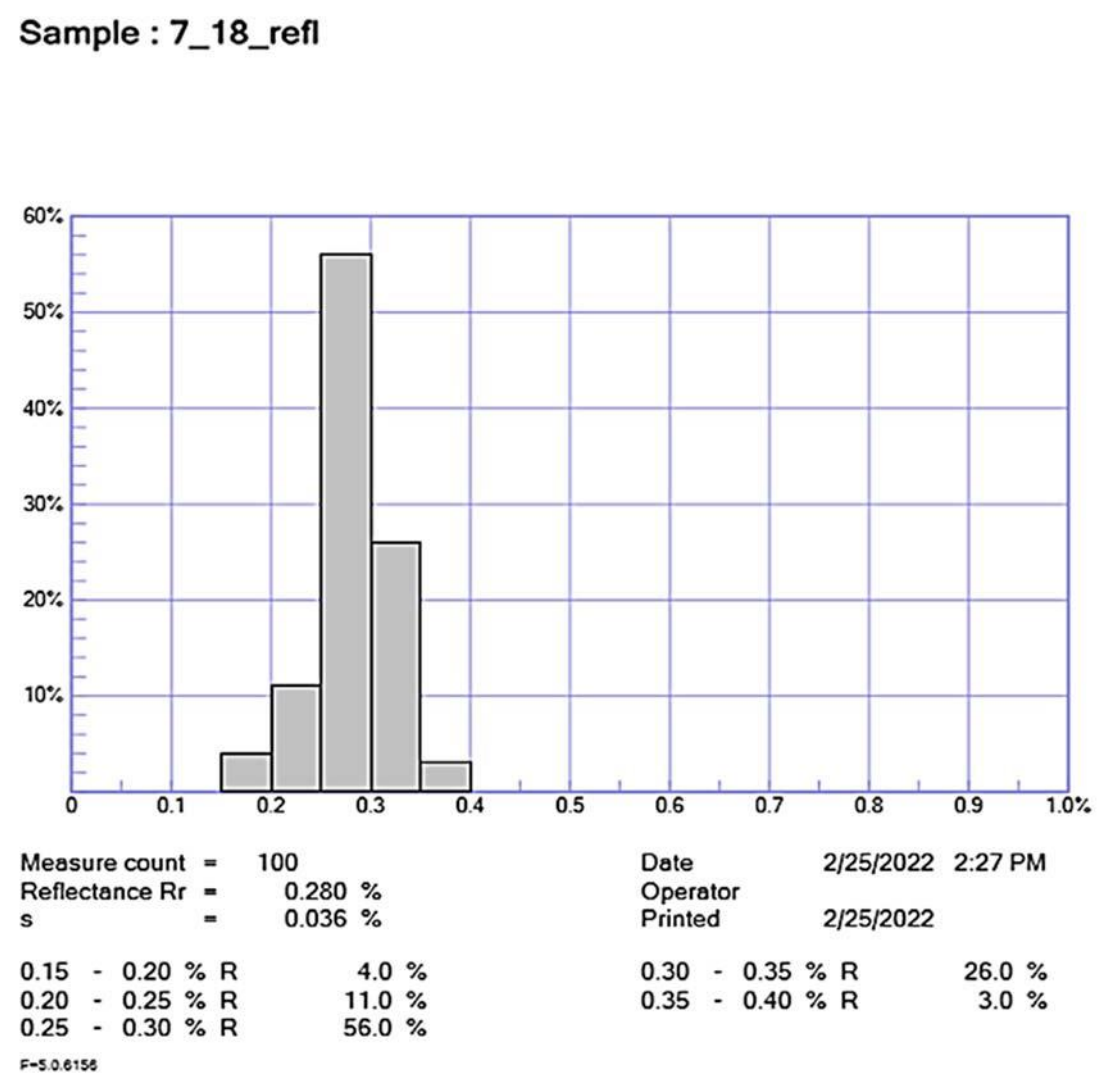

Histogram of the reflectance measurements of sample #I-18/7

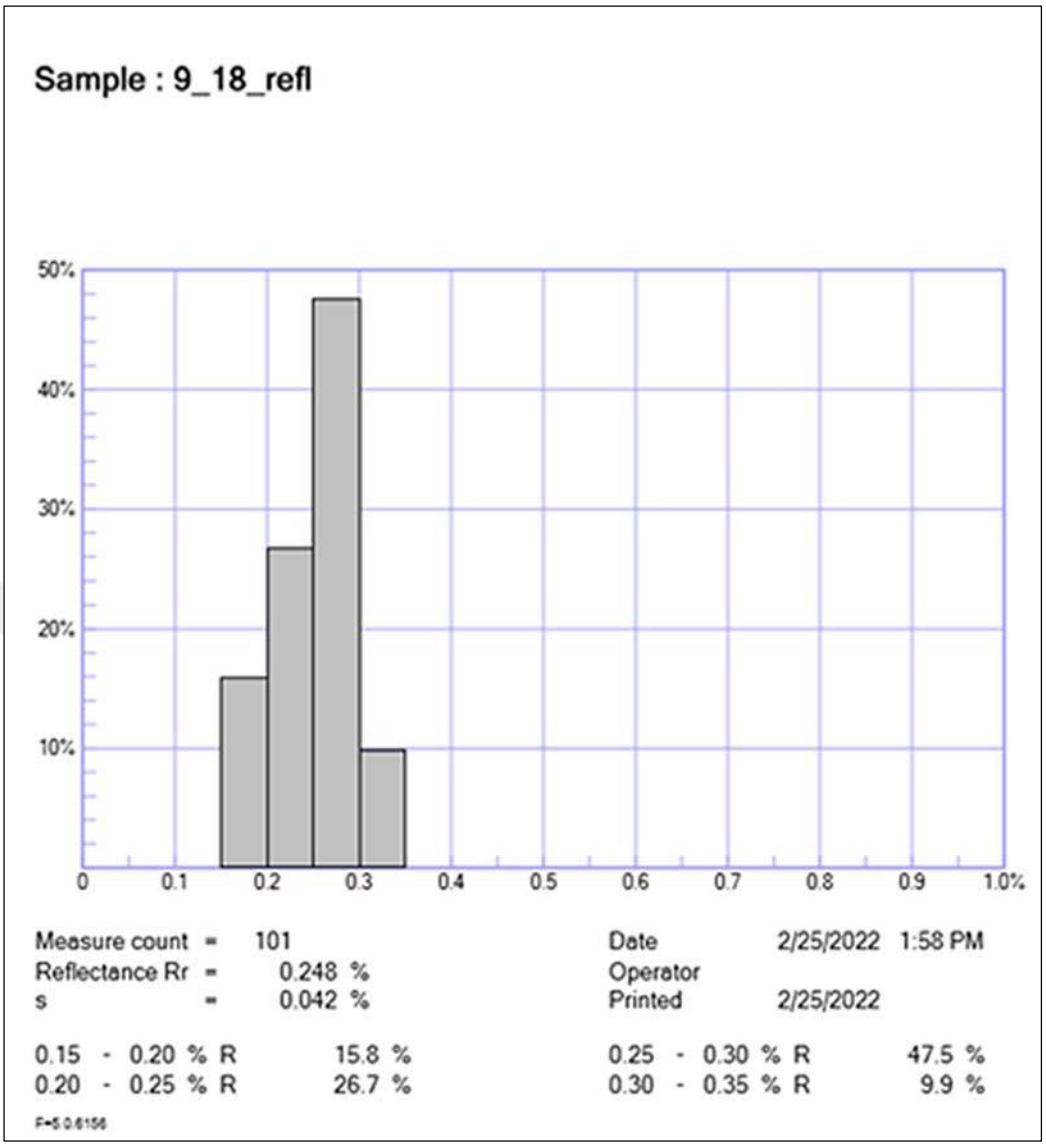

Histogram of the reflectance measurements of sample #I-18/9

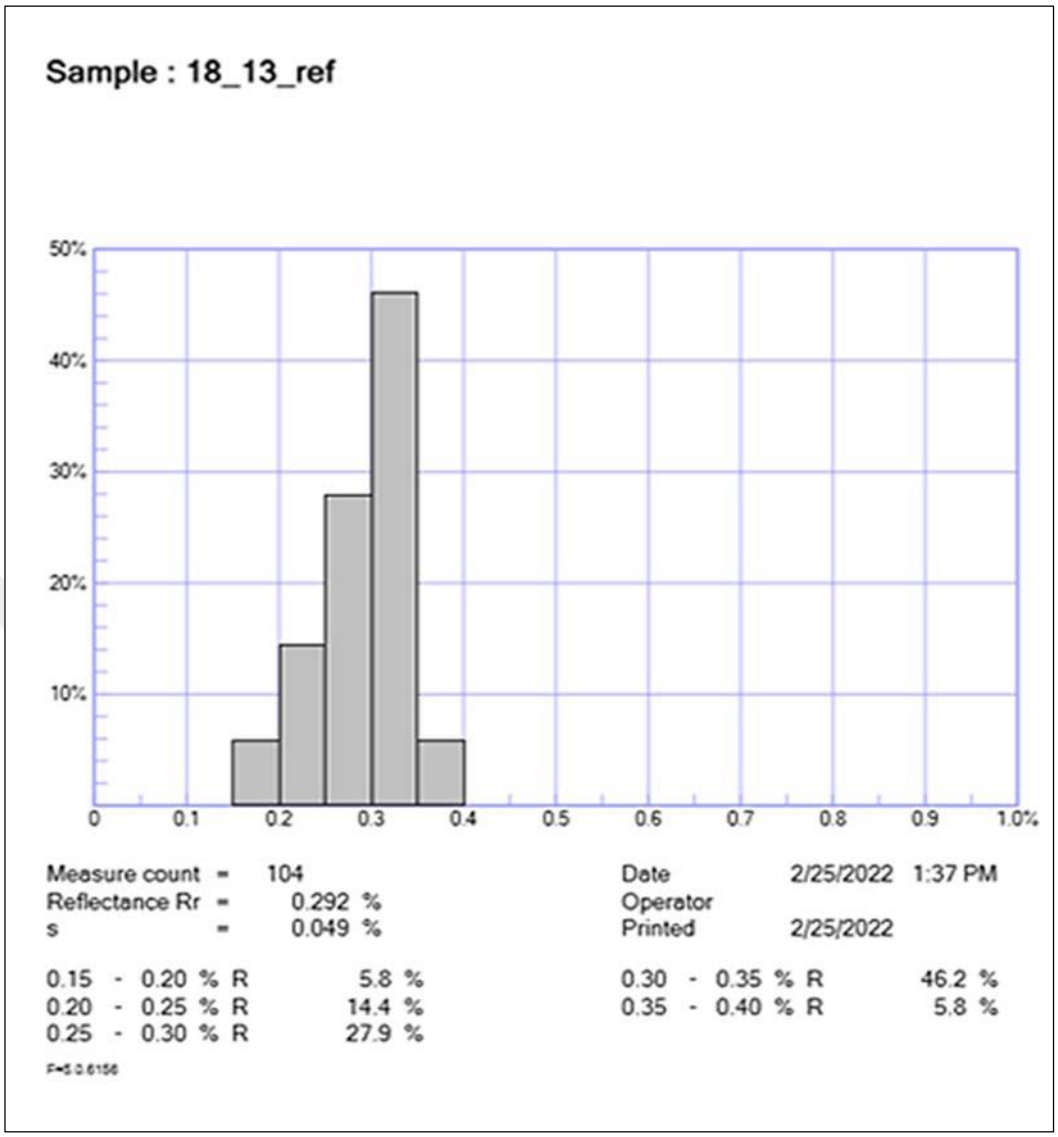

Histogram of the reflectance measurements of sample #I-18/13

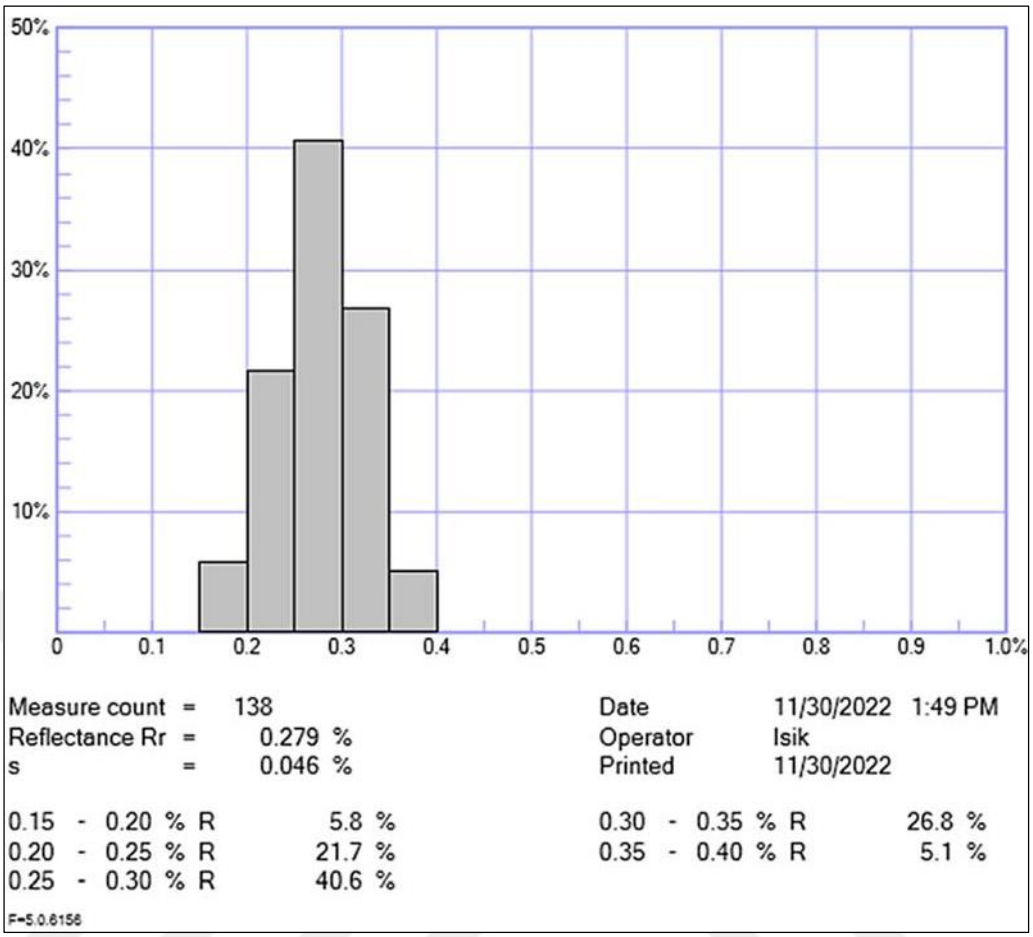

Histogram of the reflectance measurements of sample #I/23-39.

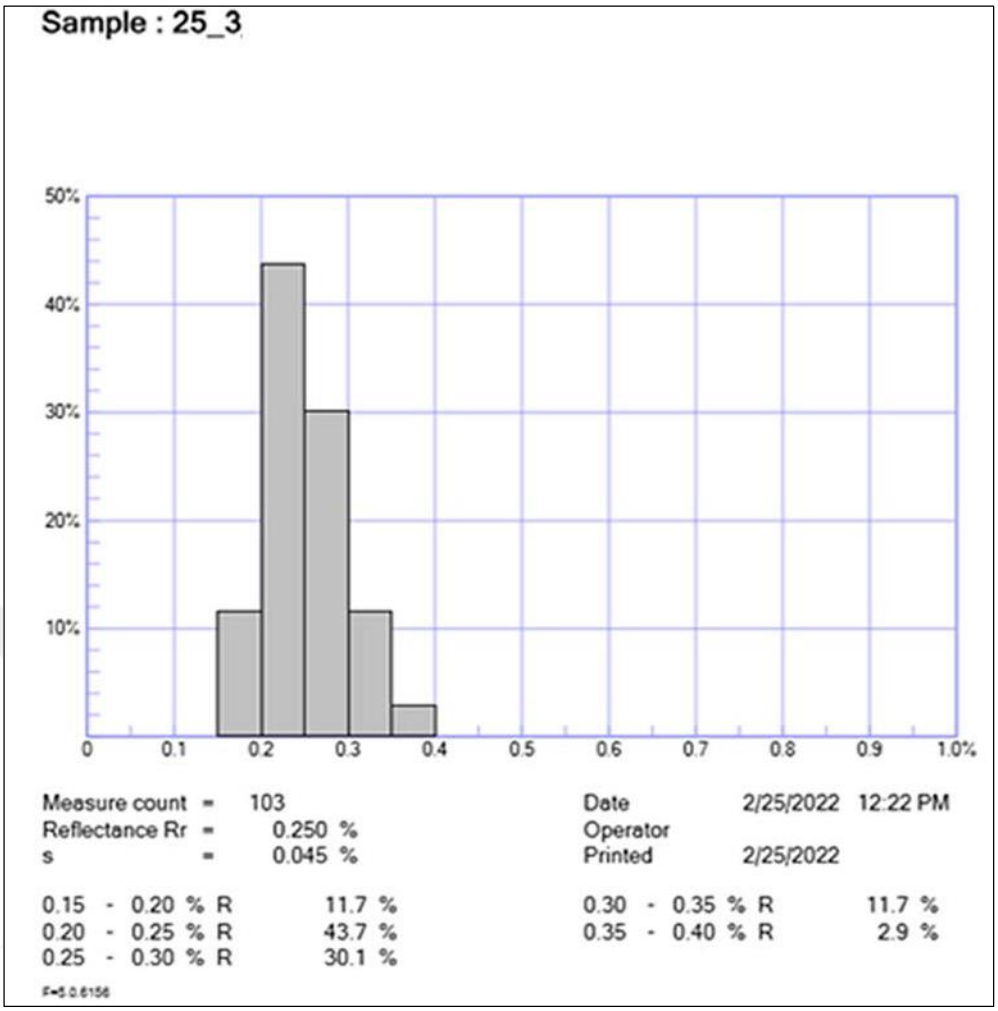

Histogram of the reflectance measurements of sample #I-25/3

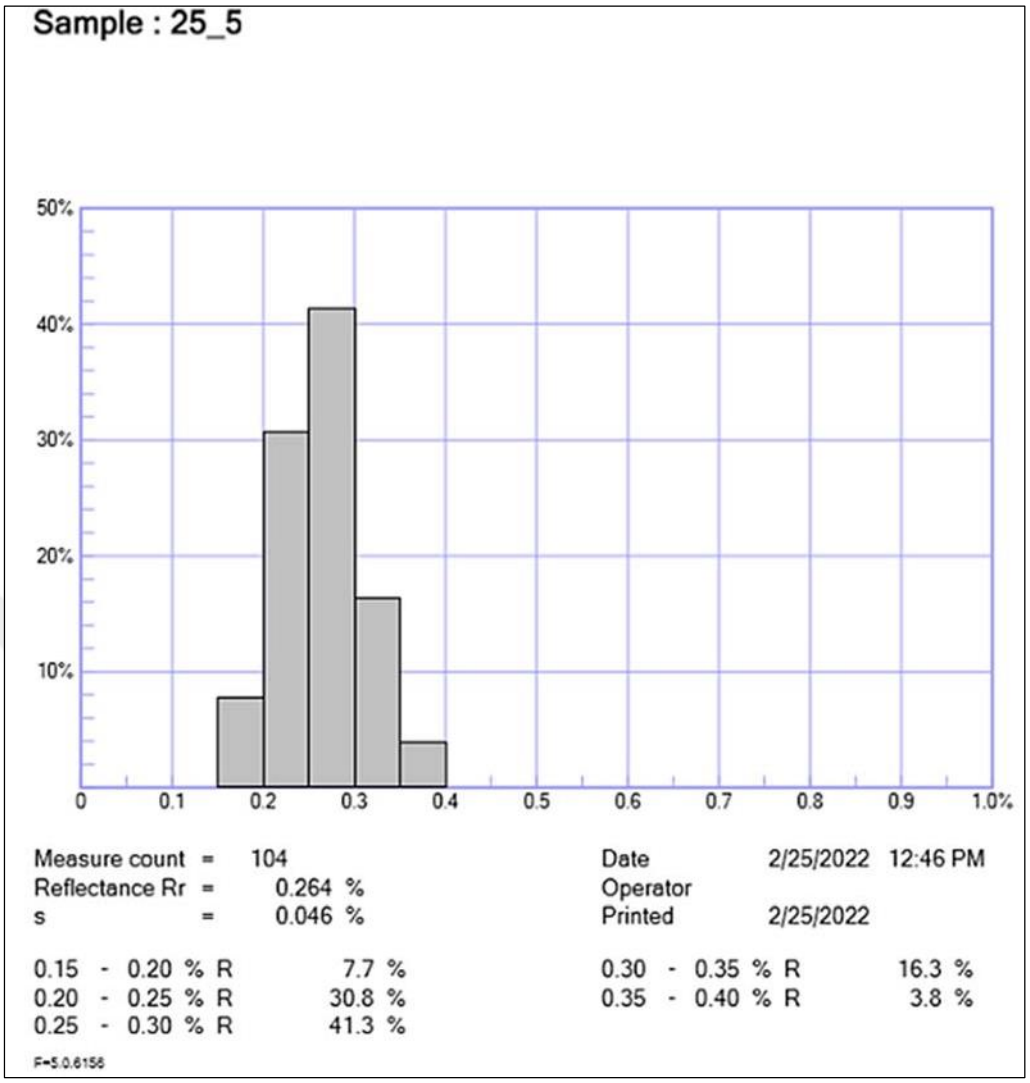

Histogram of the reflectance measurements of samples #I-25/5

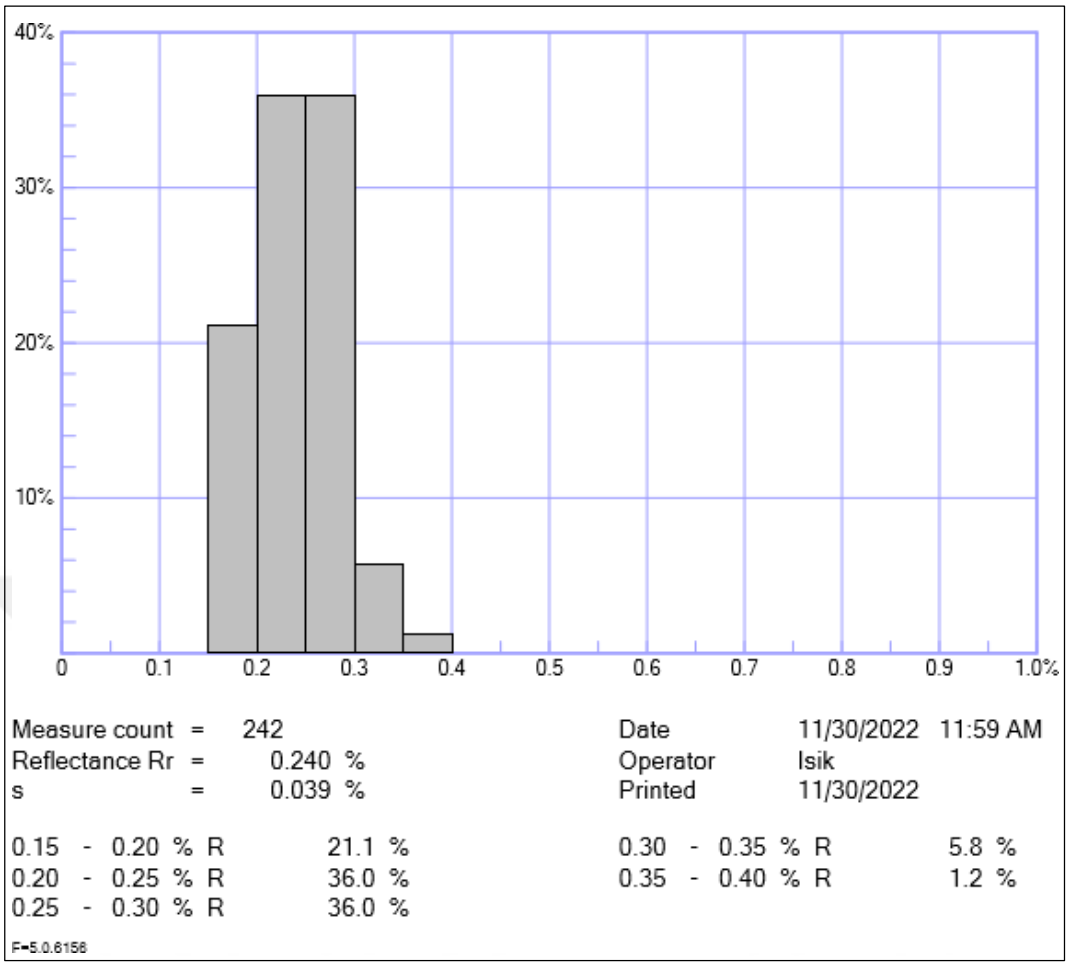

Histogram of the reflectance measurements of samples #I-25/6

APPENDIX VI: XRD Analysis

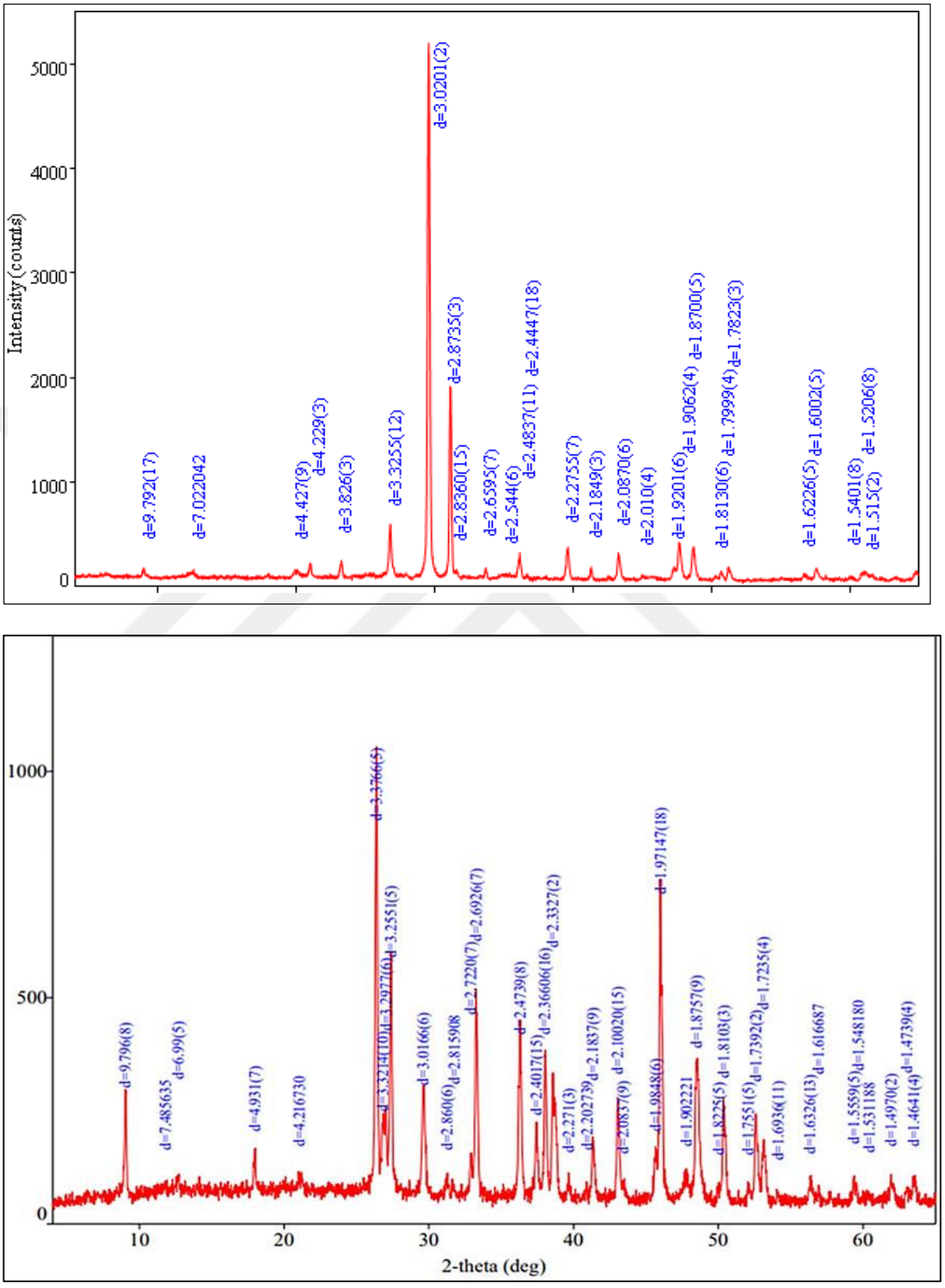

The diffractograms of I-18/32and I-23/50

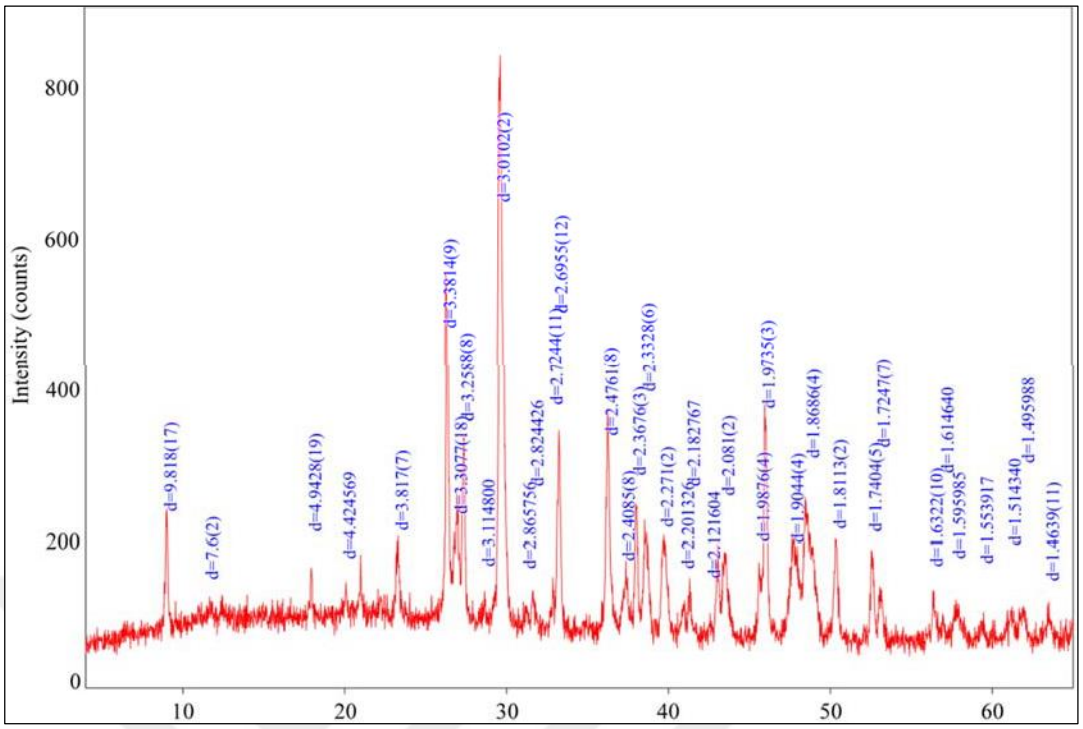

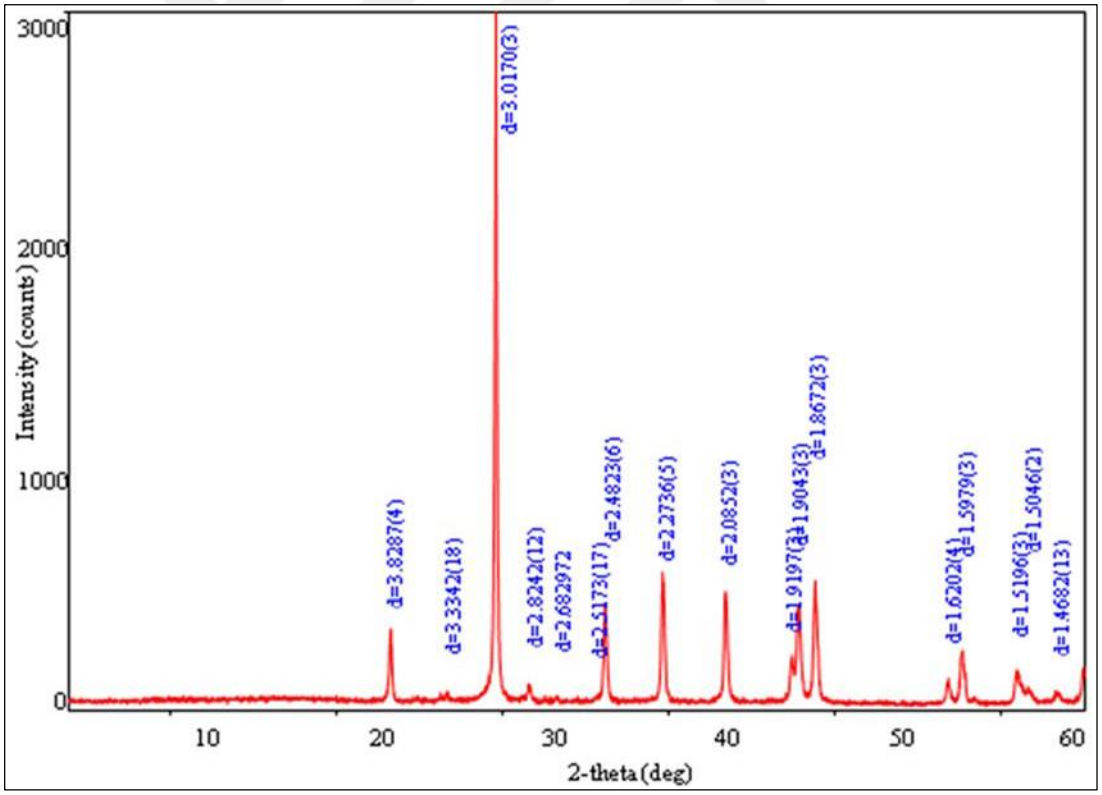

The diffractograms of I-25/1 and I-25/8

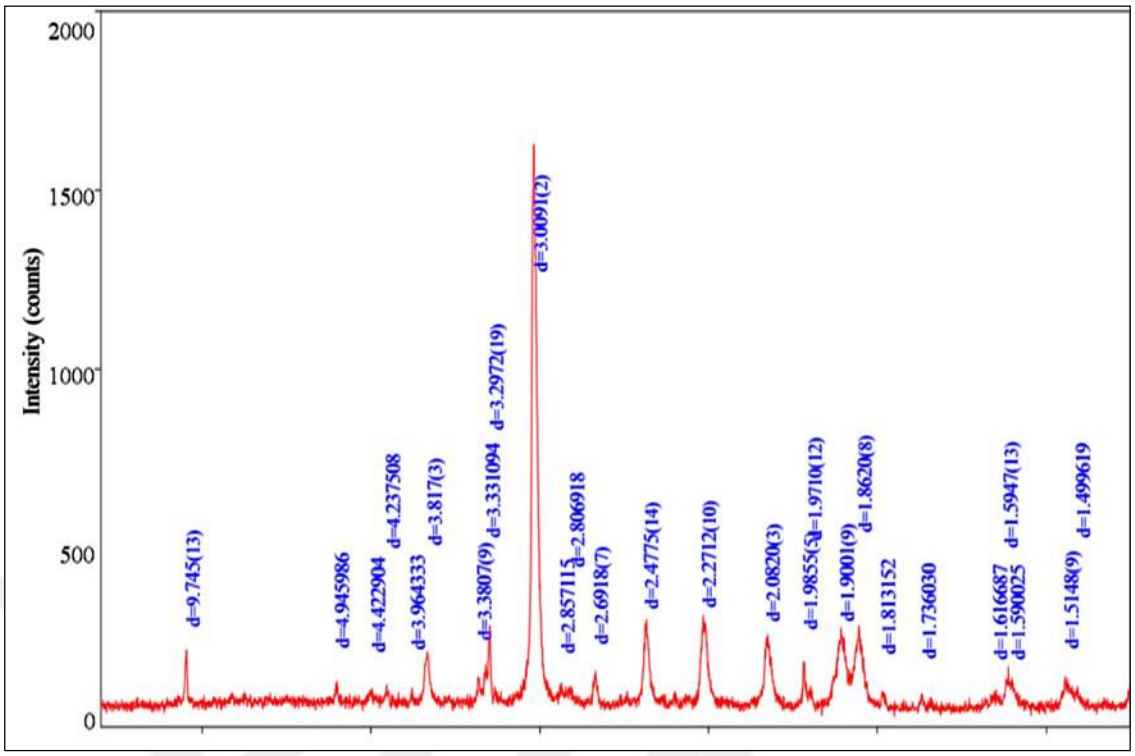

The diffractogram of sample I-25/9

APENDIX VII: SEM-EDX Analysis

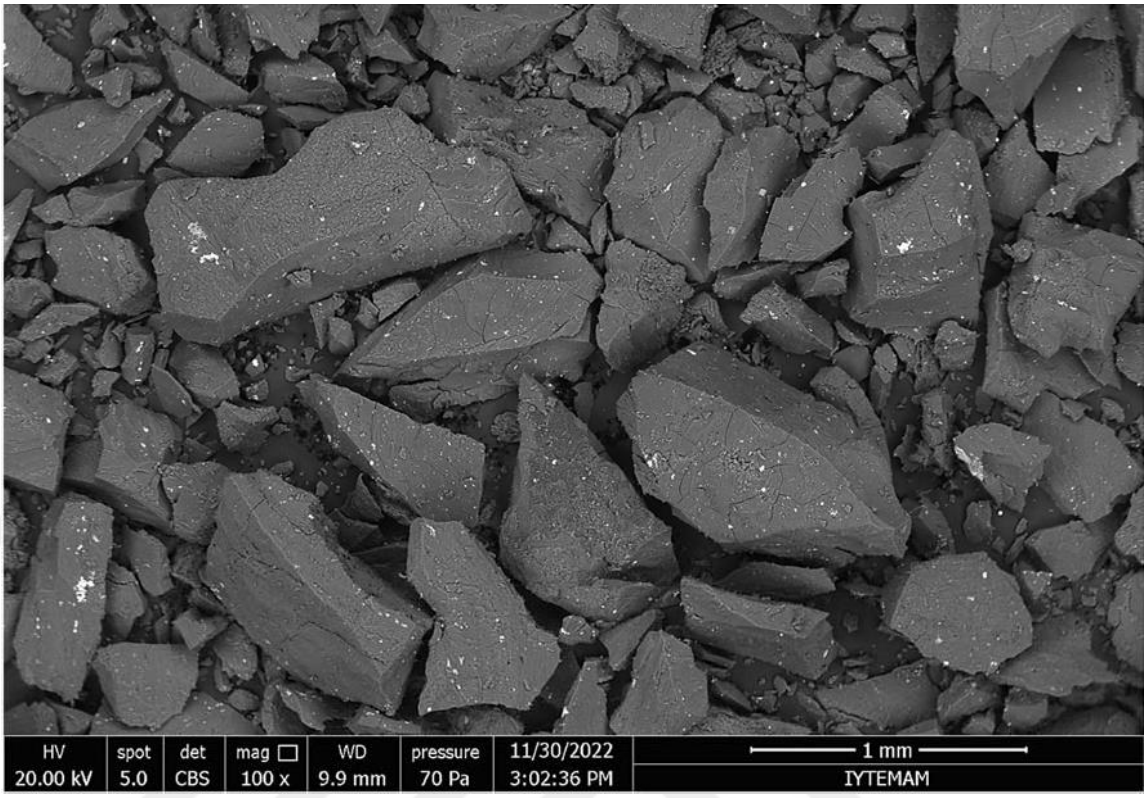

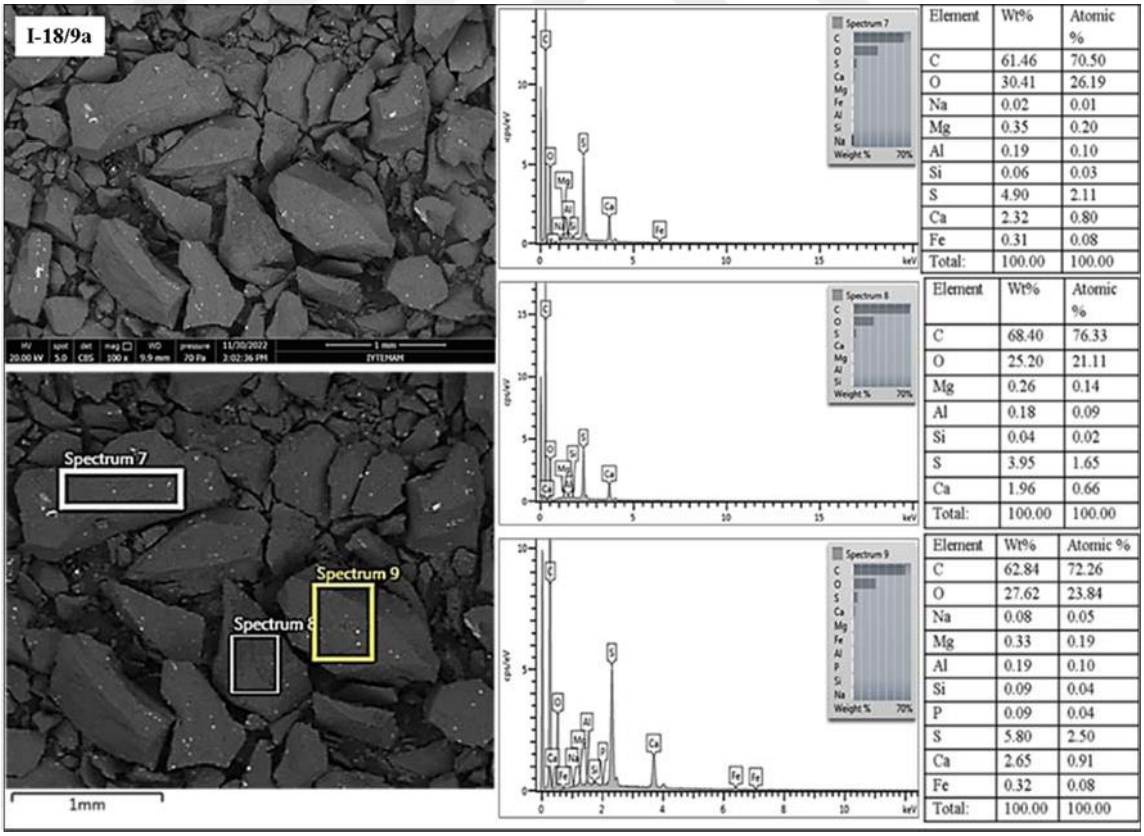

Element	Wt%	Atomic %
C	61.46	70.50
O	30.41	26.19
Na	0.02	0.01
Mg	0.35	0.20
Al	0.19	0.10
Si	0.06	0.03
S	4.90	2.11
Ca	2.32	0.80
Fe	0.31	0.08
Total:	100.00	100.00

Element	Wt%	Atomic %
C	68.40	76.33
O	25.20	21.11
Mg	0.26	0.14
Al	0.18	0.09
Si	0.04	0.02
S	3.95	1.65
Ca	1.96	0.66
Total:	100.00	100.00

Element	Wt%	Atomic %
C	62.84	72.26
O	27.62	23.84
Na	0.08	0.05
Mg	0.33	0.19
Al	0.19	0.10
Si	0.09	0.04
P	0.09	0.04
S	5.80	2.50
Ca	2.65	0.91
Fe	0.32	0.08
Total:	100.00	100.00

SEM-EDX results of sample I-18/9a.

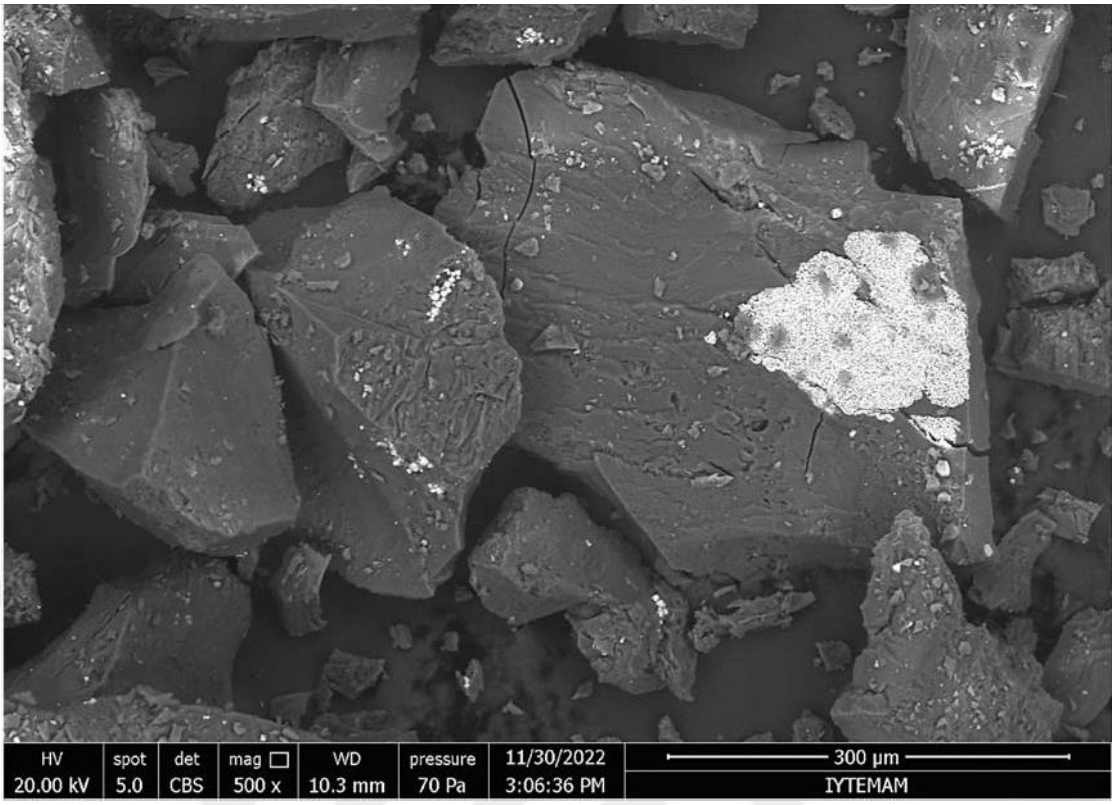

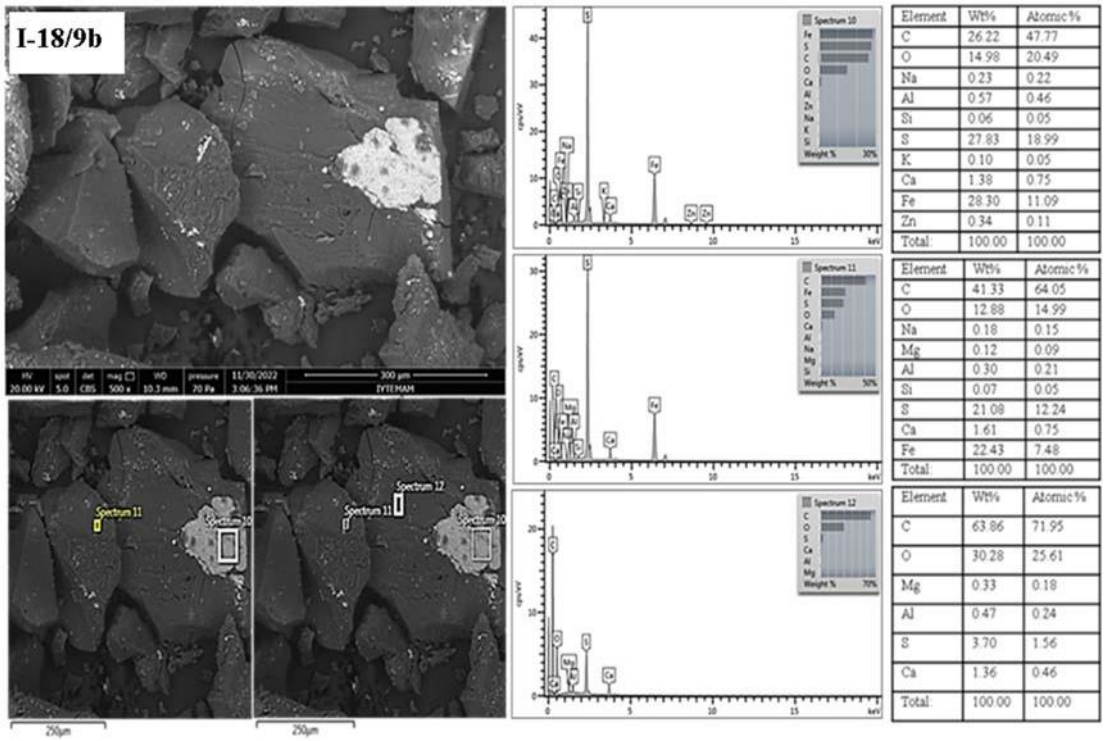

Element	Wt%	Atomic %
C	26.22	47.77
O	14.98	20.49
Na	0.23	0.22
Al	0.57	0.46
Si	0.06	0.05
S	27.83	18.99
K	0.10	0.05
Ca	1.38	0.75
Fe	28.30	11.09
Zn	0.34	0.11
Total	100.00	100.00

Element	Wt%	Atomic %
C	41.33	64.05
O	12.88	14.99
Na	0.18	0.15
Mg	0.12	0.09
Al	0.30	0.21
Si	0.07	0.05
S	21.08	12.24
Ca	1.61	0.75
Fe	22.43	7.48
Total	100.00	100.00

Element	Wt%	Atomic %
C	63.86	71.95
O	30.28	25.61
Mg	0.33	0.18
Al	0.47	0.24
S	3.70	1.56
Ca	1.36	0.46
Total	100.00	100.00

SEM-EDX results of sample I-18/9b

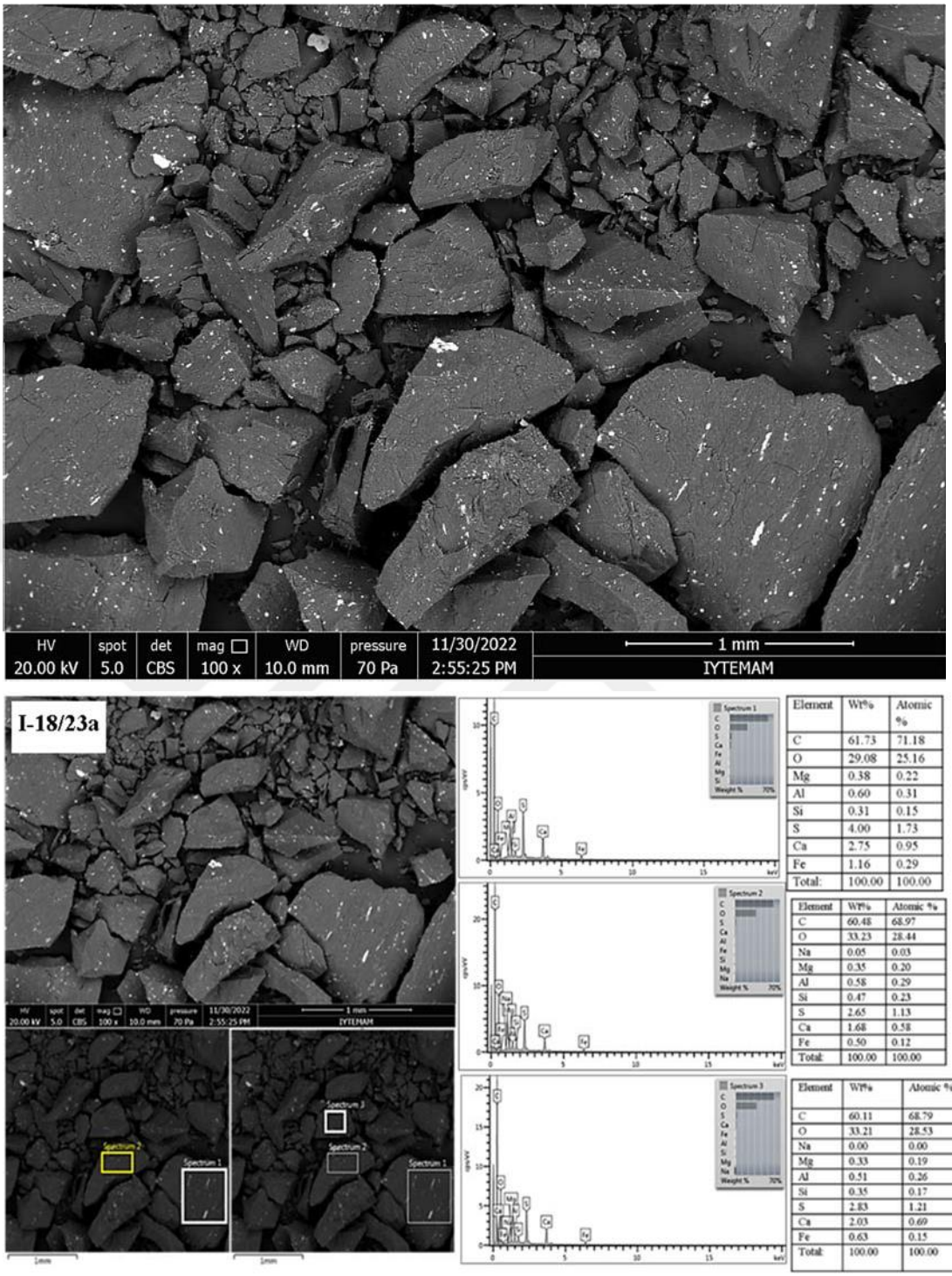

Element	Wt%	Atomic %
C	61.73	71.18
O	29.08	25.16
Mg	0.38	0.22
Al	0.60	0.31
Si	0.31	0.15
S	4.00	1.73
Ca	2.75	0.95
Fe	1.16	0.29
Total:	100.00	100.00

Element	Wt%	Atomic %
C	60.48	68.97
O	33.23	28.44
Na	0.05	0.03
Mg	0.35	0.20
Al	0.58	0.29
Si	0.47	0.23
S	2.65	1.13
Ca	1.68	0.58
Fe	0.50	0.12
Total:	100.00	100.00

Element	Wt%	Atomic %
C	60.11	68.79
O	33.21	28.53
Na	0.00	0.00
Mg	0.33	0.19
Al	0.51	0.26
Si	0.35	0.17
S	2.83	1.21
Ca	2.03	0.69
Fe	0.63	0.15
Total:	100.00	100.00

SEM-EDX results of sample I/18-23a

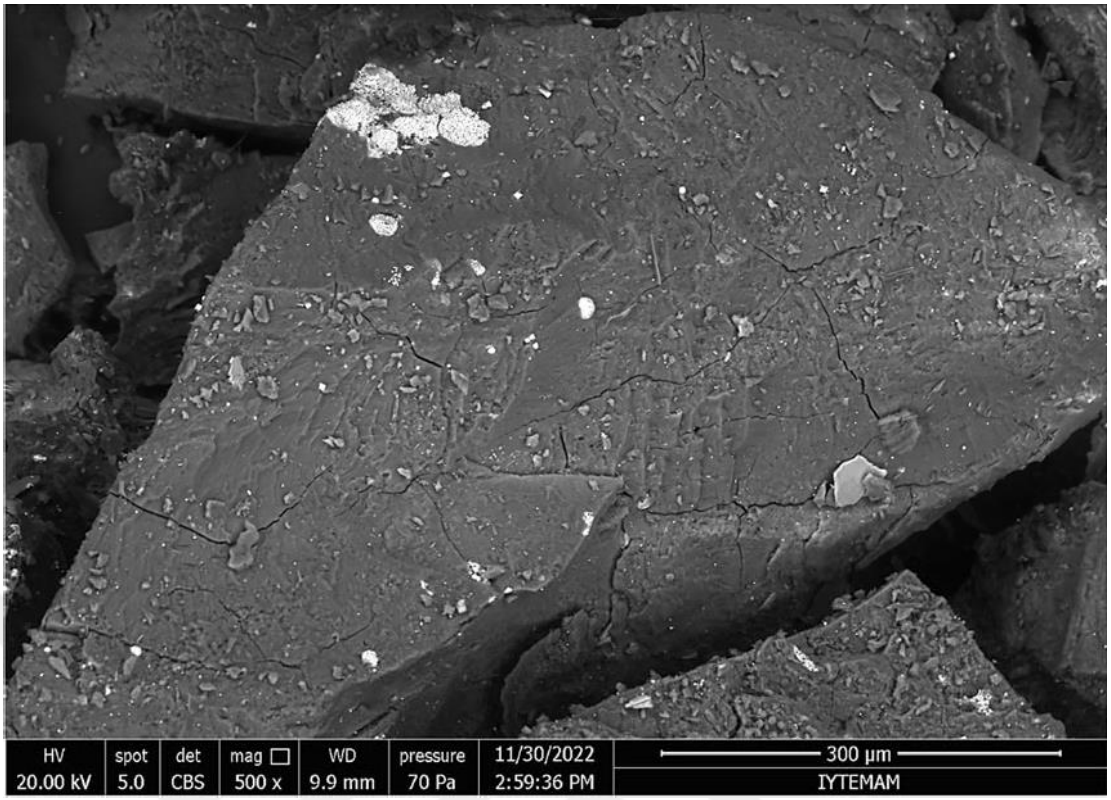

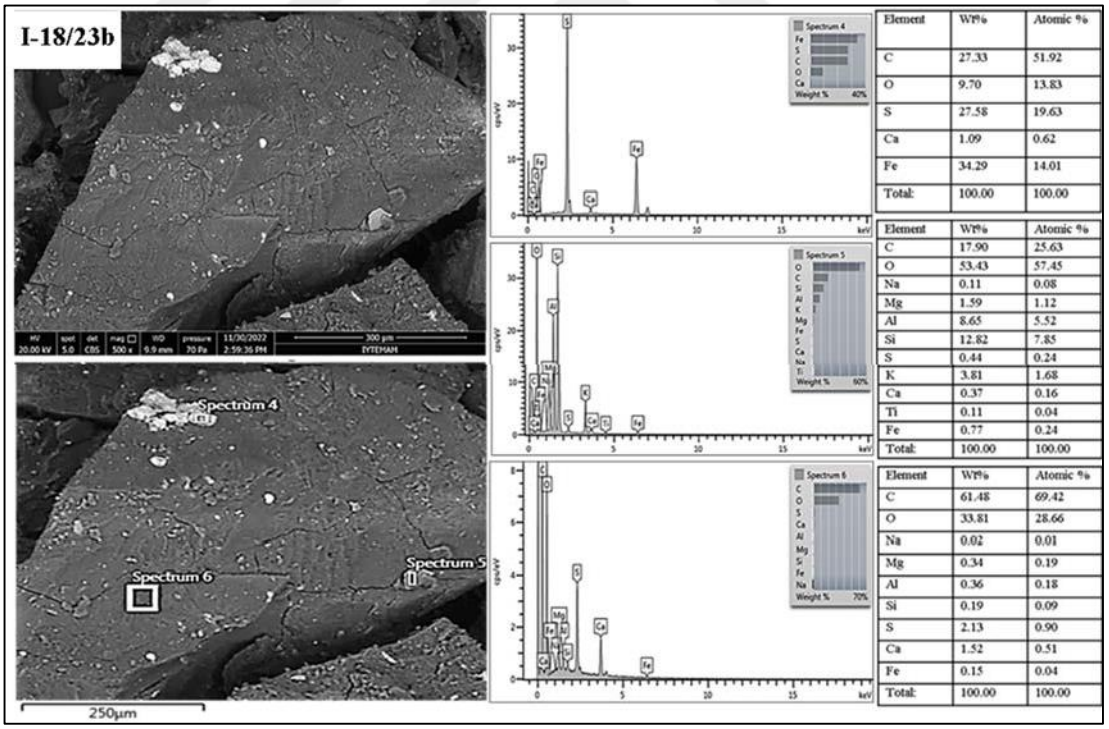

Element	Wt%	Atomic %
C	27.33	51.92
O	9.70	13.83
S	27.58	19.63
Ca	1.09	0.62
Fe	34.29	14.01
Total:	100.00	100.00

Element	Wt%	Atomic %
C	17.90	25.63
O	53.43	57.45
Na	0.11	0.08
Mg	1.59	1.12
Al	8.65	5.52
Si	12.82	7.85
S	0.44	0.24
K	3.81	1.68
Ca	0.37	0.16
Ti	0.11	0.04
Fe	0.77	0.24
Total:	100.00	100.00

Element	Wt%	Atomic %
C	61.48	69.42
O	33.81	28.66
Na	0.02	0.01
Mg	0.34	0.19
Al	0.36	0.18
Si	0.19	0.09
S	2.13	0.90
Ca	1.52	0.51
Fe	0.15	0.04
Total:	100.00	100.00

SEM-EDX results of sample I-18/23b

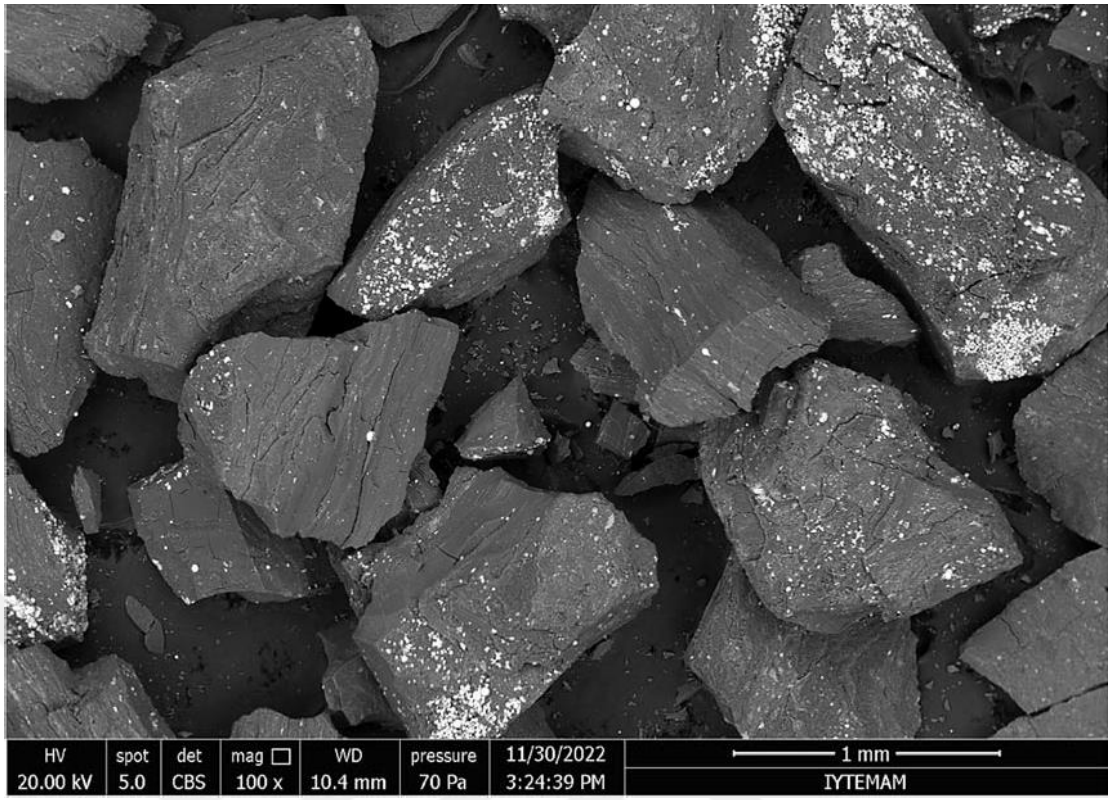

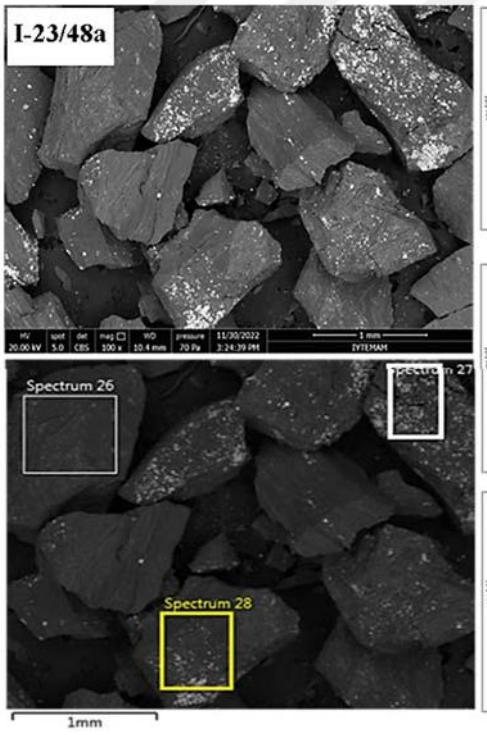

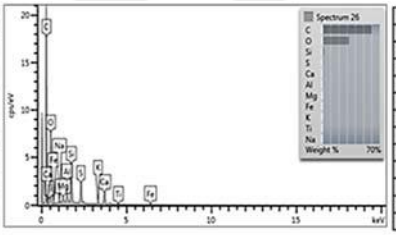

Element	Wt%	Atomic %
C	60.49	69.04
O	32.52	27.87
Na	0.05	0.03
Mg	0.35	0.20
Al	1.22	0.62
Si	2.19	1.07
S	1.42	0.61
K	0.16	0.06
Ca	1.26	0.43
Ti	0.06	0.02
Fe	0.27	0.07
Total:	100.00	100.00

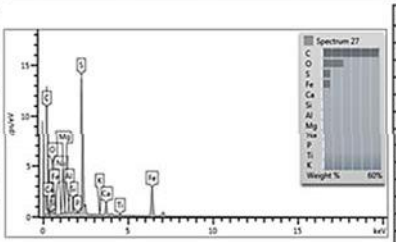

Element	Wt%	Atomic %
C	58.38	72.06
O	22.14	20.52
Na	0.11	0.07
Mg	0.18	0.11
Al	0.53	0.29
Si	0.73	0.38
P	0.07	0.03
S	8.39	3.88
K	0.05	0.02
Ca	1.16	0.43
Ti	0.06	0.02
Fe	8.19	2.18
Total:	100.00	100.00

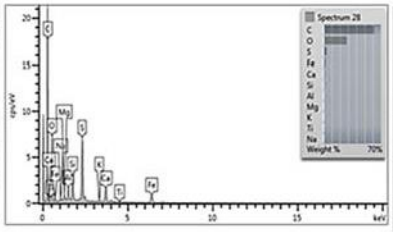

Element	Wt%	Atomic %
C	61.76	71.46
O	28.38	24.65
Na	0.05	0.03
Mg	0.29	0.16
Al	0.67	0.35
Si	1.19	0.59
S	3.83	1.66
K	0.09	0.03
Ca	1.40	0.48
Ti	0.06	0.02
Fe	2.29	0.57
Total:	100.00	100.00

SEM-EDX results of sample I-23/48a

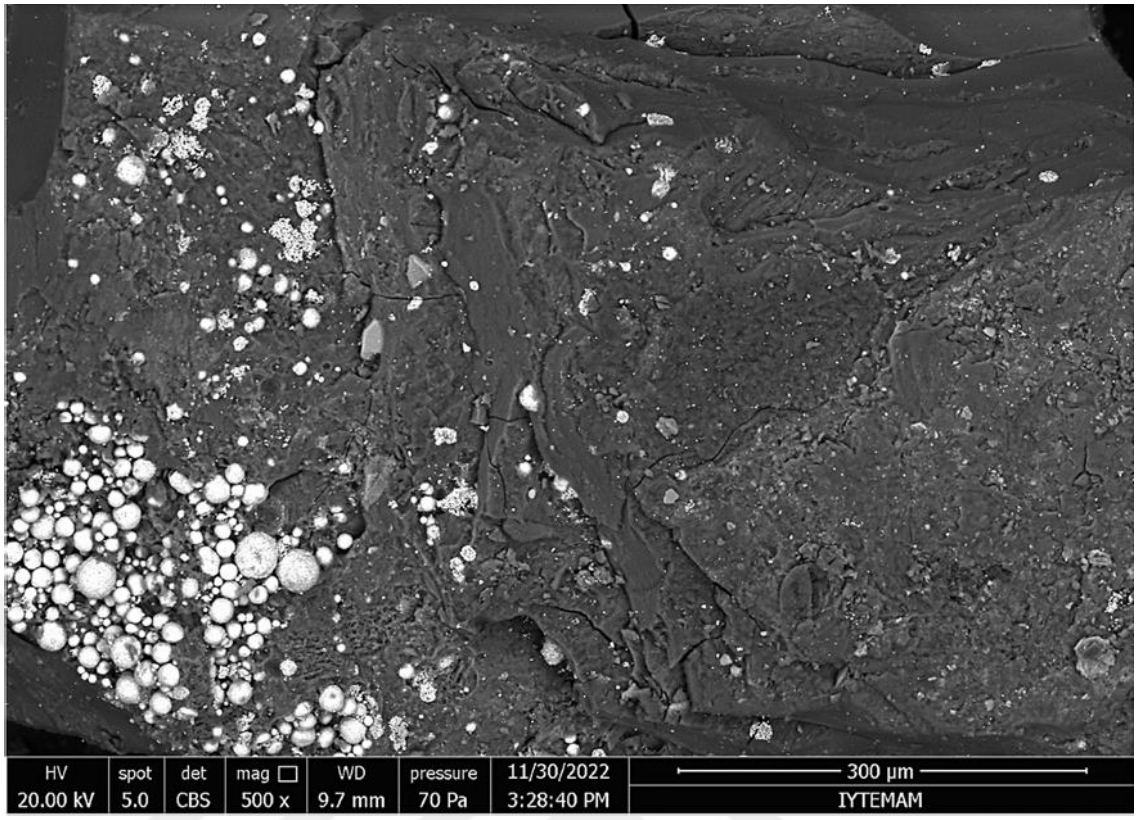

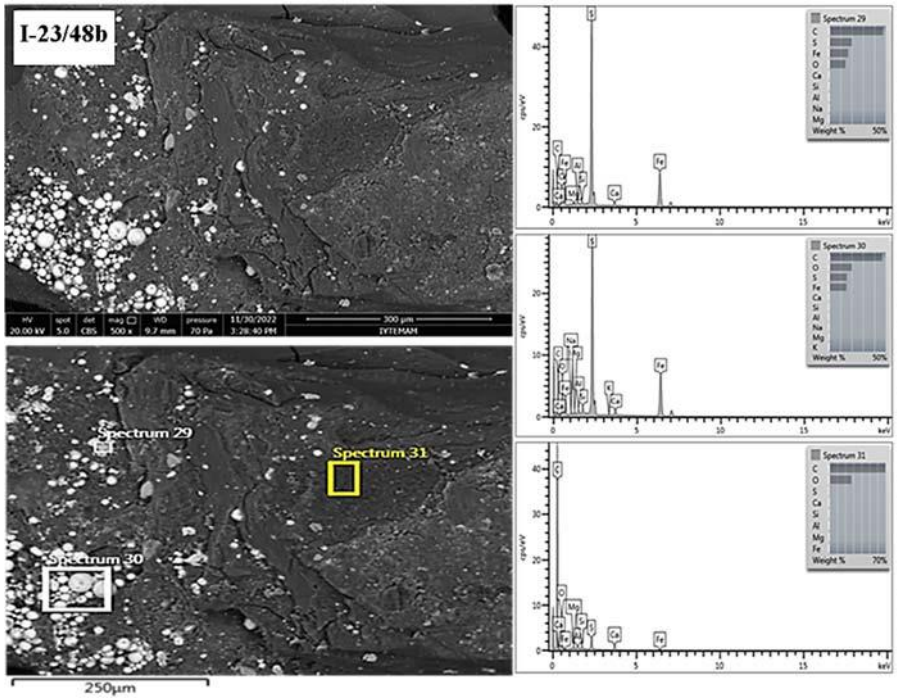

Element	Wt%	Atomic %
C	46.88	65.15
O	20.12	21.00
Na	0.27	0.20
Mg	0.13	0.09
Al	0.33	0.21
Si	0.53	0.32
S	15.66	8.15
K	0.06	0.02
Ca	0.60	0.25
Fe	15.41	4.61
Total:	100.00	100.00

Element	Wt%	Atomic %
C	47.52	67.95
O	14.47	15.53
Na	0.13	0.10
Mg	0.04	0.03
Al	0.14	0.09
Si	0.24	0.15
S	20.09	10.76
Ca	0.48	0.20
Fe	16.90	5.20
Total:	100.00	100.00

Element	Wt%	Atomic %
C	69.48	76.13
O	27.58	22.69
Mg	0.21	0.11
Al	0.25	0.12
Si	0.26	0.12
S	1.24	0.51
Ca	0.89	0.29
Fe	0.10	0.02
Total:	100.00	100.00

SEM-EDX results of sample I-23/48b

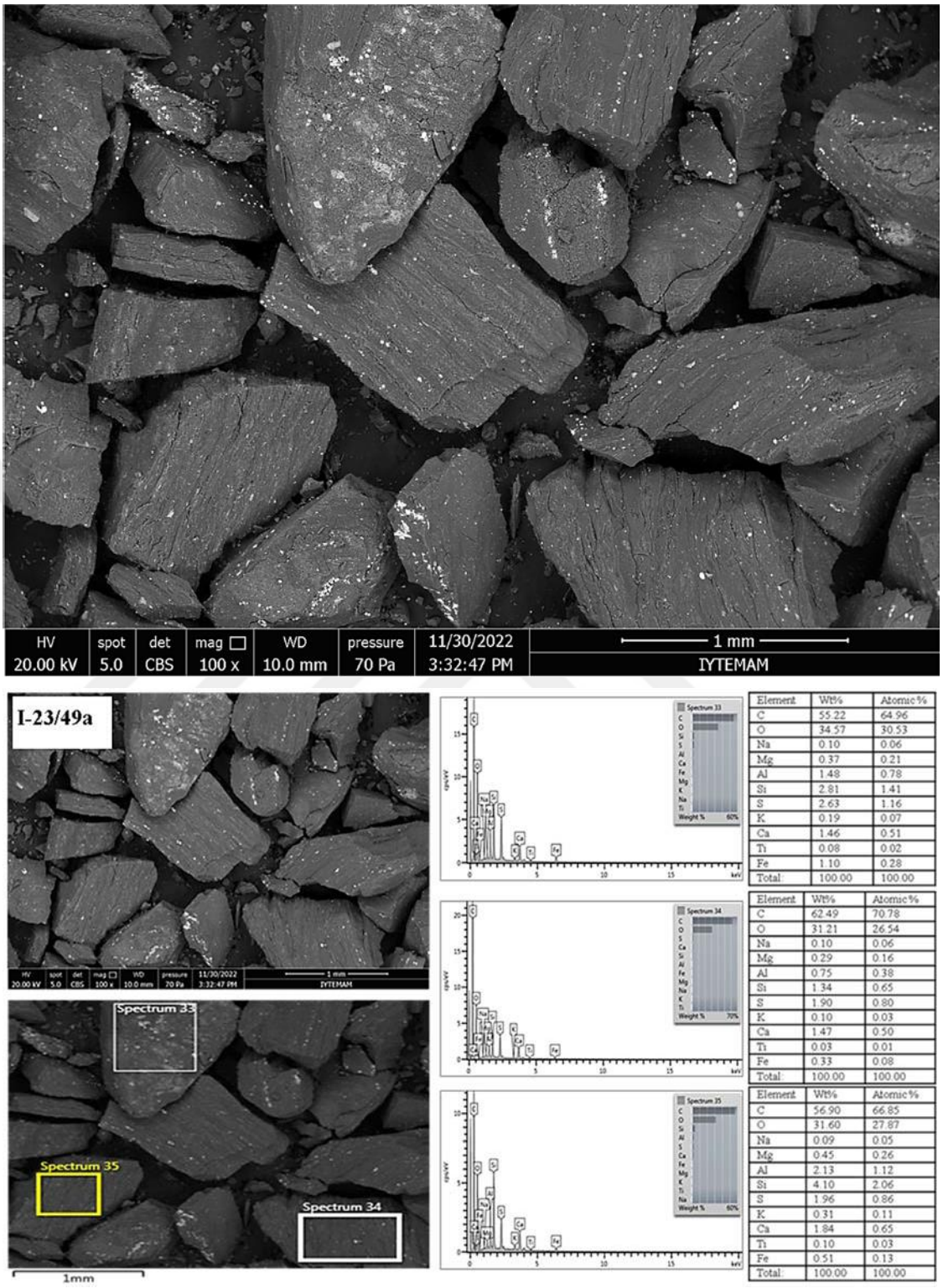

Element	Wt%	Atomic %
C	55.22	64.96
O	34.57	30.53
Na	0.10	0.06
Mg	0.37	0.21
Al	1.48	0.78
Si	2.81	1.41
S	2.63	1.16
K	0.19	0.07
Ca	1.46	0.51
Ti	0.08	0.02
Fe	1.10	0.28
Total:	100.00	100.00

Element	Wt%	Atomic %
C	62.49	70.78
O	31.21	26.54
Na	0.10	0.06
Mg	0.29	0.16
Al	0.75	0.38
Si	1.34	0.65
S	1.90	0.80
K	0.10	0.03
Ca	1.47	0.50
Ti	0.03	0.01
Fe	0.33	0.08
Total:	100.00	100.00

Element	Wt%	Atomic %
C	56.90	66.85
O	31.60	27.87
Na	0.09	0.05
Mg	0.45	0.26
Al	2.13	1.12
Si	4.10	2.06
S	1.96	0.86
K	0.31	0.11
Ca	1.84	0.65
Ti	0.10	0.03
Fe	0.51	0.13
Total:	100.00	100.00

SEM-EDX results of sample I-23/49a

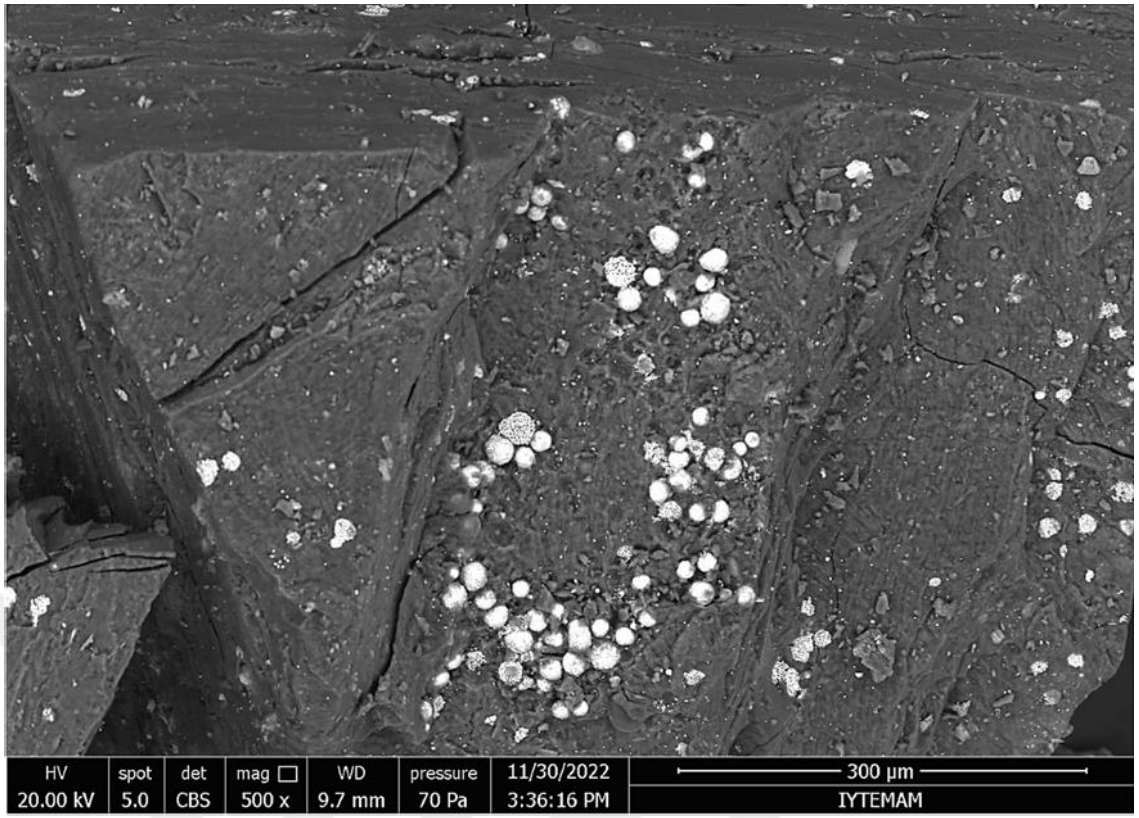

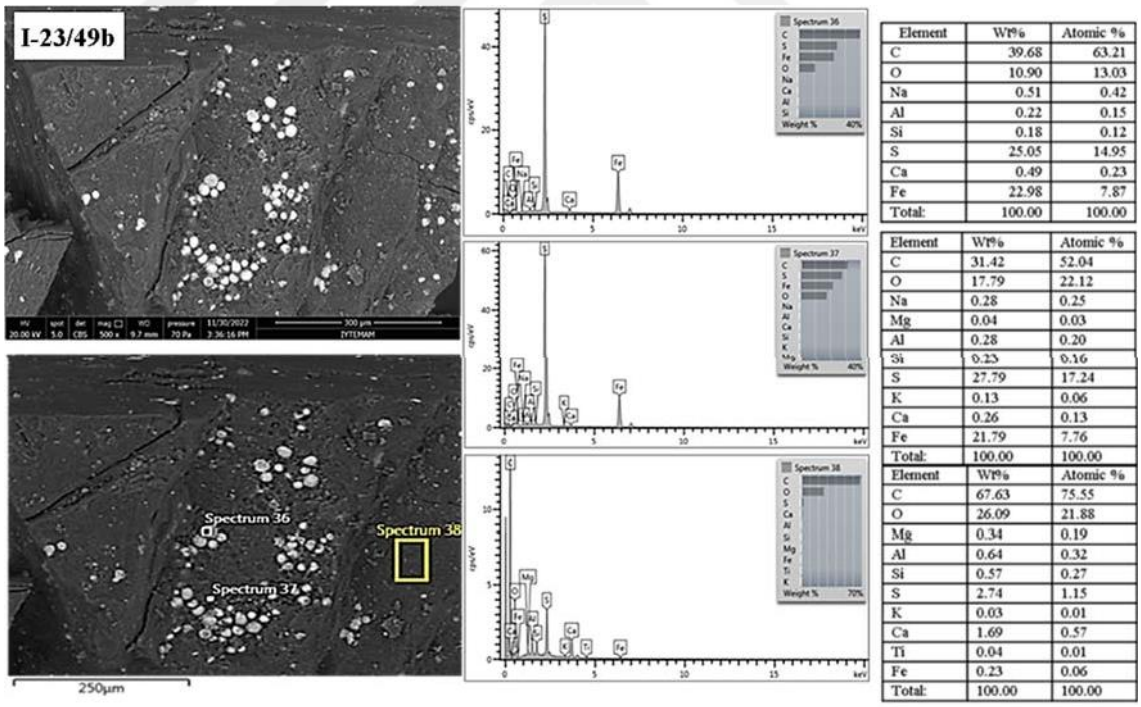

Element	Wt%	Atomic %
C	39.68	63.21
O	10.90	13.03
Na	0.51	0.42
Al	0.22	0.15
Si	0.18	0.12
S	25.05	14.95
Ca	0.49	0.23
Fe	22.98	7.87
Total:	100.00	100.00

Element	Wt%	Atomic %
C	31.42	52.04
O	17.79	22.12
Na	0.28	0.25
Mg	0.04	0.03
Al	0.28	0.20
Si	0.23	0.16
S	27.79	17.24
K	0.13	0.06
Ca	0.26	0.13
Fe	21.79	7.76
Total:	100.00	100.00

Element	Wt%	Atomic %
C	67.63	75.55
O	26.09	21.88
Mg	0.34	0.19
Al	0.64	0.32
Si	0.57	0.27
S	2.74	1.15
K	0.03	0.01
Ca	1.69	0.57
Ti	0.04	0.01
Fe	0.23	0.06
Total:	100.00	100.00

SEM-EDX results of sample I-23/49b

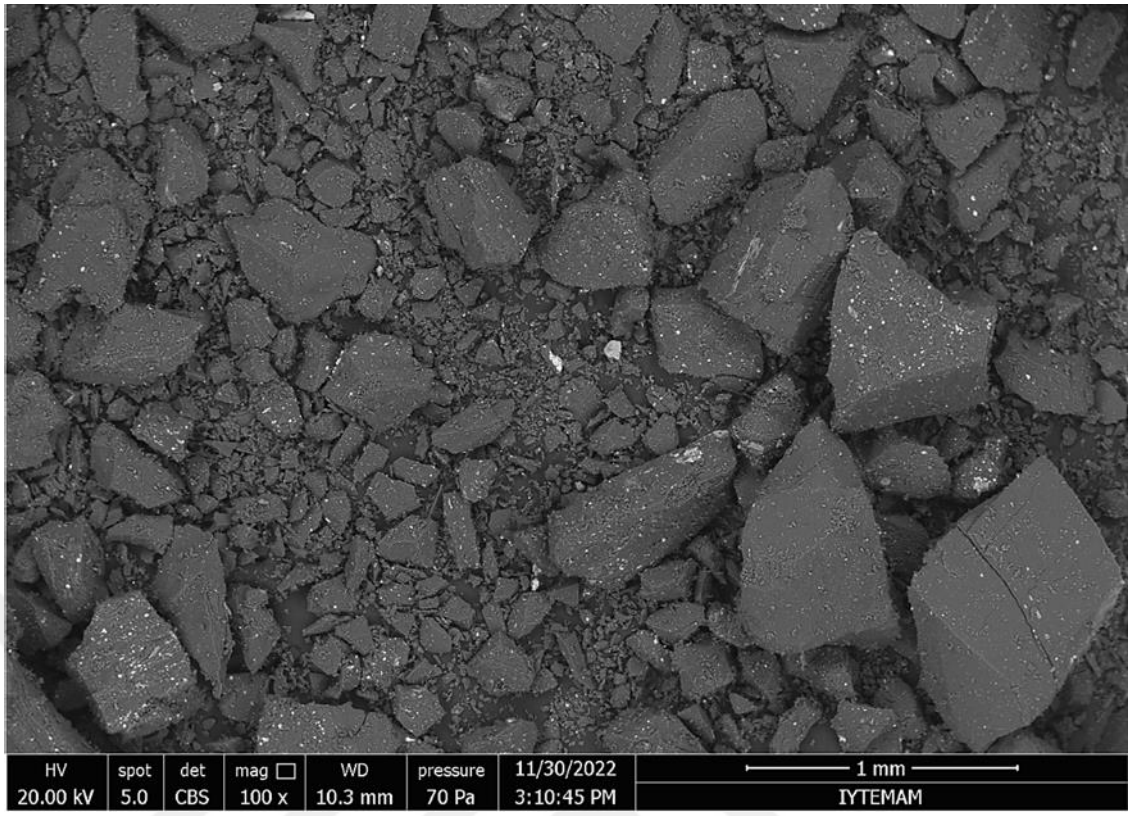

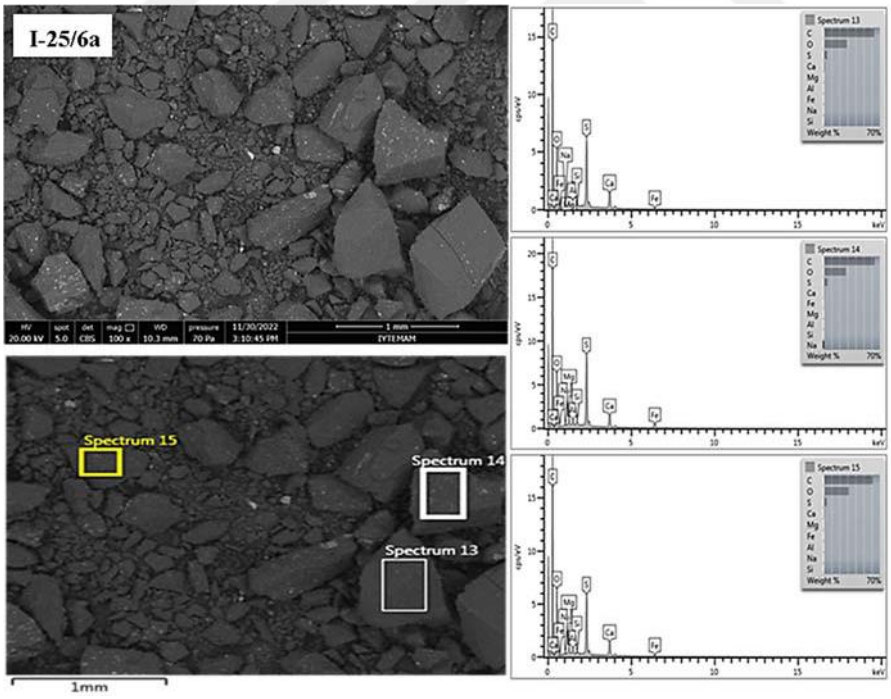

Element	Wt%	Atomic %
C	62.98	71.74
O	29.30	25.06
Na	0.08	0.05
Mg	0.49	0.27
Al	0.34	0.17
Si	0.07	0.03
S	4.63	1.98
Ca	1.84	0.63
Fe	0.28	0.07
Total:	100.00	100.00

Element	Wt%	Atomic %
C	63.40	72.50
O	28.01	24.05
Na	0.02	0.01
Mg	0.43	0.24
Al	0.31	0.16
Si	0.25	0.12
S	5.02	2.15
Ca	1.40	0.48
Fe	1.17	0.29
Total:	100.00	100.00

Element	Wt%	Atomic %
C	61.41	70.02
O	31.67	27.11
Na	0.08	0.05
Mg	0.45	0.25
Al	0.32	0.16
Si	0.04	0.02
S	4.18	1.79
Ca	1.51	0.52
Fe	0.34	0.08
Total:	100.00	100.00

SEM-EDX results of sample I-25/6a

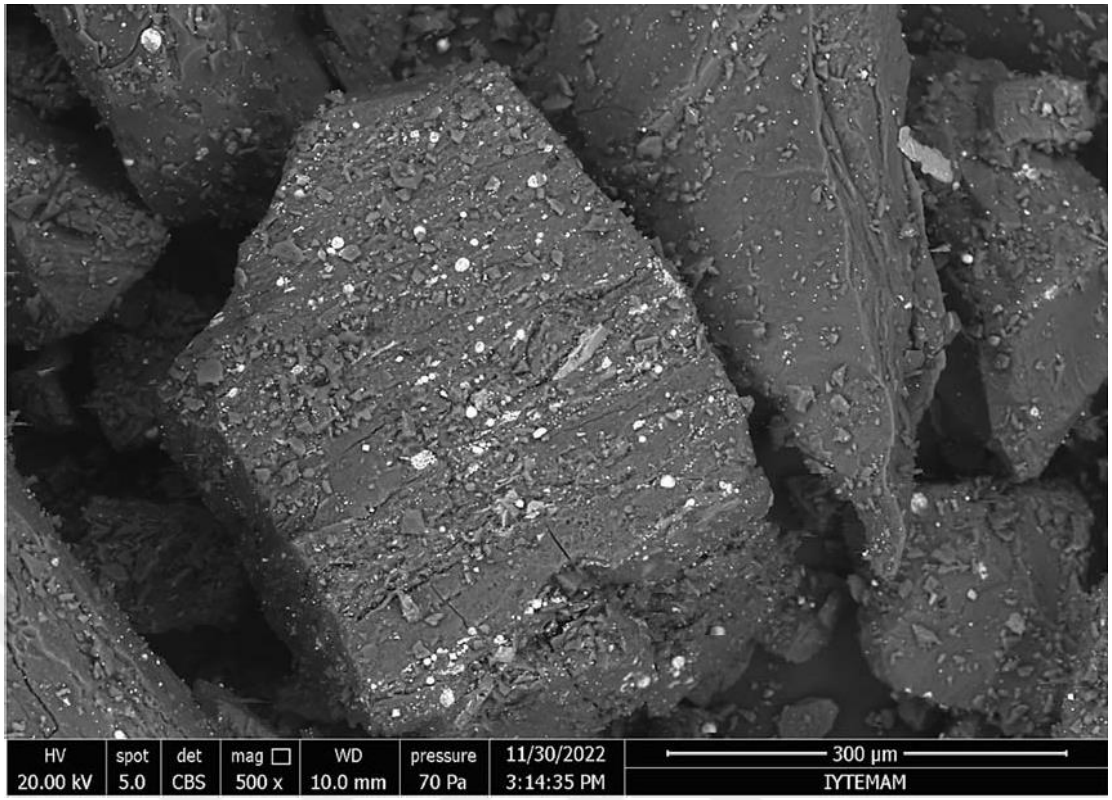

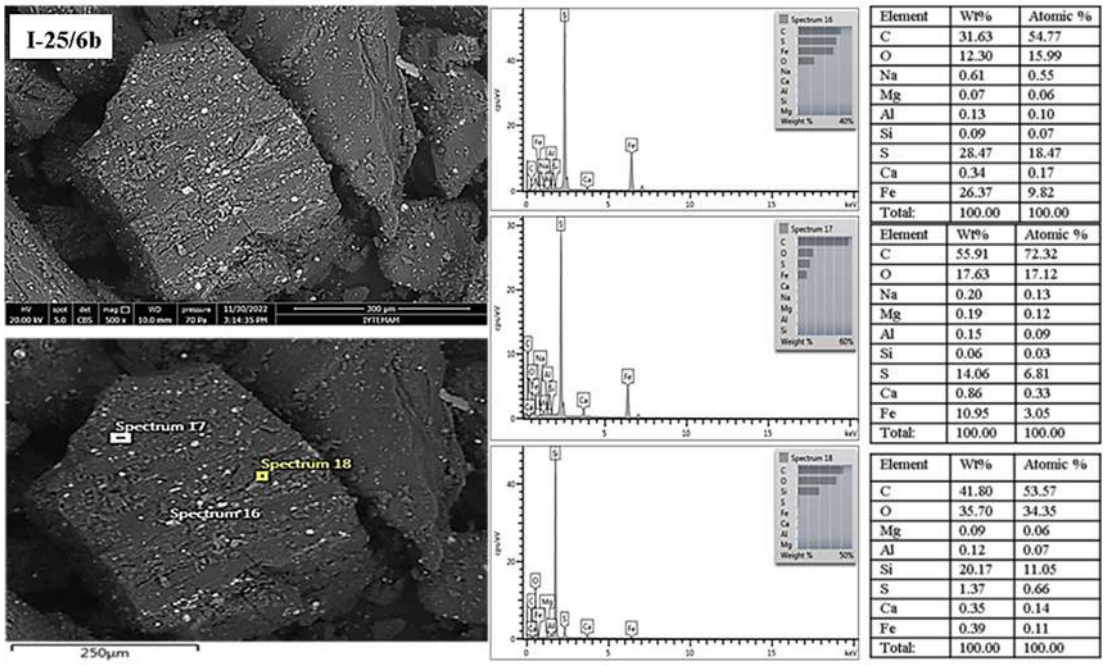

Element	Wt%	Atomic %
C	31.63	54.77
O	12.30	15.99
Na	0.61	0.55
Mg	0.07	0.06
Al	0.13	0.10
Si	0.09	0.07
S	28.47	18.47
Ca	0.34	0.17
Fe	26.37	9.82
Total:	100.00	100.00

Element	Wt%	Atomic %
C	55.91	72.32
O	17.63	17.12
Na	0.20	0.13
Mg	0.19	0.12
Al	0.15	0.09
Si	0.06	0.03
S	14.06	6.81
Ca	0.86	0.33
Fe	10.95	3.05
Total:	100.00	100.00

Element	Wt%	Atomic %
C	41.80	53.57
O	35.70	34.35
Mg	0.09	0.06
Al	0.12	0.07
Si	20.17	11.05
S	1.37	0.66
Ca	0.35	0.14
Fe	0.39	0.11
Total:	100.00	100.00

SEM-EDX results of sample I-25/6b

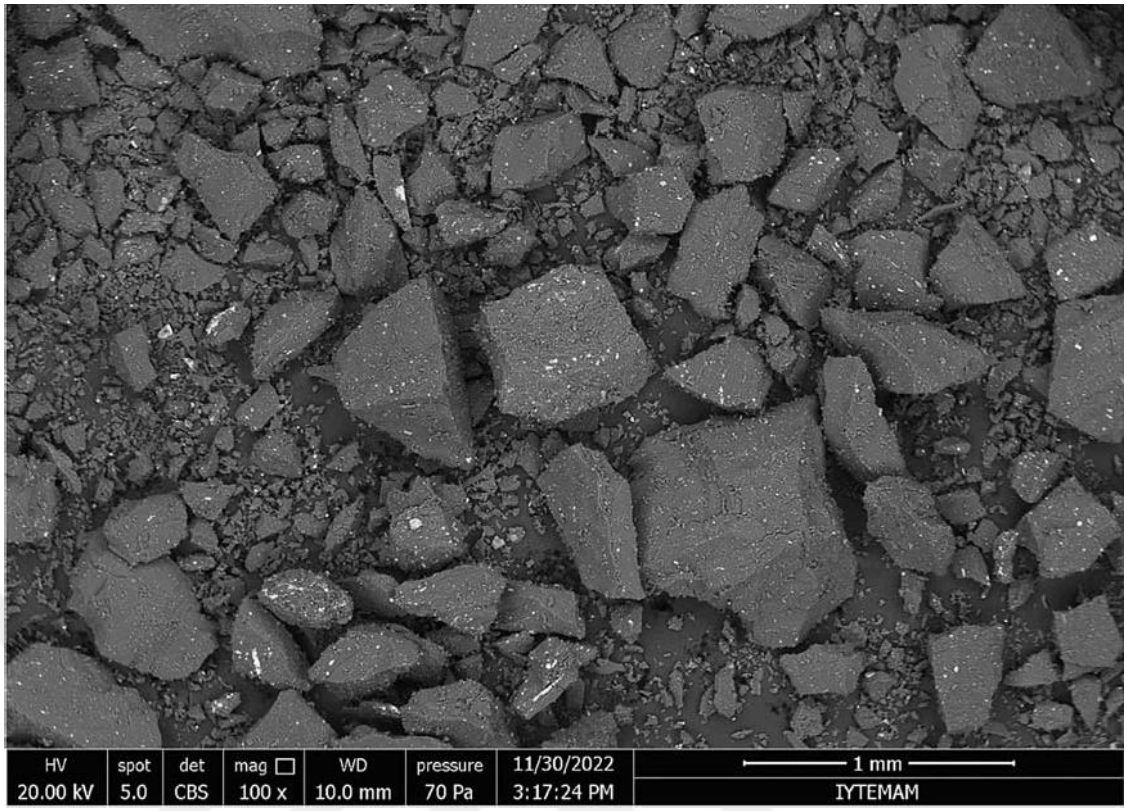

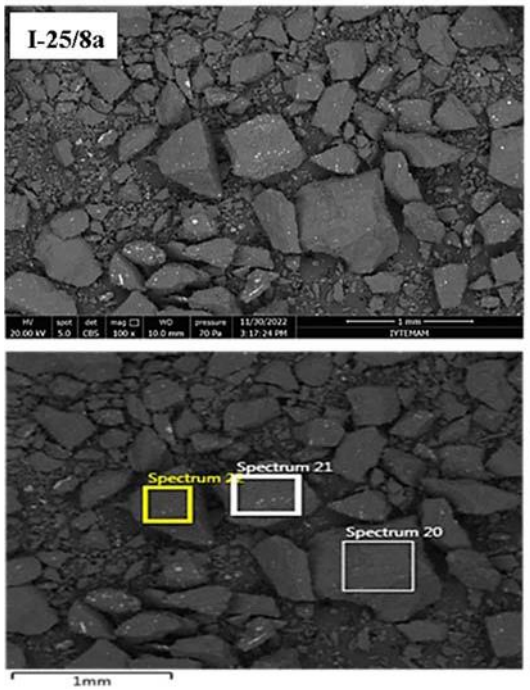

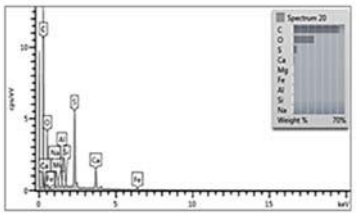

Element	Wt%	Atomic %
C	59.33	68.40
O	32.93	28.51
Na	0.06	0.04
Mg	0.30	0.17
Al	0.22	0.11
Si	0.18	0.09
P	0.08	0.04
S	4.62	2.00
Ca	0.90	0.31
Fe	1.37	0.34
Total:	100.00	100.00

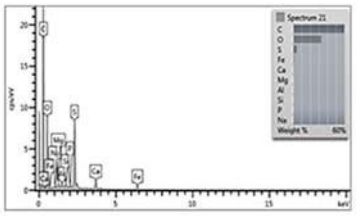

Element	Wt%	Atomic %
C	62.47	71.67
O	28.66	24.68
Na	0.05	0.03
Mg	0.47	0.26
Al	0.24	0.12
Si	0.17	0.08
S	5.37	2.31
Ca	2.13	0.73
Fe	0.45	0.11
Total:	100.00	100.00

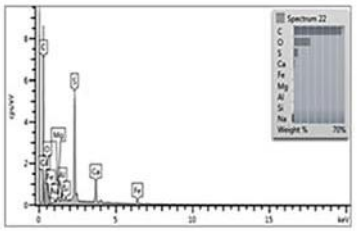

Element	Wt%	Atomic %
C	65.27	75.17
O	23.46	20.28
Na	0.04	0.02
Mg	0.35	0.20
Al	0.23	0.12
Si	0.09	0.04
S	7.14	3.08
Ca	2.37	0.82
Fe	1.05	0.26
Total:	100.00	100.00

SEM-EDX results of sample I-25/8a.

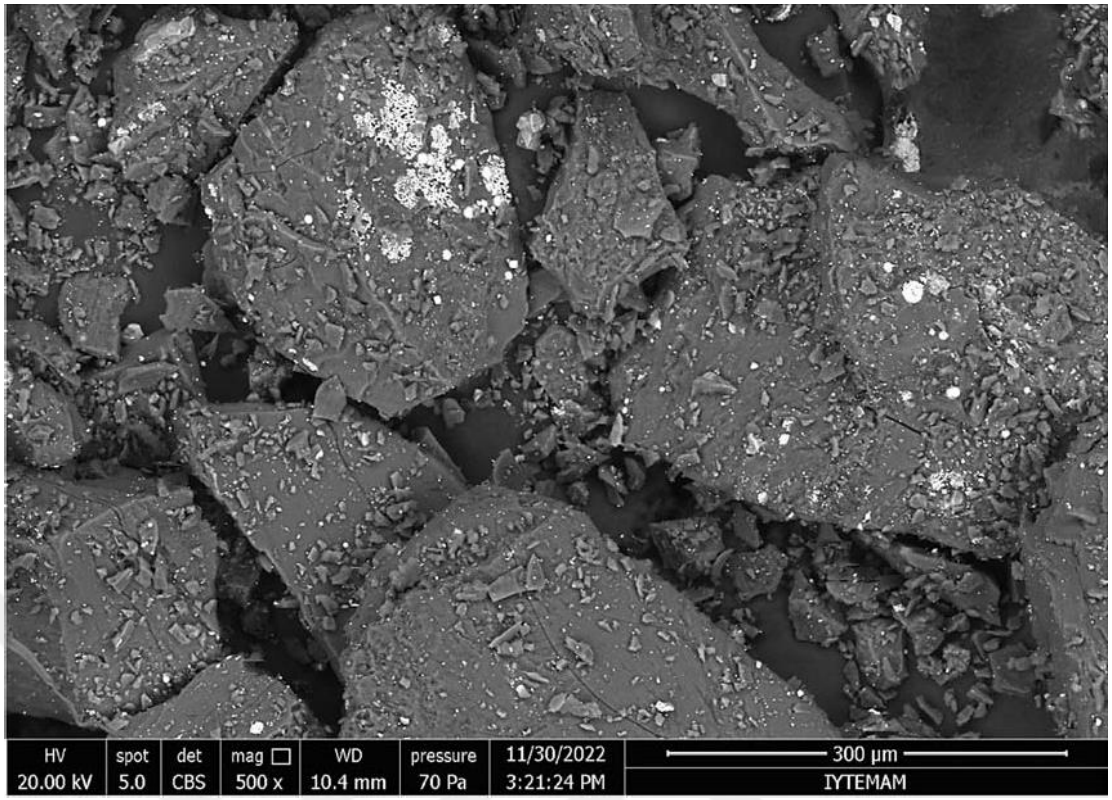

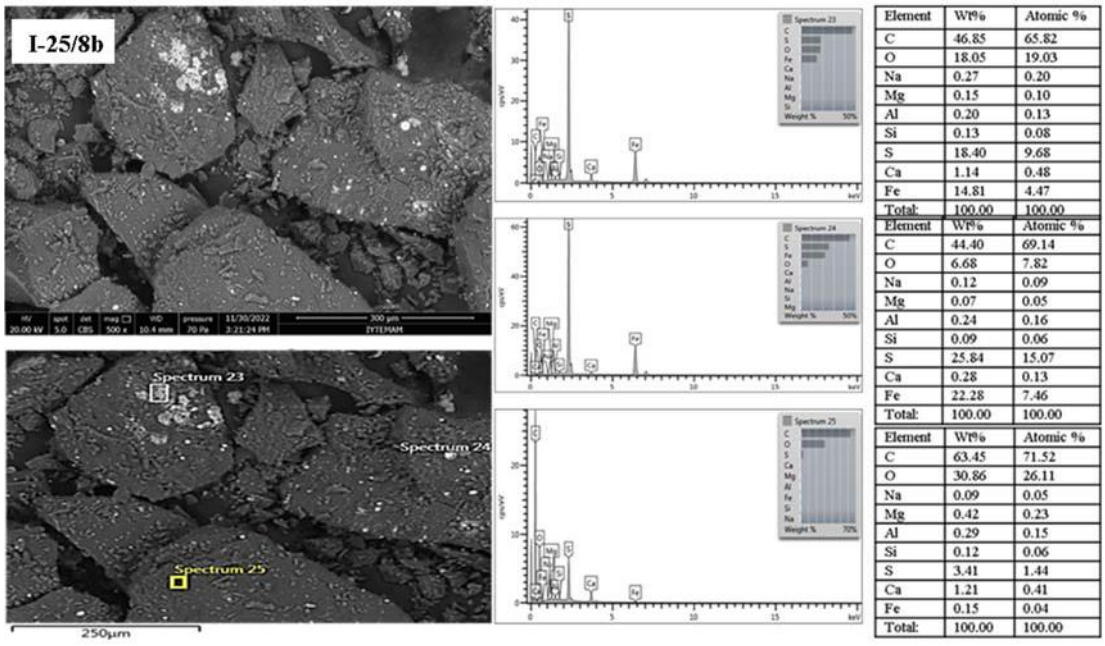

Element	Wt%	Atomic %
C	46.85	65.82
O	18.05	19.03
Na	0.27	0.20
Mg	0.15	0.10
Al	0.20	0.13
Si	0.13	0.08
S	18.40	9.68
Ca	1.14	0.48
Fe	14.81	4.47
Total:	100.00	100.00

Element	Wt%	Atomic %
C	44.40	69.14
O	6.68	7.82
Na	0.12	0.09
Mg	0.07	0.05
Al	0.24	0.16
Si	0.09	0.06
S	25.84	15.07
Ca	0.28	0.13
Fe	22.28	7.46
Total:	100.00	100.00

Element	Wt%	Atomic %
C	63.45	71.52
O	30.86	26.11
Na	0.09	0.05
Mg	0.42	0.23
Al	0.29	0.15
Si	0.12	0.06
S	3.41	1.44
Ca	1.21	0.41
Fe	0.15	0.04
Total:	100.00	100.00

SEM-EDX results of sample I-25/8a.

APPENDIX VIII: Petrographic analysis of inorganic samples





Examination of inorganic samples under the Olympus Bx41TF polarizing microscope at Torbalı Vocational School of the Dokuz Eylül University.

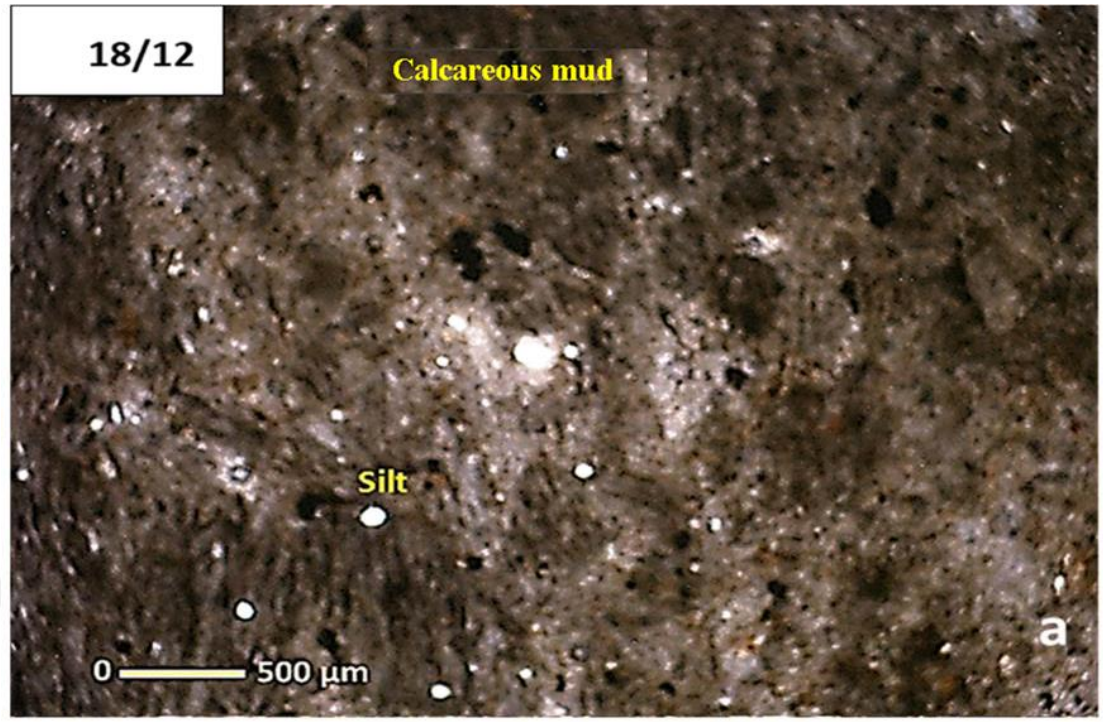
18/12
Calcareous mud
Silt
0
500 µm
a

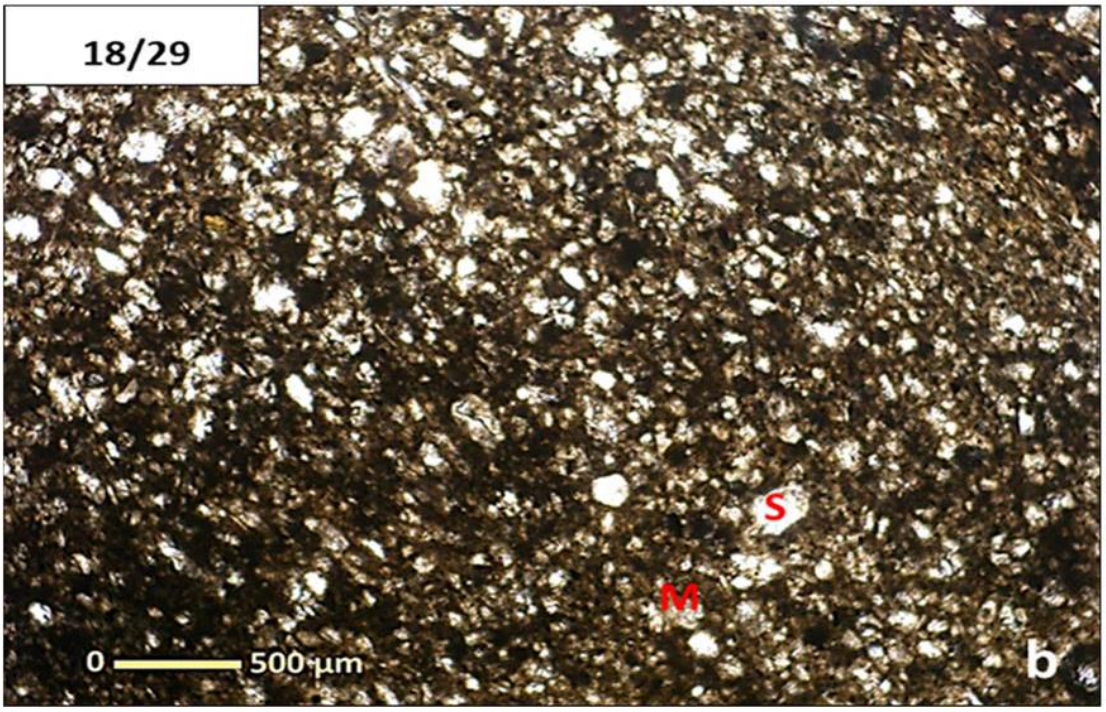
18/29
S
M
0
500 µm
b

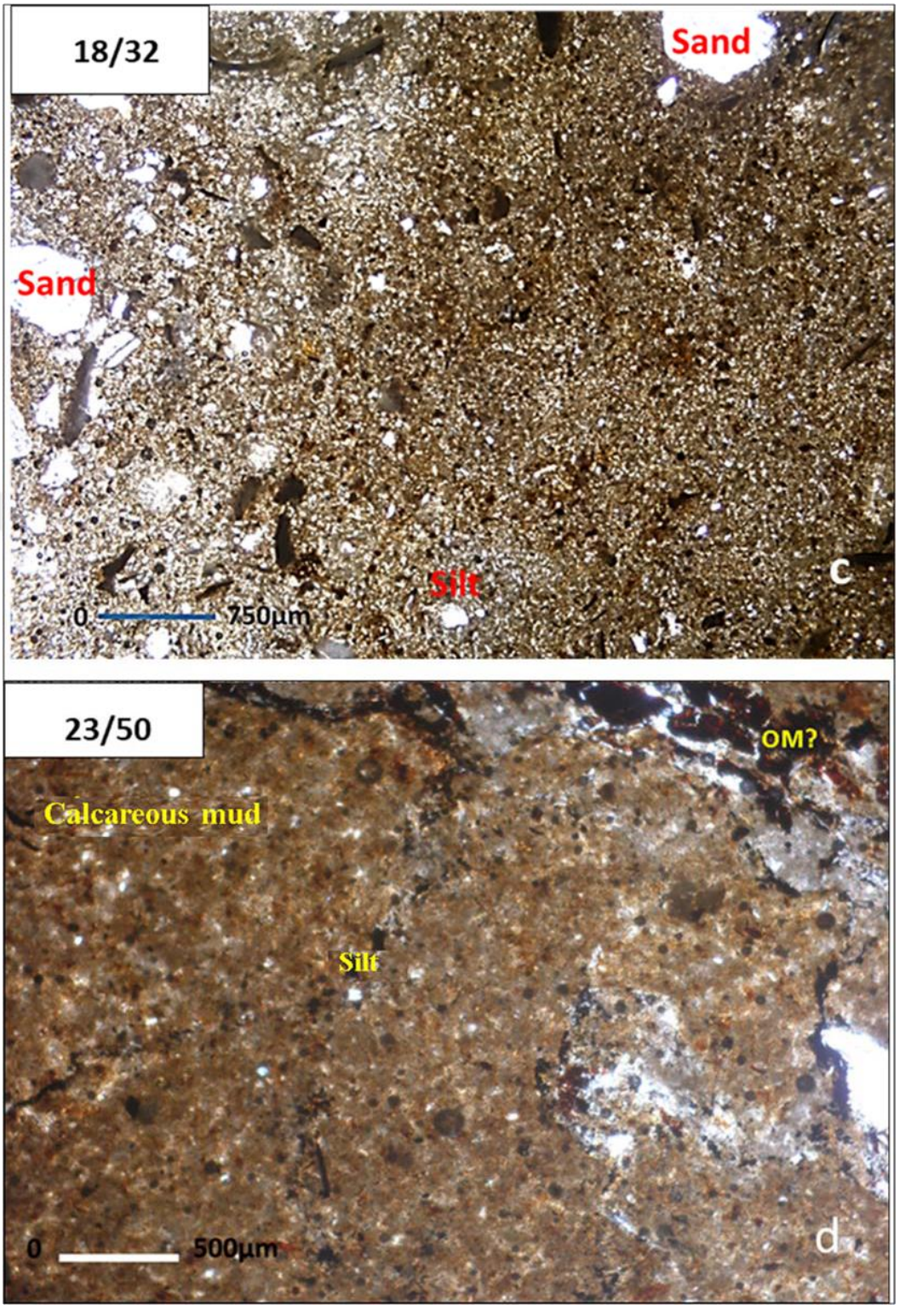
18/32
Sand
Sand
Silt
0
750µm
c
23/50
OM?
Calcareous mud
Silt
0
500µm
d

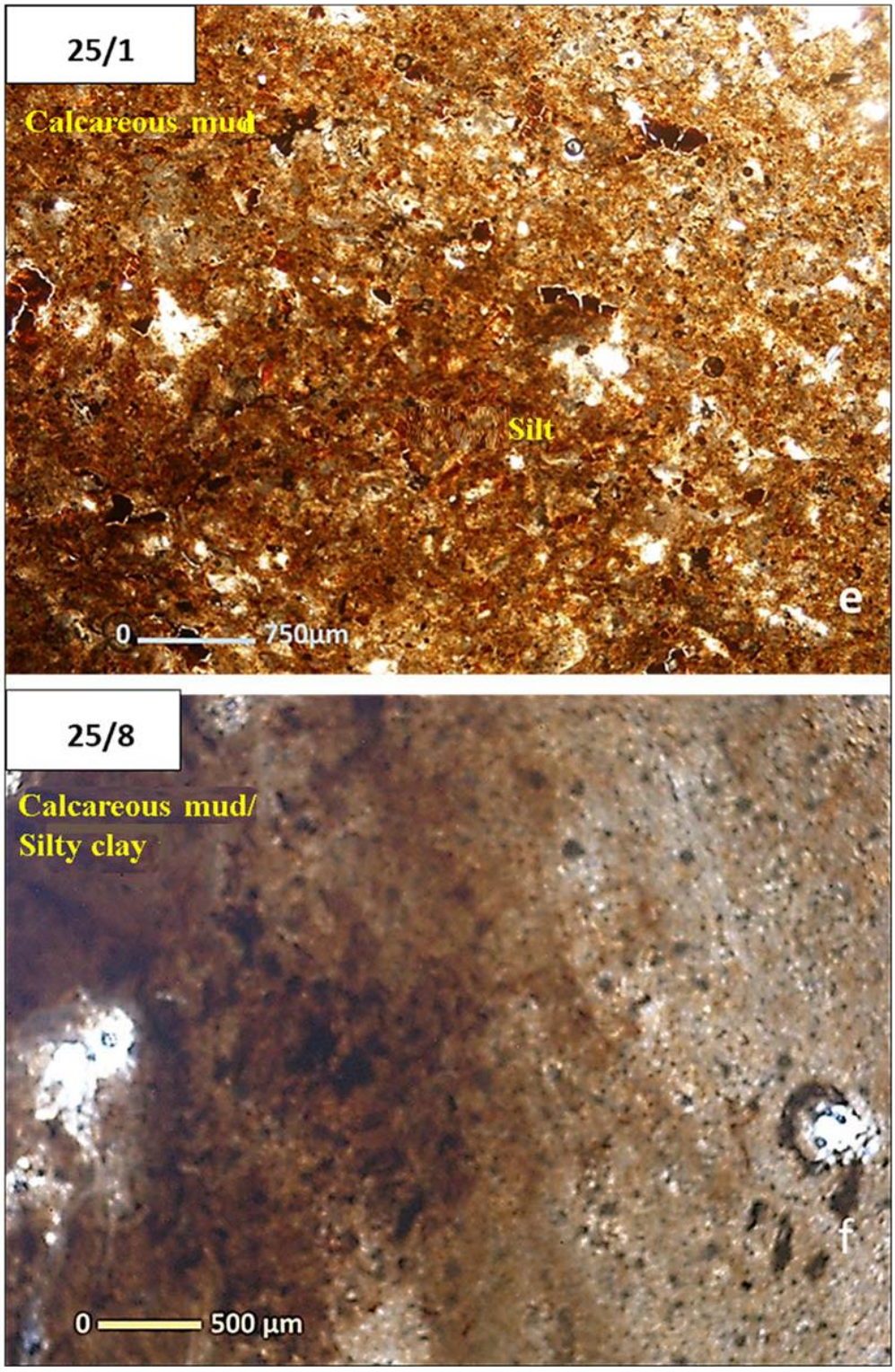
25/1
Calcareous mud
Silt
0
750µm
e
25/8
Calcareous mud/
Silty clay
0
500 µm
f

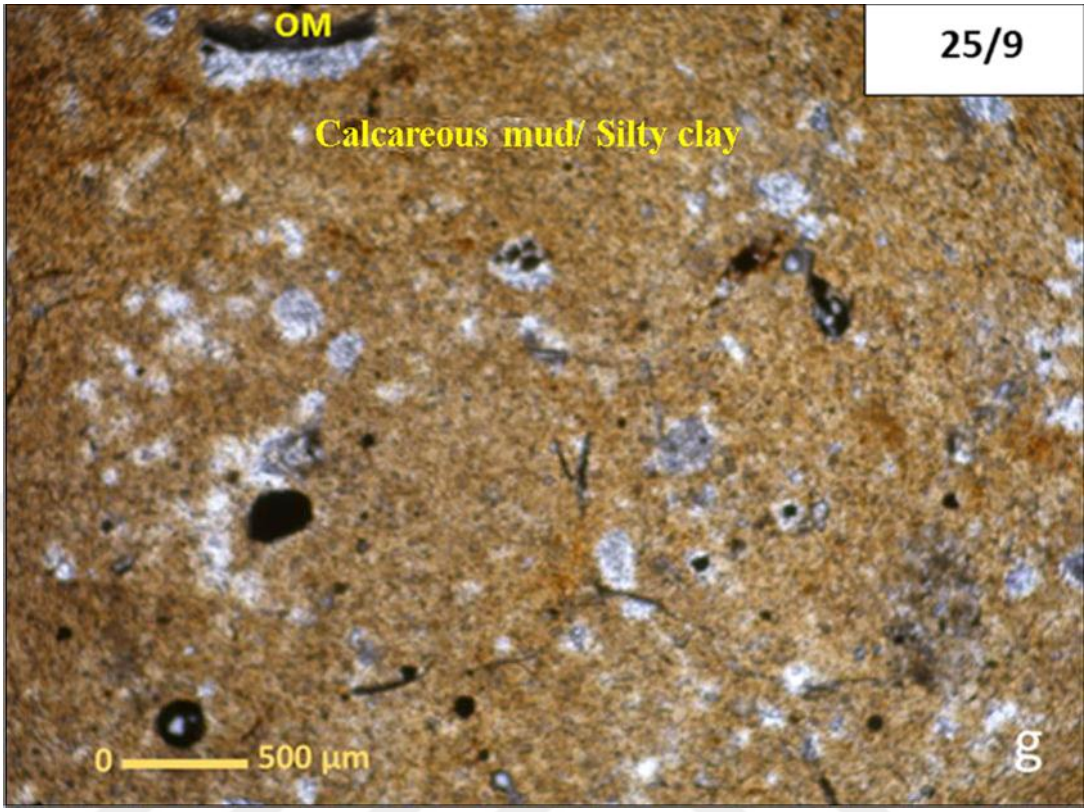

a) Above the coal sample I-18/12, (b) Interlayer of the coal sample no I-18/29 (Abbreviation: S; Sand, M; Mica flakes originating from metamorphic basement, mudstone rich in organic matter), (c) I-18/32 bottom of the coal seam (sand grains derived from metamorphic basement), (d) Above the coal seam sample no I-23/50 (OM; charred organic matter, red colour is due to Fe oxides), (e) Sample no. I-25/1, (f) Sample no. I-25/8, (g) Sample no. I-25/9 (F; feldspar or metamorphic rock grain, OM; charred plant remains).